TRANSITION METAL AND RARE EARTH METAL MODIFIED SOL-GEL TITANIA: A VERSATILE CATALYST FOR ORGANIC TRANSFORMATIONS

Thesis submitted to the

Cochin University of Science and Technology

By

Shali N.B

In partial fulfillment of the

requirements for the degree of

Doctor of Philosophy
In
Chemistry

Under the Faculty of Science

Department of Applied Chemistry
Cochin University of Science and Technology
Cochin-682 022, Kerala, India.

April 2006

Take up one idea. Make that one idea your life - think of it, dream of it, live on idea. Let the brain, muscles, nerves, every part of your body, be full of that idea and just leave every other idea alone. This is the way to success.
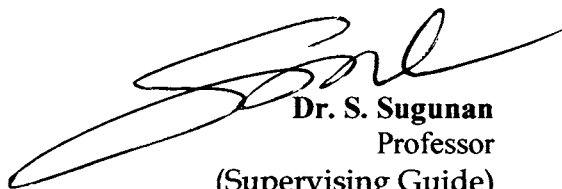
Swami Vivekananda

DEPARTMENT OF APPLIED CHEMISTRY
COCHIN UNIVERSITY OF SCIENCE AND TECHNOLOGY
COCHIN- 682 022, KERALA, INDIA.

10-04-2006

CERTIFICATE

Certified that the present work titled **"Transition metal and rare earth metal modified sol-gel titania: a versatile catalyst for organic transformations"** submitted by Ms. Shali N.B is an authentic record of research work carried out by her under my supervision at the Department of Applied Chemistry in partial fulfillment of the requirements for the Degree of Doctor of Philosophy of the Cochin University of Science and Technology, and that no part thereof has been submitted before for award of any other degree.

Dr. S. Sugunan
Professor
(Supervising Guide)
Department of Applied Chemistry
Cochin University of Science and Technology
Kochi-22.

DECLARATION

I hereby declare that the work presented in this thesis entitled **"Transition metal and rare earth metal modified sol-gel titania: a versatile catalyst for organic transformations"** is an authentic work carried out by me independently under the supervision of Dr. S. Sugunan, Professor in Physical Chemistry, Department of Applied Chemistry, Cochin University of Science and Technology, and has not been included in any other thesis submitted previously for award of any other degree.

Kochi-22

Shali N. B.

10-04-2006

Acknowledgements

really unforgettable. To mention a few other friends in the lab are Radhika, Salini, Kochurani, Ramanathan, Ajitha teacher, Reshmi, Joyes teacher and Bolie. My sincere thanks to Dr. Suja, Dr. Sunaja, Dr. Sanjay, Dr. Fincy and Dr. Bejoy for their timely help and unstinting cooperation. It is a pleasure to mention the long and fruitful companionship of my dear friends Kannan, Ambily and Rekha.

On this occasion, I would like to record my deep love for my mother Saraswathy Balan, and my sister Shabi for their constant and affectionate encouragement and care which proved to be useful in fulfilling this venture. The acknowledgement would be incomplete without mentioning my in-laws. Without their love and support, I couldn't complete this doctoral work.

My final and greatest debt is of course to my beloved husband Sunil, who has now suffered through my research work. Without his constant encouragement and incessant moral support, I couldn't complete my dream work. Last of all I recall how much I have missed my little Adithyakrishna who has adjusted so much even in his tender years and I promise to spend a lot more time with him than I did in the last one year.

Shali N.B

Preface

The science and practice of catalysis is central to most activities in chemical industry. In recent years, catalysis has become an important route to improvement of environmental quality by helping in the abatement of air pollution and the reduction of industrial waste. As materials become more and more sophisticated, the precursors used for their manufacture are likely to increase in complexity of synthesis, motivating the development of new types of catalysts to meet these requirements. Indeed, the burgeoning interest in nanotechnology will undoubtedly have an impact on the preparation of metal oxides. The aim of catalysis research is to apply the catalyst successfully in economically important reactions.

We briefly review the preparation of titania and their modified forms through sol-gel route. Sol-gel route allows the precise control of the synthetic conditions and hence of the factors relevant to catalytic activity, such as purity, stoichiometry, homogeneity and microstructural properties of the catalyst or the catalyst support. Characterization using various physico-chemical techniques and a detailed study of acidic properties are also carried out. The prepared catalysts have proved their value in many organic reactions as environmentally friendly replacements for established reagents responsible for unacceptable chemical waste. Some reactions of industrial importance such as epoxidation of cyclohexene, hydroxylation of phenol, alkylation of arenes, dehydrogenation of cyclohexane and cyclohexene, photooxidation of benzhydol as well as photodegradation of methyl orange have been selected in the present venture.

The present research work is organized into 11 chapters. The first chapter lays the foundations. It describes the history, importance and fundamental concepts of heterogeneous catalysis. A brief introduction and literature survey on titania and their modified forms is also done in this chapter. The materials and the experimental methods employed in the work are discussed in the second chapter. Further needs and directions in terms of instrumentation and methods are briefly treated in this section. The eighth chapter gives an overview about various aspects of photocatalysis. Results and discussion regarding the characterization and catalytic activity are discussed in the rest of the chapters. The last chapter gives the summary of the work done during the research period. A consolidated and systematic investigation on both transition metals and rare earth metals incorporated titania systems clearly indicate their great versatility in organic transformations. Ongoing developments, still at an early stage are focusing on new environmentally benign applications of titania based catalysts.

CONTENTS

Abstract

3   Physico Chemical Characterisation

Abstract

4   Epoxidation of Cyclohexene

Abstract

5   Hydroxylation of Phenol

Abstract

6   **Alkylation of Arenes**

Tert-butylation of Phenol

Abstract

Methylation of Aniline

Abstract

Methylation of Anisole

Abstract

Chapter *1*

Introduction and Literature survey

Abstract

Tightening environmental legislation is driving the fine and specialty chemical industries to consider alternative processes that avoid the use of conventional mineral acids. The use of heterogeneous catalysis in these processes would vastly simplify catalyst removal, minimizing the amount of waste formed. Heterogeneous catalysis is indeed a field where new challenges appear continuously, more and more charming and intriguing. Solid acids especially those based on sol-gel titania and their modified forms are beginning to play a significant role in the greening of fine chemicals manufacturing processes. A wide range of important organic reactions can be efficiently catalyzed by these materials, which can be designed to provide different types of acidity as well as high degrees of reaction selectivity. This research work concentrates on the preparation of titania and to study the influence of transition metals and rare earth metals on its physico chemical properties, considering their relevance for environmental applications.

1.1 General Introduction

Although catalysis is a mature field, it remains at the center of most industrial processes, accounting for about a quarter of the world's gross domestic product. The development of catalysis, from the Greek *(kata,* wholly; *lyein,* to loosen), as a concept has been accorded to Berzelius (1779-1848) who rationalized the "catalytic power" of certain substances as an ability to "awaken affinities, which are asleep at a particular temperature, by their mere presence and not by their own affinity"[1-2]. Berzelius' definition highlights the fact that, at the beginning at least, the focus of catalysis was placed on accelerating reaction rates. Even before Berzelius coined this term, human beings have used catalysts in the fermentation of drinks and preparation of cheese. All biological processes in living beings function through enzymatic processes. It is likely that even the very first organic molecule that formed on earth were produced by catalysis. Various definitions of catalysis have been proposed but an early definition offered by Wilhelm Ostwald in 1895 is still widely in use: "Catalysts are substances which change the velocity of a reaction without modification of the energy factors of the reaction". The original definition of catalysis has stood the test of time. The catalysts aid the attainment of chemical equilibrium by reducing the potential energy barrier in the reaction path. The success of catalysis relies on the ability of the catalyst to modify the kinetics of the chemical system being catalyzed. Specifically, a catalyst accelerates chemical reactions by opening alternative mechanisms with lower activation barriers[3]. The quantitative aspects of catalysis take the form of reaction mechanisms that account for such matters as reaction

stoichiometry, nature of the chemical interaction, geometric and electronic factors[4].

It is unfortunate that, in certain quarters, the science of catalysis is regarded as something of a "black art" largely because of the difficulty in achieving a full catalyst characterization and providing an explicit correlation of catalytic performance with catalyst structure. The choice of a suitable catalyst for a particular reaction depends on the stability of the complexes formed between the reactant and/or product and the catalyst. Catalyst efficiency is assessed in terms of three parameters; activity, selectivity and life time. As more complex catalytic processes were developed, however, the emphasis shifted towards improving their selectivity. A reaction that is highly selective towards the desired product(s) is bound to consume less reactants, minimize the need for expensive and difficult separation processes, and create less polluting byproducts. A selective catalyst will facilitate the formation of one product molecule while inhibiting the production of other different molecules, eventhough thermodynamically the formation of all the products is feasible. A molecular level control of the selectivity of the catalysts is arguably the single most important challenge in this field. One of the major problems that have bedeviled the operation of heterogeneous catalysis is a progressive loss of activity with catalyst use.

The phenomenon of catalysis is very widespread in chemistry and has enormous practical consequences in our daily lives. It plays a decisive role in the production of medicines, of synthetic fabrics for clothing, and of material such as plastics. It is widely applied in the processing of foods, in the manufacture of many valuable chemicals, and in the production of fuels for

making energy readily available for transportation and for internal heating. It is also crucial in many processes occurring in living things, where enzymes are the catalysts. Finally, it is very important in the preservation of our environment, as demonstrated by its vital contribution in making lead free gasoline a reality and by its role in decreasing pollution from automobile exhaust gases.

Catalytic technologies have played a vital role in the economic development of the chemicals industry in the 20th century, with a total contribution of ~20% of world GNP. In the 21st century, we can expect the drive towards cleaner technologies brought about by public, legislative and corporate pressure to provide new and exciting opportunities for catalysis and catalytic processes[5]. The area of catalysis is sometimes referred to as a "foundational pillar" of green chemistry. Catalytic reactions often reduce energy requirements and decrease separations due to increased selectivity; they may permit the use of renewable feedstocks or minimize the quantities of reagents needed[6].

The catalytic reactions can be classified into homogeneous, heterogeneous as well as enzymatic reactions depending on the physical state of the catalyst. As we entered the 21st century, the three principal fields of catalysis science, enzymatic, heterogeneous and homogeneous are in a stage of vigorous development, with the understanding of structure-function-mechanism reaching unprecedented heights in each field. There are clear cut correlations between homogeneous, heterogeneous and enzymatic catalysis through the dynamic nature of structure for these processes. The flexibility of structure is necessary in all three cases for the catalytic cycle to operate

efficiently, and these dynamic structural changes are complex and may occur either at the active sites or removed from the active site but influencing the bonding or lifetime of reaction intermediates nevertheless. In heterogeneous catalysis, the aim is to maximize the catalytic activity and reaction rate for reactions, which occur at known active sites on the solid surface.

Heterogeneous catalysis is important for its technological applications. Whilst there is much excellent and potentially valuable homogeneous catalytic chemistry in the academic literature, its application on the manufacturing scale is often restricted by economic, environmental, regulatory and safety considerations. Heterogeneous systems, on the other hand have the attractions like easier catalyst recovery, higher product selectivity, costless disposal of the used catalyst, design of continuous flow reactors and generally, they are accepted in the much versatile chemistry they offer. It is related to such diverse branches of science including chemical kinetics, thermodynamics, mass and heat transfer, solid state physics, surface physics and surface chemistry. Accordingly, understanding of the phenomenon requires the knowledge of these fields, and the methodology of experimental research is equally wide ranging. It is truly a multidisciplinary subject.

1.2 Solid Acid Catalysts

Solid acid catalysts have served as important functional materials for the petroleum refinery industry, such as in the cracking processes, and for the production of chemicals[7]. At present about 180 industrial processes using solid acids are in operation, featuring acids such as zeolites, oxides, mixed oxides including heteropoly acids and phosphates. A rapidly growing area of

heterogeneous catalysis is for environmental pollution control. The efficient use of solid catalysts and reagents that stay in a phase separate from the organic compounds can go a long way to achieving these goals[8]. Solid acid catalysts are generally categorized by their Bronsted and/or Lewis acidity, the strength and number of these sites, and the morphology of the support (e.g., surface area, pore size). High product selectivity can depend on the fine tuning of these properties. The synthesis of pure Bronsted and pure Lewis acid catalysts attracts a great degree of academic interest, although the latter is harder to achieve because Bronsted acidity often arises from Lewis acid-base complexation[9].

Most of the solid acid catalysts used in various chemical transformations are based on inorganic oxides. In most cases, these oxides are to be modified chemically or physically so as to get the desired catalytic activity for a particular reaction. Oxides, because of their ability to take part in the exchange of electrons, protons or oxide ions are used as catalysts in both redox as well as acid base catalysis[10]. In metal oxides, coordinative unsaturation is principally responsible for the ability towards adsorption and catalysis of various reactions. The exposed cations and anions of the metal oxide surfaces form acidic and basic sites as well as acid-base pairs. Besides this, the variable valency of the cation results in the ability of the oxides to undergo oxidation and reduction.

In recent years much attention has been centered on the use of solid acids such as metal oxides, mixed metal oxides and supported metal oxides as they form a wide variety of catalysts in industrially useful reactions[11]. It has been shown that the type of support material used is a critical factor in the

performance of the resulting supported catalyst or reagent in an organic reaction system[12]. The main factors that should be considered when employing a material as a support are

- Thermal and chemical stability during the reaction process and for batch reactions during the separation stage.
- Accessibility and good dispersion of the active sites.

1.3 Titania

Titanium is a chemical element in the periodic table that has the symbol Ti and atomic number 22. The element was given its name after the "Titans", the sons of the earth goddess in Greek mythology. It is a light, strong, lustrous, corrosion resistant (including resistance to sea water and chlorine) transition metal with a white-silvery-metallic colour. Titanium is used in strong light-weight alloys (most notably with iron and aluminium) and its most common compound, titanium dioxide is used in white pigments. Substances containing titanium are called titaniferous. It ranks 9th in the order of abundance among the elements present in the earth's crust and 4th most abundant structural unit. Titanium was discovered by the reverence William Gregor in 1791, who was interested in minerals. He recognized the presence of a new element, now known as titanium, in menachanite, a mineral named after menaccan in Cornwall (England). Several years later, the element was rediscovered in the ore rutile by a German chemist, Klaproth. The pure elemental metal was not made until 1910 by Matthew A. Hunter, who heated $TiCl_4$ together with sodium in a steel bomb at 700-800°C. Titanium is known for its rare combination of properties such as 'lighter than iron', 'stronger than

aluminium' and 'corrosion resistant as platinum' and has been called the wonder metal. Even traces of nonmetal impurities affect its physical properties[13,14]. Titanium dioxide does not occur in nature, but is derived from ilmenite or leuxocene ores. It is also readily mined in one of the purest forms, rutile beach sand. Since it falls group IV of the periodic table, it shows the characteristic valence of 4, but in addition to that di, tri and pentavalent valence states are reported in some compounds.

There are two allotropic forms and five naturally occurring isotopes of this element; Ti-46 through Ti-50 with Ti-48 being the most abundant (73.8%). One of titanium's most notable characteristics is that it is as strong as steel but is only 60% its weight. Titanium's properties are chemically and physically similar to zirconium.Titania is one of the top 20 inorganic chemicals of industrial importance. Although it is used in some non-pigmentary applications, the chemical and industrial interest in the oxides of titanium solely derives from the importance of dioxides as a white pigment in paints. It is due to its high opacity, relative chemical inertness and from the comparative abundance of titanium ores. The industrial use of titania has increased many folds recently in the field of its expanded applications as photochromic and photovoltaic sensors[15]. Titania acts as a photosensitiser for photovoltaic cells, and when used as an electrode coating in photoelectrolysis cells can enhance the efficiency of electrolytic splitting of water into hydrogen and oxygen. Because of its very high tensile strength (even at high temperatures), light weight, extraordinary corrosion resistance, and ability to withstand extreme temperatures, titanium alloys are principally used in aircraft, armour plating, naval ships, spacecraft and missiles. It is used in steel alloys to reduce grain

size and as a deoxidiser but in stainless steel it is employed to reduce carbon content. Titanium is often alloyed with aluminium (to refine grain size), vanadium, copper (to harden), iron, manganese, molybdenum and with other metals.Welded Titanium pipe is used in the chemical industry for its corrosion resistance and is growing its use in petroleum drilling especially offshore for its strength, light weight and corrosion resistance. Use of titanium in consumer products such as golf clubs, bicycles, laboratory equipment, wedding bands, and laptop computers is becoming more common.

Titanium dioxide is the most widely used white pigment (titanium white or pigment white 6) because of its brightness and very high refractive index, in which it is surpassed only by diamond. When deposited as a thin film, its refractive index and colour make it an excellent refractive optical coating for dielectric mirrors. The refractive index determines the opacity that the material confers to the matrix in which the pigment is housed. Hence, with its high refractive index, relatively low levels of titania pigment is required to achieve a white opaque coating. TiO_2 is also an effective opacifier[16] in powder form, where it is employed as a pigment to provide whiteness and opacity to products such as paints, coatings, plastics, papers, inks, foods and most toothpastes. In cosmetic and skin care products, titanium dioxide is used both as a pigment and a thickner, and in almost every sunblock with a physical blocker, titanium dioxide is found both because of its refractive index and its resistance to discoloration under ultraviolet light. This advantage enhances its stability and ability to protect the skin from ultraviolet light. Titanium is used as a white food dye and as a tattoo pigment. Paints made with titanium dioxide are excellent reflectors of infrared radiation and are therefore used extensively

by astronomers and in exterior paints. It is also used in cement, in gemstones, and as a strengthening filler in paper. TiO_2 powder is chemically inert, resists fading in sunlight, and is very opaque: this allows it to impart a pure and brilliant white colour to the brown or gray chemicals that form the majority of household plastics. Paint made with titanium dioxide does well in severe temperatures, is somewhat self-cleaning, and stands up to marine environments. Star sapphires and rubies get their asterism from the titanium dioxide present in them. Titanium dioxide is also used extensively in the handmade soap crafts as a colorant/pigment. Titanates are compounds made with titanium dioxide[17]. Barium titanate has piezoelectric properties, thus making it possible to use it as a transducer in the interconversion of sound and electricity.

Titanium dioxide is also used in resistance type lambda probes (a type of oxygen sensor). Even in mildly reducing atmospheres titania tends to lose oxygen and become sub stoichiometric. In this form the material becomes a semiconductor and the electrical resistivity of the material can be correlated to the oxygen content of the atmosphere to which it is exposed. Hence titania can be used to sense the amount of oxygen (or reducing species) present in an atmosphere[18]. The photocatalytic activity of titania results in thin coatings of the material exhibiting self cleaning and disinfecting properties under exposure to UV radiation. These properties make the material a candidate for applications such as medical devices, food preparation surfaces, air conditioning filters, and sanitaryware surfaces. Sol-gel produced titania gels induce the formation of apatite and the coatings have the ability to bond with bone i.e., titania gel coated implants are bioactive[19,20].

1.4 Crystalline Modifications of titania

Titania can exist in the crystalline as well as amorphous forms. The amorphous form of titania is photocatalytically inactive[21]. There are three crystalline forms of TiO_2; anatase, rutile and brookite. Anatase and rutile have been extensively studied for photocatalytic applications with the former found to be the most suitable for photocatalytic applications[22,23]. Brookite is not commonly available and has not been tested for photocatalysis. Rutile derives its name from the Latin *rutilus*, red, in reference to the deep red color observed in some specimens when viewed by transmitted light. Small rutile needles present in gems are responsible for "star" sapphires, "star" rubies and other "star" gems, an optical phenomenon known as asterism. It was on account of the steeper pyramid of anatase that the mineral was named, by RJ Haüy in 1801, from the Greek *anatasis*, "extension," the vertical axis of the crystals being longer than in rutile. Another name commonly in use for this mineral is octahedrite, a name which, indeed, is earlier than anatase, and given because of the common (acute) octahedral habit of the crystals. Brookite was named for Henry James Brooke, English mineralogist.

Anatase and rutile are both tetragonal in structure while the brookite structure is orthorhombic. Anatase is obtained in processes under kinetic control whereas processes involving Ostwald ripening lead to the equilibrim phase; ie, rutile. In case of all the crystalline forms, each of Ti^{4+} ions are surrounded by an irregular octahedron of oxide ions, but the number of edges shared by the octahedral increases from two in rutile to three in brookite and to four in anatase. Both in rutile and anatase the six oxide ions surrounding the Ti^{4+} ions can be grouped into two. The two oxygen atoms are farthest from Ti^{4+}

and the other four oxide ions are relatively closer to Ti^{4+}. In rutile these distances are 2.01A° and 1.92A° respectively and in the anatase they are 1.95A° and 1.91A°. In case of brookite the farthest oxide ions are only ones, which are equidistant from Ti^{4+} ions.

All the three forms consist of TiO_6^{2-} octahedral and the manner by which these octahedral bond to each other are different for anatase, rutile and brookite. In rutile, two (out of twelve) edges are shared forming a linear chain. If each titanium octahedral was represented by a building block[24], then the basic structural unit of rutile can be represented as in figure 1.1. For rutile, the linear chains are then joined to each other by the sharing of corner oxygen atoms, producing the overall rutile structure. Any spatial effect beneficial to the edge sharing polycondensation between TiO_6^{2-} octahedra results in the rutile phase formation.
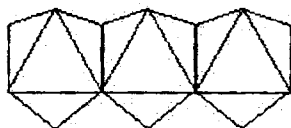
Figure 1.1 The fundamental structural unit of rutile

Anatase has four edges shared per octahedron and no corner oxygen sharing. The basic growth units possible for anatase are shown in figure 1.2[25]. This figure shows (a) two edges are shared per octahedron forming a right angled configuration and (b) the third and fourth edges are shared into and out of adjacent layers. Effectively the arrangement of these octahedra gives the overall structure of anatase. The complete structure of both anatase and rutile has been thus described[26].
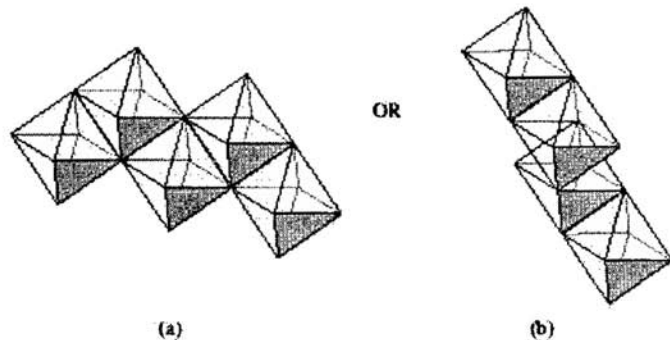
Figure 1.2 The fundamental structural units of anatase

The octahedral linkage in brookite is such that three edges are shared per octahedron[27]. The basic unit structure of brookite formed by TiO_6^{2-} octahedra is shown in figure 1.3.
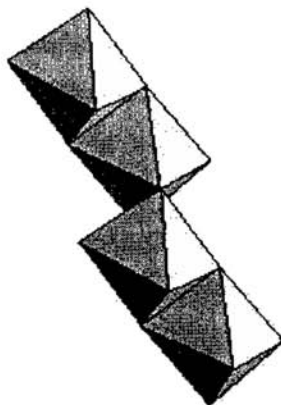
Figure 1.3 The fundamental structural units of brookite

Table 1.1

A comparative study of physical characteristics of different crystalline modifications of Titania

Physical Characteristics	Anatase	Rutile	Brookite
Colour	Brown to black Also yellow and blue	Black or reddish brown in large thick crystals	Dark brown to greenish
Luster	Adamantine to submetallic	Adamantine to Submetallic	Adamantine to Submetallic
Transparency	Opaque crystals	Transparent in thin crystals	Opaque crystals
Crystal System	Tetragonal 4/m 2/m 2/m	Tetragonal; 4/m 2/m 2/m	Orthorhombic 2/m 2/m 2/m
Fracture	Subconchoidal	Conchoidal to uneven	Subconchoidal and uneven
Hardness	5 – 6	6 - 6.5	5.5 - 6
Specific gravity	3.8 – 4.1	4.2 + (slightly heavy)	3.9 – 4.1
Streak	White	Brown	Light brown to white

1.5 Anatase to Rutile transformation

Usually, amorphous titania crystallizes into anatase below 400°C, which is further converted to rutile from 600°C to 1100°C[28]. The anatase to rutile transformation is a metastable to stable transformation and therefore

there is no unique phase transformation temperature as in the case of equilibrium reversible transformation[29]. The rates of transformation largely depend on the particle size or the size of impurities[30]. The temperature for the transition can vary from 400 to 1100°C depending on the type and amount of additives, powder preparation method, reaction atmosphere, oxygen to metal coordination, particle size, morphology, degree of agglomeration and so on. At atmospheric pressure, the transformation is time and temperature dependent and is also a function of impurity concentration[31-39].

The complexity of the transition is typically attributed to the reconstructing nature. The transition is a nucleation growth process and follows the first order rate law with an activation energy of ~90Kcal/mol. The mechanism by which the additives either inhibit or promote the anatase to rutile phase transformation has been related to the defect structure of titania, i.e, the concentration of oxygen vacancies or Ti interstitials. It was suggested that the additives, which increases the concentration of oxygen vacancies would also tend to promote the transformation, while some additives would retard the transformation by increasing the lattice defect concentration of Ti interstitials in titania[40].

The mechanism for the formation of anatase and rutile using sol-gel route has been well described in the literature[41, 42]. In solution, two octahedra undergo condensation to form a new bond. (Figure 1.4a) The placement of the third octahedron determines the formation of either rutile (Figure 1.4b) or anatase/brookite (Figure 1.4c,d). The first option (Figure 1.4b) occurs when the titania octahedra forms a bond such that a linear arrangement results. The linear arrangement is the most stable structure since the electrostatic repulsive

energy is minimized, thus thermodynamically; the basic structure of rutile is favored. The second option (Figure 1.4c) occurs when the octahedrons bond together at right angles to give the basic unit structure for anatase. The third option is possible when the octahedron edges share a bond as shown in Figure 1.4d. This option is the basic growth unit for both anatase and brookite.
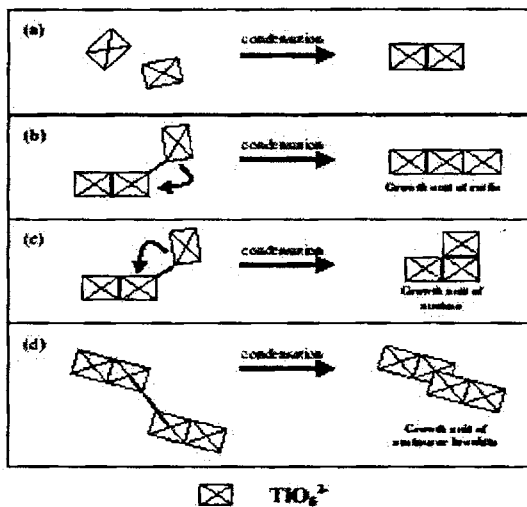
Figure 1.4 (a) Condensation of two octahedra, (b) growth unit of rutile,
(c) growth unit of anatase and (d) growth unit of anatase and brookite

As the brookite and anatase octahedra bonds involve edge sharing, the chances of interaction to form these two configurations (Figure 1.4c,d) are increased as the reaction temperature increases. The higher energy upon collision at 90°C enables the third octahedron to overcome the electrostatic repulsion and form either anatase or brookite. Anatase is more likely to occur than brookite since it can be formed by either of the two pathways.

1.6 Methods of Preparation

The development and preparation of heterogeneous catalysts were considered more as alchemy, than science, with the predominance of trial and error experiments[43-45]. However this approach is time consuming, expensive, does not offer on the assurances of the final results and discourages osmosis between catalysis and other related sciences, such as analytical or solid state chemistry, spectroscopy etc. The preparation methods of catalysts have been reported to directly affect the activity of the mixed oxide systems[46-48]. Thus it is not surprising that catalysis follow a solitary route up until the 1970's, when the idea of scientific bases for the preparation of catalysts began to develop. A brief outline of some of the commonly adopted preparation routes are discussed herewith.

a) Precipitation or coprecipitation - It is one of the most widely employed preparation methods and may be used to prepare either single component catalysts and supports or mixed catalysts. In this method, one or more soluble salts, which contain the metal of interest, are neutralized through the addition of a base to form a precipitate or coprecipitate of the corresponding metal oxides[49-50].

b) Impregnation – In this method, a certain volume of solution containing the precursor of the active phase is contacted with the solid support, which, in a subsequent step, is dried to remove the imbibed solvent. The maximum loading is limited by the solubility of the precursor in the solution. The operating variable is the temperature, which

influences both the precursor solubility, solution viscosity and as a consequence the wetting time[51-52].

c) Ion Exchange – This method consists of replacing an ion in an electrostatic interaction with the surface of a support by another ion species. Catalyst systems, which need a charge compensating ions, are ideal materials for ion exchange. It is important to adjust the pH in order to maximize electronic interaction between the support and the metal precursor[53].

d) Deposition-Precipitation– The two processes involved in this method are precipitation from bulk solutions or from pore fluids and interaction with the support surface. This method allows the preparation of catalyst with smaller particle sizes in better dispersion with large surface area and allows incorporation of higher loading of the active components[54].

e) Adsorption – This method allows the controlled anchorage of a precursor in an aqueous solution on the support. The term adsorption is used to describe all processes where ionic species are attracted electrostatically by charged sites on a solid surface.

f) Chemical vapour deposition - In chemical vapour deposition (CVD), deposition is taking place by adsorption or reaction from the gas phase[55-57]. It is a very versatile process for the production of catalytic materials and is possible to deposit target species on the materials with almost any shape and size and it is also possible to produce almost any metal and nonmetallic material as well as compounds such as oxides, carbides, nitrides, intermetallics and many others.

g) Sol-gel process – It is a homogeneous process, which results in a continuous transformation of a solution into a hydrated solid precursor (hydrogel). The nanoscale chemistry involved in sol-gel methods is a more direct way to prepare highly divided materials. These particles continue to increase in size until a metal oxide gel is formed[58-64].

1.7 The beginning of sol-gel science

Sol-gel processing methods were first used historically for decorative and constructional materials. Many of the earlier technologies became lost in the Dark ages after the decline of the Roman Empire, and probably the next significant development was the discovery of "water glass" by Von Helmont. He dissolved silicate materials in alkali and found that on acidificaton a precipitate of silica equal in weight to the original silicate materials was obtained. In 1779 Bergman reported that if the correct amount of dilute acid was used the mixture gelled on acidification. This preparation of a silica gel led to a series of applications remarkably similar to those of today's s sol-gel chemistry. In the 19th century, many oxide materials like zirconia, copper zirconate, uranium oxide, and zirconopyrophyllate were prepared from hydroxide gels. Today sol-gel methods are reaching their full potential, enabling the preparation of new generations of advanced materials not easily accessible by other methods yet using, mild, low energy conditions[65].

1.8 Sol-gel Processing

A colloid is a suspension in which the dispersed phase is so small (~1-1000nm) that gravitational forces are negligible and interactions are dominated

by short range forces such as van der waal's attractions and surface charges. The inertia of dispersed phase is so small that it exhibits Brownian movement, a random walk driven by momentum imparted by collisions with molecules of the suspending medium. A sol is a colloidal suspension of solid particles in liquid[66].

Sol-gel process can be classified based on the starting materials. The commonly used routes are the colloidal sol-gel and polymeric sol-gel depending on whether the precursor is a metal organic compound or an aqueous solution of an inorganic salt[67]. In both cases, the chemistry is dominated by the high electropositive character of metal atoms. Another important factor is the greater ability to vary their coordination number and geometry depending on the size and charge of the ion, the number of d-electrons, the crystal field stabilization energy and the nature of the surrounding electrons[65]. Most of the synthetic schemes reported are based on the use of alkoxide precursors. Alkoxides of many individual metals are available commercially and can be manipulated easily to control the chemistry of the process[68-69]. The chemical basis for the sol-gel route is similar to the well known polymerization process.

Colloidal sol-gel route involves a precipitation-peptisation process[70]. Addition of water precipitates the corresponding hydroxides, which is washed and subsequently peptized by adding electrolytes such as HCl/HNO_3 to obtain the respective sol. Further processes for obtaining titania xerogels include sol-gel conversion, drying of the corresponding gel. Thus obtained porous xerogel is calcined to get the catalyst powder. The particle size of the sol can be affected by the type and amount of acid employed as a peptizing agent and also

by the time in the hydrolysis process[71]. One fundamental difference between the colloidal and the polymeric gel is that in colloidal gel, the sol-gel transition being caused by physicochemical effect without the creation of a new chemical bonding in contrast to a chemical reaction, a polymerization or a polycondensation reaction as in the case of a polymeric gel.

If a monomer can make more than two bonds, then there is no limit on the size of the molecule that can form. If one molecule can reach its macroscopic dimensions so that it extends throughout the solution, the substance is said to be a gel. The gel point is the time (or degree of the reaction) at which the last bond is formed that completes this giant molecule. Thus, a gel is a substance that contains a continuous solid skeleton enclosing a continuous liquid phase. The continuity of the solid structure gives the elasticity to the gel. Gels can also be formed from particulate sols, when attractive dispersion forces cause them to stick together in such a way as to form a network. The characteristic feature of the gel is obviously not the type of bonding; polymeric gels are covalently linked, particulate gels are established by van der Waals forces. The bonds may be reversible as in the particulate systems or permanent as in polymeric gels. The particulate systems include some of the most successful commercial applications of sol-gel technology, such as nuclear fuel pellets and Ludox colloidal silica[66]. In some cases, inorganic polymers are combined with colloidal particles to great advantage. Key parameters which are in principle controllable via sol-gel processing of the catalyst materials are as follows[65].

« High specific surface area.

« Controlled pore size distribution.

«   Stable pore structure under preparation and reaction conditions.

«   Active material distributed on pore surfaces, not in the bulk.

«   Active material homogeneously and effectively distributed over surface.

«   High purity of active material.

«   Easy control of composition for multi component catalytic species.

«   Effective control of crystalline or amorphous structure as desired.

«   Mechanical properties adapted to desired operating environment.

«   Catalyst resistant to chemical or physical blocking of active sites.

1.9 Stability of Sols

The stability and coagulation of sols is the most intensively studied aspects of colloidal chemistry. Sols can be stabilized either electrostaically or sterically. In steric stabilization, coagulation is prevented by use of thick adsorbed layer of organic molecules, which constitute a steric barrier. Thus it discourages the close approach of the particles entropically as well as enthalpically.

Usually aqueous systems are stabilized by electrostatic double layer. Since the electrons surrounding a nucleus do not constitute a spatially and temporally uniform screen, every atom is a fluctuating dipole. This effect creates an attraction between atoms, known as van der Waal's or dispersion energy, which is proportional to the polarizabilities of atoms and inversely proportional to the sixth power of their separation. The van der Waal's forces result from three types of interactions; permanent dipole - permanent dipole (keesom forces), permanent dipole- induced dipole (Debye forces), and

transitory dipole -transitory dipole (London forces). When atoms are far apart, the movement of their electrons is uncorrelated, but upon closer approach the electrons will distribute so as to minimize the energy of the system. The transitory dipoles formed in this way produce net attraction, although the net permanent dipole moment is zero. These dipoles fluctuate with a period of ~ 10^{-16}s; thus if the atoms are separated by a distance greater than ~30nm, by the time the electromagnetic wave travels from one atom to the another, the electron distribution of the first atom has changed. This is called the retardation of the dispersion forces, and results in reduced attraction; only the unretarded forces are of importance in colloids.

The attractive dispersion forces is approximately additive, so that it becomes important for particles of colloidal dimension, and represents the attractive forces tending to cause flocculation of colloids. The stabilization of colloids by electrostatic repulsion is successfully described by the DLVO theory (named after its principal creators, Derjaguin, Landau, Verwey and Overbeek). The net forces between the particles in suspension is assumed to be the sum of the attractive van der Waal's forces and the electrostatic repulsion created by the charges adsorbed on the particles. The repulsive barrier depends on the two types of ions that make up the double layer; charge determining ions that control the charge of ion on the surface of the particle and counter ions that are in solution in the vicinity of the particle and act to screen the charges of the potential determining ions[66].

For hydrous oxides, the charge determining ions are the H^+ and OH^- ions, which establish charge on the particles by protonating or deprotonating the MOH bonds on the surface of the particles.

$$M\text{-}OH + H^+ \quad M\text{-}OH_2^+$$

$$M\text{-}OH + OH^- \quad M\text{-}O^- + H_2O$$
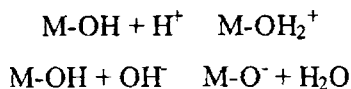
The ease with which protons are added or removed from the oxide depends on the nature of the metal atom. The pH at which the particle is neutrally charged is called the point of zero charge. At pH>PZC, the particle is negatively charged, whereas at pH<PZC, the particle becomes positively charged. The point of zero charge for titania is 6 while that of silica is 2.5.

1.10 Advantages of sol-gel process

 ✎ The temperature required for all stages apart from densification are low, frequently close to room temperature. Thus thermal degradation of both the material itself and any entrapped species is minimized, and high purity and stoichiometry can be achieved.

 ✎ Precursors such as metal alkoxides and mixed alkyl/ alkoxides are frequently volatile and easily purified to very high levels (e.g., by distillation or sublimation) using techniques developed for the microelectronics industry. This further contributes to high purity products.

 ✎ Since organometallic precursors involving different metals are frequently miscible, homogeneous controlled doping is easy to achieve.

 ✎ The chemical conditions are mild. Hydrolysis and condensation are catalyzed by acids and bases, but extreme pH conditions may easily be avoided, especially by the use of "two step" methods in which acid catalyzed hydrolysis is followed by rapid neutralization or buffering. In this way pH sensitive organic species (e.g. dyes) and even biological

species including enzymes and whole cells may be entrapped and still retain their functions.

✥ Highly porous materials and nanocrystalline materials may be prepared in this way.

✥ By appropriate chemical modification of the precursors, control may be achieved over the rates of hydrolysis and condensation, and over colloid particle size and the pore size, porosity and pore wall chemistry of the final material.

✥ Using functionalised precursors, covalent attachment of organic and biological species to porous silicate glass structures is possible.

✥ By controlling the ageing and drying conditions, further pore size and mechanical strength control may be achieved.

✥ By using organometallic precursors containing polymerisable organic ligands, materials may be produced which contain both inorganic and organic polymer networks.

✥ Entrapped organic species may serve as templates for creation of pores with controlled size and shape. Subsequent removal of these species (for example by heat or strong acid treatment) leaves "molecular footprints" with potential as catalytic sites.

✥ Since liquid precursors are used i is possible to cast ceramic materials in a range of complex shapes and to produce thin films or fibres as well as monoliths without the need for machining or melting.

✥ The optical quality of the materials is often good, leading to applications for optical components.

✎ The low temperature of sol-gel process is generally below the crystallization temperature for oxide materials, and this allows the production of unusual amorphous materials[65-66].

1.11 Limitations Of Sol-Gel Process

Despite all these advantages, sol-gel materials are not without limitations. The precursors are often expensive and sensitive to moisture, limiting large scale production plants to specialized applications such as optical coatings. The process is also time consuming particularly where careful ageing and drying are required. Although this need not be a limiting factor where long continuous production runs are envisaged, it does mean that the total volume of material in the processing line is inevitably significantly higher than in faster processes. Finally the problem of dimensional change on densification, and of shrinkage and stress cracking on drying, although not insuperable, do require careful attention. These significant limitations emphasize the need to optimize the sol-gel materials to exploit their advantages to the maximum in applications where they can provide properties not attainable by other methods[65-66].

1.12 Tungsten, Molybdenum and Chromium based catalysts

The interactions between metal oxides and the oxide supports have attracted much attention because of the wide application of the supported metal oxide systems. It is well known that the supported oxides of transition metals are widely used as catalysts for various reactions. The industrial importance of supported chromium oxide catalysts has motivated a large number of studies

relating to its specific surface properties and catalytic behaviour. Oxide–oxide interactions are considered as a separate group of phenomena occurring at the catalyst surface during the stages of both preparation and use[73]. With the advancements of the physico chemical techniques in the recent years a detailed characterizations of these systems are being carried out to understand the true picture of the chemical and molecular states of chromia stabilized over various supports and results are well documented in the literature [74-81]. Although these systems are extensively studied, there are still some points of disagreements about the surface structures of chromium oxide species stabilized on various supports and about the true nature of these species in various catalytic processes[82]. These systems find their applications in polymerization reactions, and many catalyzed reactions such as dehydrogenation of alkanes, dehydrocyclisation, catalytic reforming, hydrodesulphurisation and partial oxidation of hydrocarbons.

Molybdenum supported catalysts constitutes the most important catalysts for petroleum hydrotreating. These catalysts are used mainly to saturate unsaturated hydrocarbons to remove sulphur, nitrogen, oxygen and other metals from different petroleum streams[82-86]. In many reactions catalyzed by molybdenum oxide, the active component is often employed on supported oxide, viz, alumina, titania and silica or mixed with oxides such as vanadium. It is well established that the efficiency of the supported molybdenum oxide catalysts mainly depend on the dispersion of active phase which in turn can be greatly influenced by the nature of the supported oxide and the method of the preparation of the catalysts[87]. Titania supported molybdenum represents the basic form of catalysts in many hydrotreating reactions. Presently partial

oxidation of methane, vapour phase ammoxidation of toluene, water gas shift reaction and photocatalytic degradation of organic compounds in aqueous systems are also highly performed on the Mo/TiO_2 catalysts[88-91]. Supported tungsten oxides catalyzing different reactions such as WO_3/Al_2O_3 for propene metathesis, WO_3/SiO_2 for olefin disproportionation and WO_3/Fe_2O_3 for the reduction of NO_x in combustion flue gases. Titania supported tungsten oxide catalysts are very efficient for various heterogeneous reactions such as alkene isomerisation and disproportionation. Acid properties of tungsten-based catalysts have also been employed to improve alkane isomerisation, a very important step in the synthesis of high octane rating phenol[92-95]. The properties of bulk tungsten oxides were studied in hexane reforming[96-97] and heptane hydrocracking[98]. It has been reported that platinum containing WO_x/TiO_2 catalyze the conversion of n-butane and of n-pentane[99].

1.13 Rare Earth metals based catalysts

Rare earths or rare earth related compounds have a significant role to play in materials science and technology due to their splendid and exotic properties[100-104]. During the last few years, much endeavour has been undertaken in order to understand the phenomenon that underlies the catalytic behaviour of multicomponent and multiphase oxide-based heterogeneous catalysts. Most have been especially interested in the systems containing lanthanide oxides, such as La_2O_3, Pr_6O_{11}, CeO_2, Tb_4O_7, Nd_2O_3 and Sm_2O_3, because pertinent information on the real role played by these in partial as well as total oxidation is still rather scarce[105-111]. Rare earth oxides can be classified

as solid base catalysts on the basis of ^{18}O binding energy studies. They exhibit activity as oxidation catalysts and have low work functions.

1.14 Titania as a catalyst and catalyst support

Titania presents increasing interest as a catalyst or support. However its low surface area is an important disadvantage for catalytic applications[112-114]. This has been partially overcome by the application of new synthesis procedures in order to obtain titania with a high specific surface area[115-117]. Nevertheless for many applications, supported oxides are more efficient and therefore titania supported catalysts are also interesting as a catalyst as well as a support. It is well known that the synthesis conditions determine to a great extent morphological characteristics such as homogeneity, size and distribution of pores[118].Similarly the dispersion, the oxidation state and the structural features of the supported species may strongly depend on the support.

Each application that is based on titania requires a specific crystal structure and specific size. Thus it is important to develop synthetic methods in which the size and structure of the nanocrystals can be controlled. Anatase titania has been prepared by various methods such as sol-gel, hydrothermal, combustion synthesis, vapor hydrolysis and inert gas condensation. Anatase titania powders can also be prepared from fluorine complexed titanium (IV) aqueous solution using microwave irradiation[119]. But the obtained materials do not show photocatalytic activity, probably due to a considerable fluoride content that is in the range of 2-5%. TiO_2 nanotubes and nanorods were synthesized by the sol-gel template method. Titania sol with narrow particle size distribution was synthesized using $TiCl_4$ as the starting material[120].

Nanocrystalline anatase powders with particle sizes from 8 to 38nm have been synthesized by hydrothermal treatment of aqueous $TiOSO_4$ solutions and TiO_2–nH_2O amorphous gel[121]. Anatase nanocrystallites of about 7nm in diameter can be prepared from titanyl sulphate in alcohol-water solutions below 100°C[122]. It has been reported that nanosize rutile titania particle can be synthesized via a hydrothermal method without mineralizers[123]. Cheng Wang *et al* synthesized a mixture of nanocrystalline anatase and rutile in mixed organic media with the variation of alcohols in the media under mild conditions[124].

The porous anatase form, as compared to the rutile phase, is of greater importance and interest due to its better catalytic properties. Therefore, a key goal is to prepare anatase nanoparticles, with high surface area, uniform particle size and pore structure, and a high anatase–rutile transformation temperature[125]. Phonthammachi *et al* reported the synthesis of mesoporous titania by sol-gel route using titanium glycolate as precursor[126]. Nanocrystalline powders of anatase and rutile type of titania with different morphology and particle size 13–50 nm were prepared by a hydrothermal treatment of complex titanyl oxalate acid $H_2TiO(C_2O_4)_2$ (0.28 and 0.07 M) aqueous solutions[127]. Under the conditions of high temperature hydrolysis of 0.28 M $H_2TiO(C_2O_4)_2$ aqueous solution, the formation of mesoporous anatase particles (60–100 nm, TEM) containing non-intersecting (7–27 nm, TEM) pores with encapsulated solution was observed while hydrothermal treatment of 0.07 M aqueous solutions did not lead to the formation of mesoporous TiO_2. The formation mechanism of mesoporous anatase particles was suggested considering the process as recrystallization of primary grains aggregates.

Titania particles were prepared by water in oil emulsion system, where titanium tetraisopropoxide was dropped into the microemulsion solution and the titania particles were formed by the hydrolysis reaction in the core of the microemulsion[128]. In yet another method, titania sols, gels and nanopowders have been produced by the controlled hydrolysis of tetraisopropyl titanate in sodium bis (2-ethylhexyl) sulfosuccinate reverse micelles[129]. Ku Yuan Chen *et al* synthesized titania by the thermal hydrolysis of titanium tetrachloride in a mixed solvent (acetone/water)[130]. Titanium dioxide nanoparticles were prepared via a photoassisted sol-gel method in which ultraviolet light radiation was used in the preparation process of TiO_2 colloid[131]. A simple and efficient methodology has been established for the selective synthesis of anatase and rutile as well as their mixtures with various precursors using ultrasound irradiation[132]. Titania gel and films were prepared from Ti-EDTA complex solutions as new ceramic precursors[133]. Similarly, porous titania coatings were prepared by spin coating anhydrous titanium ethoxide – ethanol solutions in a controlled humidity atmosphere[134].

Yinghong *et al* synthesized a thermally stable mesoporous titania with a crystalline frame work and ordered large pores using a block copolymer as a structure directing agent, followed by a hydrothermal process[135]. The crystalline frame work, high specific surface area, large pore size and high thermal stability of these new materials are expected to afford better activity towards photocatalytic reactions, in particular those concerned with bulky molecules and high space velocity. Kartini *et al* reported a new route to the synthesis of mesoporous titania with full anatase crystalline domains using a block copolymer surfactant[136]. Mesoporous titania with regulated pore size as

well as high specific surface area was prepared from titanium alkoxide and various carboxylic acids with different alkyl chain lengths[137].

TiO$_2$ materials are having complex shapes such as hollow fibres, wools, textiles and nanotubes. This technique has great potential for a wide variety of applications such as catalysts, photocatalysts and filters, because tailored hierarchical architectures of titania with macroscopic morphologies and microscopic pore structures are successfully produced. Monodisperse hollow nanocylinders consisting of crystalline titania particles have been directly prepared in a porous alumina membrane by a deposition technique using an aqueous solution system of titanium tetraflouride[138]. The morphology transcription of various templates using a direct growth technique in aqueous solutions provided crystalline titania. Titania hollow fibers with porous walls were prepared by a chemical solution deposition techniques using TiF$_4$ aqueous solution[139,140]. Bimodal mesoporous titania powders with high photocatalytic activity were prepared by hydrolysis of titanium tetraisopropoxide in the presence of HCl/HNO$_3$ or NH$_4$OH under ultrasonic irradiation[141].

1.15 Modified titania systems

The most widely used industrial catalysts consist of metal oxide particles. Titania is well known for its catalytic applications. Over decades, many studies have been carried out in order to modify the structural as well as textural properties of titania. The properties of titania can be modified by doping with various metal oxides. Modification of the single oxides with different anions like PO$_4^{3-}$, WO$_4^{2-}$, F$^-$, SO$_4^{2-}$ etc[142-148]. have been found to enhance the acidity and certain physico chemical properties of the catalyst like

thermal stability, mesoporosity etc. However the textural properties of these anion modified metal oxides are very poor. The ageing time and temperature can be used as new parameters to modify the textural properties of titania aerogels[149].

It has been reported that silica addition has a significant influence on the surface properties of titania[150-156]. There is an enrichment in the reactivity with respect to Bronsted acid in the titania-silica mixed oxide system. The addition of silica increases the specific surface area of titania and also increases the anatase-rutile transformation, and was found to increase with the increase in silica. Silica addition to titania results in high temperature pore stability[157]. High surface area TiO_2 $-Al_2O_3$ were found to have higher surface area, greater porosity and enhanced specific surface acidity[158-161]. Copper loaded titania systems are prepared and their structural characterization suggest negligible interaction of copper cluster with the titania support[162]. Nano á-Fe_2O_3 in a titania matrix was prepared by the sol-gel route and the crystallographic data shows the presence of anatase and rutile[163-166]. The structural modification of titania using lanthana and Yttria is also repoertd [167-169]. Neodymium doped titania nanostructured thin films help promoting the electron trapping, thereby increasing the lifetime of holes, which are responsible for the photocatalytic oxidation[170-173]. The properties of titania can also be modified by doping with oxides like V_2O_5[174], SnO_2[175], MgO[176], ZrO_2[177-178], PtO_2[179-180], WO_3[181], Cr_2O_3[182-183] etc. Jong Ho Lee *et al* prepared $ZnO-TiO_2$, $CdS-TiO_2$, $ZnS-TiO_2$, and $Ag-TiO_2$ by ultrasonic spray pyrolysis of metal salt aqueous solution in which TiO_2 particles were suspended[184]. The effect of metal cations like Li,Rb[185], Ca,Sr, Ba[186],Mo[187],Pt[188], Ta[189], In[190],

Ag^{191}, Co^{192} etc. on the crystalline phase stability of titania has also been successfully carried out. Recently much attention is paid to the applications of nitrogen doped titania[193-195].

1.16 Surface Acidity Measurements

The acid-base properties of metal oxide catalysts can significantly affect the final selectivity of heterogeneous catalysts[196]. The surface acidity of the catalysts is closely related to the activity, selectivity and stability of solid acids. The acidity required for transformation of reactants into valuable products or byproducts can be quite different[197]. Solid acid catalysts are appealing since the nature of surface acid sites are known and their chemical behaviour in acid catalyzed reactions can be rationalized by means of existing theories and models. The dependence of catalytic properties on the acid properties of solid catalysts demand accurate methods for surface acidity measurements[198].

Various methods have been used to determine the nature, strength and the concentration of acid centers on the surface. The indicator method is used as a method for the determination of acid sites, but it suffers from the disadvantage that both Bronsted and Lewis acidity are measured without any distinction[199-200]. Though this method is successful in the case of homogeneous aqueous solutions of acids, it fails in the case of heterogeneous solids.

Temperature programmed desorption of base molecules is based on desorbing volatile amines such as ammonia, pyridine, n-butyl amine or quinoline that has been allowed to absorb on a solid, by heating it at a programmed rate. This simple and inexpensive method is normally used to

measure the number and strength of acid sites on solid catalysts[201-202]. An excess of the base is adsorbed, and what is considered to be physically adsorbed is then removed by prolonged evacuation. Whatever left on the surface, after this is a measure of total acid sites. The TPD of ammonia is used frequently as a probe molecule because of its small molecular size, stability and strong basic strength. The method is thus used to characterize the acid site distribution and further to obtain the quantitative amounts of acid sites in the specified temperature range[203]. Since ammonia and pyridine can adsorb both on Bronsted and Lewis acid sites, the selective determination of acid sites is impossible in this technique. However 2,6-dimethyl pyridine (2,6-DMP) can be preferentially adsorbed on the Bronsted acid sites[204-206]. So, to estimate the Bronsted acidity, DMPY is used as the adsorbent molecule.

1.17 Test Reactions for Acidity

The acidity of a catalyst can also be determined by using appropriate test reactions. The most widely used examples include decomposition of alcohols[207-208], cracking of aromatic hydrocarbons[209] and isomerisation of alkenes[210]. Cumene is a conventional model compound for catalytic studies because it undergoes different types of reactions over different types of active sites. Over Bronsted acid sites, however cumene is cracked to benzene (plus propene) via a carbon cation mechanism[211]. Over dehydrogenation sites, however cumene is converted to á-methyl styrene. The production of other products like ethyl benzene and toluene is minimal. Selectivity in the alcohol decomposition reaction is regarded as a typical test reaction for investigating the acid base properties of the catalytic sites on the metal oxides[212-213].

Although the mechanism of gas phase alcohol dehydration/dehydrogenation remains poorly known and controversial[214-216], it is generally accepted that the highest activities in the dehydration to cyclohexene are related to acid sites, while dehydrogenation to cyclohexanone is generally associated to basic/redox sites[214-222].

Boorman *et al* studied the surface acidity of fluoride, cobalt and molybdenum modified ã-alumina systems by infrared spectroscopy of adsorbed pyridine and correlated with the reactivity for cumene conversion[223]. The acidic and catalytic properties of alumina as well as fluoride and sodium modified alumina were also characterized by FTIR spectroscopy of adsorbed pyridine and t-butyl cyanide, and by cumene and thiophene decomposition[224]. Redox and catalytic behaviour of chromium oxide supported on zirconia is investigated in detail through the reaction of cumene using a pulse technique[225]. It has been known that cracking of cumene takes place at medium acid sites of the catalyst while the active site for the dehydrogenation of cumene is Cr^{3+}.

The surface acid strength of sulphate doped titania-silica mixed oxide is determined by the Hammett indicator methods. A good correlation is found between the cumene cracking and the acidity of the catalysts[226]. The correlation between the acidic properties of nickel supported on titania-zirconia and catalytic activity for acid catalysis is also studied[227]. Rana *et al* carried out the cumene cracking reaction on pure support as well as sulfided Mo, CoMo and NiMo catalysts in a plug flow microreactor at 400°C and atmospheric pressure and arrived at the conclusion that the cumene cracking activity over supported catalysts is attributed to the Bronsted sites like sulfhydryl groups[228].

Liu *et al* studied the acidity for catalytic cumene cracking reaction in the assembly of wormhole aluminosilicate mesostructures from zeolite seeds[229]. The surface acidity diagnosis and catalytic activity of AISBA materials is done by TPD of ammonia and in the cumene cracking reaction[230]. The role of various additives and their impregnation sequence in flourided Ni-Mo/Al₂O₃ catalysts in cumene cracking and hydrocracking and in thiophene HDS reaction has been investigated[231]. Fleisch *et al* studied the hydrothermal dealumination of Faujasite and the influence of dealumination in the cumene cracking reaction[232]. The realumination efficiency of dealuminated HZSM-5 zeolites was studied, evaluating the change in the cracking activity of cumene[233]. Landau *et al* synthesized the alumina catalytic material prepared by grafting wide pore MCM-41 with an alumina multilayer and characterized its surface acidity in cumene cracking and isopropanol dehydration[234].

A comparative study of physical, acidic and catalytic properties of pillared clays, transition metal pillared clays and pillared acid activated clays are carried out. The obtained improvement in acidity is mainly of the Bronsted type, which is very clear from both cyclohexanol decomposition and cumene cracking reaction[235-236]. Bautista *et al* studied the influence of acid base properties of amorphous AlPO₄ and several inorganic solids in the gas phase dehydration and dehydrogenation of cyclohexanol[237]. The cyclohexanol decomposition reaction is also carried out effectively over copper containing spinel catalysts[238] and alumina supported Pt-Co bimetallic catalysts[239]. Anita Rachel *et al* evaluated the acid base properties of CuO/ZrO₂ catalysts in the dehydrogenation of cyclohexanol[240]. The effect of copper loading on zirconia in the dehydrogenation activity is illustrated. The dehydration of cyclohexanol

over zeolites, silicaaluminophosphates and chromite catalysts is carried out and observed the presence of acidic and basic centers of probably different strengths[241].

1.18 Reactions selected for the present study

Among various catalysts in use, acid catalysts account for a majority of applications both in terms of volume and economy. The catalytic role of solid acids is very clear from all the investigated reactions. Since the incorporation of transition metal and rare earth metal in the crystalline framework of titania improves its structural as well as textural characteristics, the prepared systems can be used as a versatile catalyst for organic transformations. Titania, being a catalyst as well as a photocatalyst our study is focusing the reactions in both categories. The catalytic reactions like epoxidation of cyclohexene, hydroxylation of phenol, tert-butylation of phenol, methylation of aniline as well as anisole, dehydrogenation of cyclohexane and cyclohexene were carried out. The photocatalytic degradation of methyl orange as well as photooxidation of benzhydrol is successfully carried out over the prepared systems.

1.19 Objectives of the present work

- ∞ To prepare titania, transition metal as well as rare earth metal incorporated titania catalysts through particulate sol-gel route.
- ∞ To investigate the surface properties of the prepared systems by techniques such as XRD, TG/DTG, FTIR, SEM, UV-Vis DRS and BET surface area-pore volume measurements.

ଔ To explore the surface acidic properties of the prepared catalysts using various independent techniques such as TPD of ammonia, TG analysis of adsorbed 2,6-DMP and test reactions like cumene cracking and cyclohexanol decomposition.

ଔ To study the catalytic activity of the systems towards liquid phase epoxidation of cyclohexene as well as hydroxylation of phenol.

ଔ To study the catalytic activity of the prepared systems in the industrially important alkylation reactions such as tert-butylation of phenol, methylation of aniline and anisole.

ଔ To evaluate the catalytic activity of the prepared systems towards the dehydrogenation of cyclohexane and cyclohexene.

ଔ To explore the photocatalytic activity of the prepared systems towards the photooxidation of benzhydrol and methyl orange degradation.

References

1   R. Larsson, "Perspectives in Catalysis in Commemoration of Jons Jacob Berzelius", CWK Gleerup (1981).

2   J. Berzelius, "Jahres-Bericht uber die Fortschritte der Physichen Wissenschaffen", Tubingen, 15 (1836).

3   Fransisco Zaera, J. Phys. Chem. B, 106 (2002) 4043.

4   M.A. Keane, J. Mat. Sci, 38 (2001) 4661.

5   J.H. Clark, C.N. Rhodes, RSC Clean Technology Monographs, Cambridge (2000).

6   Paul T. Anastas and Mary M. Kirchoff, Acc.Chem. Res, 35 (2002) 686.

7   Toshio Okuhara, Chem. Rev, 102 (2002) 3641.

8   James H. Clark, Acc.Chem. Res, 35 (2002) 791.

9   Karen Wilson and James H. Clark, Pure Appl. Chem, 72 (2000) 1313.

10   J. Haber, "Perspectives in Catalysis" Blackwell Scientific Publications (1992) 371.

11   Werer Weiss and Robert Schlogl, Topics in Catalysis, 13 (2000) 75.

12   J.H. Clark, D.J. Macqarrie, J. Chem..Soc. Dalton Trans, (2000) 101.

13   F.A. Cotton and G. Wilkinson, 3rd Ed., Advanced inorganic chemistry, Wiley & Sons Inc (1996).

14   J.K. Burdett, T. Hughbands, IM. Gordon, J.W. Jr. Smith, J. Am. Chem. Soc, 109 (1987) 36-39.

15   C. J. Barbe, M. Gratzel, Mat. Res. Soc. Symp. Proc, (1996) 43.

16   E. J. Mezey, "Vapour Deposition", C. F. Powell, J. H. Olxey, J.M. Blocher, (Eds), Wiley, New York, (1966) p.423.

17   M. Z C. Hu, G. A. Muller, E. A. Payzant, C. J. Rown, J. Mat. Sci, 35

(2000) 2927.

18   H. Nishizava, M. Katsube, J. Solid State Chem, 131 (1997) 43.

19   M. E. Patsi, J. A. Hautaniemi, H. M. Rahiala, T. O. Peltola and I. M. O. Kangasniemi, J. Sol-gel Sci and Tech, 11 (1998) 55.

20   P. Li and K. de Groot, J. Biomed, Mater. Res, 27 (1993) 1495.

21   D. Chen, M. Sivakumar and A.K. Ray, Chem. Eng. Mineral Process, 8 (2000) 505.

22   K. Okamoto, Y. Yamamoto, H. Tanaka and A. Itaya, Bull. Chem. Soc. Japan, 58 (1985) 2015.

23   V. Augugliaro, al. Palmisano and A. Sclafani, Environ. Chem, 16 (1988) 89.

24   M.Gopal, W.J. Moberly Chan and L.C. Jonghe, J. Mat. Sci, 32 (1997) 6001.

25   Y. Zheng, E. Shi, Z. Chen, L. Wenjun and H. Xingfang, J. Mat. Chem, 11 (2001) 1547.

26   S. Waston, D. Beydoun, J. Scott and R. Amal, J. Nanoparticle Res, 6 (2004) 193.

27   X. Bokhimi, A. Morales, M. Aguilar, J.A. Toledo-Antonio and F. Pedraza, Int. J. Hydrogen Energy, 26 (2001) 1279.

28   E.F. Heald, C.W. Weiss, Am. Mineral, 57 (1972) 10.

29   Jingzhe Zhao, Zichen Wang, Liwei Wang, Hua Yang and Muyu Zhao, J. Mat. Sci. Lett, 17 (1998) 1867.

30   M. Ocana, J.V. Garcia Romos, C.J. Sema, J. Am. Ceram. Soc, 75 (1992) 201.

31   J. L. Hebrard and P. Nortier, J. Am. Ceram. Soc, 73 (1990) 79.

32   Hoag Kyu Park and Young Tae Moon, ibid, 79 (10) (1996) 2727.

33   K.I. Hadjhvanov and D.G. Kissurski, Chem. Soc. Rev, (1996).

34   C. Martin and I. Martin, J. Mater. Sci, 30 (1995) 3847.

35   V. S. Lusvardi, M. A. Barteau and W. R. Dolinger, J. Phys. Chem, 100 (1996) 183.

36   F. Molino and J.M. Barthez, Phys. Rev, 53 (1) (1996) 921.

37   M.T. Harris and C.H. Byres, J. Non-Crys. Sol. 103 (1998) 49.

38   S.D. Beck and R.W. Siegel, J. Mater. Res, 7 (10) (1992) 2840.

39   A. Fahmi and L. Ahdjoudj, Surf. Sci, 529 (1996) 352.

40   R.D. Shannon and J.A. Pask, J. Am. Ceram. Soc, 48 (1965) 391.

41   Z. Tang, J. Zhang, Z. Cheng and Z. Zhang, Mat. Chem. Phys, 77 (2002) 314.

42   S. Yin, R. Li, Q. He and T. Sato, Mater. Chem, 75 (2002) 76.

43   B. Imelik, J.C. Vedrine (Eds), Catalyst Characterization: Physical Techniques for Solid Materials, Plenum Press, New York (1994).

44   K. Morikawa, T. Shirsaki, M. Okada, Adv. Catal, 20 (1969) 97.

45   J.J. Burton, R.L. Garten (Eds.) L.L. Murrell in Advanced Materials in Catalysis, Chap. 8, Academic Press, New York (1977).

46   Q. Fu, A. Weber, M. Flytzani-Stephanopoulos, Catal. Lett, 77 1-3 (2001) 87.

47   P. Moriceau, B. Grzybowska, Y. Barbaux, G. Wrobel, G. Hecquet, Appl. Catal. A: Gen, 168 (1998) 269.

48   M.J. Holgado, S. San Roman, P. Malet, V. Rives, Mater. Chem. Phys, 89 (2005) 49.

49   O.V. Krylob, "Catalysis by nonmetals", Academic Press, New York (1970).

50   D.M. Whittle, A.A. Mirzaei, J.S.J. Hargreaves, R.W. Joyner, C. J. Kiely, S.H. Taylor, G.J. Hutchings, Phys. Chem. Chem. Phys, 4 (2002) 5915.

51   W. Zou, R.D. Gonzalez, Catal. Lett, 12 (1992) 73.

52   A.L. Bonivardi, M.A. Baltanas, J. Catal, 125 (1990) 243.

53   W. Zou, R.D. Gonzalez, Catal. Lett, 152 (1995) 291.

54   F. Pinna, Catal Today, 41 (1998) 129.

55   J. Haber, Pure Appl. Chem, 63 (1991) 1227.

56   C.F. Powell, J.H. Oxley, J.M. Blocher Jr, (Eds.) Vapour Deposition, Wiley, New York (1996).

57   H.O. Pierson, Handbook of Chemical Vapour Deposition–Principles, Technology and Applications, Noyes Publications, New Jersey (1992).

58   L.C. Klein, Ann. Rev. Mat. Sci, 15 (1985) 227.

59   B.E. Yoldas, J. Sol-Gel Sci. Tech, 1 (1993) 65.

60   S.J. teichner, G.A. Nicolaon, M.A. Vicarini, G.E.E. Gardes, Adv. Colloid Interface Sci, 5 (1976) 245.

61   T. Lopez, P. Bosch, M. Moran, R. Gomez, J. Phys. Chem., 97 (1993) 1671.

62   V. Lafond, P.H. Mutin, A. Vioux, J. Mol. Catal. A: Chem, 182-183 (2002) 81.

63   C. Palazzo, L. Olivia, M. Signoretto, G. Strukul, J. Catal, 194 (2000) 286.

64   M. Gotic, S. Popovic, M. Ivanda, S. Music, Mater. Lett, 57 (2003) 3186.

65   John D. Wright, "Sol-gel materials – Chemistry and Applications", Overseas Publishers (2001) p.8.

66   C. Jeffrey Brinker, George W. Scherer, "Sol-gel Science- The physics and Chemsitry of Sol-gel Processing" Academic Press, London (1989).

67   L. Shi, N.B. Wong, K.C. Tin and C.Y. Chung, J. Mat. Sci. Lett, 16 (1997) 1284.

68   B.E. Yoldas, Amer. Ceram. Soc. Bull, 54 (1995) 285.

69   A.J. Rubin, Mater. Sci. Res, 17 (1984) 45.

70   R.J.R. Uhihom, K. Keizer and A.J. Burggraaf, J. Membrane. Sci, 66 (1992) 1023.

71   Yu-Ting Wong, Ning Bew Wong, Li Shi, J. Mat. Sci, 38 (2003) 973.

72   B. E. Yoldas, Amer. Ceram. Soc. Bull, 54 (1975) 289.

73   R.P. Viswanath, P. Wilson, App. Catal. A: Gen, 201 (2000) 23.

74   F.D. Hard castle, I.E. Wachs, J. Mol. Catal, 46 (1988) 173.

75   M. Jehng, A.M. Turek, I.E. Wachs, App. Catal. A: Gen, 83 (1992) 179.

76   J. Engweiler, J. Nickl, A. Baiker, K. Kohler, C.W. Schlapfer, A. von Zelewsky, J. Catal, 145 (1994) 141.

77   J.P. Hogan, J. Polym. Sci, Part A-1 8 (1970) 2637.

78   Ch. Fountzoula, H.K. Matralis, Ch. Papadopoulou, G.A. Voyiatzis, Ch. Kordulis, J. Catal, 172 (1997) 391.

79   B.M. Weckhuysen, I.E. Wachs, R.A. Schoonheydt, Chem. Rev, 96 (1996) 3327.

80   G. Deo, I.E. Wachs, J. Phys. Chem, 95 (1991) 5889.

81   F. Cavani, M. Koutyrev, F. Trifiro, A. Bartolini, D. Ghisletti, R. Iezzi, A. Santucci, G.D. Piero, J. Catal, 158 (1996) 236.

82   B.M. Weckhuysen, A.A. Verberckmoes, A.L. Buttiens, R.A. Schoonheydt, J. Phys. Chem, 98 (1994) 579.

83   F. Massooth, Adv. Catal, 27 (1978) 265.

84   P. Grange, Catal. Rev. Sci. Eng, 21 (1980) 135.

85   B.M. Reddy, K.V.R. Chary, V.S. Subramanyan, N.K. Nag, J. Chem. Soc. Faraday Trans, I 81 (1985) 1665.

86   K.Y.S. Ng, E. Gulari, J. Catal, 95 (1985) 33.

87   Komandur V. R. Chary, Kondakindi Rajender Reddy, Chinthala Praveen Kumar, Catal. Commun, 2 (2001) 277.

88   S.K. Maity, M.S. Rona, S.K. Bej, J. Ancheyta Juarez, G.M. Dhar, T.S.R.P. Rao, Appl. Catal, 205 (2001) 215.

89   N.D. Spencer, J. Catal, 109 (1988) 187.

90   M. Laniecki, M. Matecka Gryez, F. Domka, Appl. Catal, 196 (2000) 293.

91   A.D. Paola, E.G.Lopez, S. Ikeda, G. Mara, B. Ohtani, L. Palmisano, Catal. Today, 75 (2002) 87.

92   B.G. Baker and N.J. Clark, Stud. Surf. Sci. Catal, 30 (1987) 483.

93   L.H. Gielgens, M.C.H. Van Kampen, M.M. Broek, R. Van Hardeveld and B. Ponec, J. Catal, 154 (1995) 201.

94   V.M. Benitez, C.A. Querini, N.S. Figoli and R.A. Comelli, Appl. Catal. A: Gen, 178 (1999) 205.

95   V.Logie, G. Maire, D. Michel and J.L. Vignes, J. Catal, 188 (1999) 90.

96   A. Katrib, V. Logie, N. Saurel, P. Wehrer, L. Hilaire and G. Maire, Surf. Sci, 30 (1997) 754.

97   V. Logie, P. Wehrer, A. Katrib and G. Maire, J. Catal, 189 (2000) 438.

98   E. Ogata, Y. Camiya and N. Ohta, J. Catal, 29 (1973) 296.

99   S. Eibl, R.E. Jentofit, B.C. Gates and H. Knizinger, Phys. Chem. Chem. Phys, 2 (2000) 2565.

100   J.R. Barkley, L.H. Brixner, E.M. Hogan, Symposium on the Applications of Ferroelectrics, York Town Heights, New York, 1971.

101   J.R. Barkley, L.H. Brixner, E.M. Hogan, R.K. Waring, J. Ferroelectr. 3 (1972) 191.

102   J. Sapriel, R. Vacher, J. Appl. Phys, 48 (1977) 1191.

103   B.H. Doreswamya, M. Mahendraa, M.A. Sridhara, J. Shashidhara Prasada , P.A. Varugheseb, K.V. Sabanc, George Varghesec, J. of Molecular Structure, 659 (2003) 81.

104   E.S. Putna, J.M. Vohs, R.J. Gorte, and G.W. Graham, Catal Lett, 54 (1998) 17.

105 A. Burrows, C.J. Kiely, J.S.J. Hargreaves, R.W. Joyner, G.J. Hutchings, M.Y. Sinev, Y.P. Tulenin, J. Catal. 173 (1998) 383.

105 J.S.J. Hargreaves, G.J. Hutchings, R.W. Joyner, S.H. Taylor, Appl. Catal. A: Gen, 227 (2002) 191.

106 B.M. Reddy, P. Lakshmanan, A. Khan, J. Phy. Chem. B, 108 43 (2004) 16863.

107 Friebe, O. Nuyken, H. Windisch, W. Obrecht, Macromol. Chem. Phys, 203 8 (2002) 1055.

108 S. Sugunan, N.K. Renuka, Bull. Chem. Soc. Jpn, 75 (2002) 463.

109 D.H. Tsai, T.J. Huang, Appl. Catal. A: Gen, 223 (2002) 1.

110 A.G. Dedov, A.S. Loktev, I.I. Moiseev, A. Aboukais, J.-F. Lamonier, I.N. Filimonov, Appl. Catal. A: Gen, 245 (2003) 209.

111 S. Shylesh, T. Radhika, K. Sreeja Rani, S. Sugunan, J. Mol. Catal. A: Chem, 236 (2005) 253.

112 A. Fernandez, J, Leyrer, A. Gonzalez, G. Munera and W. Knozinger, J. Catal, 112 (1988) 489.

113 Z. Wei, Q. Xin, X. Guo, E. Sham, P. Grange and B. Delmon, Appl. Catal, 63 (1990) 305.

114 P. Wauthoz, M. Ruwet, T. Machej and P. Grange, Appl. Catal, 69 (1991) 149.

115 G.M. Pajonk, Appl. Catal, 72 (1991) 217.

116   E.I. Ko, Chemtech, 4 (1993) 31.

117   J. Retuert. R. Quijada and V. Arias, Chem. Mater, 10 (1998) 3923.

118   Jaime Retuert, Raul Quijada and Victor Fuenzalida, J. Mater. Chem, 10 (2000) 2818.

119   Jose A. Ayllon, Ana M. Piero, Laheen Saadoun, Elena Vigil, Xavier Domenech and Jose Peral, J. Mater. Chem, 10 (2000) 1911.

120   D.S.Lee and T.K. Liu, J. Sol-Gel Sci. Tech, 25 (2002) 121.

121   Yurii Kolen ko, Alexander A. Burukhim, Bulat R. Churagulov, Nikolai N. Oleynikov, Mat. Lett, 57 (2003) 1124.

122   M. Iwasaki, M. Hara and S. Ito, J. Mater. Sci. Lett, 17 (1998) 1769.

123   S.T. Aruna, S. tirosh and A. Zaban, J. Mater. Chem, 10 (2000) 2388.

124   Cheng Wang, Zhao Xiang Deng and Yadong Li, Inorg. Chem, 40 (2001) 5210.

125   K.M.S. Khalil, T. Baird, M.I. Zaki, A.A. El-Samahy, A.M. Awad, Colloid Surf. A, 132 (1998) 31.

126   N. Phonthammachai a, T. Chairassameewong a, E. Gulari b, A.M. Jamieson c, S. Wongkasemjit, Microporous and Mesoporous Materials, 66 (2003) 261.

127   Yury V. Kolen'ko , Victor D. Maximov, Alexei V. Garshev, Pavel E. Meskin, Nikolai N. Oleynikov, Bulat R. Churagulov, Chem Phys Lett, 388 (2004) 411.

128   Yasushige Mori, Yasushiro Okastu and Yuki Tsujimoto, J. Nanoparticle

Research, 3 (2001) 219.

129 Paul D. Moran, John R. Bartlett, Graham A. Bowmaker, James L. Woolfrey, Ralph P. Cooney, J. Sol-Gel Sci. Tech, 15 (1999) 251.

130 Kun Yuan Chen and Yu Wen Chen, J. Sol-Gel Sci. Tech, 27 (2003) 111.

131 Haimei Liu, Wengsheng Yang, Ying Ma, Yaan Cao, Jiannian Yao, Jing Zhang and Tiandou Hu, Langmuir, 19 (2003) 3001.

132 Weiping Huang, Xianghai Tang, Yanqin Wang, Yuri Koltypin and Aharon Gedanken, Chem. Commun, (200) 1415.

133 T. Nishide, M. Sato and H. Hara, J. Mat. Sci, 35 (2000) 465.

134 Y.J. Kim and L.F. Francis, J. Mat. Sci, 33 (1998) 4423.

135 Yinghong Yue and Zi Gao, Chem. Commun, (2000) 1755.

136 I. Kartini, M. Meredith, J.C. Diniz Da Costa and G.Q. Lu, J. Sol-Gel Sci. Tech, 31 (2004) 185.

137 Shoichi Takenaka, Ryoji Takahashi, Satoshi Sato and Toshiaki Sodesawa, J. Sol-Gel Sci. Tech, 19 (2000) 711.

138 Hiroaki Imai, Yuko Takei, Kazuhiko Shimizu, Manabu Matsuda and Hiroshi Hirashima, J. Mater. Chem, 9 (1999) 2971.

139 Hiroaki Imai, Manabu Matsuta, Kazuhiko Shimizu, Hiroshi Hirashima and Nobuaki Negish, J. Mater. Chem, 10 (2000) 2005.

140 Hiroaki Imai, Manabu Matsuta, Kazuhiko Shimizu, Hiroshi Hirashima and Nobuaki Negish, Solid state Ionics, 151 (2002) 183.

141 Jiaguo Yu, Jimmy C. Yu, Mitch K. P. Leung, Wingkei Ho, Bei Cheng, Xiujian Zhao and Jincai Zhao, J. Catal, 217 (2003) 69.

142 T. Lopez, J. Navarrete, R. Gomez, O. Novaro, F. Figueras and H. Armendariz, Appl. Catal, 125 (1995) 217.

143 M. Hino and K. Arata, J. Chem.Soc. Chem. Commun, (1980) 851.

144 G. Larsen, E. Lotero, M. Nabity, L.M. Petkovic and D.S. Shobe, J. Catal, 164 (1996) 246.

145 S.K. Samantary, K. Parida, J. Mat. Sci, 39 (2004) 3549.

146 S. Sugunan, T. Radhika and H. Suja, React. Kinet. Catal. Lett, 79 (1) (2003) 27.

147 Kalathiparambil Rajendrapai Sunajadevi and Sankaran Sugunan, React. Kinet. Catal. Lett, 82 (1) (2004) 11.

148 J.P. Chen, R.T. Yang, J. Catal, 139 (1993) 277.

149 Dong Jin Suh and Tae Jin Park, J. Mater. Sci. Lett, 16 (1997).

150 Jaime Retuert, Raul Quijada and Victor M. Fuenzalida, J. Mater. Chem, 10 (2000) 2818.

151 Y.Y. Huang, B.Y. Zhao, Y.C. Xie, Appl. Catal. A: Gen, 171 (1998) 65.

152 B. Karmakar and D. Ganguly, Ind. J. of Tech, 22 (1987) 282.

153 M. Yoshinka, K. Hirota and O. Yamaguchi, J. Am. Ceram. Soc, 80 (10) (1997) 2749.

154 S. Rajeshkumar, C. Suresh, A.K. Vasudevan, N.R. Suja, P. Mukundan and K.G.K. Warrier, Mater. Lett, 38 (1999) 161.

155 Z. Liu, R.J. Davis, J. Phys. Chem, 98 (4) (1994) 1253.

156 Tatsuro Horiuchi, Toyohiko Sugiyama, Ken-Ichi Ushiki, J. Mat. Sci. Lett, 17 (1998) 15.

157 K.G.K. Warrier, S. Rajeshkumar and C.P. Sibu, G. Werner, J. Porous Mat, 8 (2001) 311.

158 G.S. Walker, E. Williams and A.K. Bhattacharya, J. Mat. Sci, 32 (1997) 5583.

159 A. Martucei, F. Innocemzi, E. Traversa, J. Ceram. Soc. Japan, 107 (12) (1997) 5583.

160 E. Sanchez, T. Lopez, R. Gomez, J. Mater. Sci, 32 (21) (1997) 5583.

161 S. Rajeshkumar, S.C. Pillai, U.S. Hareesh, P. Mukundan and K.G.K. Warrier, Mat. Lett, 43 (2000) 286.

162 Jeffrey C. Wu, I. Hsiang Tseng and Wan Chen Chang, J. Nanoparticle Res, 3 (2001) 113.

163 T.K. Kundu, M. Mukherjee, D. Chakravorthy and T.P. Sinha, J. Mat. Sci, 33 (1998) 1759.

164 B. Pal, M. Sten and G. Noyani, J. Mater. Chem, 59 (3) (1999) 254.

165 F.C. Gennari and D.M. Pasquevich, J. Mater. Sci, 33 (1998) 1571.

166 Y. Wang, H. Cheng, Y. Hao, J. Ma, W. Lia nd S. Cai, J. Mater. Sci, 34 (1999) 3721.

167 C.P. Sibu, S. Rajeshkumar, P. Mukundan and K.G.K. Warrier, Chem. Mater, 14 (2002) 2876.

168 K.N.P. Kumar, K. Keizer, A. Burggraaf, J. Mater. Chem, 3 (1993) 141.

169 Yu Ting Wong, Ning Bew Wong, Li Shi, J. Mater. Sci, 38 (2003) 973.

170 Andrew Burns, W.Li, C. Baker and S.I. Shae, Mat. Res. Symp. Proc. Vol. 703 (2002).

171 Yibing Xie, Chunwei Yuan, Xiangzhong Li, Colloids and Surfaces A: Physicochem. Eng. Aspects 252 (2005) 87.

172 Andrew Burns, G. Hayes, W. Lia, J. Hirvonen, J. Derek Demareed, S. Ismat Shah, Materials Science and Engineering B 111 (2004) 150.

173 B.M. Reddy, I. Ganesh, I. Reddy, J. Mater. Sci. Lett, 17 (22) (1998) 1913.

174 M. Schneider, A. Baiker, U. Scharf and A. Wokaaun, J. Catal, 150 (2) (1994) 311.

175 Weon Pil Tai and Kozo Inoue, Mat. Lett, 57 (2003) 1508.

176 T. Lopez, J. Hernandez, R. Gomez, X. Bokhimi, J.L. Bolday, E. Munoz, O. Novaro, Langmuir, 15 (1999) 5689.

177 J. Yang, J.M.F. Ferreira, Mat. Res. Bull, 33 (3) (1998) 389.

178 Jianguo Huang, Izumi Ichinose, Toyoki Kunitake and Aiko Nakao, Nano Lett, 2 (6) (2002) 669.

179 E. Sanchez, T. Lopez, R. Gomez, Solid State Chem, 122 (2) (1996) 309.

180 V. Keller, P. Bernhardt and F. Garin, J. Catal, 215 (2003) 129.

181 Tetsu Tatsuma, Shuichi Saitoh, Pailin Ngaotrakanwiwat, Yoshihisa Ohko and Akira Fujishima, Langmuir, 18 (2002) 7777.

182 A.M. Veneziaz, L. Palmisano, M. Schiavello, J. Solid State Chem, 114 (2) (1995) 364.

183 H. Scheider, A. Baiker, U. Scharf, A. Wokaun, J. Catal, 146 (2) (1994) 546.

184 Jong Ho Lee, Kyeong Youl Jung, Seung Bin Park, J. Mater. Sci, 34 (1999) 4089.

185 T. Lopez, J. Hernandez, R. Ventura, F. Gomez, F. Tzompantzi, E. Sanchez, X. Bolkhimi and A. Garcia, J. Mol. Catal, A; Chem, 167 (1) (2001) 101.

186 H. Julio Andrade Gamboa and Daniel M. Pasquevich, J. Am. Ceram. Soc, 71 (11) (1992) 2934.

187 M. Nagain, J. Takadv, S. Qmi, J. Phys. Chem. B, 103 (46) (1999) 10180.

188 K.T. Ranjit, B. Viswanathan, J. Photochem and Biology, 108 (1999)

5273.

189 X. Fang, P. Hing, J.T. Oh, H.S. Fong, X. Chen and M. Wu, J. Mater. Process. Tech, 113 (1-3) (2001) 474.

190 H. Yuan, L.D. Zhang, Chemical J. Chinese Universities, 20 (1999) 1007.

191 Asha Vasudevan, P.P. Rao, S.K. Ghosh, G.M. Anilkumar, A.D. Damodaran and K.G.K. Warrier, J. Mater. Sci. Lett, 16 (1) (1997) 8.

192 M. Iwasaki, M. Hara, H. Kadawa, H. Tada, S. Ito, J. Colloid Interface Sci, 224 (1) (2000) 202.

193 Y. Liu, X. Chen, J. Li, C. Burda, Chemosphere, 61 (2005) 11.

194 Hiroshi Irie, Seitaro Washizuka, Norio Yoshino and Kazuhito Hashimoto, Chem. Commun, (2003) 1298.

195 T. Norikawa, R. Ashai, T. Ohwaki, K. Aoki and Y. Raga, J. Appl. Phys Lett, 40 (2001) 561.

196 K. Tanabe, "Solid acids and Bases and their Catalytic Properties", Academic Press, New York (1970) 103.

197 M. Guisnet, "Catalysis by Acids and Bases", B. Imelik *et al,* (Eds), Stud Surf sci Catal, 20, Elsevier, Amsterdam (1985) 283.

198 M.R. Guisnet, Acc. Chem. Res, 23 (11) (1990) 393.

199 H.A. Benesi, J. Am. Chem. Soc, 21 (1956) 5490.

200 H.A. Benesi, J. Am. Chem. Soc, 61 (1957) 970.

201 J. Klinowshi, Chem. Rev, 91 (1991) 1459.

202 B.K. Hodnett and J.B. Moffat, J. Catal, 88 (1984) 253.

203 A.M. Tonejc, M. Goti, B. Grzeta, S. Music, S. Popovi, R. Trojko, A. Turkovi, I. Musevic, Mater. Sci. Eng, 40 (1996) 177.

204 Trilochan Mishra, Kulamani Parida, Appl. Catal A: Gen, 166 (1998)

123.

205   H.C. brown, R.B. Johanneson, J. Am. Ceram. Soc, 75 (1953) 16.

206   H.A. Benesi, J. Catal, 28 (1973) 176.

207   M.A. Barteau, Chem. Rev, 96 (1996) 1413.

208   M. Ai, Bull. Chem. Soc. Japan, 50 (1977) 2597.

209   J. Sabati, F.E. Massoth, M. Tokarz, G.M. Tsai and J. Mc. Cauley, Proc. 8th Int. Cong. In Catal, Berlin, 4 (1984) 735.

210   J.T. Miller, P.T. Hopkins, B.L. Meyers, G.J. Ray, R.T. Roginski, G.W. Zajac and N.H. Rosenbaum, J. Catal, 138 (1992) 138.

211   J. Klinowski, J.M. Thomas, C.A. Fyfe and G.C. Gobbi, Nature (London) 296 (1982) 533.

212   H. Nollery, G. Ritler, J. Chem. Soc. Faraday Trans, 80 (1984) 275.

213   C. Bezouhanava, M.A. al-Zihari, Catal. Lett, 11 (1991) 245.

214   R.A.W. Jonstone, J. Liu, D. Wittaker, J. Chem. Soc, Perkin Trans, (1998) 1287.

215   M.C. Cruz-Costa, L.F. Hodson, R.A.W. Jonstone, J. Liu, D. Whittaker, J. Mol. Catal. A, 142 (1999) 349.

216   R.A.W. Jonstone, J. Liu, D. Whittaker, J. Mol. Catal. A, 174 (2001) 159.

217   V.Z. Fridman, A.A. Davydoy, J. Catal, 195 (2000) 20.

218   Z. Liu, Z. Xu, Z. Yuan, D. Lu, W. Chen, W. Zhou, Catal. Lett, 75 (2001) 203.

219   L.F. Silva, J. Vital, A.M. Ramos, H. Valente, A.M. Botelho, Do Rego, M.J. Reis, Carbon, 36 (1998) 1159.

220   C. Park, M.A. Keane, J. Mol. Catal. A, 166 (2001) 303.

221   H. Nur, H. Hamdan, Mater. Res. Bull, 36 (2001) 315.

222 B.M. Reddy, I. Ganesh, J. Mol. Catal. A, 169 (2001) 207.

223 P.M. Boorman, R.A. Kydd, Z. Sarbak and A. Somogyvari, J. Catal, 96 (1985) 115.

224 Zenon Sarbak, Appl. Catal. A: Gen, 159 (1997) 147.

225 Jong Rack Sohn and Sam Gon Ryu, Catal. Lett, 74 (1-2) (2001) 105.

226 K.M. Parida, S.K. Samantaray and H.K. Mishra, J. Colloid Interface Sci, 216 (1999) 127.

227 Jong Rack Sohn and Ju Suk Lee, Bull. Korean Chem. Soc, 24 (2003) 159.

228 Mohan S. Rana, S.K. Maity, J. Ancheyta, G. Murali Dhar, T.S.R. Prasada Rao, Appl. Catal A Gen, (2003) .

229 Yu Liu and Thomas J. Pinnavaia, J. Mater. Chem, 14 (2004) 1099.

230 A. Gedeon, A. Lassoued, J.L. Bonardet, J. Fraissard, Microporous and Mesoporous Mater, (44-45) (2001) 801.

231 T.H. Fleisch, R.A. Kydd and P.M. Boorman, J. Catal, 120 (1989) 413.

232 T.H. Fleisch, B.L. Meyers, G.J. Ray, J.B. Hall and C.L. Marshall, J. Catal, 99 (1986) 117.

233 T. Sano, Y. Uno, Z.B. Wang, C.H. Ahn and K. Soga, Microporous and Mesoporous Mater, 31 (1999) 89.

234 M.V. Landau, E. Dafa, M.L. Kaliya, T. Sen, M. herskowitz, Microporous and Mesoporous Mater, 49 (2001) 65.

235 R. Mokaya and W. Jones, J. Catal, 153 (1995) 76.

236 Trilochan Mishra and Kulamani Parida, Appl. Catal A; Gen, 166 (1998) 123.

237 F.M. Bautisuta, J.M. Campelo, A. Garcia, D. Luna, J.M. Marinas, R.A.

Quiros and A.A. Romero, Appl. Catal A; Gen, 243 (2003) 93.

238 N. John Jebarathinam and V. Krishnasamy, Catalysis-Modern Tends, Narosa Publishing House, New Delhi (1995) p.323.

239 G. Krishna Reddy and P. Kanta Rao, Catal. Lett, 45 (1997) 93.

240 Anita Rachel, V. Durga Kumari and P. Kanta Rao, Catalysis-Modern Tends, Narosa Publishing House, New Delhi (1995) p.346.

241 K.V.V.S.B.S.R. Murthy, B. Srinivas and S.J. Kulkarni, Catalysis-Modern Tends, Narosa Publishing House, New Delhi (1995) p.186.

Chapter 2

Materials and Methods

Abstract

    The development and preparation of heterogeneous catalysts were considered more as alchemy than science with the predominance of trial and error experiments. In the production of catalysts, even a minute change in the conditions of preparation can change the quality of the catalyst. Hence they must be thoroughly characterized before use. In the present chapter the experimental procedures used for catalyst preparation, the characterization techniques and catalytic activity measurements are described in detail. The physico chemical characterization of the prepared systems are done using techniques such as XRD, EDX, SEM, BET surface area-pore volume measurements, TG/DTG, FTIR, and Diffuse Reflectance UV-vis spectroscopy. The surface acidity measurements were done using ammonia TPD, 2,6 dimethyl pyridine adsorption studies and test reactions such as cumene cracking and cyclohexanol decomposition. Reactions of industrial importance such as epoxidation of cyclohexene, hydroxylation of phenol, tert-butylation of phenol, methylation of aniline and anisole, dehydrogenation of cyclohexane and cyclohexene are chosen for the catalytic activity measurements. Photocatalytic oxidation of benzhydrol as well as photodegradation of methyl orange is carried out over the prepared systems.

2.1 Introduction

The preparation of heterogeneous catalysis has by now lost all empirical aspects[1]. A good catalyst besides having high catalytic activity and selectivity for the desired reaction should have large specific surface area, stability and mechanical strength. These factors should be kept in mind while preparing a catalyst. The design of a catalyst covers all aspects from choice of the active phases to the method of forming particles[2]. The catalyst surface is very complex and heterogeneous with a broad classification of structurally and chemically different sites. The nature of the active sites is the most important factor in heterogeneous catalysis. A complete knowledge on the exact location, structure and electronic ground state of the active site in the catalyst is essential to establish a basic understanding about the structure activity correlations and to improve the efficiency of the catalyst for high stability and selectivity.

2.2 Catalyst preparation

Sol-gel method is used for the preparation of the catalysts. The method is a homogeneous process, which results in a continuous transformation of a solution into a hydrated solid precursor. The sol-gel syntheses have been recognized for their versatility, which allows better control of the texture, composition, homogeneity and structural properties of the final solids. The nanoscale chemistry involved in the sol-gel methods is a more direct way to prepare highly divided materials. Particulate sol-gel route is used for the preparation of titania systems using metatitanic acid as precursor. The transition metals like molybdenum, chromium and tungsten is incorporated to titania from their soluble salts. Similarly the modification of titania is done

using rare earth metals like lanthanum, praseodymium and samarium from their nitrate salt solution. For a comparative evaluation of the properties, pure titania is also prepared.

Materials

The materials used for the preparation of catalysts are given below.

Materials	Suppliers
Metatitanic Acid	Travancore Titanium Products Limited
Ammonium tungstate	Merck
Ammonium molybdate	Merck
Chromium Nitrate	Merck
Praseodymium Nitrate	Indian Rare Earth Ltd
Lanthanum Nitrate	Indian Rare Earth Ltd
Samarium Nitrate	Indian Rare Earth Ltd
Conc. Nitric Acid	Merck
Conc. Sulphuric acid	Merck
Conc. Ammonia	Merck

Methods

A detailed experimental procedure for the preparation of the catalysts is given in the flow chart in figure 2.1. The estimation of the sol is done gravimetrically before the addition of the corresponding metal solution.
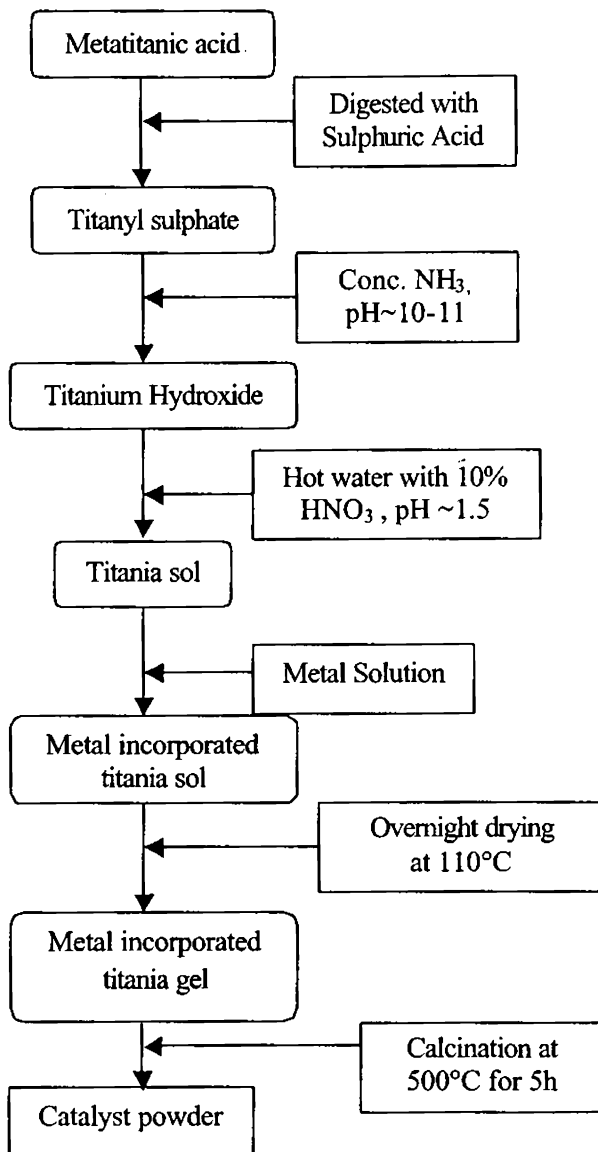
Figure 2.1 Preparation process of metal incorporated titania

2.2.1 Preparation of titania

Metatitanic acid is digested with concentrated sulphuric acid above 100°C and the resultant solution is filtered to get titanyl sulphate. Titanium hydroxide is precipitated by adding concentrated ammonia dropwise to this titanyl sulphate solution until the pH rises above 10. Then the precipitate is washed several times with hot water to remove sulphate ions totally. This titanium hydroxide is suspended in hot water at 70°C and added 10% HNO_3 with continuous stirring. A clear transparent sol is obtained at a pH of ~1.5 which is stable for months. The sol is kept for ageing for 1 day and then chemical gelation is done by slightly perturbing the pH of the stable sol with the addition of ammonia. The gel is kept in contact with the mother liquor for 1 day and then decanted off. The filtered precipitate is washed with distilled water, dried overnight at 110°C in an air oven and powdered below 100 i mesh size. The xerogel thus obtained was calcined at 500°C for 5h in a muffle furnace.

2.2.2 Preparation of metal incorporated titania

Titania sol is prepared as above and the incorporation of the metal is done in the sol phase. Transition metals like molybdenum, tungsten and chromium are incorporated from their respective aqueous salt solution such as ammonium molybdate, ammonium tungstate and chromium nitrate. Similarly rare earth metals like lanthanum, samarium and praseodymium is incorporated from their respective nitrate salt solution. 20ml of the sol is taken and estimated quantitatively. 2,6 and 10 wt % of the metal is incorporated to titania by taking corresponding amounts of the salt solution. The mixed sol is stirred

again for 3h and then gelation is done by adding ammonia drop wise. Then aging of the gel is done for a day. The gel is dried overnight and calcined at 500°C for 5h.

2.3 Catalyst notations

The catalyst systems developed for the present investigation and its designation are given below.

Notation   Systems

Ti   Pure titania

TiXy   Ti containing metals (X) such as Cr, Mo, W, La, Pr and Sm having weight % (y) of 2, 6 and 10.

2.4 Characterization techniques

In heterogeneous catalysis, the reaction occurs at the surface of the catalyst. Catalysis and catalytic surfaces hence need to be characterized by reference to their physical properties and by their actual performance as a catalyst. The most important physical properties are those relating to the surface because catalyst performance is determined by surface parameters. Any characterization of a catalyst must start with knowledge of the chemical composition of the same. It is important to know the presence and the quantity of trace elements, additives, poisons etc., in a catalyst. The amount of the sample required for any characterization is relatively small and in many cases the method is non-destructive.

The prepared catalyst systems were characterized by adopting a variety of physico-chemical properties which include BET surface area and pore volume measurements, X-Ray diffraction, Energy Dispersive X-Ray analysis, Scanning electron microscopy, Fourier Transform Infrared Microscopy, UV-Vis Diffuse Reflectance Spectroscopy and TG-DTG analysis. Before each characterization except for thermogravimetric analysis, the samples were activated at 500°C for 2h.

Materials

The materials used for catalyst characterization are

Materials	Suppliers
Liquid Nitrogen	Sterling gases Pvt. Ltd.
Potassium Bromide	Merck
Magnesium Oxide	Merck

Methods

A brief discussion of each method of characterization technique adopted along with its experimental aspects is presented in the following sections.

2.4.1 X-Ray Diffraction Analysis

X-Ray diffraction has remained the mainstay of structure determination of crystalline solids and the recent developments in technology and computing have paved the way for unequivocal determination of even macromolecular

structures with remarkable accuracy. It contains a wealth of useful information provided one can exploit and extract the same, with patience in synthesizing good materials and a healthy scientific aptitude to apply modern computational facilities[3].

Powder X-Ray diffraction is a long-range order technique sensitive to the basic periodic structure of a solid sample[4-5]. The basic principle underlying the analysis is that the scattered waves from the atoms interfere constructively, if they are in phase (coherent), and diffracted beams are formed in specific directions. These directions are governed by the wavelength of the incident radiation and the nature of the crystalline samples. Braggs law formulated by W.L. Bragg in 1913, relates the wavelength of the X-Rays to the spacing of atomic planes by the equation[6],

$$n\lambda = 2d \sin\theta$$

where n is the order of reflection, λ, the wavelength of X-Rays, θ, Bragg angle and d, the interplanar spacing.

The three main types of information in a diffraction pattern include the position, the intensity and the shape of diffraction peaks. The positions of the diffraction peaks are determined by the geometry of the crystal lattice i.e., the size and shape of the unit cell. The intensities of the peaks in a profile are related to the specific atoms in a crystal and their arrangement in the unit cell of the crystal[7]. The diffraction profile is related to the size and perfection of the crystallites and various instrumental parameters. Most of the analytical methods used for diffraction profile studies, emphasize the position variables (d spacing) as they can be accurately determined and the other two parameters

are considered when quantitative analysis/ structure refinemnt and crystallite size are required[8].

Crystallite size (L) can be determined from the corrected line broadening (â) in the sample using Scherrer equation.

$$L = K\lambda \ / \ \beta \ \cos\theta$$

Where L, λ and θ have their usual meanings, L is the mean dimension of the crystallites composing the powder sample or the thickness of the crystal in a direction perpendicular to the diffracting planes, K is a constant approximately equal to 0.9-1.0 and related both to the crystallite shape and to the way in which â and L are related.

XRD patterns were recorded in a *Rigaku D-max C X-Ray diffractometer* using Ni filtered CuKα radiation (λ=1.5406A°). The crystallite phases were identified by comparison with the standard JCPDS data file[9].

2.4.2 Diffuse Reflectance UV-Vis Spectroscopy

The diffuse reflectance UV-Vis spectroscopy is known to be a very sensitive probe for the identification and characterization of metal ion coordination. It is a non-invasive technique that uses the interaction of light, absorption and scattering, to produce a characteristic reflectance spectrum, providing information about the structure and composition of the medium. It gives information regarding electronic transition between orbitals or bands in the case of atoms, ions and molecules in gaseous, liquid or solid state. Electronic transition of transition elements are of two types, namely, metal centered transitions [d-d or (n-1) d-ns] and charge transfer (CT) transitions. d-d transitions gives information about the oxidation state and the coordination

environment of transition metal ion. (n-1) d-ns transitions are often too high in energy to be observed in the spectrum. The CT transitions are intense since they are Laporte allowed and are sensitive to the nature of donor and acceptor atoms[10-11]. Diffuse reflectance UV-Vis spectra of the samples were recorded at room temperature between 200 and 800nm using magnesium oxide as standard in *Ocean optics AD 2000* instrument with a CCD detector.

2.4.3 Thermogravimetric Analysis

Thermal analysis is a widely used analytical technique for material research[12]. Thermogravimetry or thermogravimetric analysis (TGA) provides a quantitative measurement of any weight changes associated with thermally induced transitions. The rates of these thermally induced processes are often a function of the molecular structure. TGA provides information on the thermal stability of the material. Thermal stability of a compound depends on the constituent elements present and on the type of linkages between the different elements[3]. Changes in weight result from physical and chemical bonds forming and breaking at elevated temperatures. These processes may evolve volatile products or form reaction products that result in a change of weight of the samples.

Thermal analysis techniques have great potential in the development of catalysts especially for the control and generation of active systems. They can also be successfully employed for determining the surface properties of the catalysts under favorable conditions. The application of thermal analysis methods for catalyst development is reaching a mature status and can be

expected to be exploited by many others for even studying the surface transformations that take place on catalyst surface.

In thermo gravimetric analysis, the loss of weight of a sample is being continuously recorded over a period of time under controlled heating rate. The first derivative of the thermogram (DTG) gives a better understanding of the weight loss and can also be used to determine the thermal stability of the samples. *TGAQ V2.34 thermal analyzer* was used for carrying out thermogravimetric studies. About 20mg of the samples was used at a heating rate of 20°C/min from 20 to 700°C in N_2 atmosphere. The TG data were computer processed to get thermograms. Any decomposition of the sample is indicated by a dip in the curve. These dips correspond to the weight loss due to decomposition and hence provide an idea about the species lost during the heating step. This method cannot distinguish the actual nature of the material evolved in the course of the process and is also handicapped in resolving overlapped thermal analysis. So it is seldom able to describe the process under study completely.

2.4.4 Surface Area and Pore Volume Measurements

The surface area calculated from the use of BET equation is perhaps the most popular and widely used in the literature, ever since Brunauer, Emmett and Teller (BET) derived the equation for physical adsorption of gases on solid surfaces that lead to multilayer adsorption[13]. The phenomenon of higher concentration of any molecular species at the surface than in the bulk of the solid or liquid is known as adsorption. The assumptions are that the surface is energetically uniform, that the condensation of layers of gas can proceed to

multilayers and that the adsorbed molecules do not interact laterally. The simple form of this equation that forms the basis of the BET method for the determination of surface area of solids can be written as;

$$P / [V (P_0 - P)] = 1 / V_m C + P (C-1) / V_m P_0 C$$

where V is the volume of gas adsorbed at equilibrium pressure, P and P_0 is the saturated vapour pressure of the adsorbate at liquid nitrogen temperature and C is the isothermal constant. By plotting $P / [V (P_0 - P)]$ vs P / P_0 and determining V_m from the slope and the resultant straight line in the partial pressure range of 0.05 to 0.35, the surface area can be calculated. The specific surface area can be found out using the relation,

$$A = V_m N_0 A_m / W \times 22414$$

Where N_0 is the Avogadro number, A_m the molecular cross sectional area of the adsorbate and W the weight of the sample (g).

The method is based on the phenomenon of adsorption. Nitrogen is commonly used as the adsorbate at liquid nitrogen temperature. Here we determine the volume of nitrogen gas adsorbed by a known weight of the sample at liquid nitrogen temperature. Since the area occupied by single adsorbed molecular nitrogen can be estimated, the total surface area can be calculated by multiplying the area of one molecule by the number of molecules required forming the monolayer. Adsorption varies directly with pressure and inversely with temperature. Here the temperature is held constant and the amount of nitrogen adsorbed at liquid nitrogen is measured at different relative pressures. P_0 will depend on the temperature and hence the purity of liquid nitrogen.

Simultaneous determination of surface area and total pore volume of the samples were achieved in a *Micromeritics Gemini – 2360* surface area analyzer by the low temperature nitrogen adsorption method. Previously activated samples at 500°C were degassed at 400°C under nitrogen atmosphere for 4h prior to each measurement. The pore volume is measured by the uptake of nitrogen at a relative pressure of 0.9.

2.4.5 Fourier Transform Infrared (FTIR) Spectroscopy

Infrared spectroscopy has been extensively used for identifying the various functional groups on the catalyst itself, as well as for identifying the adsorbed species and reaction intermediates on the catalyst surface[14-15]. It is one of the few techniques capable of exploring a catalyst, both in its bulk and its surface, and under the actual reaction conditions. Infrared spectrum originates from the transitions between discrete vibrational and rotational energy levels of the molecules. The IR spectrum of the compound is the characteristic of that compound and may be used for identification just like melting point, boiling point optical rotation etc. The analysis of the spectrum was done by comparing with the reported values. The most commonly used region for this purpose is the finger print region ($4000 - 600 cm^{-1}$).

Infrared spectroscopy has been widely used for characterizing the acid sites of the catalyst, which are responsible for their catalytic properties. The measurement of the intensity of IR bands due to adsorbed pyridine at a particular temperature enables one to calculate the concentration of the individual Bronsted and Lewis acid sites in a catalyst sample. It also finds

applications to identify the intermediate species in heterogeneous catalytic reactions.

The FTIR spectrum of the sample was recorded on a Nicolet Impact 4000 spectrometer using the KBr pellet method. The measured quantity of the sample was mixed with spectroscopic grade KBr and ground well. The mixture was compacted to a disc by pressing. The percentage transmittance is plotted against the wave number.

2.4.6 Energy Dispersive X-Ray (EDX) fluorescence Analysis

Energy dispersive X-Ray fluorescence analysis is one of the successful analytical methods for the qualitative and quantitative analysis of the solid samples. It allows non destructive elemental analysis of the sample[16]. The principle of EDX is based on the strong interaction of electrons with matter. When electrons of appropriate energy impinge on a sample, they cause emission of X-Rays whose energies and relative abundance depend on the composition of the sample.

The electron beam from a scanning electron micrograph used in this technique can eject an electron from the inner shell of the sample atom. The resulting inner shell electron vacancy is filled by another electron from a high energy shell in the atom. While moving from a high energy state to a lower one, this vacancy filling electrons give up some of its energy (equal to the difference in the energy between the two electronic energy levels involved) in the form of electromagnetic radiation. Since this electronic energy is fairly larger for inner shells, the radiation appears as X-rays. As all elements have a unique configuration of electronic energy levels, the X-ray pattern spectrum

will be unique for a particular element. Furthermore, under the given analysis conditions, the number of X-rays emitted by each element will be directly proportional to the concentration of that element in the sample[17].

The X-ray peak position along with the energy scale identify the element present in the sample, while the integrated peak areas after application of appropriate correction factors, can give us percentage composition of each of the elements[8]. Powdered sample is put on a double-sided carbon tape on a metal strip before analysis. EDX spectra of the samples were recorded in an EDX-JEM-35 instrument (JEOL Co. link system AN-1000-Si-Li detector).

2.4.7 Scanning Electron Microscopy (SEM)

Scanning Electron Microscopy is a well-established technique in the realm of materials science for the determination of structure. It allows the imaging of the topography of a solid surface by using back scattered or secondary electrons with good resolution of about 5nm. In this technique, a fine probe of electrons is scanned over the sample surface using deflection coils. The interaction between the primary beam and the specimen produces various signals, which are detected, amplified and displayed on a cathode ray tube screened synchronously with the beam. They can also be conveniently deflected and focused by electronic or magnetic field so that magnified real space images can be formed. The SEM has a large depth of field, which allows a large amount of the sample to be in focus at one time. The SEM also produces images of high resolution, which means that closely spaced features can be examined at a high magnification. Preparation of the samples is relatively easy since most SEMs only require the sample to be conductive. The

combination of higher magnification, larger depth of focus, greater resolution, and ease of sample observation makes the SEM one of the most heavily used instruments in research areas today. This make the technique suitable for producing very impressive, in focus images from a highly irregular structure typical of catalyst specimens. This technique is of great interest in catalysis because of its high resolution[18]. The scanning electron microscope can be used to measure not only the composition profile of a surface, but also the geometric profile of its magnetic structure.

Scanning electron micrographs of the samples were taken using *Cambridge Oxford 7060* scanning electron microscope with a resolution of 1.38eV. The powdered sample is put on a double sided carbon tape on a metal strip. It is further sputter coated with gold to minimize the charging effect and to protect the material from thermal damage by the electron beam. A film of uniform thickness, about 0.1mm, was maintained for all the samples. A serious draw back of the analysis is the charging of the particles and also the result need not be the representative of the whole sample.

2.5 Surface acidity measurements

Solid acid catalysts in many commercial processes have proved to be more economical and often produce better quality products. Being stronger acids, they have a significantly higher catalytic activity compared to conventional acid catalysts[20]. Determining the quantity and strength of the acid sites is crucial to understanding and predicting the performance of a catalyst. Therefore the main task of catalyst technologists lies in the surface acidity measurements. Quantitative analysis of model surfaces using temperature

programmed desorption technique was developed in the early 1960s. The problem of finding the most relevant method for acidity measurement is an evolutionary process. Various methods have been used to find out the nature, strength and concentration of acid centers on the surface. Some techniques can distinguish between the Lewis acidity and Bronsted acidity. A large variety of probe molecules have been utilized to ascertain the surface acidity[21]. Similarly model reactions such as cumene cracking and cyclohexanol reaction are carried out to evaluate surface acidity.

Materials

The materials used for the acidity determination of the prepared catalysts are given below.

	Materials	**Suppliers**
1	Sulphuric Acid	Merck
2	Sodium Hydroxide	Merck
3	Cumene	Aldrich
4	Cyclohexanol	CDH
5	2,6 dimethyl pyridine	Merck
6	Ammonia	Merck
7	Phenolphthalein	Merck

Methods

2.5.1 Temperature Programmed desorption of ammonia

The temperature programmed desorption technique is one of the most widely used and flexible techniques for characterizing the acid sites on oxide

surface. The method is based on desorbing ammonia adsorbed on the solids by heating it at a programmed rate. Ammonia is an excellent probe molecule for the measurement of acid property by TPD, because it can be stabilized on acid sites. Its small molecular size allows ammonia to penetrate into all pores of the solid where larger molecules commonly found in cracking and hydrocracking reactions only have access to large micropores and mesopores. Also, ammonia is a very basic molecule, which is capable of titrating weak acid sites, which may not contribute to the activity of the catalyst. The strongly polar adsorbed ammonia is also capable of adsorbing additional ammonia from the gas phase. TPD experiment describes not only the number and strength of chemisorption sites, but it may also describe the surface heterogeneity of the surface sites. In principle, any chemical interaction between the adsorbate and adsorbent can be studied by the TPD technique.

The assumption in TPD is that the desorption energy is primarily the deprotonation energy of the solid acid[3]. Thus, a stronger acid requires a higher energy to deprotonate, but this direct relationship may be modified by the type of acid sites. This technique then could provide a relative amount of weak, medium and strong acidity in a solid, depending upon the temperature in which the desorption of an adsorbed base takes place. It may be noted that the temperature range associated with weak, medium or strong acid sites is rather arbitrary. Still the information and classification of the acid sites is useful. It has also been the practice to collect the desorbing base in a medium and then titrate against a standard acid to quantify the desorbed base, according to the temperature range in which it desorbs.

Ammonia TPD measurements were carried out in the range 100-600°C in a conventional flow type apparatus using a stainless steel reactor of 30 cm length and 1cm diameter kept in a cylindrical furnace. The catalyst is pelletized and put in the reactor under nitrogen flow at 300°C. After cooling to room temperature, ammonia was injected in the absence of carrier gas flow and allowed to attain equilibrium. The excess and physisorbed ammonia was flushed out using a current of nitrogen for half an hour. Under a controlled temperature programme, the amount of chemisorbed ammonia leached out for each 100°C was absorbed in a known volume of dilute sulphuric acid. The desorbed ammonia is estimated volumetrically by titrating with sodium hydroxide solution. The amount of ammonia desorbed in the temperature ranges 100-200, 200-400 and 400-600°C was assigned as measures of weak, medium and strong acid sites respectively.

2.5.2 Thermodesorption Studies of 2,6- dimethyl pyridine

2,6-dimethyl pyridine is a useful probe molecule for the selective determination of the Bronsted acid sites[22]. Due to steric hindrance of the methyl groups, 2,6-DMP gets selectively adsorbed at the Bronsted acid sites and thus the percentage weight loss during thermal treatment will correspond to the Bronsted acidity of the sample. Previously activated catalysts were kept in a desiccator saturated with vapours of 2,6-DMP for 48h for the effective and uniform adsorption. After this, the weight loss of the adsorbed samples was measured by thermogravimetric analysis in nitrogen atmosphere at a heating rate of 20°C/minute. The fraction of weight loss in the range of 300-600°C was found out and taken as a measure of the Bronsted acidity of the sample[23].

2.5.3 Cumene cracking reaction

Cumene cracking reaction is generally used as the probe reaction to characterize the acid properties of the solid acid catalyst. Cumene cracking mainly depends on Bronsted acid sites whereas dehydrogenation occurs on Lewis acid sites[24]. The major reactions taking place during the cracking of cumene are dealkylation to give benzene and propene and dehydrogenation to give á-methyl styrene. Thus it is possible b compare both Lewis and Bronsted acid sites in a catalyst through cumene conversion reaction. The vapour phase cumene cracking reaction is carried out in a fixed bed down flow vertical glass reactor. The reaction conditions are optimized and the product distribution of all the prepared systems is compared under the optimized conditions. The product analysis was achieved by using a gas chromatograph, comparing with authentic samples.

2.5.6 Cyclohexanol decomposition reaction

Cyclohexanol decomposition reaction may be used to characterize the acidity of solid acid catalyst. The amphoteric nature of cyclohexanol permits their interaction with acidic and basic sites resulting in dehydration and dehydrogenation. The reaction usually gives two types of products; cyclohexene and cyclohexanone. The selectivity to a particular product is determined by the acid base properties of the catalyst[25]. The reaction was carried out in a fixed bed down flow glass reactor and the reaction conditions are optimized. The catalyst samples are compared under the optimized reaction conditions and the liquid products were analyzed by using a gas chromatograph.

2.6 Catalytic activity measurements

The role of a catalyst in bringing about a chemical reaction is a stimulating one. In order to test the catalytic activity of the prepared systems, reactions are carried out both in liquid as well as vapour phase. In the present case, epoxidation of cyclohexene and hydroxylation of phenol is carried out in the liquid phase. Alkylation of aromatics to give various industrially important products can be successfully carried out in vapour phase over the prepared catalytic systems. All the systems are effective in dehydrogenating cyclohexane and cyclohexene. Titania, being a well known photocatalyst, the influence of modified metals on its photocatalytic activity is studied in detail. Photocatalytic oxidation of benzhydrol and photodegradation of methyl orange were done over the prepared catalysts.

Materials

The materials used for the catalytic activity measurement is as follows.

	Materials	Suppliers
1	Cyclohexene	Merck
2	Cyclohexane	Merck
3	TBHP in water	Aldrich
4	Phenol	Merck
5	Hydrogen peroxide	SD Fine-Chem Ltd
6	Tert-butanol	Qualigens
7	Aniline	Merck
8	Methanol	SD Fine-Chem Ltd

9	Anisole	Merck
10	Benzhydrol	SD Fine-Chem Ltd
11	Methyl orange	Merck
12	Acetonitrile	Merck

Methods

A brief description of the experimental procedure for the different types of reactions studied is given below. The catalytic activity was expressed as the percentage conversion and the selectivity for a product is expressed as the amount of the particular product divided by the total amount of products multiplied by 100.

2.6.1 Liquid Phase Reactions

Epoxidation of cyclohexene and hydroxylation of phenol was carried out in liquid phase. The reactants in the required molar ratio and a definite amount of the catalyst were taken in a 50ml round bottom flask fitted with a water condenser. The whole set up is placed in an oil bath put on the top of a magnetic stirrer. The temperature of the oil bath can be adjusted according to the requirement for a particular reaction and kept constant with the help of a dimmerstat. The product analysis was done using gas chromatograph (*Chemito*) equipped with Flame ionization detector and a capillary column.

2.6.2 Gas Phase Reactions

Applicability of the liquid phase reaction is often limited by low temperature requirement below the boiling point of the least boiling

component of the reaction mixture. Reactions can be done at much higher temperatures in the vapour phase set up where the reactants will be in the gas phase, which undergo reaction over the catalyst surface. Tert-butylation of phenol, methylation of aniline and anisole, dehydrogenation of cyclohexane and cyclohexene were done in vapour phase. These reactions were conducted at atmospheric pressure in the presence of N_2 in a fixed bed, vertical, down flow reactor inserted into a double zone furnace. A temperature controller was used to maintain the temperature of the reaction. The reactant was fed into the reactor with the help of a syringe pump at a controlled flow rate. The condensed reaction mixture was collected downstream from the reactor in a receiver connected through a cold water circulating condenser. The products were collected at regular intervals and analyzed gas chromatographically.

2.6.3 Photochemical reactions

The photocatalytic cativity of the prepared systems towards the oxidation of benzhydrol as well as the degradation of methyl orange is intensively studied. The reactios were carried out in a Heber photoreactor (multilamp type, model HML-MP88) containing concentrically arranged eight numbers of 8W mercury lamps of 365nm wavelength. In the methyl orange degradation, the extent of degradation was determined by using a *Shimadzu UV-Vis spectrophotometer* (UV-160A) at λ_{max} of 660nm. The product analysis of the photooxidation of benzhydrol was done gas chromatographically.

Reference

1   S.P.S. Andrew, CHEMTECH, 9 (1979) 180.

2   M. Campanati, F. Fornasari, A. Veccari, Catal Today, 77 (2003) 299.

3   B. Viswanathan, S. Sivasnker and A.V. Ramaswamy, "Catalysis-Principles and Applications.", Narosa Publishing House, New Delhi, p.92

4   H.P. Klug and L.E. Alexander, "X-Ray Diffraction procedures" John Wiley & sons, New York.

5   D.L. Bish and J.E. Post, Structures and Structure determination, Eds. H.G. Karge and J. Weitkamp, Springer 1999, "Modern Powder diffraction"

6   J.W. Niemantsverdriet, "Spectroscopy in Catalysis" Weinheim, New York, 1995.

7   D.K. Chakrabarthy, "Solid-state Chemistry" New Age International Ltd. New Delhi (1996) p.14

8   Clive Whiston, "X-Ray methods-Analytical Chemistry by open learning" John Wiley, New York (1987) Ch.3.

9   H.Lipson, H.Steeple, "Interpretation of X-Ray Powder Diffraction Patterns" Macmillan, London (1970) p.261.

10 G. Ertl, H. Koninger, J. Weitkamp, "Handbook of Heterogeneous Catalysis" Vol.2, VCH, Weinheim (1997) p.646.

11 H.G. Hecht, "Modern aspects of Reflectance Spectroscopy" W.W. Wendlandt (Eds), plenum Press, New York (1968)

12 M. Kamruddin, P.K. Ajikumar, S. Dash, A.K. Tyagi and Baldev Raj, Bull. Mater. Sci, 26 (2003) 449.

13 S. Brunauer, P.H. Emmette and E. Teller, J Am. Chem. Soc, 60 (1938) 309.

14 H. Knozinger, Catal. Today, 32 (1996) 71.

15 I.E. Wachs, "Characterisation of Catalytic Materials" Butterworth - Heinemann: Manning, (1992).

16 Kurt W. Kolasinski, Surface Science-Foundations of catalysis and Nanoscience. John Wiley & Sons, Ltd. (2001).

17 Hobart H. Willard, Lynne L. Merritt Jr, John A.Den, Frank A. Settle Jr, "Instrumental methods of Analysis", CBS Publishers, New Delhi (1986).

18 A. Howie, "In characterization of Catalysts", J. Thomas and R.M. Lambert Eds, John Wiley, New York (1980) 89.

19 G. Ertl, H. Koninger, J. Weitkamp, "Handbook of Heterogeneous Catalysis" Vol.2, VCH, Weinheim (1997) p.256.

19 D.K. Chakrabarthy, "Adsorption and Catalysis by solids", Wiley Eastern Ltd, New Delhi (1990) p.166.

20 P.A. Jacobs, "Characterization of Heterogeneous catalysts", F. Delanney (Eds), Elsevier, Amsterdam (1985) 311.

21 A. Corma, C. Rodellas and V. Hornes, J. Catal, 88 (1984) 374.

22 H.A. Benesi, J. Catal, 28 (1973) 176.

23 A. Satsuma, Y. Kamiya, Y. Westi, T. Hattori, Appl. Catal. A; Gen, 253 (2000) 194.

24 S.M. Bradley, R.A. Kydd, J. Catal, 141 (1993) 239.

25 M. Ai, Bull. Chem. Soc. Jpn, 50 (1997) 2579.

Chapter *3*

Physico Chemical Characterization

Abstract

The physico chemical characterization of both transition metal and rare earth metal incorporated titania systems were done in the present chapter. A detailed investigation was performed by different techniques such as X-Ray diffraction analysis, Energy dispersive X-Ray analysis, Surface area and pore volume measurements, TG-DTG analysis, FTIR spectroscopy, Scanning electron microscopy and UV-Vis diffuse reflectance spectroscopy. The evaluations of acid sites were done by two independent techniques such as TPD of ammonia and TGA of adsorbed 2,6-dimethyl pyridine. Test reactions such as Cumene cracking reaction and Cyclohexanol decomposition reaction were also carried out over the prepared systems to get an insight to the nature of surface acid site distribution.

3.1 Introduction

Catalysis plays a prominent role in our society. The catalyst characterization is a lively and highly relevant discipline in catalysis. It deals with the material science of the catalysts on a more or less mesoscopic scale, whereas the ultimate goal of fundamental catalytic research is to characterize the surface of a catalyst at the microscopic scale[1-2]. In heterogeneous catalysis, the reaction occurs at the surface. Catalysis and catalytic surfaces need to be characterized with reference to their physical properties and by their actual performance as a catalyst[3]. The most important properties are those relating to the surface because catalyst performance is determined by surface parameters. The catalytic properties of a surface are determined by its composition and structure. The surface acidity also plays a crucial role in determining the catalytic efficiency. Nanosize titania is attractive for many applications because of its large effective surface area which enhances the surface reactions.

3.2 Physical Characterization

Several approaches can be adopted to investigate fundamental relations between the state of a catalyst and its catalytic properties. Physical methods like X-Ray diffraction analysis (XRD), Energy dispersive X-Ray analysis (EDX), Surface area and pore volume measurements, TG-DTG analysis, Fourier ransform Infrared (FTIR) spectroscopy, Scanning electron microscopy (SEM) and UV-Vis diffuse reflectance spectroscopy were employed to characterize the prepared catalysts. The results are discussed in the following sections.

3.2.1 X-Ray diffraction analysis (XRD)

Powder X-Ray diffraction (XRD) was used for crystal phase identification, estimation of the anatase to rutile ratio and of the crystallite size of each phase present. Figures 3.1 to 3.3 illustrate the X-Ray diffraction patterns of the pure as well as modified titania systems calcined at 500°C. The XRD data of the prepared systems agree well with the standard values given in the JCPDS data cards, thus confirming the crystalline phases of titania. The diffraction lines for anatase are observed at 2θ values 25.5, 37.4, 48 and 53° while that of rutile type appear at 27, 36, 41 and 54°.

The selection of calcination temperature is of critical importance in catalysis. In the case of mixed metal oxides, substantially elevated temperature may be required to cause mixing by diffusion of individual species to form a desired compound or crystal phase. The crystalline phase formation also depends on the calcination temperature. It has been reported that the transition of amorphous titania to crystalline titania takes place at 350°C for pure titania. An earlier study on the kinetics of the anatase to rutile transformation has shown that the transformation involves an overall contraction or shrinking of the oxygen structure and a co-operative movement of ions. The transformation needs to overcome both the strain energy for the oxygen ions to reach their new configuration and the energy necessary to break the Ti-O bonds as the titanium ions redistribute. A high activation energy is required for this purpose (over 420 KJ/mol) and so the phase transition takes place only at a high temperature[4]. Also the phase transformation is generally accompanied with the crystal growth. In the present case, the titania samples calcined at 500°C contain only the characteristic peaks of anatase[5].
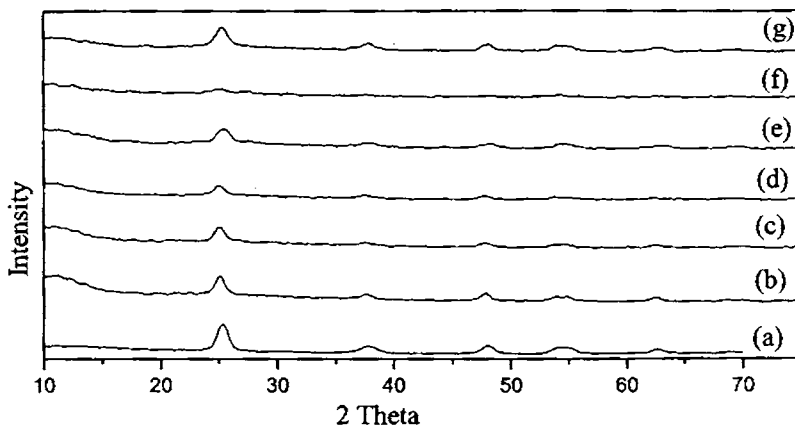
Figure 3.1

XRD profiles of (a) Pure Ti, (b) TiCr2, (c) TiMo2, (d) TiW2, (e) TiLa2, (f) TiPr2 and (g) TiSm2

The low peak intensity in the metal incorporated titania samples reveal the lowering of crystallinity after incorporation of the corresponding metal. Anatase is the predominant phase in all transition metal incorporated systems. But the rare earth metals like praseodymium is capable of enhancing the anatase to rutile phase transformation whereas samarium and lanthanam incorporated systems stabilises the anatase phase considerably. Prevention of agglomeration through metal incorporation accounts for the stabilisation of the anatase phase. The characteristic peak of the incorporated metal oxide was not evidenced even at the 10 wt. % metal loading. This might indicate either the dispersity of the incorporated metal oxide species or the small crystallinity of these species particle diameter i.e., particle size below the detection limit of

XRD.Another possibility is that the added metal species are present in the form of solid solution. The bulk structure remains virtually unchanged by the incorporation of the metals.
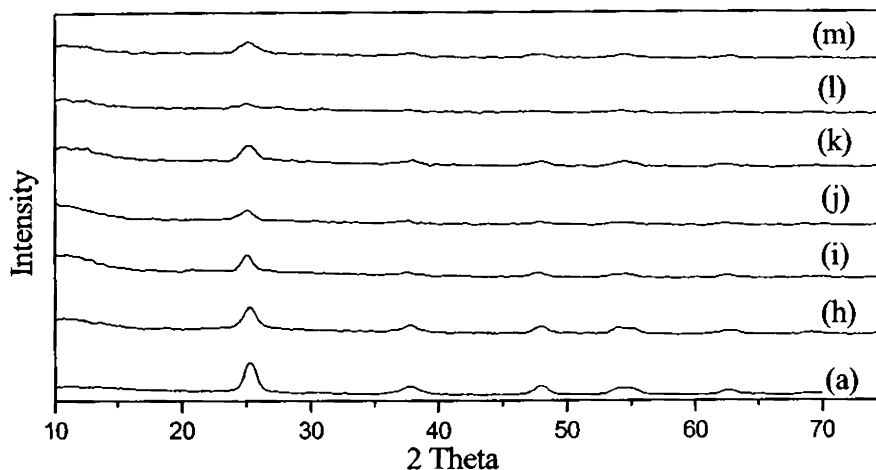
Figure 3.2

XRD profiles of (a) Pure Ti, (h) TiCr6, (i) TiMo6, (j) TiW6, (k) TiLa6, (l) TiPr6 and (m) TiSm6.

The average crystallite size is calculated using Scherrer equation[6-7] from the 101 reflection of anatase is given in tables 3.1 and 3.2. The crystallite size decreases with the increase in the percentage of the metal incorporated. This may be due to the interaction of the incorporated metal with the titania network, and thus hinder the growth of the particles. Praseodymia incorporated systems show a more or less different behavior. Among those systems, the highest crystallite size is shown by 10% praseodymium incorporated ones.

These systems are found to be less crystalline and the powder XRD patterns clearly indicate the rutile phase present.
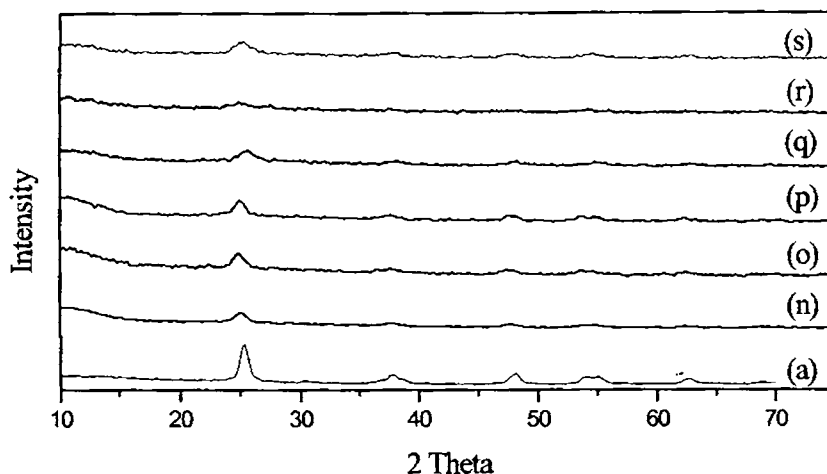
Figure 3.3

XRD profiles of (a) Pure Ti, (n) TiCr10, (o) TiMo10, (p) TiW0, (q) TiLa10, (r) TiPr10 and (s) TiSm10.

3.2.2 Surface Area and Pore Volume Measurements

The variation in surface area, pore volume and crystallite size with transition metals as well as rare earth metals loading is presented in tables 3.1 and 3.2. The surface area of titania is increased considerably in the presence of small amounts of other transition metals as well as rare earth metals. Further, there is a remarkable improvement in the high temperature stability of pores upon metal incorporation. This is in agreement with the observation reported

by Kumar[8] *et al* and Gopalan and Lin[9]. The improvement in the textural characteristics can be attributed to the better intaraction between titania and the incorporated metals. Upon calcinations, the oxides of the incorporated metals are distributed uniformly in the titania gel matrix.

Table 3.1

Surface area, Pore volume and Crystallite size of the prepared systems

Catalyst	Surface area (m^2/g)		Pore volume (X 10^{-6}m^3/g^{-1})	Crystallite Size (X 10^{-9}m)	Pore Diameter (X 10^{-9}m)
	BET	Langmuir			
Ti	79.3	192.2	0.1	8.6	5.6
TiMo2	104.0	214.2	0.1	9.0	5.0
TiMo6	117.0	220.7	0.2	7.7	5.5
TiMo10	117.0	306.7	0.1	6.7	4.8
TiCr2	90.5	192.1	0.1	8.6	5.8
TiCr6	101.7	267.4	0.2	7.4	9.4
TiCr10	112.0	290.8	0.2	6.0	8.2
TiW2	111.0	303.3	0.2	9.5	5.8
TiW6	112.0	290.1	0.2	8.5	5.4
TiW10	119.6	304.0	0.2	6.2	5.4

Among different metal incorporated systems, there was no significant variation in the surface area values. Addition of transition metal species causes a further setback to the crystallization and sintering process, which is evident from the higher surface area of the samples in comparison with pure titania.

The metal oxide species along with incorporated ones prevent the agglomeration of titania particles resulting in a higher surface area.

Table 3.2

Surface area, Pore volume and Crystallite size of the prepared systems

Catalyst	Surface area (m^2/g)		Pore volume (X 10^{-6}m^3/g^{-1})	Crystallite Size (X 10^{-9}m)	Pore Diameter (X 10^{-9}m)
	BET	Langmuir			
TiLa2	110.7	308.2	0.2	8.9	6.2
TiLa6	111.2	289.0	0.3	8.5	9.4
TiLa10	106.0	276.3	0.2	7.1	7.6
TiPr2	112.0	292.5	0.2	7.1	5.4
TiPr6	116.7	295.5	0.1	9.0	4.8
TiPr10	129.8	336.1	0.2	10.8	4.6
TiSm2	105.2	276.6	0.3	7.4	10.3
TiSm6	107.0	285.6	0.3	4.6	11.6
TiSm10	116.5	113.4	0.3	4.4	11.00

Assuming the pores are cylindrical, the average pore diameter is calculated using the formulae, $d = 4Vp/Sp$, where d is the average pore diameter, Vp is the pore volume and Sp is the surface area[10]. From the results, a gradual increase in the pore diameter is seen with the percentage of metal incorporation upto 6 wt% metal loading and thereafter the average pore diameter decreases when 10 wt% of the metal is incorporated. There is a reduction in crystallite size of the systems as the percentage of the metal incorporated increases. According to Ding and Liu, the decrease in grain size increases the rate of grain growth process. The reduction in crystallite size is

proposed to be due to segregation of the incorporated metal cations at the grain boundary, which inhibits the grain growth by restricting the direct contact of grains.

3.2.3 Energy Dispersive X-Ray Fluorescence Analysis (EDX)

The elemental compositions of the prepared catalytic systems determined by EDX analysis is presented in table 3.3. The percentage of the metal retained in the systems upon calcinations at 500°C is also given. The results clearly indicate that the expected catalyst profile can be successfully achieved by the present preparation method since the amount of the metal incorporated is close to the expected value except in the case of molybdenum and tungsten incorporated systems. This can be due to the loss of tungstate and molybdate ions as soluble ammonium tungstate during the gelation process.

Table 3.3

EDX data for titania as well as their modified analogues

Catalyst	TiO_2	Metal	Catalyst	TiO_2	Metal
Ti	100		TiLa2	97.0	3.0
TiMo2	99.0	1.0	TiLa6	90.4	9.6
TiMo6	96.1	3.9	TiLa10	86.0	14.0
TiMo10	94.1	5.9	TiPr2	96.3	3.7
TiCr2	97.0	3.0	TiPr6	89.9	10.1
TiCr6	90.9	9.1	TiPr10	86.0	14.0
TiCr10	86.6	13.5	TiSm2	96.4	3.6
TiW2	99.0	1.0	TiSm6	90.5	9.5
TiW6	97.1	2.9	TiSm10	85.4	14.6

3.2.4 Scanning Electron Microscopy (SEM)

The scanning electron micrograms of representative samples are given in Fig. 3.4 and 3.5. The particles tend to agglomerate upon the incorporation of transition metals as well as rare earth metals. As a consequence, the particle size also increases. The results obtained from XRD can be well correlated with the SEM results.
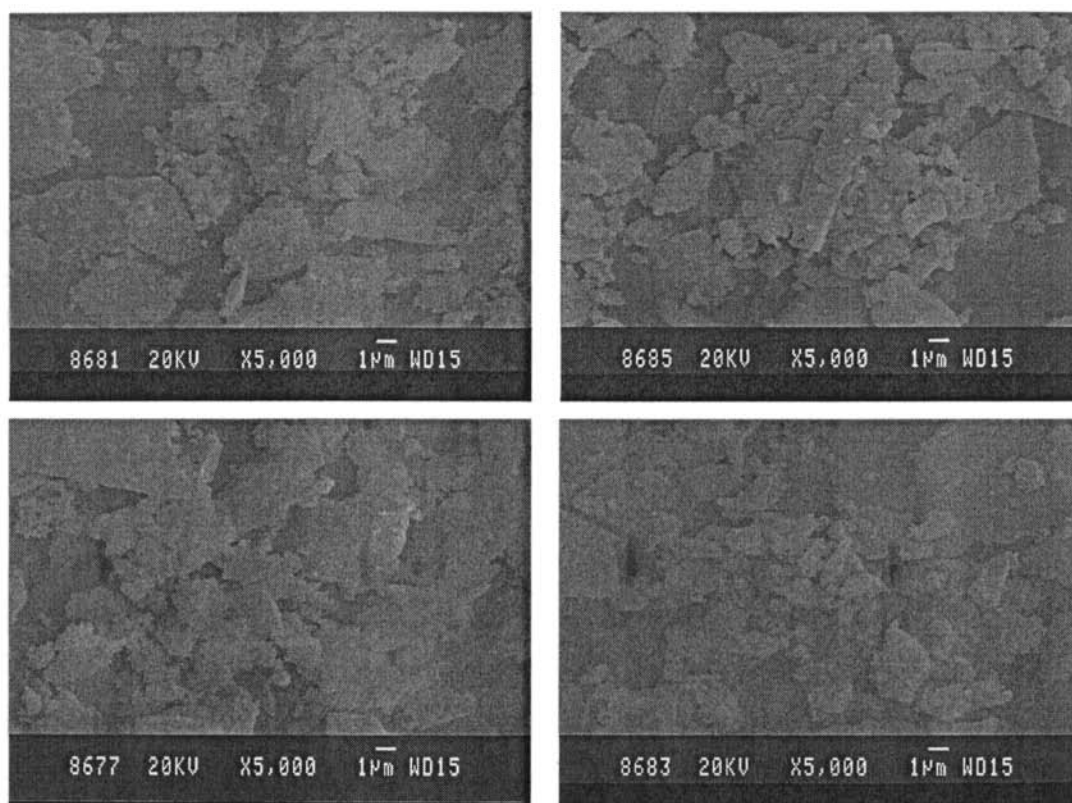
Figure 3.4

Scanning Electron Micrographs of (a)Ti (b)TiMo6, (c) TiCr6, (d) TiW6
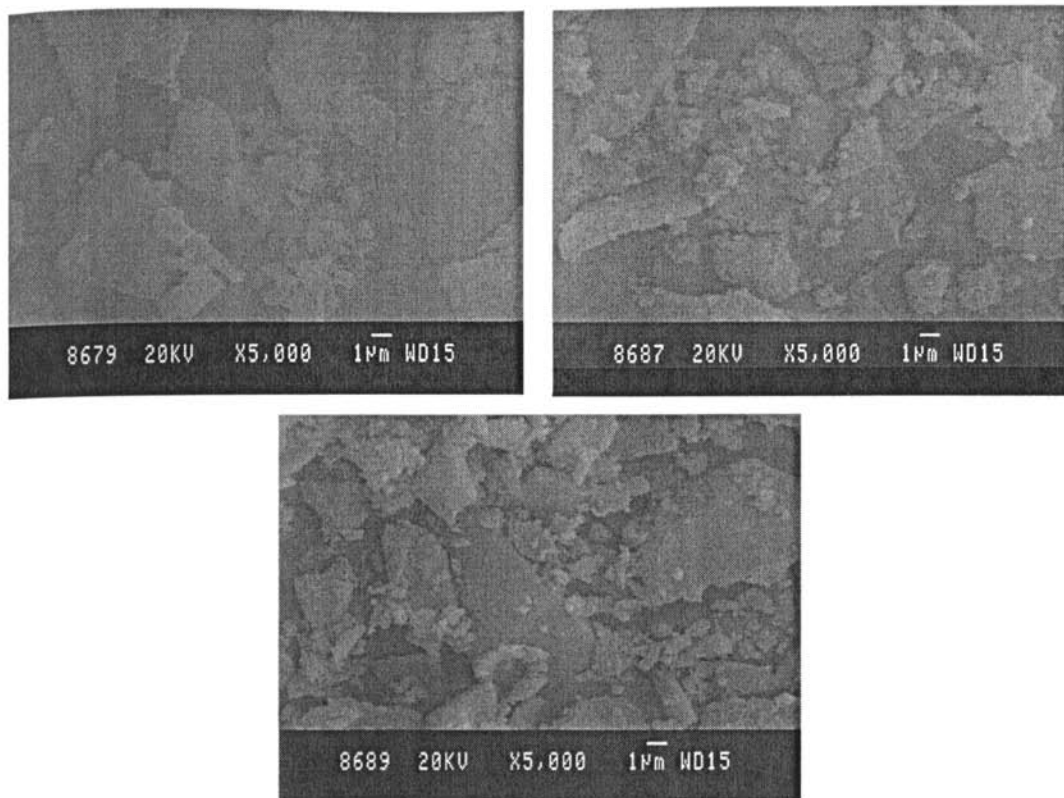
Figure 3.5

Scanning Electron Micrographs of Rare Earth Metal modified titania systems

The scanning electron micrographs of the representative samples calcined at 700°C are presented in figure 3.6. With the increase in calcination temperature, the particles grow bigger in size due to sintering effect of the grains. The presence of other metal cations retards the grain growth of titania particles. The distribution of the oxides of the incorporated metals may be more or less in the intergranular region and decrease the diffusion barrier at the anatase - anatase grain contact.
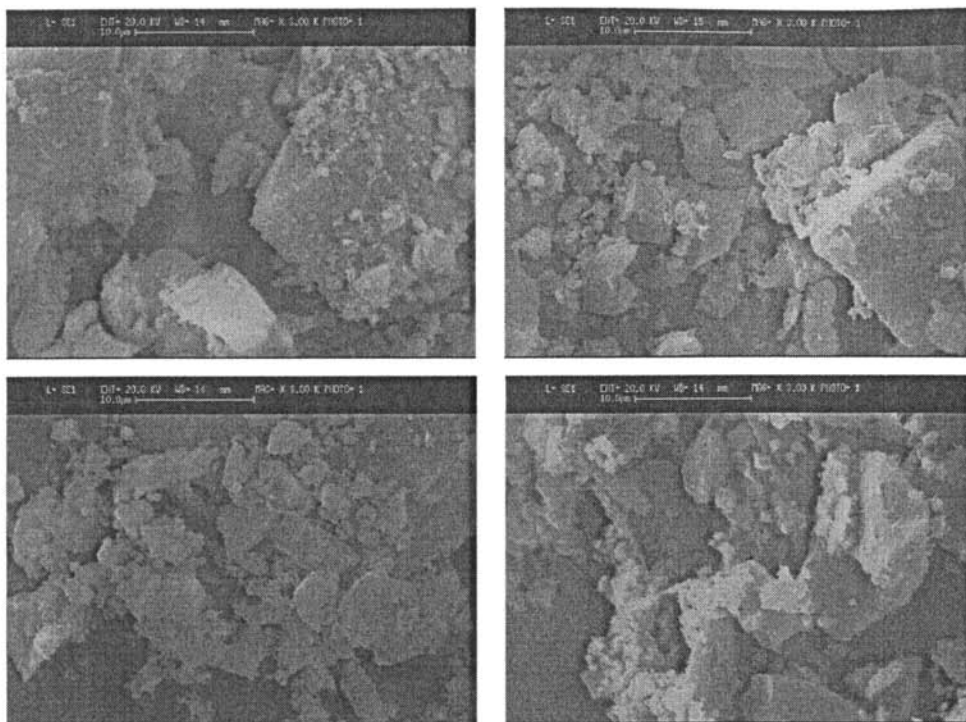
Figure 3.6

Scanning Electron Micrographs of (a) Ti, (b) TiCr10,

(c) TiSm10 and (d) TiPr10 calcined at 700°C.

3.2.5 Thermogravimetric Analysis

The thermal stability of the samples was examined by TG-DTG analysis. Thermogravimetric curve for representative systems are presented in figures 3.7 and 3.8. The mathematically obtained differential curve is also plotted in order to clarify the weight loss processes. The high thermal stability of metal incorporated titania systems is clear from TG/DTG curve.
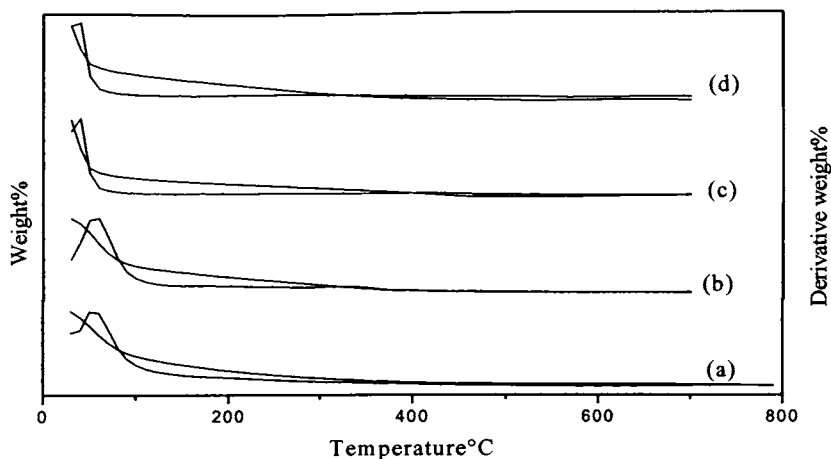
Figure 3.7

TG/DTG of (a) Pure Ti (b) TiMo6 (c) TiCr6 (d) TiW6

TG/DTG pattern of all the systems show a continuous dehydration over the entire temperature range studied. The first step below 110°C is due to the removal of adsorbed water[11]. Another small dip in the region of 250 to 300°C may be due to the removal of structural water present in the sample. The removal of structural hydroxyls will increase the number of bridging oxygens and hence the monolithic nature of the gel[12]. There is a possibility for the additional weight loss in metal incorporated titania systems in the range 320 to 350°C due to the decomposition of nitrates that become incorporated in the gel matrix. In all these thermograms, no apparent weight loss is observed upto 600°C after transformation of metal salts to corresponding metal oxides.
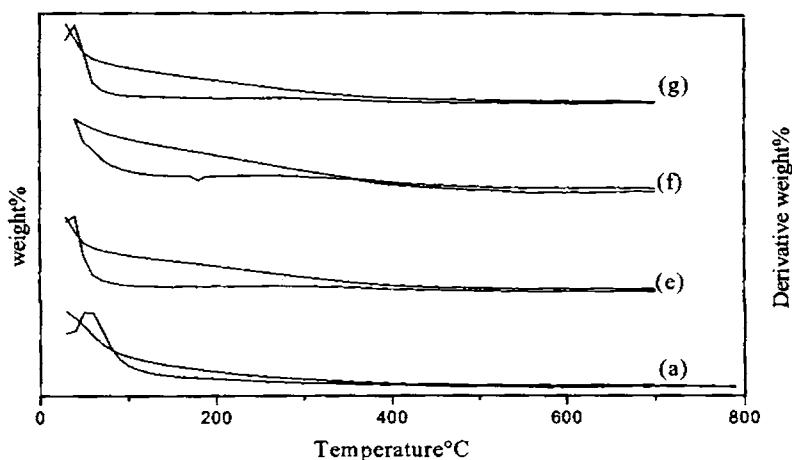
Figure 3.8

TG/DTG of (a) Pure Ti   (e) TiSm6   (f) TiLa6 (g) TiPr6

3.2.6 UV-Vis Diffuse Reflectance Spectroscopy

UV-Vis diffuse reflectance spectral analysis of titania as well as their modified analogues is carried out. The wavelength is shifted to lower wavelength region upon metal incorporation. As from the relationship of the absorption edge λ_g and the band gap energy E_g, λ_g = 1240/E_g (eV), the band gap energy of all the prepared systems are calculated and it is given in table 3.4. It has been reported for pure anatase, the significant increase in the absorption at wavelengths shorter than 380 nm can be assigned due to the intrinsic band gap absorption of anatase[13]. The band gap energy estimated for pure anatase is 3.53eV in the present case. This value is slightly higher than the reported value for anatase (3.2-3.3eV)[14]. The band gap energy observed for TiO_2 Degussa P25

and Hombikat UV-100 reported in the literature is about 3.5ev[15]. The band gap is a strong function of titania particle size for diameters less than 10nm because of the well known quantum size effect[16]. The interface interaction (matrix support effect) and changes in the coordination and ligand environment and the interatomic distances of titania microdomains also results in the changes in the band gap absorption edge[17-24]. Modification with other metal ions has a significant impact on the electronic properties of titania. But a direct relationship with the percentage of metal incorporation and the band gap energy of titania couldn't be obtained in the present study.

Table 3.4

λ_{max} and band gap energy obtained from UV-Vis DRS analysis

Catalyst	λ_{max} (nm)	Band gap Energy (eV)	Catalyst	λ_{max} (nm)	Band gap Energy (eV)
Ti	350.7	3.5			
TiMo2	299.3	4.1	TiLa2	299.1	4.1
TiMo6	341.5	3.6	TiLa6	250.0	5.0
TiMo10	332.7	3.7	TiLa10	254.3	4.9
TiCr2	322.5	3.9	TiPr2	287.7	4.3
TiCr6	295.1	4.2	TiPr6	264.6	4.7
TiCr10	523.6	2.4	TiPr10	268.9	4.6
TiW2	290.6	4.3	TiSm2	270.3	4.6
TiW6	321.0	3.9	TiSm6	309.6	4.0
TiW10	277.7	4.5	TiSm10	277.7	4.5

UV-Vis DRS is used to probe the band structure or molecular energy levels in materials since the UV light excitation creates the photogenerated electrons and holes. Thus information about the properties of metal oxides can be obtained from diffuse reflectance UV-Vis spectroscopy. This finds applications in the field of photocatalysis.
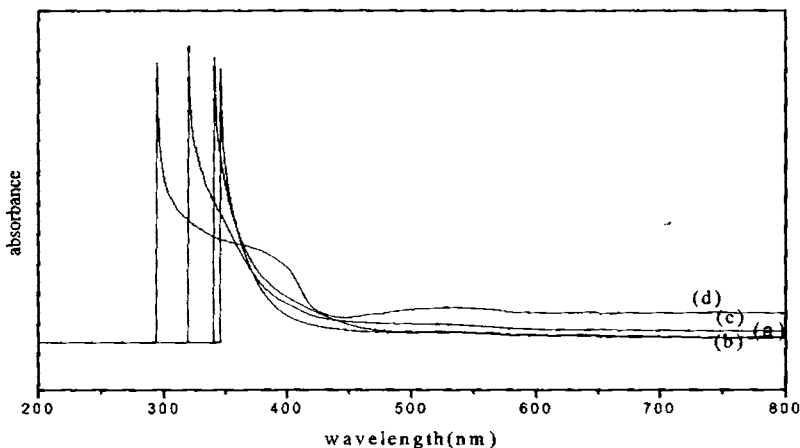
Figure 3.9

UV-Vis Diffuse Reflectance Spectra of (a) Ti (b) TiMo6 (c) TiCr6 (d) TiW6

Titania is a well known semiconductor oxide with a measured band gap energy. Characteristic absorption band for tetrahedrally coordinated titanium appear at about 300-400 nm. The absorption is associated to the $O^{2-} \rightarrow Ti^{4+}$ charge transfer corresponding to the electronic excitation from the valence band to the conduction band. In the presence of higher amounts of chromium, the spectrum shows a different behaviour. The peak is observed at a wavelength of 523.58nm and the charge transfer transition for tetrahedrally coordinated titanium gets overlapped with this broad peak. The additional band

near 600 nm is attributed to the $^4A_{2g} \rightarrow {}^4T_{1g}$ transitions for Cr(III) ions in an octahedral environment[25]. However Cr(III) $\rightarrow$ Ti(IV) charge transfer transitions which may be alternatively described as excitation of an electron of Cr(III) to the conduction band of TiO_2 cannot be ruled out[26].
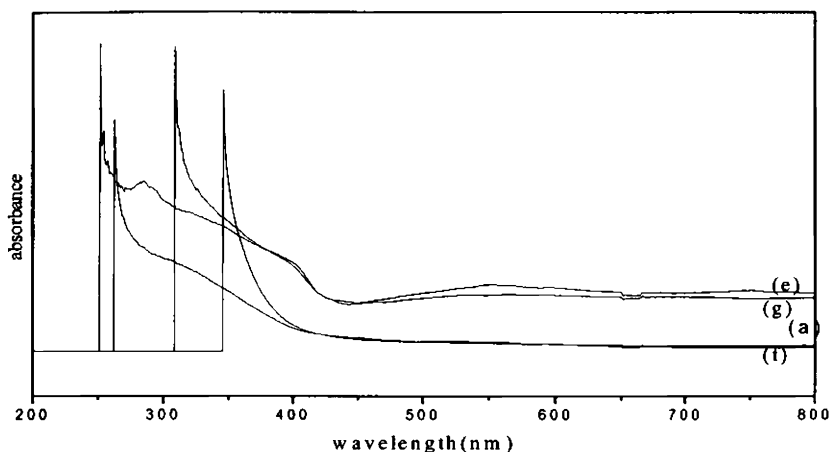
Figure 3.10

UV-Vis Diffuse Reflectance Spectra of (a) Ti (e) TiLa6 (f) TiPr6 and (g) TiSm6

3.2.7 Fourier Transform Infrared (FTIR) Spectroscopy

Figures 3.11 to 3.14 present the FTIR spectra of the representative systems calcined at 500°C. The spectra for pure titania shows a characteristic absorption bands at 1613 cm^{-1} corresponding to the bending vibrations of adsorbed molecular water. A small peak at 3430 cm^{-1} corresponds to the stretching vibrations of OH groups. It has been reported that the oxide supports

generally terminate with surface OH groups, which are quite polar and give strong IR bands[27] in the 3000-4000 cm^{-1} and 1600-1700 cm^{-1}.
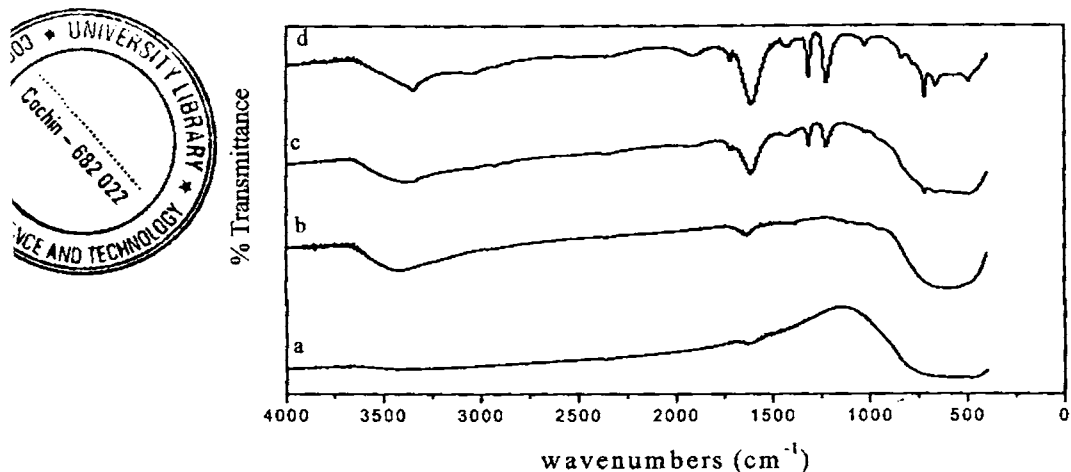
Figure 3.11
FTIR spectra of (a) Ti (b) TiCr6 (c) TiMo6 and (d) TiW6

Additional band around 480 cm^{-1} are also observed which is the characteristic peak of titania. The vibration modes of anatase skeletal O-Ti-O bonds in the range of 400-900cm^{-1}with a maximum at around 474 cm^{-1} is also reported in literature[28-30]. The peaks present in the tungsten modified titania systems at 650-950 cm^{-1} points to the presence of some tungsten oxides formed in between the crystal lattices of titania during calcination. In molybdena incorporated systems, another small peak having a lower intensity is observed in the region 1050-900°C which is attributed to the terminal Mo=O vibrations. Some sort of Ti-O-M bonding in rare earth modified titania systems is also evident from their respective FTIR spectrum.
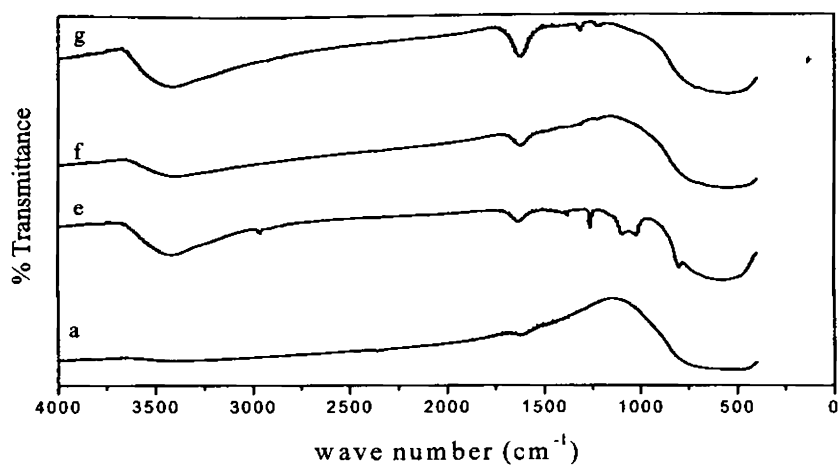
Figure 3.12

FTIR Spectra of (a)Ti, (e) TiLa6, (f)TiPr6 and (g) TiSm6
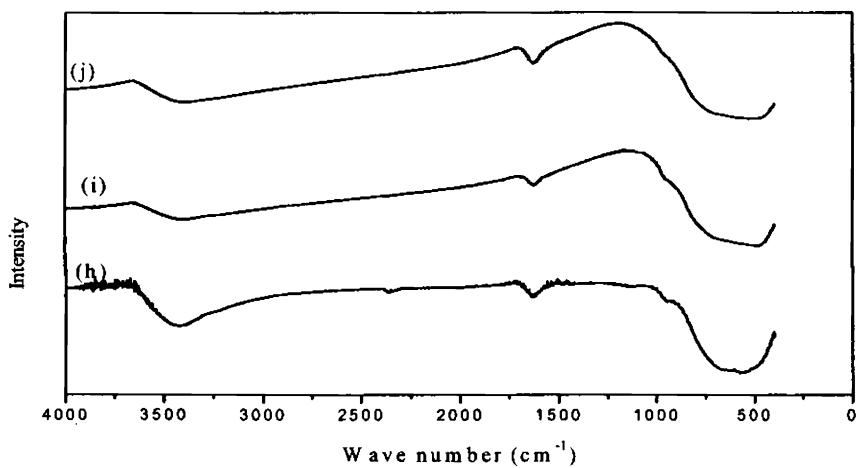
Figure 3.13

FTIR Spectra of (h) TiCr10, (i) TiMo10, (j) TiW10
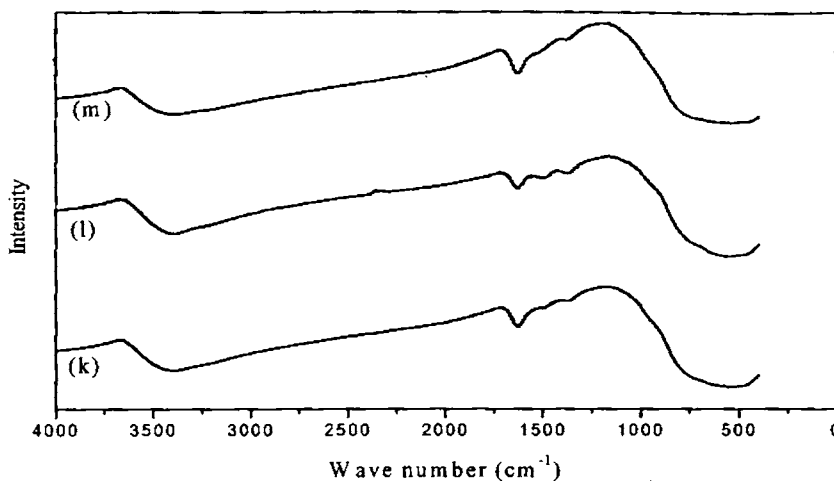
Figure 3.14

FTIR Spectra of (k) TiLa10, (l) TiPr10 and (m) TiSm10.

3.3 Surface Acidity Measurements

Solid acid catalysts are the backbone of major processes of refining and of petrochemistry. In reactions occurring by acid catalysis, the activity, selectivity and stability of the solid acids are obviously determined to a large extent by their surface acidity (i.e., the number, nature, strength and density of their acid sites)[31]. The acidity of solids often plays a significant role when they are used as supports of catalytic species. Interaction of the support with the active components (support effect) can influence their catalytic properties. Moreover, for certain reactions, new paths involving the joint participation of the acid sites and other types of sites can occur. The rate and selectivity of reactions that do not occur by acid catalysis can also be affected by acidity.

This has been shown in the case of oxidation of hydrocarbons on transition metal oxides.

The amount of acid or acidity, as a function of the acid strength, is an interesting feature of solid catalysts. The surface properties of anatase titania strongly depends on the presence of impurities. Tanabe *et al* proposed a hypothesis, which explains well the mechanism of formation of acid sites in binary oxides and predicts whether the acid sites will be of the Bronsted or Lewis type. The hypothesis applies to a case where small amount of the metal oxide (guest) is introduced into a matrix metal oxide (host). The portion of a guest is considered to be 1-10 atom. According to the hypothesis, the acid site is formed by an excess of negative or positive charge in a model structure of the binary oxide[32-33].

3.3.1 Temparature Programmed Desorption (TPD) of Ammonia

Given the great use and versatility of solid acids, it is very important to derive accurate methods for characterizing their acidity and predicting their value as catalysts. The methods most frequently based on the chemisorption of basic compounds. Basic molecules such as ammonia[34-36], pyridine[37] and n-butyl amine are the generally used probe molecules. Among these molecules, ammonia is most widely used; being a small molecule, it has greater accessibility to almost all acidic sites including the weak ones[38]. The acid site distribution pattern can be classified into weak (desorption at 100-200°C), medium (200-400°C) and strong (400-600°C) acid sites. Total acidity is also shown as the sum of amount of ammonia desorbed from the entire temperature region. The amount of ammonia desorbed at 100°C may contain some amount

of physisorbed ammonia too. Tables 3.5 and 3.6 give the strength of acid sites of titania and modified titania systems determined by ammonia TPD method.

Table 3.5

Influence of transition metal on the acid site distribution of titania

Catalyst	Amount of Ammonia desorbed (mmol/g)			
	Weak (100-200°C)	Medium (200-400°C)	Strong (400-600°C)	Total (100-600°C)
Ti	0.20	0.12	0.03	0.27
TiMo2	0.19	0.23	0.08	0.42
TiMo6	0.60	0.33	0.13	0.89
TiMo10	0.57	0.52	0.20	1.13
TiCr2	0.26	0.18	0.14	0.48
TiCr6	0.33	0.20	0.31	0.69
TiCr10	0.43	0.05	0.27	0.73
TiW2	0.19	0.09	0.12	0.39
TiW6	0.17	0.23	0.20	0.45
TiW10	0.45	0.13	0.12	0.64

From the table, it is revealed that pure titania possesses comparatively lower amount of acid sites. Considerable enhancement in the surface acidity was observed upon metal modification. The TPD data of metal modified systems show a gradual increase in the acidity with the increase of the percentage of the metal incorporated. The combination of titania with both transition metals and rare earth metals probably generates stronger acid sites and more acidity as compared with the separate components. The nature of

acid sites is greatly altered by the nature of the ions incorporated into the lattice. The change in the distribution may be a coupled effect of the crystalline as well as structural changes. The change in the acid strength distribution for the different systems may be related to the interaction of the added metal cations with titania.

Table 3.6

Influence of rare earth metal on the acid site distribution of titania

Catalyst	Amount of Ammonia desorbed (mmol/g)			
	Weak (100-200°C)	Medium (200-400°C)	Strong (400-600°C)	Total (100-600°C)
Ti	0.20	0.12	0.03	0.26
TiLa2	0.10	0.01	0.19	0.29
TiLa6	0.13	0.05	0.17	0.33
TiLa10	0.12	0.11	0.15	0.35
TiPr2	0.11	0.13	0.13	0.36
TiPr6	0.25	0.16	0.20	0.58
TiPr10	0.37	0.30	0.27	0.72
TiSm2	0.01	0.05	0.15	0.21
TiSm6	0.08	0.05	0.10	0.24
TiSm10	0.10	0.07	0.09	0.24

3.3.2 Thermodesorption Studies of 2,6-Dimethyl Pyridine

The thermodesorption study of 2,6-dimethylpyridine was carried out with an intention of obtaining a comparative evaluation of the Brönsted acidity in the samples. Upon thermal treatment, 2,6-DMP gets desorbed at different

temperature ranges depending on the strength of the acidic sites on which they are adsorbed. Lahosse *et al* found that using 2,6-DMP, which is s a stronger base than pyridine, they were able to detect by IR, Bronsted acidity at the surface of titania-alumina mixed oxides, but only Lewis acidity when using pyridine[39-40]. 2,6-dimethyl pyridine cannot coordinate to Lewis acid sites because of steric hindrance. The acid site distribution obtained from desorption of 2,6-DMP can be tabulated as in table 3.7 and 3.8.

Table 3.7

Influence of transition metals loaded on Bronsted acid site distribution of titania from 2,6-DMP desorption studies

| Catalyst | Relative weight (%) loss of 2,6-DMP desorption | | | |
	Weak (300-400°C)	Medium (400-500°C)	Strong (500-600°C)	Total (300-600°C)
Ti	0.56	0.38	0.09	1.03
TiMo2	3.50	3.62	0.41	7.53
TiMo6	0.74	3.43	3.93	8.10
TiMo10	3.54	3.64	0.95	8.13
TiCr2	2.71	2.77	0.50	5.98
TiCr6	3.57	3.57	0.42	7.56
TiCr10	3.72	2.83	0.49	7.04
TiW2	2.53	1.37	0.52	4.78
TiW6	3.16	2.73	0.19	6.08
TiW10	2.78	1.92	1.28	5.98

Satsuma *et al* reported that the coordinatively adsorbed 2,6-dimethyl pyridine on Lewis acid sites could be eliminated by employing a purging temperature above 300°C[41]. Thus it can be concluded that the amount of 2,6-DMP adsorbed at temperatures above 300°C originates exclusively from Bronsted acid sites. It has also been reported that the IR bands corresponding to dimethyl pyridine associated with Lewis acid sites disappeared with an increase in the desorption temperature[42]. Those molecules adsorbed at strong acid sites desorb only at high temperatures while those adsorbing on weak and medium acidic sites desorb at relatively low temperatures. Desorption below 300°C was omitted in the calculation since it contains contribution from the Brönsted as well as weak Lewis acid sites. So for a crude approximation, it may be assumed that the desorption in the range 300 to 400°C arises from the weak sites and those in the range 400 to 500°C corresponds to medium acid strength while the strong acid sites give desorption above 500°C.

From the tables, it can be concluded that the relative amounts of Bronsted acid sites increases by the incorporation of transition metals as well as rare earth metals into the crystal lattice of titania. Thus a clear relationship was found between the metal content and the acid strength as well as density; both increased with the increase of metal content. Comparatively higher amounts of Bronsted acid sites are present in the transition metal modified titania systems than that of rare earth modified ones. The highest Bronsted acidity is shown for molybdena incorporated titania systems. A Bronsted acid site also requires a hydroxyl group, and it is postulated that the number of sites was limited by the availability of hydroxyl species.

Table 3.8

Influence of rare earth metals loaded on Bronsted acid site distribution of titania from 2,6-DMP desorption studies

Catalyst	Relative weight (%) loss of 2,6-DMP desorption			
	Weak (300-400°C)	Medium (400-500°C)	Strong (500-600°C)	Total (300-600°C)
Ti	0.56	0.38	0.09	1.03
TiLa2	1.05	1.99	0.13	3.17
TiLa6	0.98	1.56	1.41	3.95
TiLa10	1.01	2.56	0.51	4.08
TiPr2	1.52	1.73	0.53	3.78
TiPr6	2.15	1.38	0.50	4.03
TiPr10	2.73	1.08	0.57	4.38
TiSm2	0.57	0.99	0.57	2.13
TiSm6	1.38	0.73	0.47	2.58
TiSm10	1.31	1.05	0.87	3.23

3.3.3 Gas Phase Cumene Cracking Reactions

Model reactions constitute an efficient means for measuring the surface acidity of the solids especially in terms of the nature, strength and density of the acid sites. Cumene cracking reaction is a test reaction for the simultaneous determination of Bronsted as well as Lewis acidity. The major reactions occurring during cumene conversion may be grouped into dealkylation (cracking) and dehydrogenation. Dealkylation of cumene yields benzene and propene whereas dehydrogenation gives α-methyl styrene[43]. Another

possibility is the cracking of the alkyl chain to give ethylbenzene. Ethylbenzene on dehydrogenation give styrene. The cumene conversion reaction can be schematically represented as shown in Fig. 3. 15. The reaction conditions are optimised in terms of flow rate and reaction temperature. The cumene conversion and relative product selectivity could be correlated with the surface acidic properties as established by the following sections. All the reactions were performed over 0.5g TiLa6 catalyst.
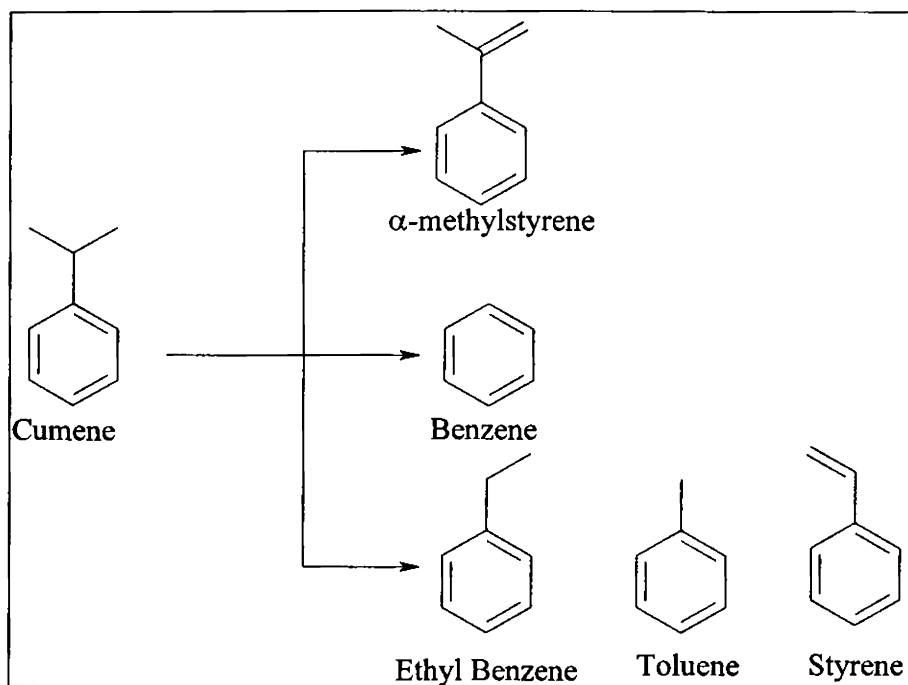
Figure 3.15

General Scheme for Cumene Cracking Reaction

A. Effect of temperature

Figure 3.16 shows the influence of reaction temperature on cumene conversion and product selectivity. The reactions were carried in a temperature range from 300 to 450°C at a flow rate of 4ml/h. The enhancement in catalytic activity with temperature is very clear from the figure. The selectivity to α-methyl styrene increases with temperature upto 400°C and ~~therefore~~ *after* decreases when the temperature reaches 450°C, with a simultaneous increase in the selectivity of the dealkylated products. At higher temperatures, there is a possibility for some of the Bronsted acid sites to get converted to Lewis acid sites. Hence dehydrogenation is favoured at higher temperatures. Considering the cumene conversion and percentage α-methyl styrene selectivity, the optimum temperature chosen was 400°C.
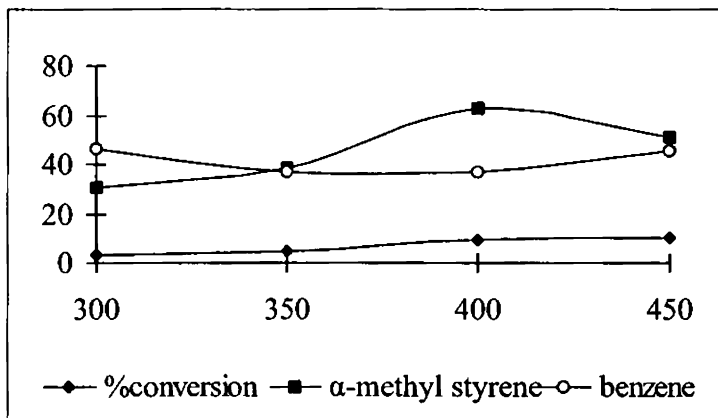
Figure 3.16

Influence of Reaction Temperature on cumene conversion and product selectivity

Amount of the catalyst-0.5g TiLa6, Flow rate-4ml/h, Duration-2h

---

B. Effect of flow rate

Figure 3.17 demonstrates the effect of flow rate on cumene cracking reaction. The flow rate depends on the residing time of the reactants on the catalyst surface. Increase in flow rate increases the ~~flow rate~~ *percentage conversion* and then decreases beyond an optimum value. An optimum flow rate of 4ml/h was chosen for all the reactions considering the cumene conversion as well as product selectivity.
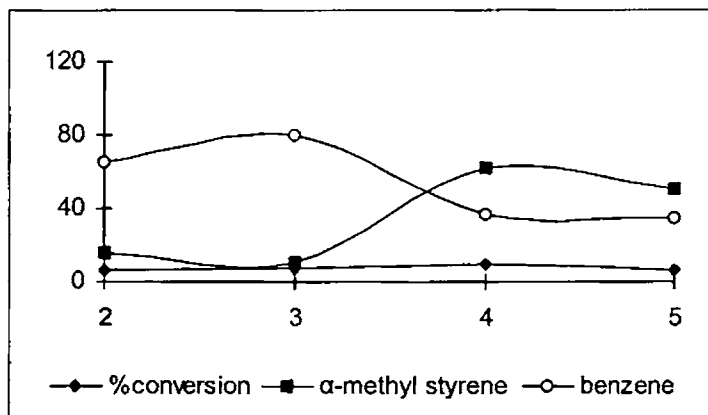
Figure 3.17

Influence of Flow Rate on cumene conversion and product selectivity

Amount of the catalyst-0.5g TiLa6, Temperature-400°C, Duraton-2h

C. Effect of time on stream

The reaction was carried out for a continuous 7h run over the prepared catalysts and the product analysis was done at a regular time intervals of 1h. The results obtained are presented in figure 3.18. The catalytic activity was found to decline gradually with reaction time. The decrease in overall conversion is associated with a rapid decrease in the amount of benzene

produced and must result from poisoning of active acidic sites on the surface by polymerization of the propene produced by the cumene dealkylation[44]. The decrease of catalytic activity may also be due to the coke formation during the reaction[45].
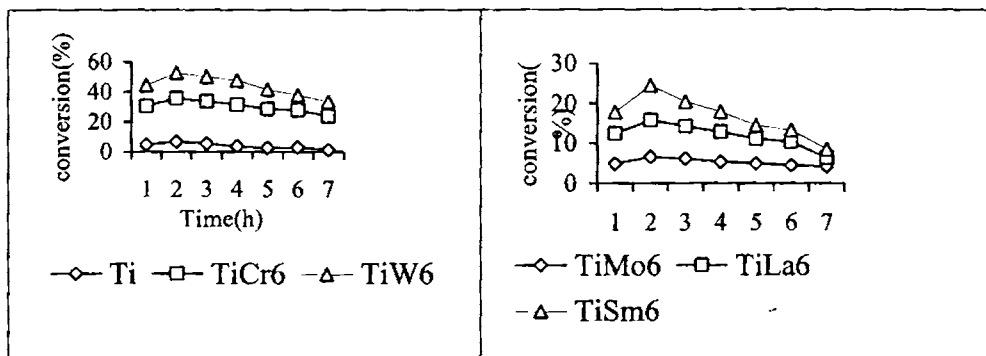
Figure 3.18

Influence of time on stream over the prepared catalysts

D. Comparison of different systems

The cumene conversion reactions were carried out for different catalytic systems under the optimized reaction temperatures. The optimized reaction conditions include a reaction temperature of 400°C and a flow rate of 4ml/h. The catalytic activity along with the selectivity to different products for both transition metals and rare earth metals incorporated titania systems are given in tables 3.9 and 3. 10. The trend in the product selectivity is obviously different for transition metal as well as rare earth metal modified systems. The incorporation of transition metals into titania results in the formation of benzene as the major product whereas the rare earth metal modification enhances the selective formation of α-methyl styrene.

Table 3. 9

Influence of Transition Metals in the cumene conversion

Catalyst	Conversion of Cumene (wt%)	Selectivity (%)	
		α-methyl styrene	Benzene
Ti	6.6	35.4	8.0
TiMo2	15.6	17.5	77.8
TiMo6	31.0	12.1	84.6
TiMo10	43.6	7.5	86.4
TiCr2	16.0	47.0	52.0
TiCr6	29.0	41.6	55.4
TiCr10	38.7	41.1	59.4
TiW2	14.5	48.2	50.8
TiW6	17.2	38.2	61.7
TiW10	23.6	36.8	62.1

Amount of the catalyst-0.5g, Temperature-400°C, Duraton-2h

Flow rate-4ml/h

From 2,6-dimethyl pyridine desorption studies, it is seen that molybdena incorporated systems are having comparatively high abundance of Bronsted acid sites and samaria incorporated ones having least number of Bronsted acid sites. The results support the benzene selectivity obtained from cumene cracking reaction. There is a direct relationship between the percentages of metal incorporated as well as the percentage cumene conversion. As the percentage of the metal loaded increases, a regular increase in the percentage benzene selectivity with a concomitant decrease in the α-methyl styrene selectivity is observed.

Table 3. 10

Influence of Rare Earth Metals in the cumene conversion

Catalyst	Conversion of Cumene (wt%)	Selectivity (%)	
		α-methyl styrene	Benzene
Ti	6.6	35.4	8.0
TiLa2	8.4	75.3	24.1
TiLa6	9.2	62.5	37.1
TiLa10	11.6	57.1	41.1
TiPr2	11.8	52.7	47.3
TiPr6	25.3	42.1	47.5
TiPr10	30.3	35.6	63.7
TiSm2	6.9	85.6	14.1
TiSm6	8.7	85.4	14.6
TiSm10	9.5	84.3	16.6

Amount of the catalyst-0.5g, Temperature-400°C, Duraton-2h

Flow rate-4ml/h

The cumene conversion over the metal oxide catalysts depends on the surface acidity. A good correlation is obtained between the percentage cumene conversion as well as the total acidity obtained from NH_3 TPD. Another one to one correlation is obtained between the percentage benzene selectivity as well as the Bronsted acidity obtained from 2,6-DMP thermodesorption. The results are presented in figures 3.19 to 3.22.
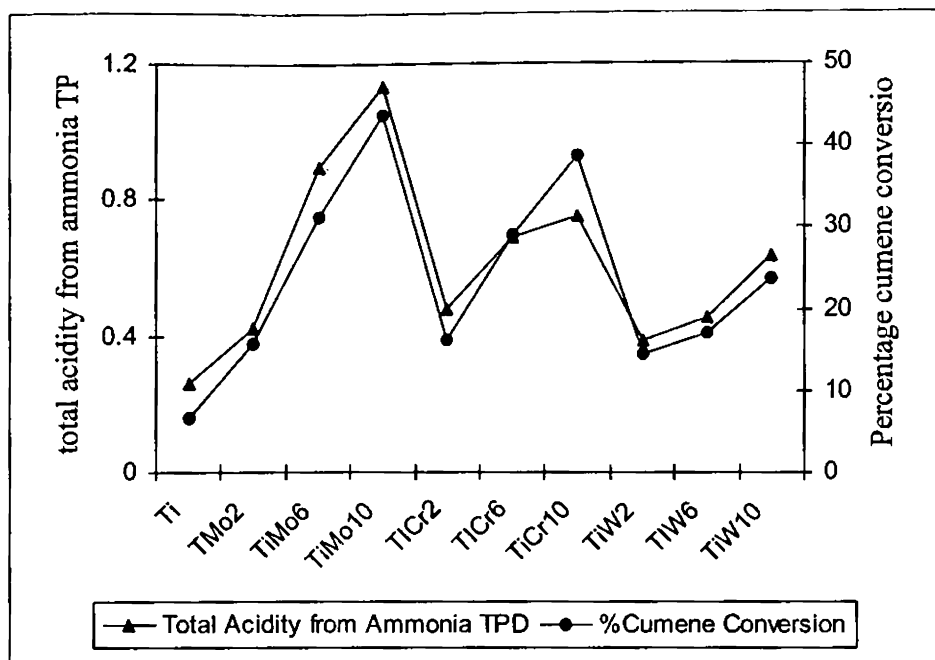
Figure 3.19

Correlation between cumene conversion and total acidity
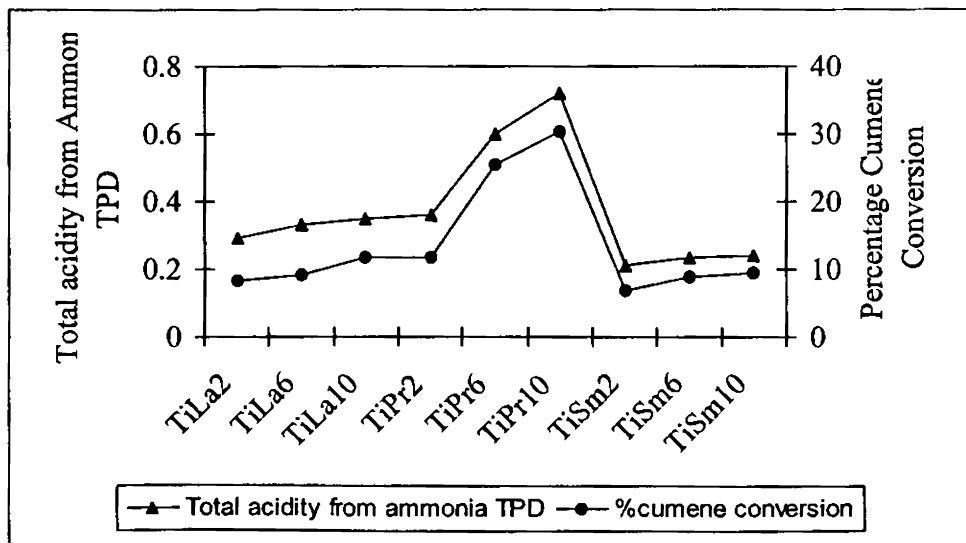
Figure 3.20

Correlation between cumene conversion and total acidity
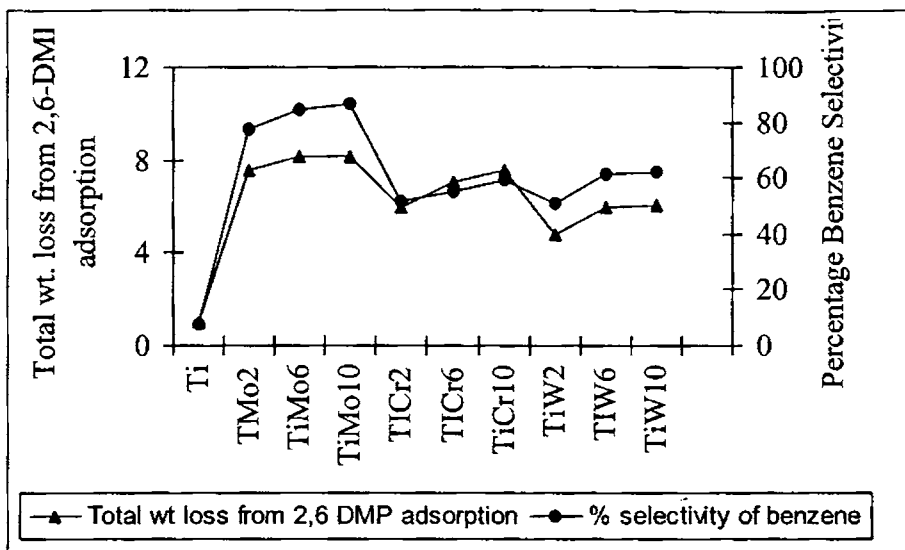
Figure 3.21

Correlation of benzene selectivity with Bronsted acicity
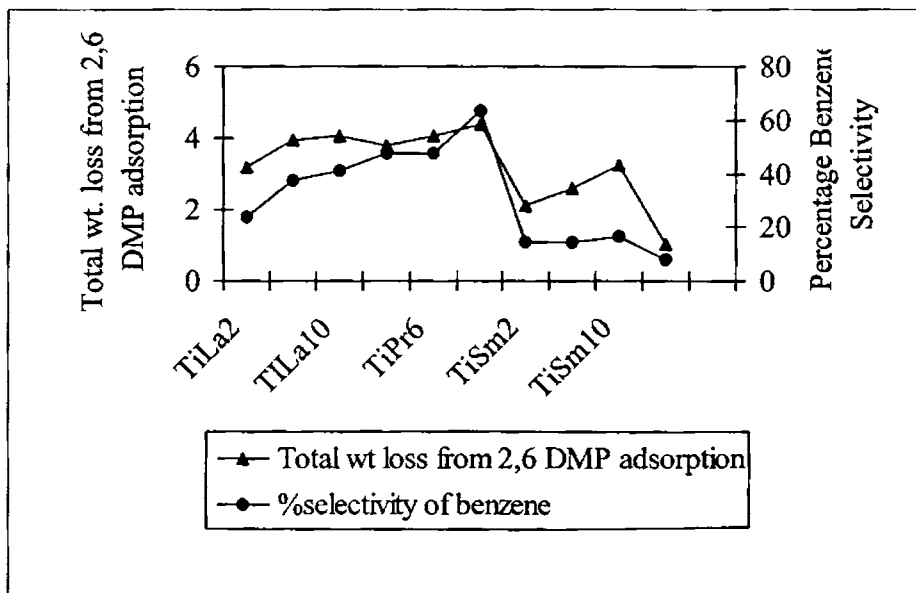
Figure 3.22

Correlation of benzene selectivity with Bronsted acicity

E Mechanism of the reaction

Cumene conversion reaction was carried out over different types of solid acid catalysts and in all the cases the involvement of Bronsted as well as Lewis acid sites is quite evident. Zenon Sarbak *et al* arrived at the conclusion that the high selectivity of alumina and their surface modified ones in cumene dealkylation can be related both to the presence of Bronsted acid sites and strong Lewis centers[46]. Corma *et al* reported that the dealkylation of cumene requires the presence of a small number of Bronsted acid sites, which are capable of formation of a σ-complex with the ipso form of the cumene molecule[47]. Bautista et al have proposed a different mechanism[48,49]. These authors assume that the Bronsted acid sites take part in the protonation of the cumene molecule, which yields a π-complex of the aromatic ring and subsequently this complex is transformed to a σ-complex. In view of these results, a high activity in dealkylation is due to the presence of Bronsted acid sites. The redox and catalytic behaviors of chromium oxide supported on zirconia has been studied. It was found that Cr^{6+} species existing on the surface of the catalyst were responsible for the formation of strong acid sites and the catalytic activity for cracking of cumene[50].

A Friedel Crafts mechanism, involving initial protonation of aromatic ring followed by the cleavage of the ring side chain bond, is generally accepted for the cumene dealkylation over acidic catalysts[51]. This mechanism provides a route to the poisoning of the catalyst through coke formation, since the cracked side chain may polymerize on the acidic surface. Cracking of cumene to benzene is generally attributed to the action of Brönsted sites by a carbonium

ion mechanism while dehydrogenation of cumene yields α–methylstyrene as the major product, the formation of which has been ascribed to the Lewis acid sites. A plausible mechanism of cumene conversion reaction is represented in figure 3.23.
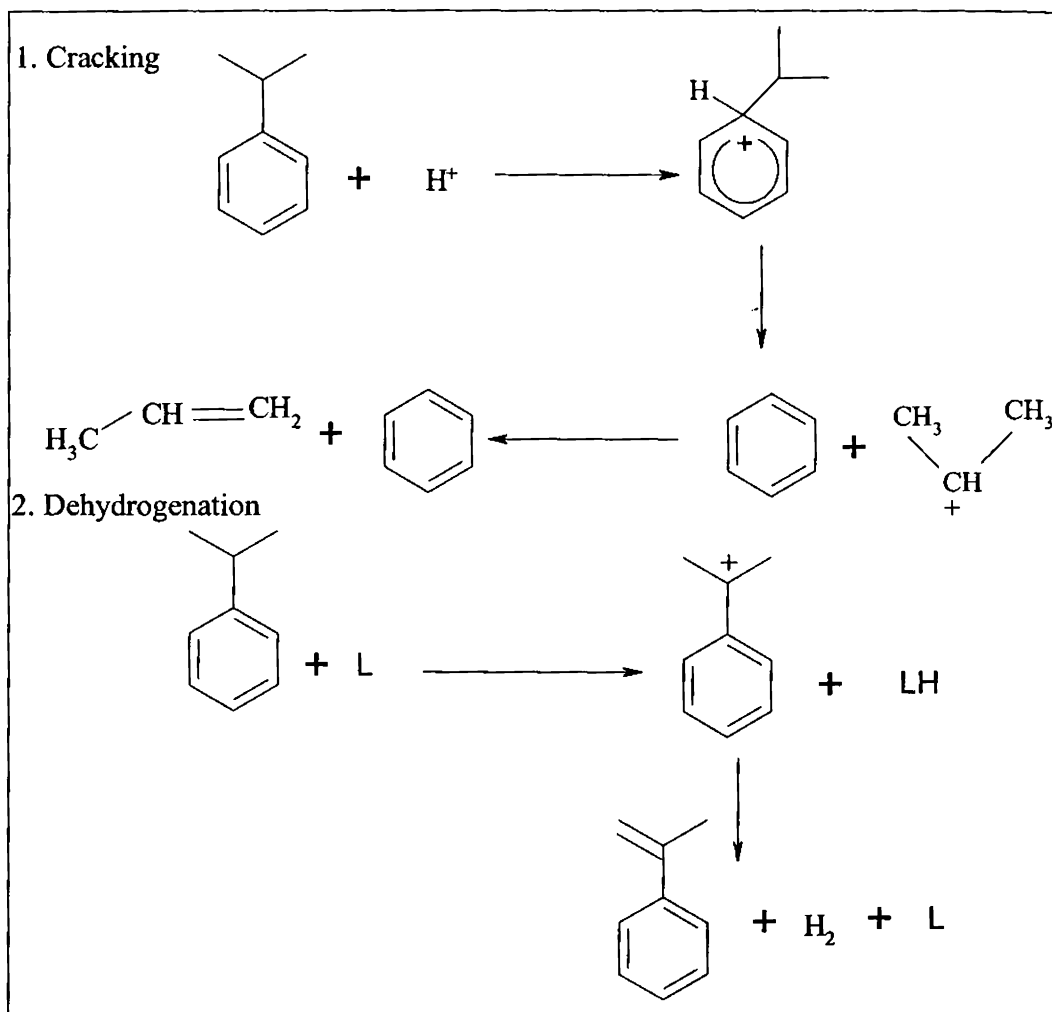
Figure 3.23 Mechanism of Cumene Conversion Reaction

3.3.4 Cyclohexanol Decomposition Reaction

The decomposition of cyclohexanol is used as a probe reaction to characterize the acid-base properties of the catalysts[52]. The dehydrogenation reaction usually competes with the dehydration of the starting compound to an olefin, which is produced in a variable proportion depending on the particular catalyst and the reaction conditions. The amphoteric nature of the alcohol permits its interaction of both acidic and basic centers[53-54]. The dehydrogenation and dehydration resulting in the formation of cyclohexanone[55] and cyclohexene is shown in figure 3.24. Other possible products in this reaction include methyl cyclopentene, cyclohexane, phenol and benzene. The optimum reaction conditions for cyclohexanol decomposition were determined by carrying out the reaction at various reaction temperature and flow rate.
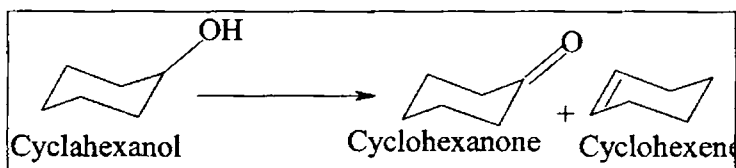
Figure 3.24

Scheme of Cyclohexanol decomposition Reactions

A. Effect of temperature

The effect of reaction temperature on the decomposition of cyclohexanol is studied over the temperature range from 250 to 400°C. The conversion and selectivity to different products is given in figure 3.25. The percentage cyclohexanol decomposition increases with the increase in reaction

temperature from 250 to 350°C and thereafter no appreciable change in the percentage conversion is observed. The percentage selectivity remains more or less the same with the increase in the reaction temperature upto 350°C. But at higher temperatures, there is a reduction in the cyclohexene selectivity. There is a chance for the decomposition of surface hydroxyl ions leading to the formation of stronger Lewis acid centers, which can form other products like methyl cyclopentanes. The optimum reaction temperature chosen in the present study is 350°C.
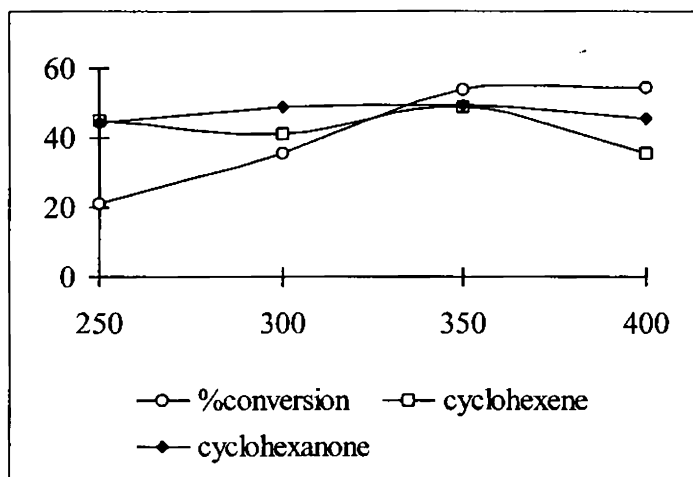
Figure 3.25

Influence of Reaction temperature on the decomposition of cyclohexanol

Flow rate-4ml/h, Duration-2h, 0.5 g TiLa6 catalyst

B. Effect of flow rate

The effect of flow rate on the decomposition of cyclohexanol is investigated in detail and the results are presented in figure 3.26. The reaction is carried out at a temperature of 350°C over TiLa6 catalyst. The percentage

conversion increases initially upto 5ml/h and thereafter it decreases. When the flow rate is high, there is a drastic reduction in the percentage cyclohexanol conversion due to the decrease in contact time between the catalyst and the reactant. Maximum conversion as well as selectivity is obtained when the flow rate is 5ml/h.
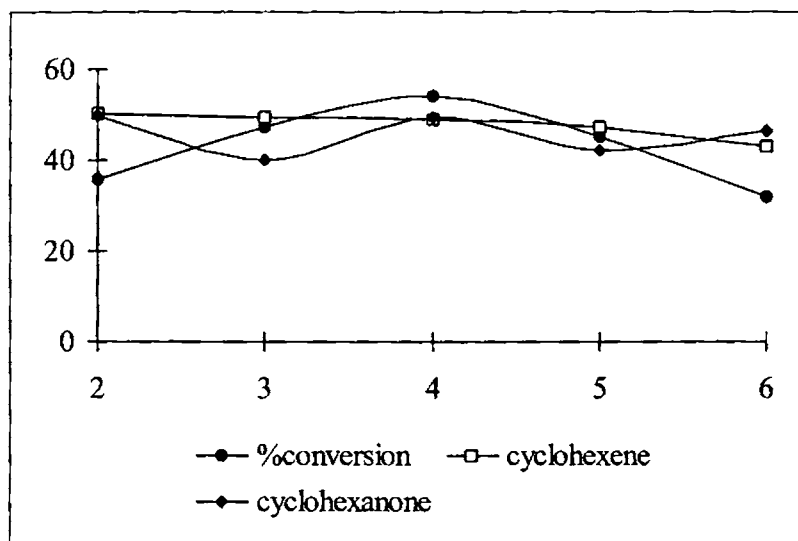
Figure 3.26

Effect of flow rate on the decomposition of cyclohexanol

Temperature-350°C, time-2h, 0.5g TiLa6

C. Effect of time on stream

Figure 3.27 illustrates the time on stream stability of the prepared catalysts at a reaction temperature of 350°C and a flow rate of 4ml/h. Good catalytic activity is shown by all the systems. The deactivation of titania occur immediately after 2h but in modified systems, the deactivation start only after

4h. The deactivation of the catalyst is due to the thermal decomposition of cyclohexanol and cyclohexanone to carbonaceous compounds or due to the presence of surface oligomers resulting from poly condensation of cyclohexanone[56]. The cyclohexene produced in this reaction also ascribed to have a high capacity for deactivating the catalysts on account of the ease with which they can give rise to surface carbonaceous compounds.
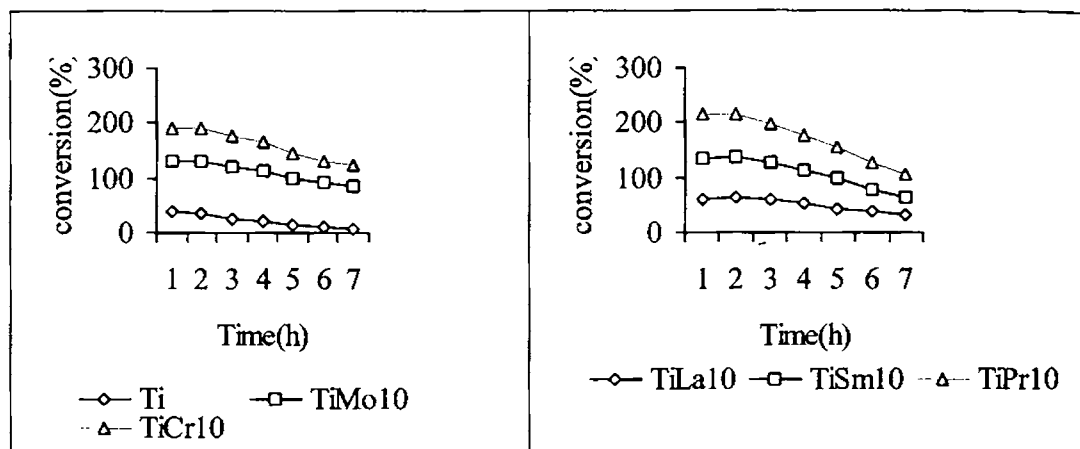
Figure 3.27

Influence of time on stream over the prepared catalysts

D. Catalyst comparison

The catalytic performance of the prepared systems was compared under the optimized reaction conditions and the results are presented in tables 3.11 and 3.12. The improvement in catalytic activity of pure titania upon modification with transition metals and rare earth metals is clearly understood from the results. All the systems are found to be highly selective to cyclohexene formation. Reports suggest that weak and medium acid centers on the surface of the catalyst are responsible for the formation of cyclohexene.

The present work also agrees with the above conclusion. A very good correlation is obtained between the weak and medium acidity obtained from ammonia TPD and the percentage cyclohexanol decomposition. The results are presented in figures 3.28 and 3.29.

Table 3. 11

Influence of Transition Metals in the decomposition of cyclohexanol

Catalyst	Conversion of	Selectivity (%)	
	Cyclohexanol (wt%)	Cyclohexene	Cyclohexanone
Ti	20.7	85.4	13.2
TiMo2	35.8	89.3	10.3
TiMo6	81.1	83.1	13.5
TiMo10	98.9	80.3	19.0
TiCr2	52.6	78.9	21.3
TiCr6	55.1	81.6	18.3
TiCr10	58.5	80.2	19.2
TiW2	25.7	83.7	16.1
TiW6	58.6	80.2	18.7
TiW10	60.0	82.3	15.7

Reaction Temperature-350°C, Catalyst weight-0.5g, Flow rate-4ml/h, Duration-2h

The nature and amount of the metals incorporated also have a crucial role in determining the catalytic activity of the prepared systems. With the increase in the amount of the incorporated metal, there is an improvement in the catalytic activity of the prepared systems towards the decomposition of cyclohexanol. The transition metal incorporated systems are having higher selectivity to cyclohexene compared to rare earth metal incorporated systems.

The rare earth metals are capable of increasing the number of basic sites over titania support which is reflected from their higher cyclohexanone selectivity.
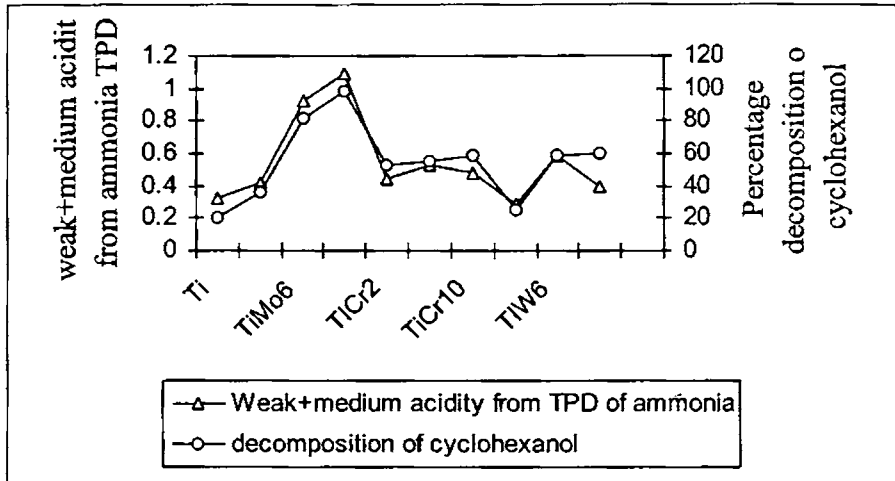
Figure 3.28, Correlation between percentage cyclohexanol decomposition and weak+medium acidity from ammonia TPD
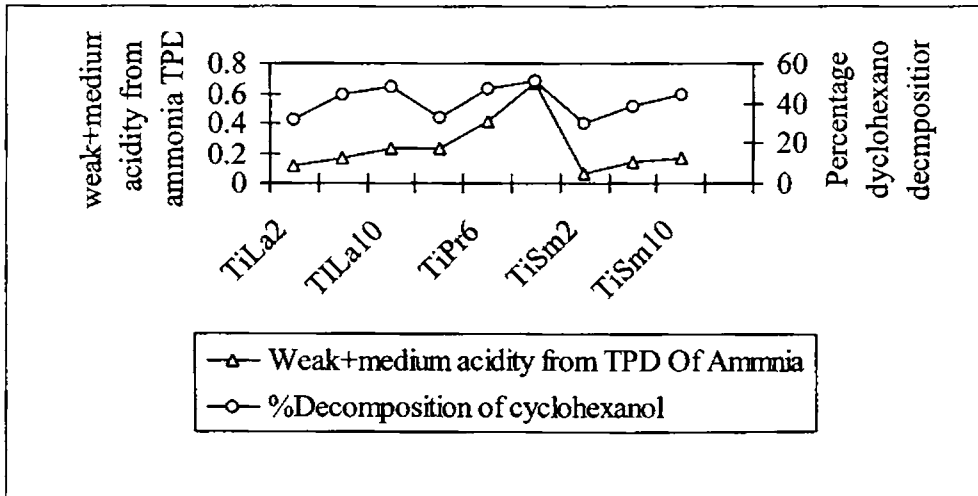
Figure 3.28, Correlation between percentage cyclohexanol decomposition and weak + medium acidity from ammonia TPD

Table 3. 12

Influence of Rare Earth Metals in the decomposition of cyclohexanol

Catalyst	Conversion of Cyclohexanol (wt%)	Selectivity (%)	
		Cyclohexene	Cyclohexanone
Ti	20.7	85.4	13.2
TiLa2	32.3	63.2	36.6
TiLa6	44.1	49.0	49.3
TiLa10	48.4	47.2	52.2
TiPr2	32.8	53.9	44.0
TiPr6	47.7	54.2	46.0
TiPr10	51.1	48.8	50.3
TiSm2	30.0	58.6	41.3
TiSm6	39.2	52.1	47.4
TiSm10	44.5	53.3	42.6

Reaction Temperature-350°C, Catalyst weight-0.5g, Flow rate-4ml/h, Duration-2h

E. Mechanism of the Reaction

Although the mechanism of gas phase alcohol dehydrogenation and dehydration remains poorly known and controversial, it is generally accepted that the highest activities in the dehydration to cyclohexene are related to acid sites, while dehydrogenation to cyclohexanone is generally associated to basic/ redox sites[57-61]. Bronsted acid sites are directly involved in the alcohol dehydration mechanism. It is similar to the E-1 elimination in which the reaction proceeds through initial formation of carbocation. The elimination reaction on the basic site is carried out after the adsorption of cyclohexanol

through the hydrogen atom in the α-carbon, which develops a carbenium character to some degree. The strongest basic sites could be able to carry out the adsorption of the hydrogen atom of the hydroxyl group, generating an oxygen anion, thus promoting the dehydrogenation reaction[62-63]. The general mechanism of cyclohexanol decomposition over metal oxides is given in figure 3.28.
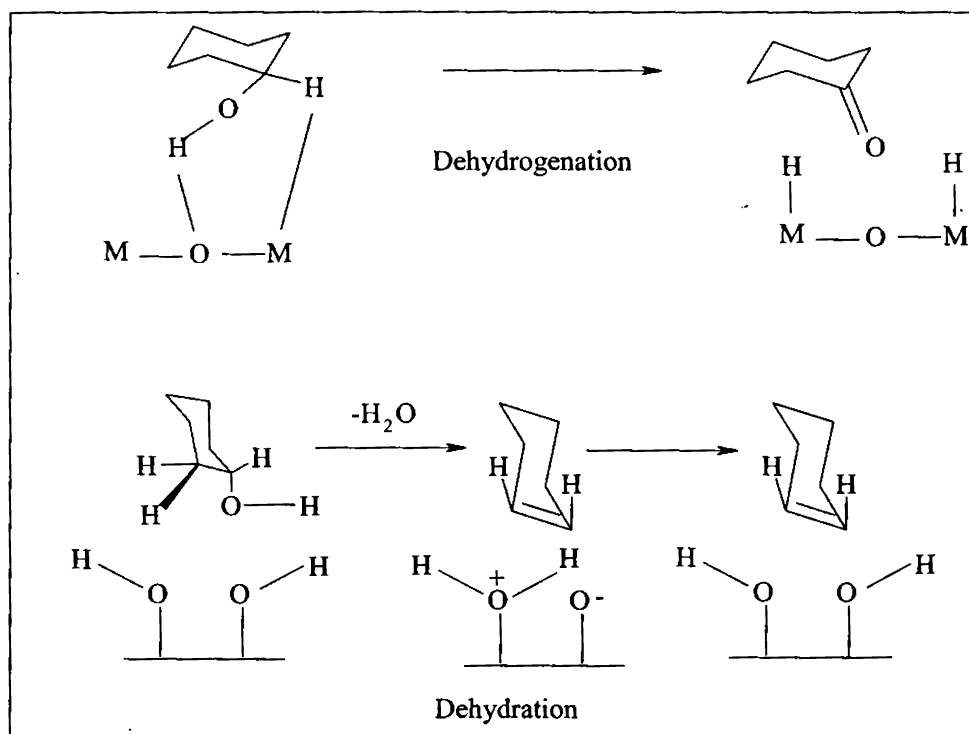
Figure 3.28

Mechanism of dehydrogenation and dehydration of cyclohexanol on oxide surface

3.4 Conclusions

Sol-gel method is highly effective for the preparation of nanosize titania having larger surface area. The elemental composition obtained from EDX analysis adds to the effectiveness of this method. Modification with transition metals and rare earth metals enhances the structural as well as textural characteristics of titania. Another important consequence is the special stabilization of the anatase phase which is the catalytically and photocatalytically stable phase of titania. The modified cations are shifting the anatase to rutile phase transformation to higher temperatures. The XRD results reveals that the incorporated metal ions are highly dispersed on the surface of the catalyst. Surface area and pore volume of the modified systems are remarkably improved by metal incorporation. The surface morphologies of the prepared systems are clearly understood from the SEM pictures. The high thermal stability of the prepared systems can be understood from the TG-DTG curves. The characteristic peaks of pure titania is obtained from the FTIR analysis. UV-Vis DRS helped in the identification of tetrahedrally coordinated titanium ions and calculation of the band gap energy of the prepared systems. The surface acidity of the systems can be assessed by means of ammonia TPD and thermodesorption of 2,6-DMP. Model reactions like cyclohexanol decomposition as well as cumene cracking successfully give an idea about the surface acid-base characteristics of the prepared systems.

References

1   J.W. Niemantsverdriet, "Spectroscopy in Catalysis", Weinheim, New York, 1995.

2   R.A. Van Santen, "Theoretical heterogeneous Catalysis", World Scientific Singapore, 1991.

3   A.V. Ramaswamy, "Catalysis Principles and Applications" Narora, New Delhi.

4   John. F. Porter, Yu-Guang Li and Chak K. Chan, J. Mat. Sci, 34 (1999) 1523.

5   R.D. Shannon and J.A. Pask, J. Amer. Ceram. Soc, 48 (8) (1965) 391.

6   H. Lipson, H. Steeple, "Interpretation of X-Ray powder diffraction patterns" Macmillan, London, (1970) 261.

7   B.D. Cullity, "Elements of X-Ray Diffraction", 2nd Edition, Addison-Wesley, Reading, WA, 1978) p.94.

8   K.N.P. Kumar, K. Keizer, A. Burggraaf, J. Mater. Sci, 3 (1993) 141.

9   R. Gopalan, Y.S. Lin, Ind. Eng. Chem. Res, 34 (1995) 1189.

10   S.K. Samantaray, T. Mishra, K.M. Parida, J. Mol. Catal. A. Chem, 156 (2000) 267.

11   J. Livage, K. Doi, C. Maziieres, J. Phys. Chem, 93 (1989) 6769.

12   C.P. Sibu, S. Rajeshkumar, P. Mukundan and K.G.K. Warrier, Chem. Mater, 14 (2002) 2876.

13   Hongmei Luo, Cheng Wang and Yushan Yan, chem. Mater, 15 (2003) 3841.

14   A.L. Linsebigler, G. Lu and J.T. Yates, Jr. Chem. Rev, 95 (1995) 735.

15   Degussa Canada Ltd, Bull. 56, Burlington, Ont, Canada.

16   V.F. Stone, Jr, R.J. Davis, Chem. Mater, 10 (1998) 1468.

17   C. Beck, T. Mallat, T. Burgi and A. Baiker, J. Catal, 204 (2001) 428.

18   R. J. Davis, Z.F. Liu, Chem. Mater, 9 (1997) 2311.

19   X. Gao and I.E. wachs, Catal. Today, 51 (1999) 233.

20   A. Fernandez, J. Leyrer, A.R. Gonzales-Elipe, G. Munuera and H. Knozinger, J. Catal, 112(1988) 489.

21   G. Lassaletta, A. Fernandez, J.P. Espinos and A.R. Gonzales-Elipe, J. Phys. Chem, 99 (1995) 1484.

22   C.K. Gorgenson, "Modern Aspects of Ligand Field Theory", North Holland, Amsterdam, 1971.

23   M.R. Boccutti, K.M. Rao, A. Zecchina, G. Leofanti and G. Petrini, Stud. Surf. Sci. Catal, 48 (1989) 133.

24   S. Klein, B.M. Weekhuysen, J.A. Martens, W.F. Maier and P.A. Jacobs, J. Catal, 163 (1996) 489.

25   M.A. Malathi, W.K. Wong, Surf. Technol, 22 (1984) 305.

26   S. Velu, N. Shah, T.M. Jyothi, S. Sivasanker, Micropor. Mesopor. Mater, 33 (1998) 61.

27   H.P. Bochnm, H. Knozinger, "Catalysis" J.R. Anderson and M. Boudart, Eds. Vol.4, Springer, Berlin (1983) Chp.2

28   G. Cristallo, E. Roncari, A. Rinaldo, F. Trifiro, Appl. Catal. A, Gen, 209 (2001) 249.

29   J.M. Gallardo-Amores, T. Armaroli, G. Ramis, E. Finocchino, G. Busca, Appl. Catal. B, Environ, 22 (1999) 249.

30   S. Doeuff, M. Henry, C. Sanchez, J. Livage, J. Non-Cryst. Solids, 89 (1987) 206.

31   Michel R. Guisnet, Acc. Chem. Res, 23 (11) (1990) 392.

32 K. Tanabe, T. Sumiyoshi, K. Shibata, T. Kiyoura and I. Kitagawa, Bull. Chem. Soc. Jpn, 47 (1974) 1064.

33 K. Tanaba, M. Misono, Y. Ono and H. Hattori, New Solid Acid and Bases (Kodansa, Tokyo, 1989) ch.3, p.108.

34 A. Auroux, A. Gervasini, J. Phys. Chem, 94 (1990) 765.

35 J. Lebars, A. Auroux, J. Therm. Anal, 40 (1993) 1277.

36 D.J. Parrillo, R.J. Gorte, W.E. Farneth, J. Am. Chem. Soc, 115 (1993) 12441.

37 S.B. Sharma, B.L. Meyers, D.T. Chen, J. Miller, D. Dumesic, Appl. Catal. A, Gen, 102 (1993) 253.

38 H. Karge, V. Dondur, J. Phys. Chem, 94 (1990) 765.

39 C. Lahousse, F. Mauge, J. Bachelier and J.C. Lavalley, J. Chem. Soc. Farad. Trans, 91 (1995) 2907.

40 G.S. Walker, E. Williams and A.K. Bhattacharya, J. Mat. Sci, 32 (1997) 5583.

41 A. Satsuma, Y. Kamiya, Y. Westi, T. Hattori, Appl. Catal. A, Gen, 194-195 (2000) 253.

42 A. Corma, C. Rodellas, V. Fornes, J. Catal, 88 (1984) 374.

43 S.M. Bradley, R.A. Kydd, J. Catal, 141 (1993) 239.

44 J.M. Lewis, R.A. Kydd and P.M. Boorman, J. Catal, 120 (1989) 413.

45 P. Wu, T. Komatsu, T. Yashima, Micropor. Mesopor. Mater, 22 (1998) 343.

46 S. Zenon, Appl. Catal. Aa, 159 (1997) 147.

47 A. Corma, J.L.G. Fiero, R. Montanana, F. Thomas, J. Mol. Catal, 30 (1985) 361.

48 F.M. Bautista, J.M. Campelo, A. Garcia, D. Leina, J.M. Marinas, A.A. Romero, J.A. Navio M. Macias, J. Catal, 145 (1994) 107.

49 F.M. Bautista, J.M. Campelo, A. Garcia, D. Leina, J.M. Marinas, A.A. Romero, Appl. Catal, 104 (1993) 109.

50 Jong Rack Sohn and Sam Gon Ryu, Catal.Lett, 74 (1-2) (2001) 105.

51 N.Y. Chen, W.W. Kaeding and F.H. Dwyer, J. Amer. Chem. Soc, 101 (1979) 6783.

52 M. Ai, Bull. Chem. Soc. Jpn, 50 (1997) 2579.

53 M.M.C.C. Costa, L.F. Hodson, R.A.W. Johnstone, J.Y. Liu, D. Whitaker, J. Mol. Catal, 142 (1999) 349.

54 D. Martin, Duprez, J. Mol. Catal, 118 (1997) 113.

55 M. Ai, Bull. Chem. Soc. Jpn, 50 (1977) 2587.

56 Y.M. Lin and I. Wang, Appl. Catal. A. Gen, 41 (1988) 53.

57 R.A.W. Jonstone, J. Liu, D. Whittaker, J. Chem. Soc. Perkin Trans, (1998) 1287.

58 R.A.W. Jonstone, J. Liu, D. Whittaker, J. Mol. Catal. A, 174 (2001) 159.

59 Y. Shinohara, T. Nakajima, S. Suzuki, J. Mol. Struct. (Theochem), 460 (1999) 231.

60 V.Z. Fridman, A.A. Davydov, J. Catal, 195 (2000) 20.

61 F.M. Bautista, J.M. Campelo, A. Garcia, D. Leina, J.M. Marinas, R.A. Quiros and A.A. Romero, Appl. Catal. A; Gen, 243 (2003) 93.

62 L. Nodek, J. Sedlaceck, J. Catal, 40 (1975) 34.

63 M. Bowker, R.W. Petits, K.C. Waugh, J. Catal, 99 (1986) 53.

Chapter 4

Epoxidation of Cyclohexene

Abstract

Titanium containing catalysts and their modification is of great importance in the liquid phase oxidations using heterogeneous catalysts. In the present chapter, the liquid phase epoxidation reaction of cyclohexene with tert-butyl hydroperoxide over the prepared titania as well as modified titania systems is analyzed in depth. The influence of various reaction parameters like reaction temperature, amount of the catalyst, nature and amount of the solvent as well as the oxidant is investigated thoroughly in various sections. The excellent activity and selectivity in the epoxidation of cyclohexene is due to highly dispersed Lewis acidic titanium sites. A plausible reaction pathway is also proposed. Here we show that cyclohexene epoxidation could be used as an important step of a greener synthesis of adipic acid.

4.1 Introduction

Epoxidation reactions are indispensable for the chemical industry because of the ease, with which they can be used to convert olefins to oxygenated molecules, so-called epoxides, by oxygen transfer reaction. Epoxides are valuable and versatile commercial intermediates used as key raw materials for a wide variety of products owing to the numerous reactions they may undergo. They are widely used in organic synthesis of fine chemicals and pharmaceuticals[1-6]. These materials are largely used for the synthesis of several perfume materials, anthelmintic preparations, epoxy resins, plasticizers, drugs, sweeteners, etc. Products formed in the epoxidation are of independent significance and/or are valuable chemicals for syntheses of biologically active substances[7]. Therefore the synthesis of an epoxide by an easier method and a low cost route is of great interest to researchers working in this field.

The direct epoxidation of alkenes has been the main process for preparing the epoxides. Epoxidation reactions of alkenes generally require the presence of a catalyst. However, several side reactions can take place, such as oxidation in the allylic positions, ring-opening of the epoxides by hydrolysis or solvolysis, epoxide rearrangement, or even total break down of the C=C double bonds. Industrial olefin epoxidation has been carried out in the presence of alkaline earth metal chlorides promoted by chlorine containing substances. This method has several disadvantages, one of which is the use of chlorine containing reagents. The epoxidation procedure using peracids is very costly and usually produces huge amounts of pollutants. It is highly desirable to replace the conventional process by an environmentally benign procedure. In

recent years, several heterogeneous and homogeneous catalysts have been shown to be effective in the selective oxidation of olefins[8-12].

There are a variety of experimental systems capable of carrying out an oxygen transfer to an alkene double bond to produce an epoxide. In a number of them the oxygen added to the olefin comes from a peroxo group, either in the form of an organic peroxide or coordinated to a transition metal. The use of cleaner oxidants than usual hazardous and costly organic peroxides for epoxidation allows the development of greener reaction. Hydrogen peroxide (H_2O_2) and tert-butyl hydroperoxide (TBHP) are more suitable from environmental point of view of green chemistry because their reduction products, water or alcohol can be easily recycled[13]. The profitability of epoxidation with hydroperoxides depends on the possible utilization of co-products, namely tert-butyl alcohol in the case of TBHP[14].

Cyclohexene epoxidation to yield cyclohexene oxide is one of the most difficult cases, in which the first two problems, namely allylic oxidation and epoxide ring opening, occur considerably. As cyclohexene oxide is an important organic intermediate consumed in the production of pharmaceuticals, plant-protection agents, pesticides, and stabilizers for chlorinated hydrocarbons much effort has been dedicated to the development of new active and selective cyclohexene epoxidation catalysts that circumvent the side reactions and the subsequent formation of large amounts of by-products. Cyclohexene epoxide is of great technical importance as it is applied in the modification of epoxy resin properties and the synthesis of new polymers, copolymers and solvents. Another very interesting application is the preparation of cyclohexanol and pyrocatechins[15]. Special attention was paid to

cyclohexene because cyclohexene epoxide could replace cyclohexanone as an intermediate in the synthesis of adipic acid, the precursor for Nylon 6-6[16]. The current production of adipic acid amounts to 2 million tones/year worldwide. It involves cyclohexanone oxidation by nitric acid and those reduction products include N_2O. Nitrous oxide is a strong green house gas, 200 times more potent than CO_2, and is partly involved in ozone layer damage.

Titania-silica mixed oxides are active and selective epoxidation catalysts[17-28], offering an efficient alternative to conventional titania on silica and titanium substituted zeolites. The unmodified as well as the methyl- and phenyl- groups modified titania-silica aerogels were active and selective in the epoxidation of cyclohexene with tert- butyl hydroperoxide[29]. Novel mesoporous TS-1 catalyst is shown to be active in epoxidation of oct-1-ene and significantly more active in epoxidation of cyclohexene than conventional TS-1[30]. The epoxidation of alkenes using titanium silicate (TS-1) as a solid catalyst and aqueous hydrogen peroxide as oxidant has been studied extensively. Interaction of titanosilicates (TS-1, TiMCM-41 and Pd $_{(n)}$-TS-1) with H_2O_2, urea- H_2O_2, and ($H_2 + O_2$) generates reactive Ti(IV)-superoxo and hydroperoxo/peroxo species[31]. The selectivity for epoxidation over these catalysts can be enhanced by controlling the type of Ti-oxo species. The organic modification of titania - silica catalysts by mono and bidendate functional groups enhanced the rate of epoxidation of cyclohexene remarkably[32]. Titanium containing carbon-silica composite catalysts showed an increased activity and epoxide selectivity[33]. This may be attributed to the hydrophobic nature of the carbon surface and the local environment of active titanium centers on the silica support. Peng Wu *et al* studied the liquid phase

alkene epoxidation activity over a novel titanosilicate with the MWW topology[34].

Chiker *et al* synthesized new mesoporous catalysts by grafting titanium on mesoporous silica SBA15 by means of titanium tetrachloride in gas phase and tested for green epoxidation of cyclohexene[16]. The selectivity in this case is 100% and epoxide yields can reach almost 100% in the case of organic hydroperoxides without any leaching of titanium species. Framework Ti-substituted and Ti- grafted MCM-41 mesoporous materials have been tested as catalysts for cyclohexene oxidation[35]. The mesoporous structure of the catalyst plays an important role in the oxidation of cyclohexene, especially when bulky TBHP was used. An increasing attention is being given recently to phase transfer oxidation catalysts in the presence of tungsten and molybdenum compounds[36], which are efficient catalysts for oxidation with hydrogen peroxide solutions of various organic substrates, viz., olefins, alcohols and aromatic hydrocarbons.

Heterogenization of alkene epoxidation catalysts was done recently to produce an appropriate material, which would allow the obtention of epoxides with high selectivity under industrial conditions[37]. Dendrimer templated mesoporous oxidation catalysts can easily be produced to have similar physical and chemical properties to MCM-41 materials and their epoxidation activity is also comparable[38]. MCM-41 supported ruthenium porphyrin ring systems are also effective in the epoxidation of cyclohexene using 2,6 dichloropyridine N-oxide as the oxidant[39]. An electron deficient iron porphyrin complex catalyzes the epoxidation of olefins by tert-butyl hydroperoxides via radical free oxidation reactions in aprotic solvent; the epoxidation reactions were markedly

influenced by reaction temperature and high yields of epoxide products were obtained with retention of stereospecificity at low temperatures[40]. Clay supported manganese (salen) complexes also catalyses the epoxidation of cyclohexene efficiently using phenyl iodate as the oxidant[41]. Marcelo Alves Moreira *et al* in his work optimized the chemo-enzymatic epoxidation of cyclohexene mediated by lipases[42]. The systems studied here involve a biocatalytic perhydrolysis followed by a peroxyacid epoxidation.

Sreethawong *et al* studied the combined effect of mesoporosity as well as metal oxide additives on the epoxidaion of cyclohexene in t-butanol-H_2O_2 system[43]. The reaction pathways, which could suitably explain the catalytic activity for the cyclohexene epoxidation, were also proposed. Since TiO_2 has been extensively used in multiple applications in the field of catalysis, especially, photocatalysis and its surface contains a number of OH groups behaving as the sites for the formation of peroxotitanium complexes, it has been believed to be one of the active catalysts for the considered epoxidation reaction[44-45]. Richard L. Brutchey prepared a new dimeric complex [(^{t}BuO)$_2$Ti{μ-O$_2$Si[OSi(O^{t}Bu)$_3$]$_2$}]$_2$ via silanolysis of Ti(O^{t}Bu)$_4$ with (HO)$_2$Si[OSi(O^{t}Bu)$_3$]$_2$. The resulting materials were found to be active and highly selective in the epoxidation of cyclohexene, yielding up to 71% of cyclohexene oxide based on oxidant (cumene hydroperoxide) after 2 h at 65°C in toluene[46]. New dioxomolybdenum(VI) complexes of tetradentate Schiff base is prepared and its catalytic activity towards the epoxidation of cyclohexene and 1-octene with *tert*-butyl hydroperoxide (TBHP) as oxidant have been studied[47].

The chapter presents an exhaustive investigation on the liquid phase epoxidation of cyclohexene over the prepared catalytic systems. The general scheme of the reaction is represented in figure 4.1. The nature of the products demonstrates that cyclohexene can suffer either epoxidation yielding epoxy cyclohexane (cyclohexene epoxide) and glycol (cyclohexane diol) or an allylic attack forming cyclohex-2-ene-1-ol (cyclohexenol) and cyclohex-2-ene-1-one (cyclohexenone). All the catalytic systems show considerable activity towards the reaction with high selectivity towards cyclohexene epoxide.
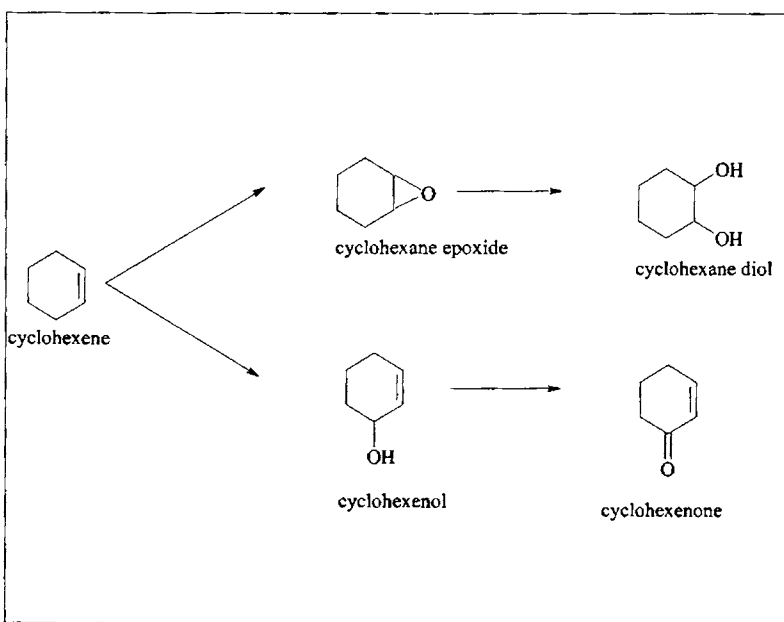
Figure 4.1

General Scheme of cyclohexene epoxidation reaction

4.2 Process optimization

The epoxidation of cyclohexene with tert-butyl hydroperoxide was carried out in a 100ml round bottom flask equipped with a reflux condenser and a thermometer. The reactor and oil bath were continuously stirred to ensure that the system was well mixed and isothermal. In a standard procedure 0.1g of the catalyst and 20mmol of cyclohexene were put into 25ml acetonitrile. The mixture was heated to 343K under stirring.10mmol TBHP (70% in water) was introduced in one lot. All the reagents used were used as such without further purification. The samples were withdrawn at different reaction times and the products were separated by filtration. The reaction mixture was analyzed with the help of a gas chromatograph using BP-1 capillary column (12m X 0.32mm). Products were confirmed by comparison with authentic samples. The reaction is conducted under various conditions and compared the activity of different systems under optimized reaction conditions.

4.2.1. Influence Of the Catalyst

Cyclohexene epoxidation reaction is conducted in acetonitrile using TBHP as the oxidant at 343K in the absence of a catalyst (blank run) and in the presence of the catalyst (0.1g TiCr6). In a blank run, even after 5h, the percentage conversion is only 1.6 and the number of detectable side products remained small at this low conversion. Under the same reaction conditions, the yield is 55.2 when conducted in presence of 0.1g of TiCr6 catalyst. From this it can be concluded that in presence of the catalyst, the reaction proceeded through a different path with lower activation energy. Hence the percentage conversion is higher in the catalyzed reaction.

4.2.2. Influence of Catalyst weight

In heterogeneous catalysis, the amount of the catalyst plays an important role in determining the rate of the reaction. To study this, the catalyst weight is varied by taking different amounts of TiCr6 catalyst under otherwise identical reaction conditions. Table 4.1 shows the influence of amount of catalyst weight on the catalytic activity and selectivity.

Table 4.1

Influence of amount of the catalyst in the epoxidation of cyclohexene

Catalyst	Conversion	Selectivity (%)		
Weight (g)	(%)	Epoxide	Diol	1-ene + 1-ol
0.05	21.9	65.1	27.0	7.9
0.1	55.2	86.6	6.6	6.7
0.15	51.9	77.2	19.2	3.6
0.20	27.7	64.1	31.2	4.7

Catalyst chosen-TiCr6, duration-5h, temperature-343K,

20ml acetonitrile, 10mmol TBHP.

In the absence of a catalyst, the conversion is negligible. Addition of 0.05g catalyst changes the percentage conversion from 1.6 to 21.9 in the epoxidation of cyclohexene. An initial sharp rise in the percentage conversion is observed when the catalyst amount is increased to 0.1g. After that the percentage conversion remains almost the same eventhough the catalyst amount is changed to 0.15g. But the percentage conversion decreases with further increase in catalyst weight. The effect of catalyst weight is more substantial when considering the epoxidation activity, but no clear correlation of catalyst weight with the percentage conversion can be established. A

gradual change in the epoxide selectivity is also noticed with the change in catalyst weight. An optimum catalyst weight of 0.1g is chosen for the present reaction, considering the percentage conversion as well as epoxide selectivity.

4.2.3. Influence of Temperature

The epoxidation of cyclohexene depended greatly on the reaction temperature. The catalytic epoxidation of cyclohexene by TBHP was carried out at various reaction temperatures from 333 to 363K and the results are given in table 4.2.

Table 4.2

Influence of temperature in the epoxidation of cyclohexene

Temperature	Conversion	Selectivity (%)		
(K)	(%)	Epoxide	Diol	1-ene + 1-ol
333	43.5	80.3	9.0	9.7
343	55.2	86.6	6.6	6.7
353	31.9	87.2	9.2	3.6
363	24.9	54.2	16.2	26.7

Catalyst chosen-0.1g TiCr6, duration-5h,

20ml acetonitrile, 10mmol TBHP

Interstingly, the product distribution varied depending on reaction temperature. The cyclohexene conversion reached about 55.2% when the temperature reaches 343K with a cyclohexene selectivity of 86.6%. The percentage conversion was 43.5 when conducted the reaction at a temperature of 333K. But as the temperature is increased, the amount of allylic oxidation products increases leading to a lower selectivity of epoxide. The percentage

cyclohexene conversion decreases with temperature beyond 343K. From the results it can be concluded that the epoxidation of cyclohexene proceeds with high activity and selectivity under gentle reaction temperature. The high conversion is not accompanied by the highest selectivity of transformation to epoxide with regard to TBHP consumed. This is due to the decomposition of TBHP to alcohol and oxygen at higher temperature.

$$(H_3C)_3C\text{-}OOH \rightarrow (H_3C)_3C\text{-}OH + 0.5\ O_2$$
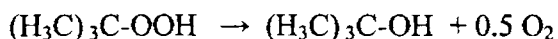
4.2.4 Influence of Oxidant

The epoxidation reaction was carried out using oxidants like hydrogen peroxide and tert-butyl hydroperoxide. A blank run was made by conducting the reaction without the addition of an oxidant and that yields negligible conversion with a poorer selectivity of cyclohexene epoxide. The results are presented in table 4.3.

Table 4.3

Influence of oxidant in the epoxidation of cyclohexene

	Conversion	Selectivity (%)		
	(%)	Epoxide	Diol	1-ene + 1-ol
No oxidant	1.2	12.4	46.3	51.1
TBHP	55.2	86.6	6.6	6.7
H₂O₂	17.4	93.3	2.4	4.3

Catalyst chosen- 0.1gm TiCr6, duration-5h,

Temperature-343K, 25ml acetonitrile

At 343K, the corresponding epoxides are obtained with 93.3% selectivity though the percentage cyclohexene conversion is only 17.4%. Here the colour of the catalyst changed to brown. This can be due to the possible formation of hydroperoxy complexes with titanium. When the epoxidation is carried out with TBHP as oxidant, the conversion is very much higher with a percentage epoxide selectivity of 86.6%. Despite its outstanding interest in green chemistry, hydrogen peroxide gives poorer results and so TBHP is preferred in the epoxidation of cyclohexene.

4.2.5. Influence of concentration of oxidant

To investigate the effect of concentration of TBHP on the rate of cyclohexene epoxidation, a series of reactions were performed with varying concentration of TBHP from 5mmol to 20mmol.

Table 4.4

Influence of concentration of oxidant in the epoxidation of cyclohexene

Concentration of TBHP (mmol)	Conversion (%)	Selectivity (%)		
		Epoxide	Diol	1-ene + 1-ol
5	21.9	67.2	29.2	3.6
10	55.2	86.6	6.6	6.7
15	43.4	66.0	19.1	15.0
20	36.2	61.0	24.9	14.2

Catalyst chosen- 0.1g TiCr6, duration-5h,

Temperature-343K, 25ml acetonitrile, Oxidant-TBHP

From the results given in table 4.4, it is evident that an optimum concentration of TBHP is needed for maximum activity as well as selectivity of the oxidant. As the concentration of TBHP increases, the rate of epoxidation of cyclohexene increases with a good selectivity of cyclohexene epoxide. The rate reaches a maximum value when 10mmol TBHP is used as an oxidant and thereafter goes on decreasing. Whatever be the concentration of TBHP, the formation of cyclohexene epoxide occurs selectively over TiCr6 catalyst.

4.2.6. Influence Of Solvent

Catalytic activity depends largely on the nature of solvent used. So it is necessary to find out an ideal solvent for the epoxidation of cyclohexene using TBHP as the oxidant. Ingold[48] *et al* reported in his work that the solvent suitable for olefin epoxidation is one, which is not a hydrogen bond donor (HBD) and is also only a relatively poor hydrogen bond acceptor (HBA). If the solvent is a strong HBA, it would be expected to deactivate the catalyst (via any surface hydroxyl groups) and also deactivate the hydroperoxide (via ROOH....HBA hydrogen bonding).

When water is used as a solvent for epoxidation, the catalyst systems showed the least activity as well as selectivity of the epoxide. The formation of another product other than the epoxide, cyclohexane diol, cyclohexenol and cyclohexenone is noticed in appreciable amounts. It has been reported[38] that when water was added to the reaction mixture, they did produce significant amounts of cyclohexene-3- (t-butyl) peroxide. A nice balance between these various solvent requirements is achieved for TiCr6 catalyst by using

acetonitrile, which may well be the optimum solvent for these epoxidation reactions.

<div align="center">

Table 4.5

Influence of solvent in the epoxidation of cyclohexene

</div>

Solvent	Conversion (%)	Selectivity (%)		
		Epoxide	Diol	1-ene + 1-ol
Water	1.0	5	19.1	13. 9
Acetonitrile	55.2	86.6	6.6	6.7
Methanol	2.1	36.3	25. 9	36.2
Isopropanol	2.3	47.0	23.2	12.3

Catalyst chosen- 0.1g TiCr6, duration-5h,

Temperature-343K, 25ml solvent, Oxidant-10 mmol TBHP

4.2.7. Effect of Amount of Solvent

The epoxidation of cyclohexene is carried out using different amounts of acetonitrile under otherwise similar reaction conditions. As the volume of acetonitrile increases there is an increase in percentage conversion as well as epoxide selectivity. When using 25ml acetonitrile TiCr6 gives a cyclohexene conversion of 55.2 with an epoxide selectivity of 86.6%. After that there is not much reduction in percentage conversion when 30ml of acetonitrile is used as the solvent. But the selectivity decreases drastically. This effect is attributed mainly but not exclusively to the side reactions presented in the scheme above. Thus the optimum volume of acetonitrile used in the present study is 25ml.

Table 4.6

Influence of amount of solvent in the epoxidation of cyclohexene

Volume of Acetonitrile (ml)	Conversion (%)	Selectivity (%)		
		Epoxide	Diol	1-ene + 1-ol
15	26.0	65.3	19.2	12.4
20	31.9	77.2	12.1	8.6
25	55.2	86.6	6.6	6.7
30	53.9	47.2	29.2	23.6

Catalyst chosen- 0.1g TiCr6, duration-5h

Temperature-343K, solvent- acetonitrile, Oxidant-10 mmol TBHP

4.2.8. Influence of reaction time

To show the influence of reaction time upon the epoxidation of cyclohexene, the reaction was carried out continuously for 8h at 343K using TBHP as the oxidant in presence of acetonitrile as solvent over the prepared catalyst systems. Figures 4.2,4.3 and 4.4 show the time courses for the epoxidation of cyclohexene over TiCr6, Ti and TiLa6 respectively. All the systems show a common trend in the activity as well as epoxide selectivity. During the initial stages of the reaction the percentage conversion increases and approaches an almost steady value within 5h. But the selectivity towards the corresponding epoxide is high upto 5h of the reaction, thereafter it drops suddenly. This may be due to the possible side reactions. These reactions afford mostly allylic oxidation products and oligomers, and thus limit the epoxidation selectivity.
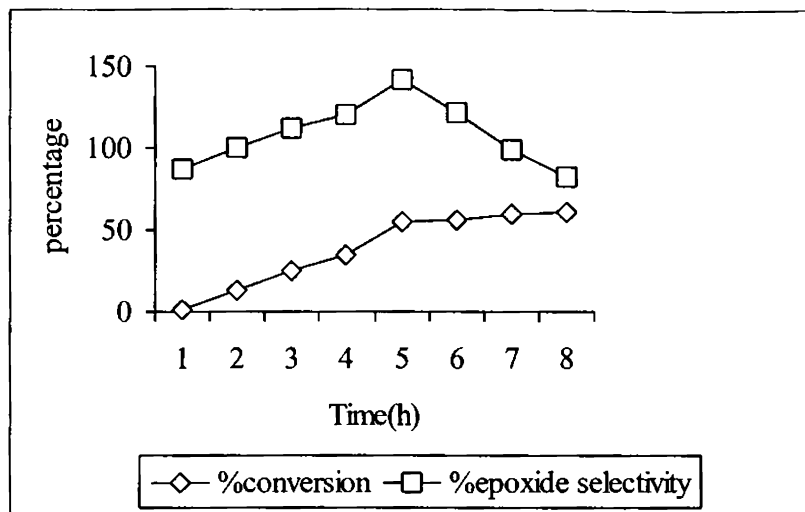
Figure 4.2

Effect of reaction time on the epoxidation of cyclohexene over TiCr6
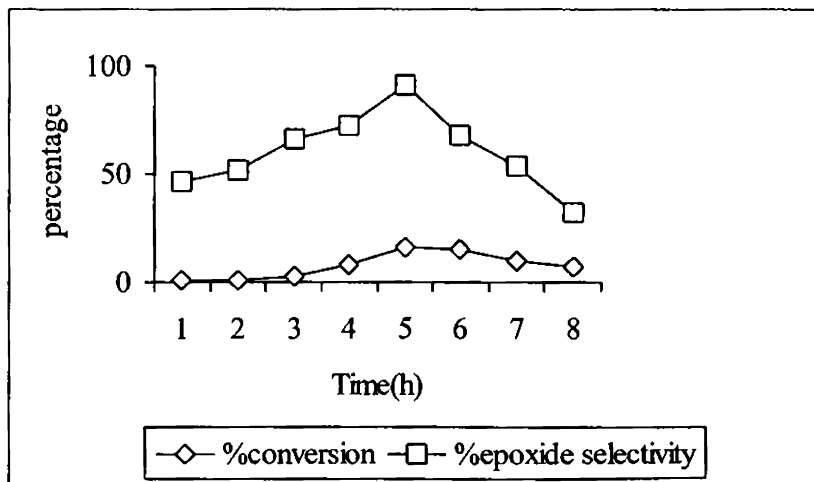
Figure 4.3

Effect of reaction time on the epoxidation of cyclohexene over Ti
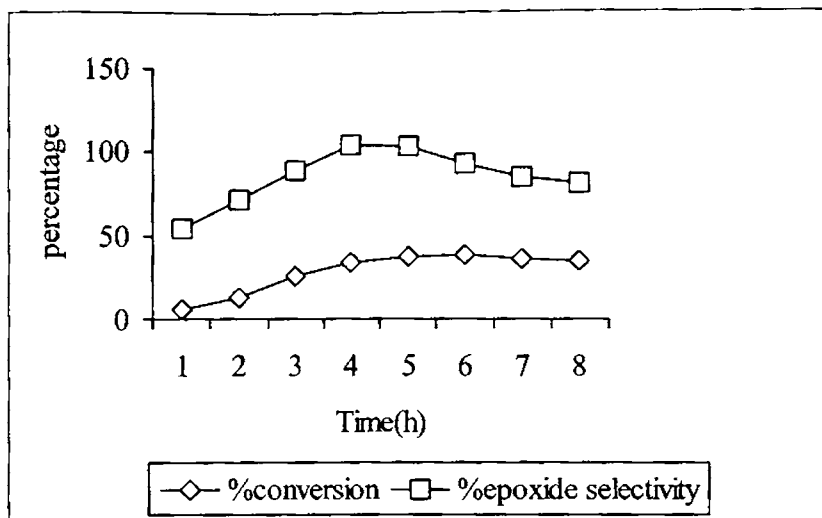
Figure 4.4

Effect of reaction time on the epoxidation of cyclohexene over TiLa6

4.3 Catalytic activity of different catalyst systems

A comparative account of the catalytic activity of various metal modified titania systems in the epoxidation of cyclohexene is given in this section. All the prepared systems were tested for activity over a reaction time of 5h under the optimized reaction conditions. (Reaction temperature of 343K using 25ml acetonitrile as solvent and 10mmol TBHP as the oxidant and 0.1g catalyst). Pure titania exhibited poor activity towards the epoxidation of cyclohexene. The interesting point to be noted is that in spite of its poor activity, pure titania shows a very good selectivity towards cyclohexene epoxide. The results of epoxidation of cyclohexene over transition metal and rare earth metal modified titania systems are presented in tables 4.7 and 4.8 respectively.

Table 4.7

Effect of transition metal on the epoxidation of cyclohexene

Systems	Conversion (%)	Selectivity (%)		
		Epoxide	Diol	1-ene + 1-ol
Ti	16.1	84.5	3.3	12.2
TiMo2	37.5	67.6	18.8	3.7
TiMo6	40.5	63.8	26.4	9.8
TiMo10	38.8	70.4	19.5	10.2
TiCr2	41.3	77.2	17.5	5.3
TiCr6	55.2	86.6	6.6	6.7
TiCr10	53.4	84.4	8.1	7.6
TiW2	34.4	85.8	11.8	2.4
TiW6	42.4	82.0	12.1	6.0
TiW10	41.1	77.4	13.3	8.3

Catalyst -0.1g, duration-5h

Temperature-343K, solvent- 25ml acetonitrile, Oxidant-10 mmol TBHP

Whatever be the nature of the metal incorporated, all the catalytic systems give cyclohexene epoxide as the major product. The selectivity to cyclohexene epoxide is higher in the case of chromium than other metals like molybdenum, tungsten, lanthanum, samarium and praseodymium modified titania systems. An attempt to investigate the influence of the metal loading on catalytic activity is quite reasonable. As expected, variation in metal loading had a significant impact on the catalytic activity. As the percentage of metal

loading increased from 2 to 6%, the conversion gradually increased, thereafter the conversion declined.

Table 4.8

Effect of rare earth metal on the epoxidation of cyclohexene

Systems	Conversion (%)	Selectivity (%)		
		Epoxide	Diol	1-ene + 1-ol
Ti	16.1	74.5	13.3	12.2
TiLa2	40.0	70.4	15.0	14.6
TiLa6	37.3	65.0	24.3	12.2
TiLa10	35.3	62.3	23.2	14.6
TiPr2	39.5	63.8	26.4	9.8
TiPr6	40.5	64.7	23.0	12.3
TiPr10	38.7	62.5	22.2	11.9
TiSm2	37.0	74.7	13.1	11.8
TiSm6	37.0	74.0	11.8	14.2
TiSm10	36.1	72.8	14.6	12.5

Catalyst –0.1g, duration-5h

Temperature-343K, solvent- 25ml acetonitrile, Oxidant-10 mmol TBHP

Synthesis via the solution sol-gel route provided access to highly dispersed Lewis acidic sites, which can effectively activate the alkyl hydroperoxide oxidant[18, 49-52]. The good epoxidation activity and selectivity of modified titania systems is attributed to the presence of isolated titanium sites. To achieve a good distribution of Ti in the modified titanium sites at the

atomic level, it is crucial to compensate the strikingly different sol-gel reactivities of Ti and modified metal precursor.

4.4 Mechanism of the Reaction

Based upon the experimental observations, the proposed pathway for cyclohexene epoxidation at the catalyst surface is schematically shown in figure 4.5. In the epoxidation of cyclohexene, the oxidant (TBHP) interacts with titanium centers and transfers oxygen to cyclohexene. Upon the exposure of TiO_2 surface with this *tert*-butyl hydroperoxide, *tert*-butyl peroxotitanium complex is formed. The peroxotitanium complex formed by the direct reaction between the prepared catalysts (containing TiO_2) and TBHP should have been considered as another candidate for an active species. This suggested that the Ti-OO-*t*-Bu is a plausible active species. The cyclohexene epoxidation is then preceded by oxygen transfer from the *tert*-butyl peroxotitanium complex to the cyclohexene double bond. The consumed complex is finally regenerated by *tert*-butyl hydroperoxide. The enhanced cyclohexene conversion in the case of metal modified titania systems may be attributed to the assistance of the added metal oxide to form tert-butyl peroxotitanium complex. The additional possibility of the added metal to form the corresponding tetra butyl peroxocomplex due to the ability of the metal to form a variety of high valent oxocomplex cannot be ignored.
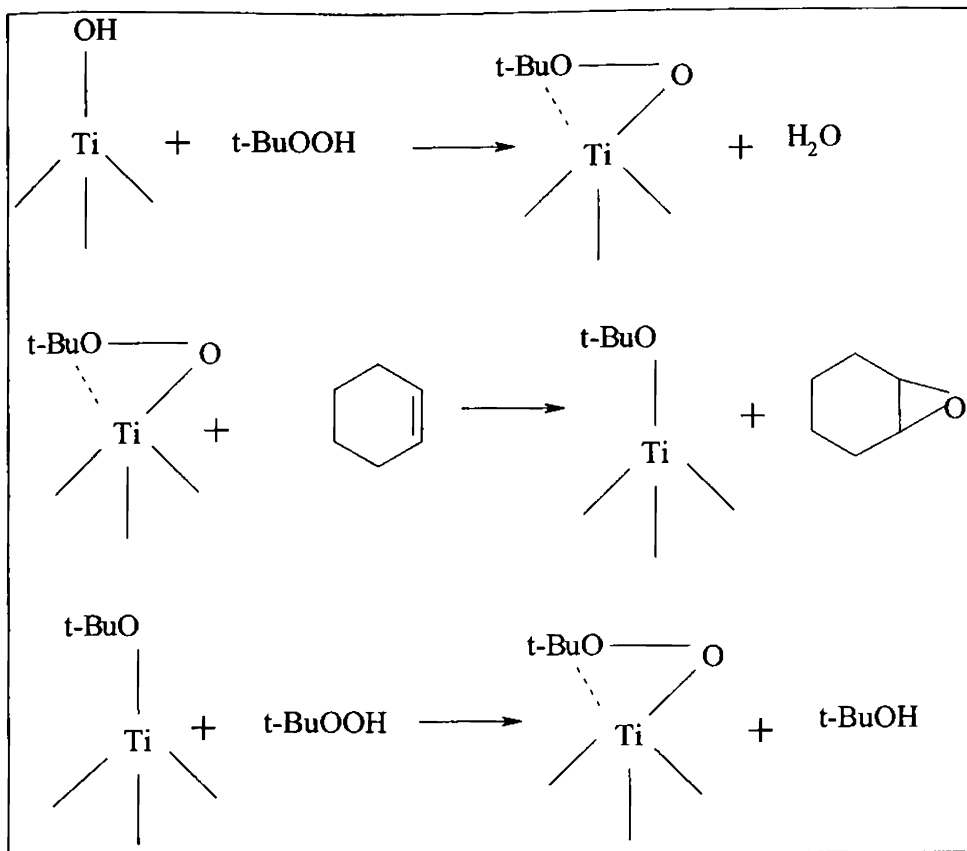
Figure 4.5

Proposed pathway for the epoxidation of cyclohexene at TiO_2 surface

4.5 Conclusions

Transition metal as well as rare earth metal modified sol-gel titania catalyst systems afford high activity and selectivity in the liquid phase epoxidation of cyclohexene. Cyclohexene epoxide is obtained as the major product during the reaction with small amounts of allylic substitution products.

The catalytic behaviour is strongly influenced by the reaction temperature, catalyst concentration, nature and amount of solvent as well as oxidant. The excellent activity and selectivity in the epoxidation of cyclohexene is due to highly dispersed Lewis acidic titanium sites. The reaction pathways, which could suitably explain the catalytic activity for the cyclohexene epoxidation, were also proposed. The activity of the prepared catalysts and their stability with time in the epoxidation of cyclohexene by tert-butyl hydroperoxide hints that it might be possible to create cleaner nylon chemistry.

References

1   I.W.C.E. Arends and R.A. Sheldon, Appl. Catal. A; Gen, 212 (2001) 175.

2   R.A. Sheldon and J. Dakka, Catal. Today, 19 (1994) 215.

3   R.A. Sheldon and J.K. Kochi, Metal catalyzed oxidations of organic compounds, Academic Press, New York, 1981.

4   R.A. Sheldon, Chemtech (1991) 566.

5   G.Centi and M.Misono, Catal. Today, 41 (1998) 287.

6   J.S. Rafelt and J.H. Clark, Catal. Today, 57 (2000) 33.

7   A.H. Hains, Methods for the oxidation compounds, Academic Press, London, 1985,108.

8   M.G. Clerici, Topics Catal, 13 (2000) 373.

9   N.N. Trukhan, V.N. Romannikov, A.N. Shamkov, M.P. Vanina, E.A. Paukshtis, V.I. Bukhtiyarov, V.V. Kriventsov, I. Yu. Danilov and O.A. Kholdeeva, Micropor. Mat. 59 (2003) 73.

10 A. Tuel and L.G. Hubert – Pfalzgraf, J. Catal, 217 (2003) 343.

11 P.T. Tanev, M. Chibwe and T. Pinnavaia, Nature, 368 (1994) 321.

12 L.Y. Chen, G.K. Chuah and S. Jaenicke, Catal. Lett, 50 (1998) 107.

13 F. Chiker, F. Launay, J.P. Nogier and J.L. Bonardet, Environ Chem Lett, 1 (2003) 117.

14 Grzegorz Lewandowski and Eugeniusz Milchert, Ind. Eng. Chem. Res, 40 (2001) 2402.

15 G. Tolstikov, Reactions of Hydroperoxide Oxidation, Nauka, Moscow, U.S.S.R (1976).

16 K. Sato, M. Aoki, R. Noyori , Science, 281 (1998) 1646.

17 S. Imamura, T. Nakai, H. Kanai and T. Ito, Catal. Lett, 28 (1994) 277.

18 R. Hutter, T. Mallat and A. Baiker, J. Catal, 153 (1995) 177.

19 S. Imamura, T. Nakai, H. Kanai and T. Ito, J. Chem. Soc – Faraday Trans, 91 (1995) 1261.

20 Z. Liu, G.M. Crumbaugh and R.J. Davis, J. Catal, 159 (1996) 83.

21 D.T. On, M.P. Kapoor and S. Kaliaguine, Chem. Commun, 1161 (1996).

22 D.C.M. Dutoit, M. Schneider, R. Hutter and A. Baiker, J. Catal, 161 (1996) 651.

23 S. Klein, S. Thorimbert and W.F. Maier, J. Catal, 163 (1996) 476.

24 R.J. Davis and Z.F. Liu, Chem. Mater, 9 (1997) 2311.

25 M. Dusi, T. Mallat and A. Baiker, J. Catal, 173 (1998) 423.

26 C.A. Muller, A. Gisler, M. Schneider, T. Mallat and A. Baiker, Catal. Lett, 64 (2000) 9.

27 T. Mallat and A. Baiker, Appl. Catal. A, 200 (2000) 3.

28 C. Beck, T. Mallat, T. Burgi and A. Baiker, J. Catal, 204 (2001) 428.

29 C.A. Muller, R. Deck, T.Mallat and A. Baiker, Topics Catal, 11 (2000) 369.

30 Iver Schmdt, Anne Krogh, Katrine Wienberg, Anna Carlsson, Michael Brorson and Claus J. H. Jacobsen, Chem. Commun, (2000) 2157.

31 Vasudev N. Shetti, P. Manikandan, D. Srinivas and P. Ratnasamy, J. Catal, 216 (2003) 461.

32 A. Gisler, C.A. Muller, M. Schneider, T. Mallat and A. Baiker, Topics Catal, 15 (2001) 247.

33 Hee-Seok Cheong, Kyoung-Ku Kang and Hyun-Ku Rhee, Catal. Lett, 86 (2003) 145.

34 Peng Wu and Takashi Tatsumi, Catal. Surveys from Asia, 8 (2004) 137.

35 L.Y. Chen, G.K. Chuah and S. Jaenicke, Catal. Lett, 50 (1998) 107.

36 M.N. Timofeeva, Z.P. Pai, A.G. Tolstikov, G.N. Kustova, N.V. Selivanova, P.V. Berdnikova, K.P. Brylyakov, A.B. Shangina and V.A. Utkin, Russian chemical Bulletin, Int. Edn, 52 (2003) 480.

37 Regina Buffon and Ulf Schuchardt, J. Braz. Chem. Soc, 14 (2003) 347.

38 Matt C. Rogers, Bamidele Adisa and David A. Bruce, Catal. Lett, 98 (2004) 29.

39 C.J. Liu, J. Org. Chem, 63 (1998) 7364.

40 Wonwoo Nam, So-Young Oh, Mi Hee Lim, Mee-Hwa Choi, So-Yeop Han and Gil-Ja Jhon, Chem. Commun, (2000) 1787.

41 J.M. Fraile, J. Mol. Catal. A: Chemical, 136 (1998) 47.

42 Marcelo Alves Moreira, Thiago Bergler Bitencourt, and Maria da Grac,a Nascimento, Synthetic Commun, 35 (2005) 2107.

43 Thammanoon Sreethawong, Yusuke Yamada, Tetsuhiko Kobayashi, Susumu Yoshikawa, J. Mol Catal A: Chem, 241 (2005) 23.

44 W.R. Moser, Advanced Catalysts and Nanostructured Materials, Academic Press, San Diego, 1996.

45 A.L. Linsebigler, G. Lu, J.T. Yates Jr., Chem. Rev. 95 (1995) 735.

46 Richard L. Brutchey, Benjamin V. Mork, Donald J. Sirbuly, Peidong Yang, T. Don Tilley, J. Mol. Catal A: Chem, 238 (2005) 1.

47 K. Ambroziak, R. Pelech, E. Milchert, T. Dziembowskaa, Z. Rozwadowski, J. Mol. Catal A: Chem, 211 (2004) 9.

48 K.U. Ingold, Darren W. Snelgrove, Philip A. MacFaul, Richard D. Oldroyd and John Meurig Thomas, Catal. Lett, 48 (1997) 21.

49 R. Hutter, T. Mallat and A. Baiker, J. Catal, 157 (1995) 665.

50 R. Hutter, T. Mallat, D. Dutoit and A. Baiker, Topics Catal, 3 (1996) 421.

51 C.J. Brinker and G.W. Scherer, Sol-Gel Science, Academic Press, Boston (1990).

52 K. Kosuge and P.S. Singh, J. Phys. Chem. B, 103 (1999) 3563.

Chapter 5

Hydroxylation of Phenol

Abstract

The organic effluents containing phenolic compounds from pharmaceutical, fine chemical and petrochemical industries, on account of their poor biodegradability, form a major threat to the ecological balance. With growing ecological concern, chemical producers have been subjected to increasing pressure to minimise the dispersion of waste chemicals. Hydroxylation of phenol is an industrially important reaction as the products, namely catechol and hydroquinone finds diverse applications. The catalytic efficiency of the prepared titania systems in the hydroxylation of phenol was carried out in liquid phase. The effects of various factors that influence this catalytic reaction such as the solvent, reaction temperature, reaction time, catalyst amount and molar ratio of phenol to H_2O_2 were investigated intensively. The performance of the catalytic systems points to its potential in the degradation of phenolic wastes.

5.1 Introduction

The development of ecologically friendly technologies is currently one of the most important goals in industrial chemistry research. This is especially true in the field of oxidation of organic compounds, where there is an urgent need to replace highly effective but wasteful and toxic stoichiometric oxidants. A possible solution to this problem consists in using technology based on catalytic oxygen transfer from "clean" oxygen donors, such as hydrogen peroxide (H_2O_2). Organic compounds such as phenols and phenolic derivatives are amongst the most common chemicals found in regular commercial manufacturing processes. On account of their poor biodegradability, these compounds form a major threat to the ecological balance. The selective oxidation of phenol to industrially useful diphenols forms a convenient route to their efficient disposal. Catechol and hydroquinone are two of the many phenolic derivatives of high value. They are widely used as photography chemicals, antioxidants and polymerization inhibitors and are also used in pesticides, flavoring agents, and in medicine [1]. Catechol was also used as an organic sensitizer in a photo electrochemical cell [2].

Mineral acids [3-5], simple metal ions [6-7] and metal complexes [8] are the traditional catalysts for this reaction, but these homogeneous catalysts are difficult to be separated and recovered from the reaction mixture, which prevents their practical utilization in phenol hydroxylation. Therefore, heterogeneous catalysis over various metal oxides and complexes, such as metal oxides or supported ones [9-11], metal complex oxides [12-13], zeolite encapsulated metal complexes[14] and hydrotalcite like compounds [15-16] have been of great interest to many researchers for a long time.

Zhang *et al.*[17] investigated the catalytic performance of naturally occurring ferritin for the selective hydroxylation of phenol with hydrogen peroxide. The removal of the interior iron containing nanoparticle from the ferritin molecule caused a substantial decrease in catalytic activity. A.Dubey *et al.*[18] carried out the hydroxylation of phenol over CuM(II)M(III) ternary hydrotalcites, where M(II) is Ni or Co and M(III) is Al,Cr,or Fe and they studied the influence of various reaction parameters on the percentage phenol conversion and the selectivity of catechol and hydroquinone formed as the major products. Hydroxylation of phenol was carried out over a series of CoNiAl ternary hydrotalcites having a (Co+Ni)/Al atomic ratio close to 2.6 and a Co:Ni atomic ratios ranging from 1:0 to 0:1 using H_2O_2 as oxidant and water as solvent [19.] Both end members of this series, namely CoAl-HT and NiAl-HT, showed negligible conversion of phenol while cooperative catalytic behaviour was noted when both the elements are present together.

The catalytic activities towards phenol hydroxylation is carried out over intrazeolitic Fe^{3+} prepared by chemical vapor deposition of $[(C_5H_5)Fe(CO)_2]_2$ inside NaY and FSM-16 zeolites. The higher activity of the Fe/NaY sample was attributed to the high dispersity of Fe ions that are located in framework positions and to the high crystallinity[20]. Wang *et al* [21]reported Cu^{2+} exchanged zeolites as efficient catalysts for phenol hydroxylation with hydrogen peroxide. Both zeolite type and copper content in the zeolite catalyst were revealed to exert critical impact upon the catalytic activity in phenol hydroxylation reaction. Mayura *et al* [22]suggested coordination polymers based on bridging methylene blue have potential catalytic activity for the liquid phase hydroxylation of phenol.

Iron containing pillared clays are found to be efficient catalysts for phenol hydroxylation reaction where the presence of redox centers in the layers or in the galleries of the materials, together with a Bronsted acid environment in the galleries of the pillared clays induces the hydroxylation of phenol reaching conversions close to 70% under microwave irradiation even at low reaction time [23]. AlFe-pillared clays are quite efficient catalysts for phenol conversion in water solutions in rather mild conditions[24]. At higher phenol content, catalytic activity loss was noticed.

An enhancement of p-selectivity has been achieved by carrying out the phenol hydroxylation reaction over TS-I/H_2O_2 system with the coexistence of benzene or cyclohexane[25]. The enhancement effect is attributed to the coexistent bulky molecules imposing significant steric restriction on the transition state, which prefers to produce the products with relatively smaller molecular sizes. Feng-Shou Xiao *et al*[26-27] synthesized a novel catalyst of copper hydroxy phosphate ($Cu_2(OH)PO_4$) that has neither microporous nor mesoporous pores and showed that they are particularly active for the wet oxidation of phenol, benzene and naphthol by hydrogen peroxide.

Wei Zhao *et al*[28] reported the synthesis of highly ordered Fe-MCM-48 by a mixed templation method. Its catalytic activity and selectivity was studied for phenol hydroxylation using hydrogen peroxide. The substituting element Fe $^{3+}$ is partially incorporated into the framework position forming a new type of active site, which raises the phenol conversion and the diphenol selectivity. The α-Fe_2O_3 / SiO_2 catalyst exhibited very good catalytic performance in phenol hydroxylation by H_2O_2 to dihydroxybenzene [29]. Fe supported catalysts containing 10 wt% of iron as oxide, on titania and alumina have been prepared

and its catalytic activity was measured in a batch reactor using ozone as the oxidizing agent. The catalytic activity indicates that phenol is degraded with a low mineralisation to CO_2 [30].

Santos *et al*[31-32] reported the aqueous phase oxidation of phenol using a series of commercial copper containing catalysts at elevated temperatures and oxygen pressures. Catalytic wet peroxide oxidation of phenol over unpromoted MnO_2/CeO_2 revealed that even after complete removal of organic carbon from the solution was achieved,an important fraction of the initial carbon was transformed into a polymeric material strongly adsorbed on the surface of the catalyst[33-35]. This deposit was shown to be responsible for the catalyst deactivation *via* physical blockage of the active sites[34]. The use of noble metal containing catalyst like platinum over alumina generates lesser build up. However, due to its weaker reactivity, longer reaction times and higher oxidation temperatures are required[33]. Hamoudi *et al* also investigated the catalytic oxidation of phenol in aqueous solution in presence of Pt and Ag promoted MnO_2/CeO_2[36]. Hocewar *et al*[37], investigating on the catalytic wet peroxide oxidation of copper containing catalysts observed that $Ce_{1-x}Cu_xO_{2-\delta}$ system was insoluble in hot acidic solutions. The same system when prepared in the form of highly dispersed copper oxide phases on CeO_2 support by sol gel route was catalytically active under mild conditions.

In the present study, the catalytic activity of pure titania, transition metal as well as rare earth metal modified titania systems towards phenol hydroxylation is carried out. Phenol Hydroxylation reaction seems to proceed along a complex pathway involving a series of consecutive reactions (Fig. 5.1)
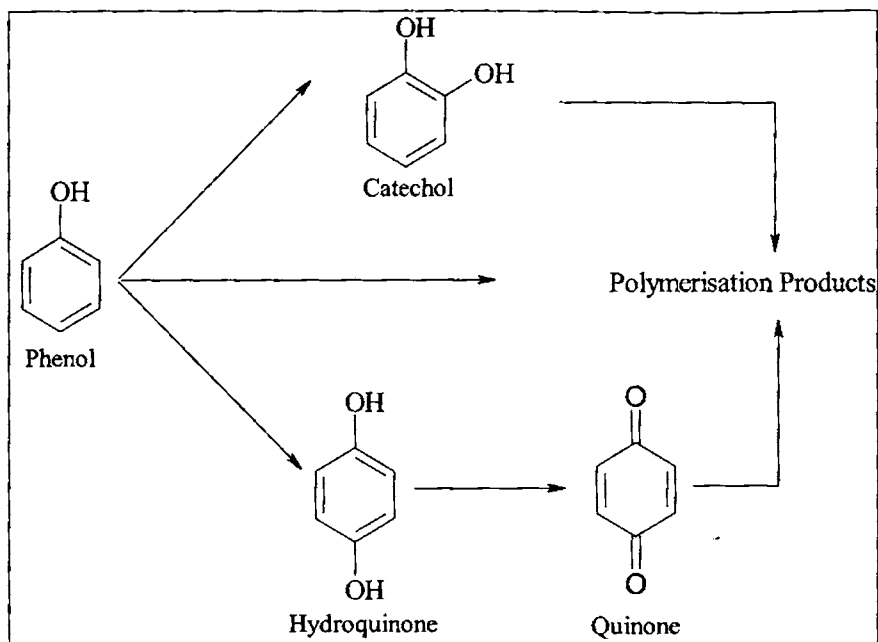
Figure.5.1

General scheme of phenol hydroxylation

5.2 Process optimization

Catalytic experiments were carried out in a round bottom flask equipped with a reflux condenser, a magnetic stirrer and a temperature controllable oil bath. The catalyst to be studied was added to start the reaction. For a typical run, 0.1 gm of the catalyst, 1mmol phenol, 5 mmol hydrogen peroxide as oxidant and 5ml water as solvent were stirred vigorously at 333K for 2h. The reaction mixture was then stirred at controlled temperature. The reaction products were analyzed at stipulated time using a gas chromatograph by taking small aliquot out. It is well known that the solvent, reaction temperature, reaction time, catalyst amount, molar ratio of phenol to hydrogen

peroxide are the main factors that influence the phenol hydroxylation and these factors are systematically investigated in the following sections.

5.2.1. Influence of catalyst

The reaction is done using phenol and hydrogen peroxide in water solvent in the absence of a catalyst (blank run) and in the presence of the catalyst (0.1gm TiCr6) at 333K. Catechol (o-diphenol), hydroquinone (p-diphenol) and benzoquinone were the major products of this reaction despite the different conditions and catalysts used. We observed a percentage conversion of 1.4 and 50.2 after 2hs in the absence and presence of catalyst respectively. Low yield for the reaction in uncatalyzed reaction is due to higher activation energy of the uncatalyzed reaction. Addition of the catalyst significantly reduced the activation energy and the reaction proceeded through a different mechanism, resulting in a higher percentage conversion.

5.2.3 Influence of reaction temperature

The activities and product selectivities in the temperature range of 323-353K for phenol hydroxylation with H_2O_2 over TiCr6 catalyst are presented in table 5.1. Obviously phenol conversion increased when the reaction temperature increases from 323 to 333K and when the temperature was above 333K, there is a remarkable reduction in phenol conversion. At 323K, phenol conversion was only 21. 1% with a hydroquinone selectivity of 51.4%. When the temperature increased to 333K, phenol conversion increased to 50.2% with hydroquinone selectivity of 61.0%. Considering both conversion and

selectivity, the reaction temperature chosen for hydroxylation reaction was 333K.

Table 5.1

Influence of reaction temperature on phenol hydroxylation

Temperature	Conversion (%)	Selectivity (%)		
		Catechol	Hydroquinone	Quinone
323	21.1	24.8	51.4	31.8
333	50.2	31.2	61.0	2.3
343	31.6	30.5	54.9	10.3
353	18.5	28.8	45.8	20.3

Amount of catalyst -0.1g TiCr6, water-5ml, Phenol: H2O2-1: 5, Duration-2h

The decrease in phenol conversion with increase in reaction temperature is consistent with the exothermic nature of the reaction. The accelerated decomposition of H_2O_2 at elevated temperatures may also contribute to the drop off in the conversion. It has been reported that the activation energy for the decomposition of H_2O_2 is lower than that for the hydroxylation of phenol [12,38]. Above 90°C, the amount of residual phenol in the reaction mixture was rather negligible. However, no peaks could be detected in the GC analysis corresponding to the products. This may be due to the overoxidation resulting in tarry products.

5.2.3. Influence of H_2O_2 to phenol ratio

Table 5.2 summarizes the influence of molar ratio of hydrogen peroxide to phenol in phenol hydroxylation over TiCr6 catalyst. A larger molar

ratio of hydrogen peroxide to phenol in the catalysis led to higher efficiency of utilization for H_2O_2. The phenol conversion first increases with the increase in the ratio to a certain extent and thereafter an increase in the H_2O_2 to phenol ratio causes a drastic reduction in the percentage conversion. The drastic reduction may be related to the overoxidation of phenol to tarry products at high peroxide concentration. The product selectivity is also influenced by the H_2O_2 to phenol molar ratio. At an optimum molar ratio of 5:1, the percentage selectivity is highest with a good product distribution.

Table 5.2

Influence of H_2O_2 to phenol molar ratio on phenol hydroxylation

H_2O_2 to phenol Ratio	Conversion (%)	Selectivity (%)		
		Catechol	Hydroquinone	Quinone
3:1	17.5	12.6	41.8	33.3
4:1	26.9	26.0	57.2	16.3
5:1	50.2	31.2	61.0	2.3
6:1	21.2	11.9	41.1	25.0
7:1	7.5	17.9	39.7	31.0

Amount of catalyst -0.1g TiCr6, water-5ml, Temperature-333K, Duration-2h

5.2.4. Influence of catalyst weight

The activities in phenol hydroxylation over TiCr6 catalyst with different catalyst amount is presented in table 5.3. Hydroxylation occurs very slowly in the absence of a catalyst. Phenol conversion increased with a catalyst amount upto 0.1g and then a further increase in catalyst amount decreases the phenol conversion. Addition of large amount of the catalyst to the reaction

mixture had a negative effect in the prepared systems. This is because a larger amount of the catalyst hastened the decomposition of hydrogen peroxide. Therefore a suitable amount of the catalyst in the catalysis was 0.1g.

Table 5.3

Influence of catalyst weight on phenol hydroxylation

Catalyst weight (g)	Conversion (%)	Selectivity (%)		
		Catechol	Hydroquinone	Quinone
0.05	19.8	17.3	7.1	75.6
0.10	50.2	31.2	61.0	2.3
0.15	45.6	22.1	31.2	40.8

TiCr6 catalyst, Temperature-333K, water-5ml, Phenol: H2O2-1: 5; Duration-2h

5.2.5. Influence of solvent

It has been reported that the solvents in this reaction has a profound influence on the phenol conversion and the product selectivity. Table 5.4 presents a summary of solvent influence in phenol hydroxylation over TiCr6 catalyst. When acetone is used as a solvent, the hydroxylation occur at a slower rate even at temperatures upto 363K. Interestingly a change from organic solvents to water led to a significant increase in phenol conversion, indicating that water was the best solvent over the prepared systems. Water is safe, cheap and environmentally friendly solvent. However the amount of water strongly affected the phenol conversion and the product selectivity. At 333K, the catalytic activity was in the order water > methanol > acetonitrile > acetone. In the present study, water is used as a solvent.

Table 5.4

Influence of solvent on phenol hydroxylation

Solvent	Conversion (%)	Selectivity (%)		
		Catechol	Hydroquinone	Quinone
Acetone	1.2	42.4	45.8	12.1
Water	50.2	31.2	61.0	2.3
Methanol	38.3	7.9	39.7	41.0
Acetonitrile	24.8	30.5	44.9	20.3

0.1 g TiCr6 catalyst, Temperature-333K, Phenol: H2O2-1: 5, Duration-2h

5.2.6 Influence of reaction time

Figure 5.2 shows the time profiles of catalytic performances of pure titania, TiCr6 and TiLa6.
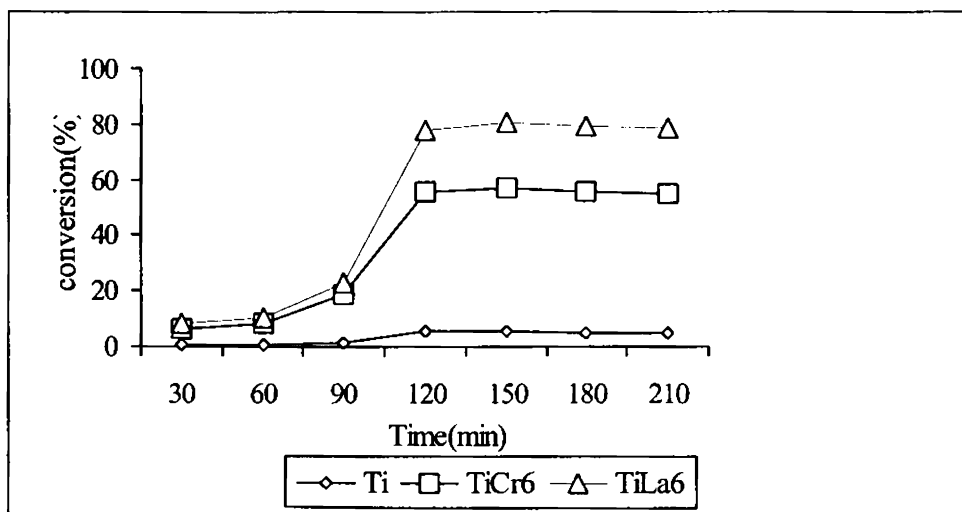
Figure 5.2

Influence of time on stream in phenol hydroxylation

Notably a relatively short reaction time resulted in incomplete conversion of phenol as well as undesirable product selectivity and the conversion increased with reaction time. There was an induction period of about 90 minutes where the systems gave marginal phenol conversions. After 90 minutes, a sharp rise was observed in the yield of diphenols. Suitably, a long reaction time was beneficial for the conversion of phenol, but its deep oxidation of hydroquinone into benzoquinone and of benzoquinone into tar could not be avoided after longer times. Therefore the reaction time of 120 minutes was suitable for phenol hydroxylation over the prepared systems

5.3. Catalytic activity of different catalyst systems

After optimization studies, catalytic activity of all the prepared systems were evaluated. The following tables 5.5 and 5.6 present the results of phenol hydroxylation over transition metal and rare earth metal loaded titania systems respectively. It is believed that the proximity of the hydroxylating agent and of the substrate molecule on or near the active catalyst site is essential for driving the reaction. In water, both phenol and hydrogen peroxide dissolve simultaneously and approach the active center, thereby generating hydroxy radicals, proposed to be the active species involved in the hydroxylation reaction. Moreover such an electrophile is easier produced and stabilized in water than in organic solvents. Possibly, the lack of hydroxylated nature for the other organic solvents may be responsible for the non-occurrence of this reaction. Furthermore when this reaction is carried out using different oxidants other than hydrogen peroxide, namely oxygen, air and tert-butyl hydroperoxide, none of them hydroxylated phenol to a significant extent under

similar reaction conditions, possibly due to the lack of generation of the active oxidant species and the solubility problems associated with the reactant and the oxidant.

Table 5.5

Influence of transition metal in the hydroxylation of phenol

Systems	Conversion (%)	Selectivity (%)		
		Catechol	Hydroquinone	Quinone
Ti	5.4	26.6	42.4	31.1
TiMo2	28.4	32.4	42.5	15.8
TiMo6	29.3	20.7	55.2	17.5
TiMo10	36.2	20.4	42.3	27.2
TiCr2	43.6	33.9	43.6	13.4
TiCr6	50.2	31.3	61.0	12.3
TiCr10	50.5	21.4	56.9	16.4
TiW2	29.8	28.7	63.2	8.7
TiW6	35.3	13.8	50.8	28.4
TiW10	45.0	34.3	35.3	19.0

0.1 g catalyst, Temperature-333K, water-5ml ,Phenol: H2O2-1: 5, Duration-2h

Pure titania gave very low conversion under the specified conditions and the metal loaded systems are highly effective in hydroxylating phenol. But no strict correlation is obtained between the catalytic activity and the catalyst properties. Among the systems incorporated with different transition metal and rare earth metals, the individual effects created by the addition of the respective species may be playing a dominating role in deciding the catalytic

activity. In all the systems, the percentage phenol conversion increases with the metal loading. This supports the active involvement of the incorporated metal in the reaction. A combined influence of various factors like the surface area, crystallite size, redox properties and the electron accepting properties may be the driving force for the reaction. Chromia loaded titania systems showed higher phenol conversion and a good diphenol selectivity.

Table 5.6

Influence of rare earth metal in the hydroxylation of phenol

Systems	Conversion (%)	Selectivity (%)		
		Catechol	Hydroquinone	Quinone
Ti	5.4	26.6	42.4	31.1
TiLa2	21.0	48.8	37.3	14.0
TiLa6	22.5	39.5	38.0	22.5
TiLa10	23.5	48.5	39.6	11.8
TiPr2	20.9	78.5	19.6	2.2
TiPr6	22.9	56.1	24.2	19.7
TiPr10	19.7	55.7	23.9	13.6
TiSm2	22.7	78.9	18.3	2.8
TiSm6	23.7	79.2	14.6	6.3
TiSm10	28.7	65.9	26.9	7.3

0.1 g catalyst, Temperature-333K, water-5ml, Phenol: H2O2-1: 5, Duration-2h

5.4 Mechanism of phenol hydroxylation

A heterogeneous-homogeneous reaction mechanism has been proposed for the liquid phase oxidation over solid catalysts [39-40]. The appearance of an induction period and the exponential increase in the percentage conversion with time in the present study support the involvement of a free radical mechanism. An induction period was quite noticeable with all the systems, the time being dependent on the system chosen. This again suggests a free radical mechanism to be operating irrespective of the catalytic system selected. The high susceptibility of the aromatic ring of phenols towards oxidation can be attributed to the possible generation of the delocalised aryloxy radical *via.* the removal of a hydrogen atom. The generation of phenoxy radicals may occur on the catalyst surface. At the same instant, catalyst surface can also trigger the homolytic cleavage of the hydrogen peroxide. A general mechanism of the reaction is sketched in Fig. 5.3. The formation of catechol and hydroquinone is believed to occur *via.* the attack of OH˙ on the benzene ring. The formation of phenoxy radicals occurs at the catalyst surface after which the propagation of the reaction can occur either in the liquid phase or on the catalyst surface. A further investigation into the course of the reaction is essential for a clear-cut prediction of the actual mechanism.

Another interesting observation was that transition metal loaded systems gave good selectivity to hydroquinone(para product) whereas rare earth metal loaded systems gave high selectivity to catechol(ortho isomer).This may be a consequence of some sort of association between the phenoxy radicals and the catalyst surface. Another possibility is that the diffusion of the radicals from the catalyst surface may be a slow process when compared with

the attack of the hydroxy radicals. Thus, before the radical gets sufficient time to drift apart the attack by the OH˙ occurs preferentially at the ortho position in case of rare earth metal loaded systems.
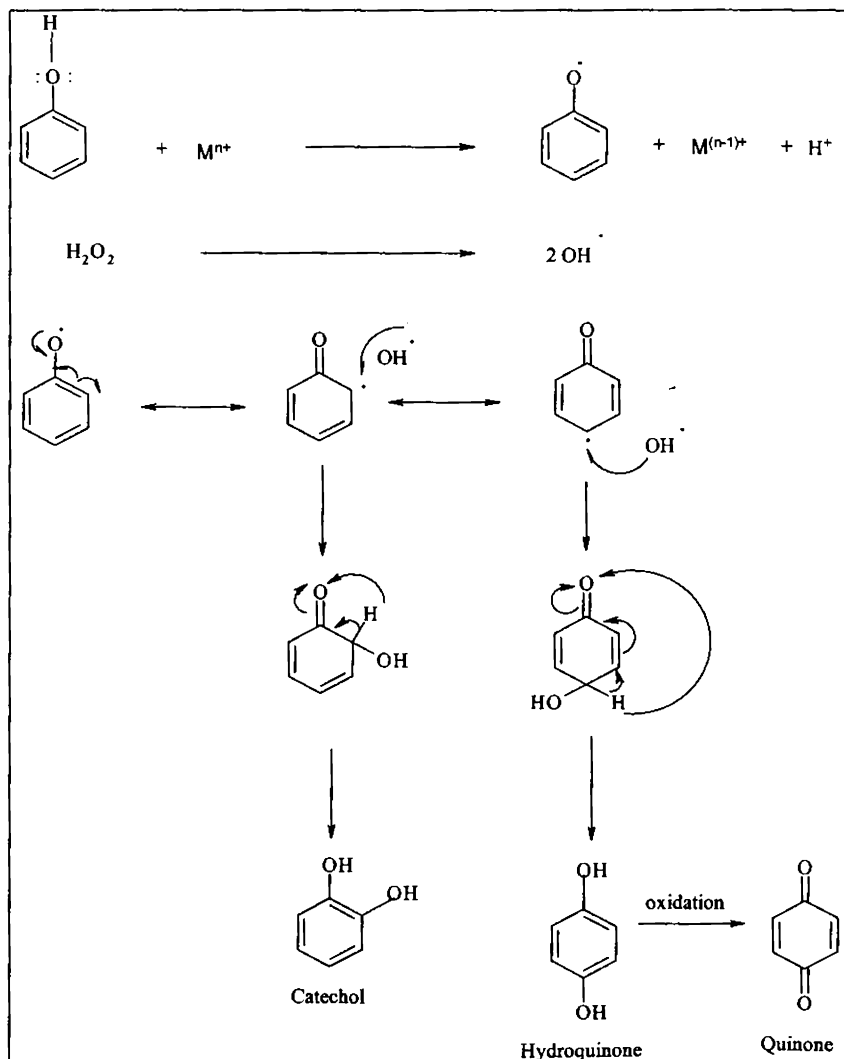
Figure 5.3 A plausible mechanism for phenol hydroxylation reaction

5.5 Conclusions

Both transition metal and rare earth metal modified titania systems are highly effective in the hydroxylation of phenol. Among various metals, chromia incorporated systems are showing highest activity as well as selectivity. Reaction variables such as temperature, catalyst concentration, nature of solvent and the molar ratio of phenol to hydrogen peroxide are indispensable factors influencing the catalytic activity of the systems. Selection of an optimum reaction time also demands prime importance in order to achieve maximum activity and selectivity of the products. In any case, metal modified titania systems seem to be a promising catalyst for the disposal of phenolic wastes.

References

1   M.Howe-Grant (Ed), Kirk-Othmer, Encyclopedia of chemical technology, 4th ed., Wiley, (1995), 996.

2   K. Tennakone, G.R.R.A. Kumara, A.R. Kumarasinghe, P.M. Sirimanne, K.G.U. Wijayantha., J. Photochem. Photobiol. A; Chem, 94 (1996) 217.

3   F. Bourdin, M. Costantini, M. Jouffret, G. Latignan.,Ger. Patent, 2,064,497 (1971).

4   C. Skepalik, Ger. Patent, 2,138,735 (1973).

5   J. Varagnat, Ind. Eng. Chem. Prod. Res. Dev, 15 (1976) 212.

6   G.A. Hamilton, J.W. Hamfin, J.P. Friedman, J. Am.Chem.Soc, 88(22) (1966) 5269.

7   M.A. Brook, L. Gatle, I.R. Lindsay, J. Chem. Soc., Perkin Trans, 2 (1982) 687.

8   D.R.C. Hytbrechts, I. Vaesen, H.X. Li, P.A. Jacobs, Catal. Lett, 8 (1) (1991) 237.

9   Ai. M, J. Catal, 54 (2) (1978) 223.

10 N. Al-Hayck, Water Res, 19 (1985) 657.

11 S. Goldstein, G. Czapski, J. Robani, J. Phys. Chem, 98 (26) (1994) 6586.

12 R. Yu, F. Xiao, D. Wang, J. Sun, Y. Liu, G. Pang, S. Feng, S. Qiu, R. Xu, C. Fang, Catal Today, 51(1) (1999) 39.

13 J. Sun, X. Meng, Y. Shi, R. Wang, S. Feng, D. Jiang, R. Xu, F. Xiao, J. Catal, 193 (2) (2000) 199.

14 M.R. Maurya, S.J.J. Titinchi, S. Chand, I.M. Mishra, J. Mol. Catal.A.Chem, 180 (2002) 201.

15 K. Zhu, C. Liu, X. Ye, Y. Wu, Appl. Catal.A; Gen, 168 (2) (1998) 365.

16 A. Dubey, V. Rives, S. Kannan, J.Mol.Catal.A, Chem, 181 (2002) 151.

17 Ning Zhang, Fengyi Li, Qi jia Fu, Shik Chi Tsang, React.Kinet.Catal.Lett, 71 (2000) 393.

18 A.Dubey, S.Kannan, S.Velu, K.Suzuki, Appl.Catal.A;Gen, 238 (2003) 319.

19 Vicente Rives, Olga Prieto, Amit Dubey and Srinivavsan Kannan, J.Catal, 220 (2003) 161.

20 Mohamed Mokhtar Mohamed, N.A.Eissa, Mat. Research Bulletin, 38 (2003) 1993.

21 Jun Wang, Jung-Nam Park, HaCheol Jeong, Kwang-Sik Choi, Xian-Yong Wei, Suk-In Hong and Chul Wee Lee, Energy and fuels, 18 (2004) 470.

22 Mannar R.Mayura, Indu Jain, Salam J.J.Titinchi, Appl.Catal.A; Gen, 249 (2003) 139.

23 Sadok Letaief, Blanca Casal, Pilar Aranda, Maria Angeles Martin-Luengo, Eduardo, Eduardo Ruiz-Hitzky, Appl.Clay.Science, 22 (2003) 263.

24 Erno E.Kiss, Lonjaua G. Ranogajec, Radmila P.Marinkovic-Neducin and Tatjana J.Vulic, React. Kinet. Catal. Lett, 80 (2) (2003) 255.

25 Toshiyuki Yokoi, Peng Wu, Takashi Tatsumi, Catal.Commun, 4 (2003) 11.

26 Feng-Shou Xiao, Jianmin Sun, Xiangju Meng, Ranbo Yu, Hongming Yuan, Dazhen Jiang, Shilum Qiu and Ruren Xu, Appl. Catal.A; Gen, 207 (2001) 267.

27 Feng-Shou Xiao, Jianmin Sun, Xiangju Meng, Ranbo Yu, Hongming

Yuan, Dazhen Jiang, Shilum Qiu and Ruren Xu, J.Catal, 199 (2001) 273.

28 Wei Zhao, Yunfei Luo, Peng Deng and Quanzhi Li, Catal Lett, 73 (2001) 199.

29 Qingsheng Liu, Jianfeng Yu, Zhenlu Wang, Piaoping Yang and Tonghao Wu, React. Kinet. Catal. Lett,73(2001) 179.

30 Gina Pecchi and Patrico Reyes, J. Sol-gel Sci and Tech, 26 (2003) 865.

31 A. Santos, E. Barroso, F.G. Ochoa, Catal. Today, 48 (1999) 109.

32 A. Santos, P. Yustos, B. Durban, F.G-Ochoa, Catal. Today, 66 (2001) 511.

33 S. Hamoudi, F. Larachi, A. Sayari, J. Catal, 177 (1998) 247.

34 S. Hamoudi, F. Larachi, A. Adnot, A. Sayari, J. Catal, 185 (1999) 333

35 S. Hamoudi, A. Sayari, K. Belkacemi, L. Bonneviot, L. Larachi, Catal. Today, 62 (2000) 379.

36 S. Hocevar, U.O. Krasovec, B. Orel, A.S. Arico, H. Kim, Appl. Catal. B: Environ, 28 (2000) 113.

37 A.Alejandre, F.Medina, P.Salagre, A.Fabregat, J.E.Sueiras, Appl. Catal. B: Environ, 18 (1998) 307.

38 R.Yu, F-S. Xiao, D. Wang, Y. Liu, G. Pang, S. Feng, S. Qiu, R. Xu, Catal. Lett, 49 (1997) 49

39 C. Meyer, G. Clement, J.C. Balaceanu, "Proc. 3rd Int. Congr. On Catalysis", Vol. 1 (1965) 184.

40 A. Sadana, J.R. Katzer, J. Catal, 35 (1974) 140.

Chapter 6

Alkylation of Aromatics

Abstract

Alkylation of aromatics is a particularly important area of industrial chemistry. In searching for more environmentally benign replacements for traditional hazardous acid catalysts, numerous solid acid catalysts have been suggested. The present chapter reveals the great versatility of titania and modified titania systems in the alkylation of aromatics. The chapter is divided into three sections. The first section deals with the tert-butylation of phenol. The second and third section depicts the methylation of aniline and anisole respectively. The products obtained find extensive use in industries related to pharmaceuticals, dyestuffs, agrochemicals, surfactants, polymers and antioxidants. The important variables affecting the activity and selectivity of the prepared catalytic systems, such as reaction temperature, flow rate and mole ratios of the alkylating agent to arene were studied. The effects of acidity on the alkylating activity of arene are also discussed.

Section A

Tert-Butylation of Phenol

6.1 Introduction

The alkylation of phenol with tert-butyl alcohol is of industrial relevance and also of academic interest. Alkyl phenols are very valuable industrial chemicals; among which tert-butylated phenols find wide variety of applications. 2-tert-butyl phenol is an intermediate for pesticides, fragrances and other products whereas 4-tert-butyl phenol is used as a raw material for the production of a variety of resins, durable surface coatings, varnishes, wire enamels, printing inks and so forth[1-2]. Other applications of 4-tert-butyl phenol include surface-active agents, rubber chemicals, antioxidants, fungicides and petroleum additives. 2,4-Di-tert-butyl phenol is an intermediate for antioxidants and 2,6-di-tert-butyl phenol is used as an antioxidant intermediate and in pharmaceuticals[3].

In general, tertiary butylation of phenol was carried out in homogeneous medium using euphoric acid, flour euphoric acid, arene euphonic acid, phosphoric acid and aluminium chloride boric acid or boron triflouride etherate as catalysts[1]. Although both homogeneous and heterogeneous catalysts are used in alkylation reaction systems, the trend is towards solid heterogeneous catalysts due to the inherent advantages of their high activity, better selectivity, ease of separation from reaction mixtures, chemical stability, reusability, environmental friendliness and absence of corrosion problems.

Tert-butylated phenols are generally prepared by reacting phenol with pure isobutylene gas or C_4 fraction of naphtha, by using a liquid acid catalyst,

giving wide product distribution. Both C- and O-alkylation are possible depending on reaction conditions such as temperature, source of isobutylene and type of catalyst. Besides due to the problems associated with unavailability, transportation and handling of isobutylene, particularly for usage in low tonnage fine and specialty chemical industry, it is advantageous to generate isobutylene in situ, amongst which cracking of methyl tert-butyl ether (MTBE) and dehydration of tert-butanol is attractive[4-6]. MTBE is a good source for the in situ generation of pure isobutylene and the coproduct; methanol can be recovered and reused. On the contrary, the dehydration of tert-butanol in situ leads to water as a coproduct in the alkylation reaction and thus different yields of the calculated product are expected vis-à-vis MTBE as an alkyl ting agent[7-8]. Other general processes for the production of alkyl phenols include the following routes.

- Reduction of acyl phenols, which are obtained by Friedel Crafts acylation of phenols or by the Fries rearrangement of phenol esters.

- Alkali fusion of alkyl benzene sulphonates, which are obtained by sulphonation of alkyl benzenes.

- Cleavage of bis (4-hydroxy phenol) alkanes either alkali catalyzed with H_2 in presence of hydrogenating catalyst or with hydrogen donor such as cyclohexanol.

- Claisen rearrangement of allyl aryl ethers into allyl phenols with subsequent rearrangement into vinyl phenols or hydrogenation to alkyl phenols.

Reports and patents concerning the catalytic reaction, which has been carried out both in the liquid and in the gas phase, are available. The catalysts

used include liquid acids, metal oxides, aluminium salt catalysts and cation exchange resins [9-32]. Sulphated titania systems[22] as well as zirconia systems[23] are also found to be highly effective for para selective tert butylation of phenol. Recently many organic chemists have been intrigued with the use of inorganic supports for use as effective and selective catalysts in some synthetic organic reaction.

Yasuhiro *et al* studied the reaction of phenol with t-butanol under a variety of conditions in the presence of silica gel[24]. They could easily prepare 2-tert butyl, 2,6-di-tert butyl and 2,4,6-tri-tert butyl phenols, all of which are hard to obtain directly by the Friedel Crafts process, by this one step reaction. Para selective butylation of phenol over silico alumino phosphate molecular sieve SAPO-11 catalyst is carried out successfully[25]. Separate studies have shown that 2- and 4- tert-butyl phenols obtained undergo easy dealkylation to phenol that increases with temperature. Sakthivel *et al* successfully carried out tert-butylation of phenol over mesoporous H-AlMCM-41 catalysts[26]. They suggested an optimum reaction conditions to get higher substrate conversion and para selectivity compared to the microporous catalysts, e.g., SAPO-11, ZSM-12, zeolite β and zeolite Y. Moderate to strong acidity, large surface area, and mesoporous nature of the H-AlMCM-41 may be responsible for the observed results. A range of iron and aluminium containing mesoporous molecular sieves FeAlMCM-41 catalysts showed superior performance in the acid catalyzed tert butylation of phenol [27].

The catalytic properties of zeolite beta in the tert butylation of phenol are reported[28]. Medium acid sites on zeolite Hβ are advantageous in producing 4-tert butyl phenol and that of strong acid sites are helpful for the formation of

2,4-di tert butyl phenol, while weak acid sites are effective in producing 2-tert butyl phenol. Zhang *et al* investigated the tert-butylation of phenol over various zeolite catalysts using tert-butyl alcohol as the alkylating agent in a down flow tubular reactor at atmospheric pressure[29]. Their study shows that zeolite Y was beneficial to this reaction with a greater selectivity of 2,4-di tert butyl alcohol. Alkylation of phenol was carried out with tert-butyl alcohol producing 4-tert butyl alcohol over a variety of zeolite catalysts, namely zeolite β, 13X zeolite, Ce-exchanged 13X zeolite, and zeolite prepared from fly ash. Zeolte β showed the highest activity for the reaction under otherwise identical conditions[30]. The alkylation reaction was found to be surface reaction controlled with negligible interparticle mass transfer resistance. Zeolite HM has a potential application in phenol alkylation with tert-butyl alcohol to produce 4-tert-butyl alcohol and 2,4-di-tert butyl alcohol with high activity and selectivity[31]. The liquid phase tert- butylation of phenol with tert-butanol in the presence of the H^+ form of the zeolites with FAU, BEA, and MOR topologies was investigated[32]. The catalytic activity and selectivity are controlled by the porous structure and acid properties of the zeolite type.

6.2 Process Optimization

The vapour phase tert-butylation of phenol was carried out in a conventional fixed bed reactor under the flow of nitrogen using 0.5g of the catalyst by changing the reagent feed ratio, the temperature and the flow rate. The catalysts were placed in the reactor and supported on either side with a thin layer of glass wool and ceramic beds. The reactor was heated to the reaction temperature with the help of a tubular furnace provided with a

temperature controller. The catalyst was activated at 500°C for 2h before the catalytic runs. Reactants were fed into the reactor using a syringe pump. The bottom of the reactor was connected to a coiled condenser and receiver to collect the products. The products obtained in the first hour were discarded and the products collected after different times-on-stream was analyzed. The activities and selectivities considered for comparison of the behaviour of the different catalysts are those obtained after 2h. The products were analyzed by Gas Chromatography (Chemito GC 1000) using BP1 capillary column (12m×0.32m) with FID detector.

In the alkylation of phenol with TBA over the prepared catalysts, 2-tert-butyl phenol (2-TBP), 4-tert-butyl phenol (4-TBP) and 2,4-di-tert-butyl phenol (2,4-DTBP) were found as the reaction products. The formation of more bulky dialkyl phenols was suppressed. According to the results from GC, no phenyl ethers and no 3-tert-butyl phenol (3-TBP) formed even at high phenol conversions under the chosen reaction conditions, which is different from the results obtained in CCl$_4$ solutions at lower reaction temperature (303, 318, 353K) reported previously[33]. The choice of proper reaction conditions is discussed in the following sections.

6.2.1 Effect of temperature

The alkylation of phenol with tert-butanol was a highly temperature dependant reaction. Most of the studies were conducted at temperatures close to the boiling point of phenol (180°C). The reaction is carried out at various reaction temperature in the range 150-300°C. From table 6.1, it is clear that at higher and lower temperatures, the percentage conversion and the selectivity to

the para product changes remarkably. When temperature was increased from 150 to 200° C, the conversion of phenol had also increased from 26.4 to 45.6%, respectively. Phenol conversion decreases when the temperature is increased beyond 200°C, which could be due to the predominant dealkylation of the product into phenol and other lower hydrocarbons over alkylation and also the diminishing availability of tert-butanol as it undergoes side reactions such as oligomerisation or aromatisation[25, 26,28].

Table 6.1

Influence of reaction temperature on the conversion and product selectivity in tert-butylation of phenol

Temperature (°C)	Conversion of Phenol (%)	Product Selectivity (%)		
		2-TBP	4-TBP	2,4-DTBP
150	26.4	23.9	68.8	7.4
200	45.6	36.0	61.3	2.7
250	17.2	16.3	77.1	6.7
300	15.2	20.0	65.3	14.7

Catalyst chosen-0.5g TiW2, Flow rate-5ml/h, Phenol: t-butanol –1:3,

Duration-2h

However at higher temperatures, enhanced para selectivity could be due to the absence of secondary alkylation reaction. Moreover coke formation might be a serious problem, which could result in fast deactivation of the catalyst. A high selectivity for the formation of 4-tert-butyl phenol is observed which increases significantly with reaction temperature. The observed increase in para selectivity with decreasing phenol conversion has also been reported for other catalysts and explained by the other diffusion kinetics of 4-TBP as

compared to the other products. A moderate reaction temperature was helpful to enhance the product selectivity. Considering the phenol conversion and the product (4-TBP) distribution, the proper reaction temperature is 200°C. At this reaction temperature, the selectivity of 4-TBP is higher at higher phenol conversions.

6.2.2 Effect of flow rate

The contact time between the catalyst and the reactants greatly influence the reaction rate. The results of phenol alkylation at different flow rates were depicted in table 6.2.

Table 6.2

Influence of flow rate on phenol conversion and product selectivity in tert-butylation of phenol

Flow rate (ml/h)	Conversion of Phenol (%)	Product Selectivity(%)		
		2-TBP	4-TBP	2,4-DTBP
4	19.5	3.5	92.7	3.8
5	45.6	36.0	61.3	2.7
6	23.9	5.6	85.3	9.1
7	20.0	6.1	77.6	16.3

Catalyst chosen-0.5g TiW2, Temperature-200°C,

Phenol: t-butanol –1:3, Duration-2h.

Very low contact time (high flow rates) may lead to poor reaction on account of the fact that little time is available for the adsorption of the reactants on the catalyst surface. At the same time very high contact time (low flow rates) mostly results in undesired reactions. The product yields also follow a

similar trend. Thus each reaction requires an optimum contact time with which maximum conversion and desired product yield is obtained. Phenol conversion increases when the flow rate increases from 4 to 5 ml/h. After that phenol conversion decreases with increasing flow rate.

6.2.3 Effect of phenol to tert-butanol mole ratio

Table 6.3 summarizes the results of butylation reaction carried out with various phenol to tert-butanol ratios. In all the cases, 4-tert-butyl phenol is observed as the major product along with small amounts of 2-tert-butyl phenol and 2,4-di-tert-butyl phenol. At an optimum molar ratio of 1:3, the catalyst systems show very good activity and selectivity.

Table 6.3

Influence of phenol:t-butanol ratio on phenol conversion and product selectivity in tert-butylation of phenol

Phenol: Tert-butanol	Conversion of Phenol (%)	Product Selectivity (%)		
		2-TBP	4-TBP	2,4-DTBP
1:1	22.7	8.1	67.3	21.4
1:3	45.6	36.0	61.3	2.7
1:5	20.6	15.3	63.7	20.8
1:7	18.6	17.9	55.8	26.3

Catalyst chosen-0.5g TiW2, Flow rate-5ml/h, Temperature-200°C, Duration-2h.

Phenol conversion increases on increasing the concentration of tert-butanol upto a phenol:t-butanol ratio of 1:3, which has been ascribed to the preferential

adsorption of t-butanol on the Bronsted acid sites as compared to phenol. Higher amount of TBA in the feed helps in promoting the alkylation, provided the alkylating agent is not consumed in non-selective parallel reactions. However further increase of phenol:t-butanol ratio results in a decline of phenol conversion while the selectivity to 2,4-di-tert-butyl phenol increases. This is due to a higher concentration of the alkylating agent in the pores, which facilitates the formation of dialkylated products.

6.2.4 Effect of time on stream

The effect of time on stream is expected to throw light on the deactivation of a particular catalyst and its influence on product selectivities. The performance of the reaction for a continuous 7h run tests the susceptibility of deactivation of the catalyst. The products were collected and analyzed after every 1h. Figures 6.1 and 6.2 represent the phenol conversion of pure and modified systems towards time on stream. The above results indicated that the catalyst is gradually deactivated with time irrespective of the reaction conditions. This deactivation is most likely due to the formation of coke, which is generated by oligomerization of excess tert-butanol. The formed coke will block the strong acid sites that are responsible for the formation of 2,4-DTBP and, thus, reduces the activity of the catalyst. In the initial hours the catalyst might absorb phenol strongly and after 2h, the catalyst activity established an equilibrium level. The phenol conversion gradually increased with time on stream in the initial reaction period for 2h and then the conversion starts

decreasing. This could be due to the formation of water molecules during the reaction, which may covert some of Lewis acid sites into Bronsted acid sites.
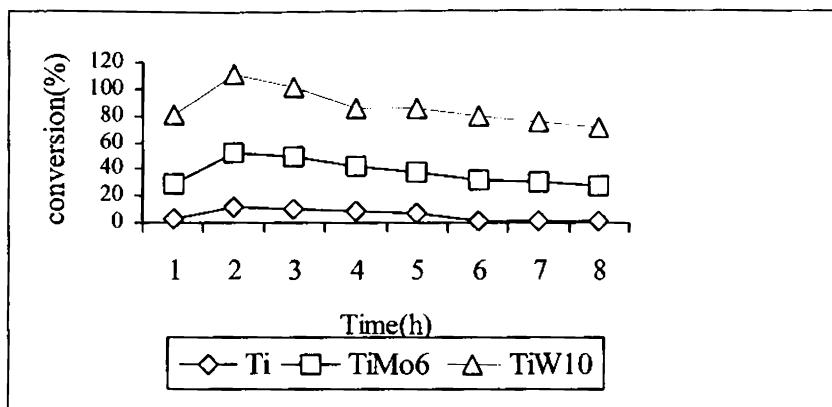
Figure 6.1

Deactivation studies on the conversion of phenol over transition metal modified titania systems
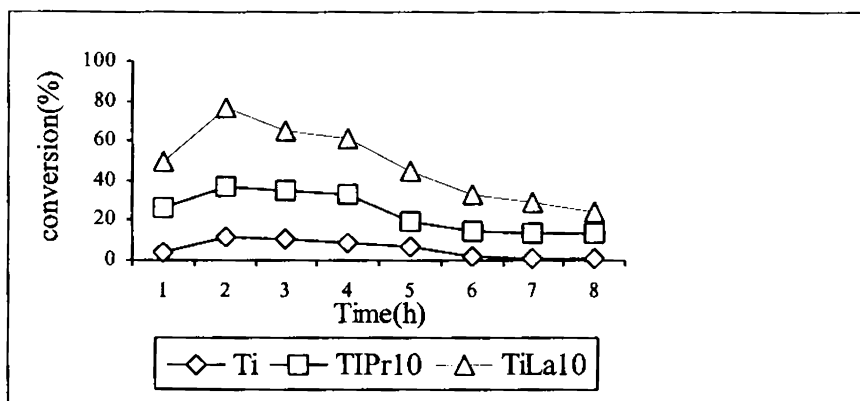
Figure 6.2

Deactivation studies on the conversion of phenol over rare earth metal modified titania systems

6.3 Comparison of Catalyst systems

A comparative study of both transition metal and rare earth metal modified systems towards the tert-butylating activity of phenol is given in this section (Tables 6.4 and 6.5).

Table 6. 4

Influence of transition metal in the tert-butylation of phenol

Systems	Conversion (%)	Selectivity (%)		
		2-TBP	4-TBP	Di-TBP
Ti	12.0	35.6	63.2	1.2
TiMo2	38.0	26.0	71.6	2.4
TiMo6	40.5	34.7	63.2	2.1
TiMo10	41.6	4.4	91.8	3.9
TiCr2	24.7	24.3	70.4	5.3
TiCr6	29.5	31.4	65.7	2.9
TiCr10	38.8	37.8	53.4	8.8
TiW2	45.6	36.0	61.3	2.7
TiW6	51.0	30.8	66.8	2.5
TiW10	58.9	14.8	82.0	3.2

Catalyst weight-0.5g, Flow rate-5ml/h, Temperature-200°C,

Phenol: t-butanol –1:3, Duration-2h

The reaction is carried out at an optimum reaction temperature of 200°C, flow rate of 5ml/h and a phenol to tert-butanol mole ratio of 1:3. Both the transition metal and rare earth metal modified systems are superior to pure

titania in the tert-butylation of phenol. Further, the reaction is carried out without the addition of catalyst under the same reaction conditions and that revealed poor conversion (~3.5%), thus indicating that the reaction was catalytic.

Table 6.5

Influence of rare earth metal in the tert-butylation of phenol

Systems	Conversion (%)	Selectivity (%)		
		2-TBP	4-TBP	Di-TBP
Ti	12.0	35.6	63.2	1.2
TiLa2	36.4	47.3	50.4	2.4
TiLa6	39.6	46.0	51. 8	2.2
TiLa10	44.6	36.6	60.9	2.5
TiPr2	14.1	31.9	66.8	1.3
TiPr6	14.7	24.6	71.0	4.5
TiPr10	25.0	3.0	89.6	7.4
TiSm2	21.6	44.1	52.3	3.5
TiSm6	35.8	46.2	52.3	1.6
TiSm10	40.8	41.6	57.1	1.3

Catalyst weight-0.5g, Flow rate-5ml/h, Temperature-200°C,

Phenol: t-butanol –1:3, Reaction time-2h

Tungsten modified systems are found to be catalytically more active than other systems. The influence of metal loading in the tert butylation of

phenol is also investigated here. As the percentage of incorporated metal increases, the catalytic activity improves considerably. All the systems give para isomer as the major product. Metal loading also has a significant impact on the para selectivity of the reaction. Except in chromia modified systems, 10% metal incorporated systems showed highest para selectivity.

In order to gain an understanding of acidity affecting the activity and selectivity of the prepared systems, the NH_3 TPD results are correlated with the catalytic activity. It has been reported that the alkylation of phenol carried out in the gas phase system at high temperature in the presence of catalysts with weak, moderate or strong acid sites are suitable for the formation of para C-alkylated product. Figures 6.3 to 6.6, gives the correlation between the products selectivity and the acidity assessed by ammonia TPD.
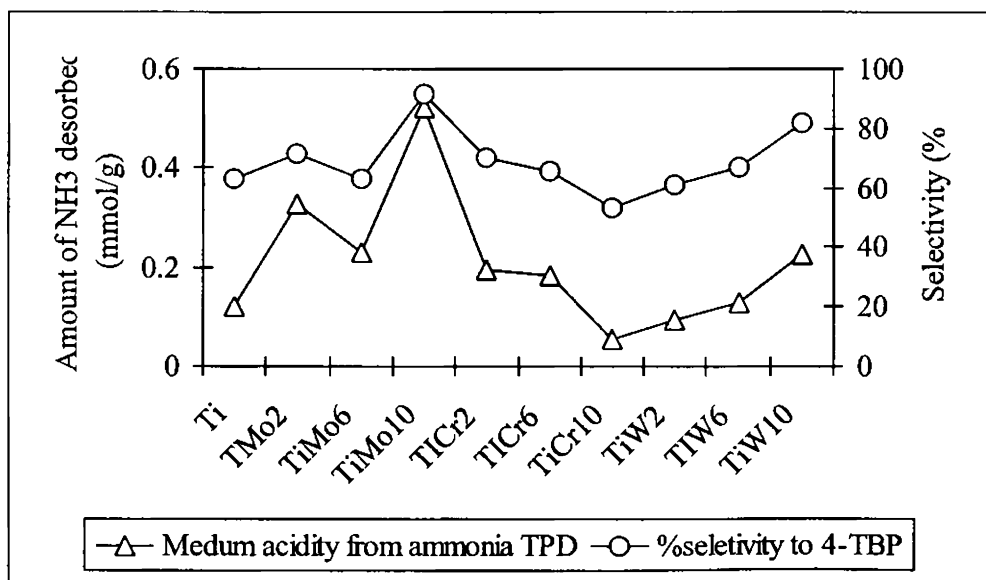
Figure 6.3

4-TBP selectivity correlated with medium acidity from NH_3 TPD

In the present study, medium and strong acid sites promote the reaction. Strong acid sites are necessary to get higher selectivity of 2,4-DTBP while medium acid sites are helpful in enhancing the selectivity of 4-TBP. The increased selectivity to the para isomer of tert-butyl phenol, which is thermodynamically more stable than that of ortho isomer, was explained as being the result of several consecutive reactions such as the isomerization and disproportionation, the dealkylation or the transalkylation involving mono and poly alkyl phenols.
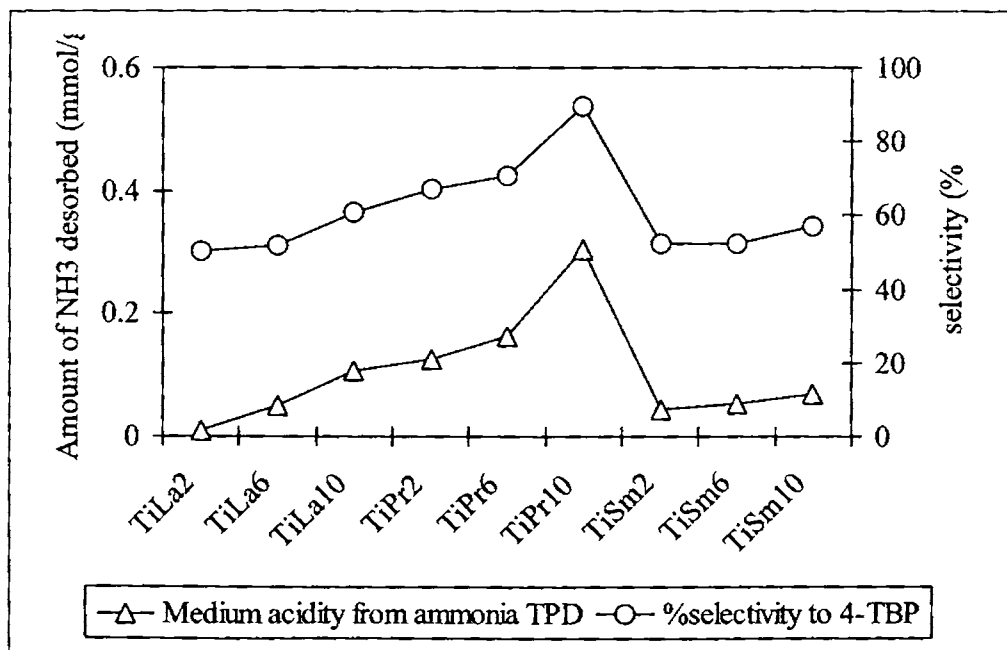
Figure 6.4

4-TBP selectivity correlated with medium acidity from NH$_3$ TPD
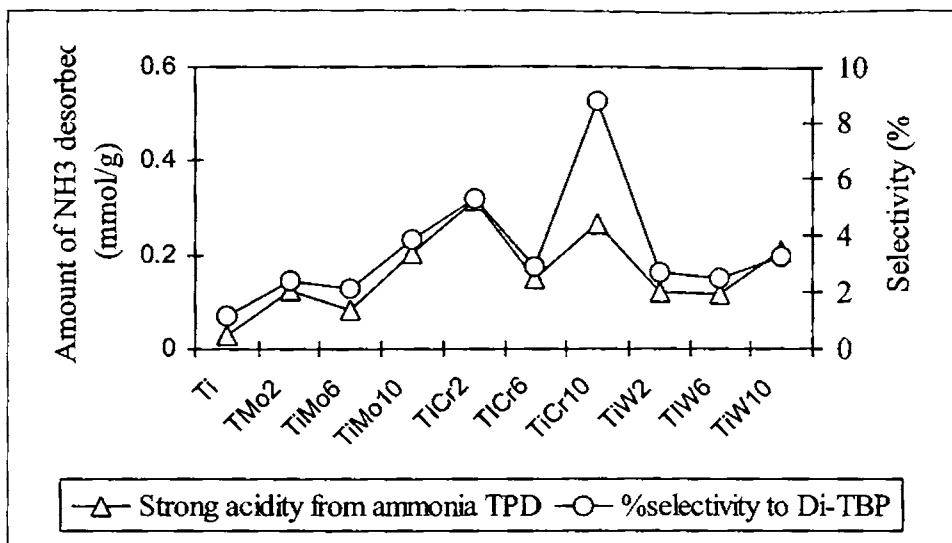
Figure 6.5

2,4-DTBP selectivity correlated with strong acidity from NH_3 TPD
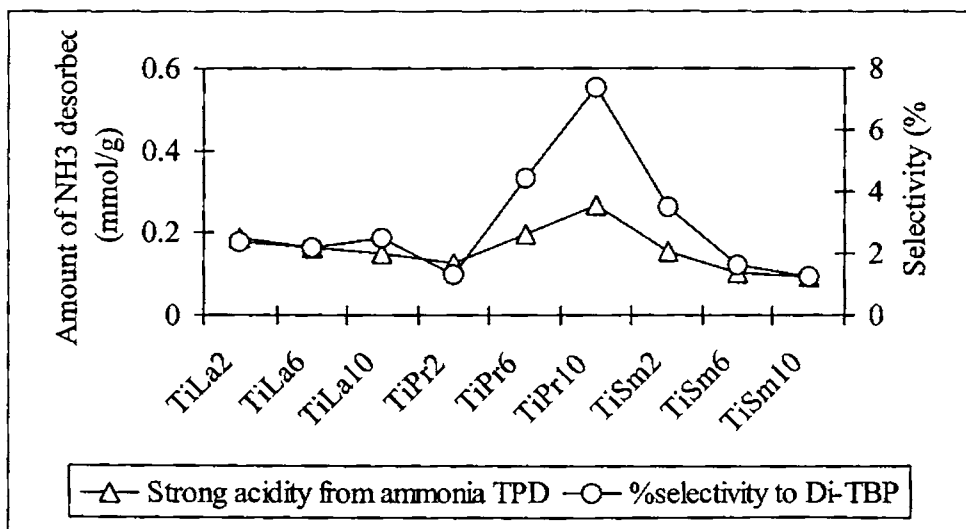
Figure 6.6

2,4-DTBP selectivity correlated with strong acidity from NH_3

It is accepted that when the product is not thermodynamically controlled, both the electronic and steric factors are very important for the alkylation reactions in heterogeneous catalysis. Generally, the electrophilic substitution may take place in the ortho and para positions of the phenyl ring. It is difficult to predict how much of the product will be the ortho isomer and how much the para isomer. On a purely statistical basis, there would be 67% ortho and 33% para, since there are two ortho positions and only one para. Moreover, the presence of phenolic group kinetically favors ortho alkyaltion. It is well known from the previous reports that the formation of 4-TBP occurs over moderate acid sites, while the formation of dialkylated products require medium or strong acid sites[25, 33].

In order to understand the role played by the structural acid sites and the weak acid sites, Subramanian *et al* carried out the alkylation experiments on SAPO-11 samples pretreated with ammonia and quinoline[25]. Phenol conversion decreased due to ammonia poisoning. Strongly adsorbed ammonia at the structural acid sites make those sites unavailable for the alkylation reaction and thus decrease the acidity. However tert-butanol was not fully converted on these samples, suggesting that the tert-butanol was mainly dehydrated at the surface hydroxyl sites. After quinoline adsorption, there is no alkylation of phenol. The large quinoline molecules essentially poison the external acid sites and also block the pore mouth of zeolites. This makes it difficult for the reactant molecule to enter and for the product molecules to diffuse out of the pores, thus preventing the reaction. Even t-butanol decomposition is suppressed to a considerable extent.
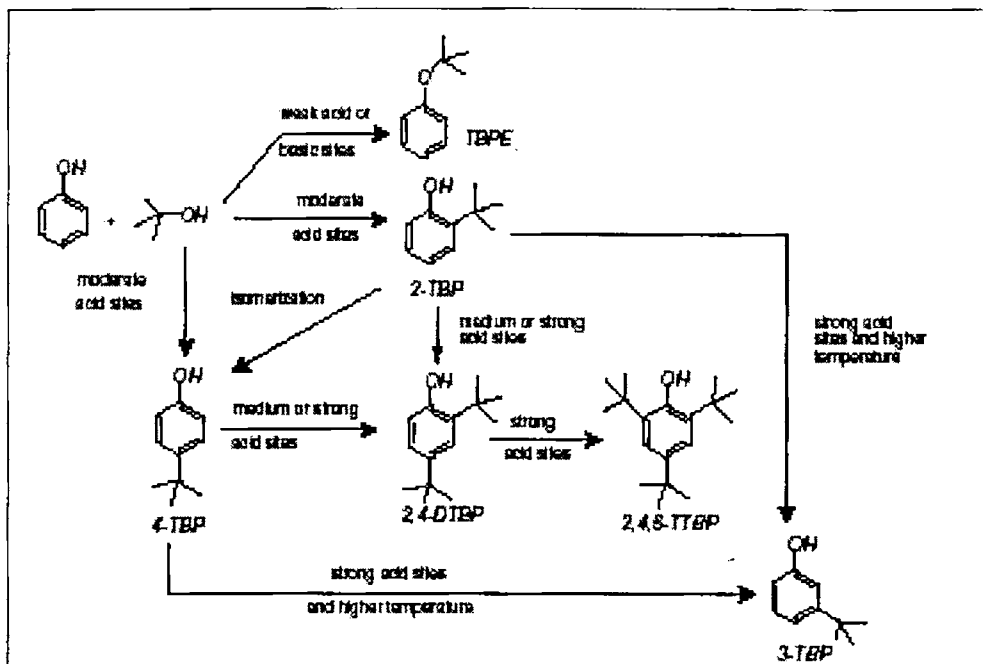
Scheme 6.1

To understand the formation of 2,4-di-tert-butyl phenol, tert-butanol was reacted with 2-tert-butyl phenol and 4-tert-butyl phenol separately and with a mixture of these two isomers. When tert-butyl phenol is mixed with a mixture of 2-TBP and 4-TBP at 175°C, apart from the disubstituted 2,4-DTBP, considerable amount of phenol is also obtained whose concentration in the product increased with the increase of reaction temperature. The amount of 2-TBP has decreased and that of 4-TBP increased. When 2-TBP alone reacted with t-butanol it undergoes appreciable alkylation to give 2,4-DTBP. It also isomerises to 4-TBP to a large extent. The geometric constraints of the catalysts significantly influence the product distribution.

6.4 Proposed mechanism of tert-butylation of phenol

From the above observations of tert-butylation of phenol, a mechanism is proposed. Phenol alkylation with tert-butanol is a typical Friedel Crafts alkylation and can be catalyzed by acid sites. The interesting aspect of this reaction is the high selectivity of alkylation at the para position. The generally accepted mechanism for aromatic alkylation is that the tertiary carbenium ion interacts with adsorbed phenol forming a π complex, which then rearranges to an σ complex by the electrophile attacking a ring carbon atom. The σ complex on proton elimination gives tert- butyl phenol. It has been suggested[34] that the Bronsted acid site interacts with the π cloud of the aromatic ring bringing the molecule parallel to the surface. This will allow alkylation at the para position easier as compared to the ortho positions. Also it has been reported that the steric hindrance in the transition state due to the substitution of bulkier tert-butyl group at the ortho positions enhances the para selectivity[25]. The complete absence of 2,6-di-tert-butyl phenol may also be due to bulkier size and only the less bulky 2,4-di-tert-butyl phenol is formed.

The reaction of tert-butylation of phenol can be catalyzed by Bronsted and Lewis acid sites. Tanabe and Nishizaki[35] and Klemm[36] *et al* suggested a vertical orientation in the adsorption of phenol molecules at Lewis acid sites, the ortho position of phenol being close to the surface and tert-butylation of phenol occurring predominantly in this position. The Bronsted acid sites strongly interact with the aromatic ring of the adsorbed phenol, thus bringing it closer to the surface and permitting tert-butylation in the ortho and para positions. It is difficult for 2-TBP to adsorb perpendicularly on Lewis acidic sites because of the bulky tert-butyl in its ortho position, the isomerization of

2-TBP to 4-TBP could not be catalyzed by Lewis acidity, hence the isomerization of 2-TBP to 4-TBP over zeolite could be promoted by Bronsted acid sites with medium acidity. Because of the same ortho effect, 2-TBP could react with tert-butanol to form 2,4-DTBP over strong bronsted acid sites, while 4-TBP could perform the same reaction, over strong Bronsted or strong Lewis acid sites to produce 2,4-DTBP.

6.5 Conclusions

Phenol alkylation with tert-butyl alcohol is successfully carried out over pure and modified titania systems. Among the prepared systems, tungsten incorporated titania is found to be a more promising catalyst for this vapour phase reaction. An interesting feature of this study is the high para selectivity. The reaction is promoted by strong and medium acid sites, where strong acid sites are helpful in producing 2,4-di-tert-butyl phenol and medium acid sites are effective to produce 4-tert-butyl phenol. A detailed study clearly indicates that under optimum conditions, higher substrate conversion and para selectivity can be obtained compared to other conventional catalysts. This will definitely open up new areas of research.

Section B
Methylation of Aniline

6.6 Introduction

Alkylation of aniline is an important reaction in organic synthesis. This reaction form products such as N-alkylated and/or C-alkylated anilines that are used as intermediates or additives in dyes, synthetic rubber, herbicides and pharmaceuticals. The synthesis of these organic intermediates is a high activity research area where the alkylation proceeds through Friedel Crafts reaction[37]. The major steps in the aniline methylation reaction may be represented by the general scheme shown in Fig. 6.7. N-methyl aniline arises from the side chain alkylation of aniline while toluidines are the products of ring alkylation. Consecutive reaction can result in N,N-dimethylaniline or N-methyl toluidines. Trans alkylation can also occur as a side reaction.

The synthesis of these compounds are reported both in open and patented literature over a wide variety of catalysts. Vanadia impregnated iron pillared montmorillonite is also found to be effective for the methylation of aniline[38]. It is observed that only moderate acidity is required for a good catalytic reaction between aniline and methanol. Nagaraju *et al* studied the vapour phase methylation of aniline with methanol or dimethyl carbonate on amorphous $AlPO_4$ and $M-AlPO_4$ (M=Cu, Ni, Fe, Co and V) and obtained a high selectivity towards N-monomethylated product of aniline[37]. No simple correlation is observed between the selectivity and the total surface acidity.
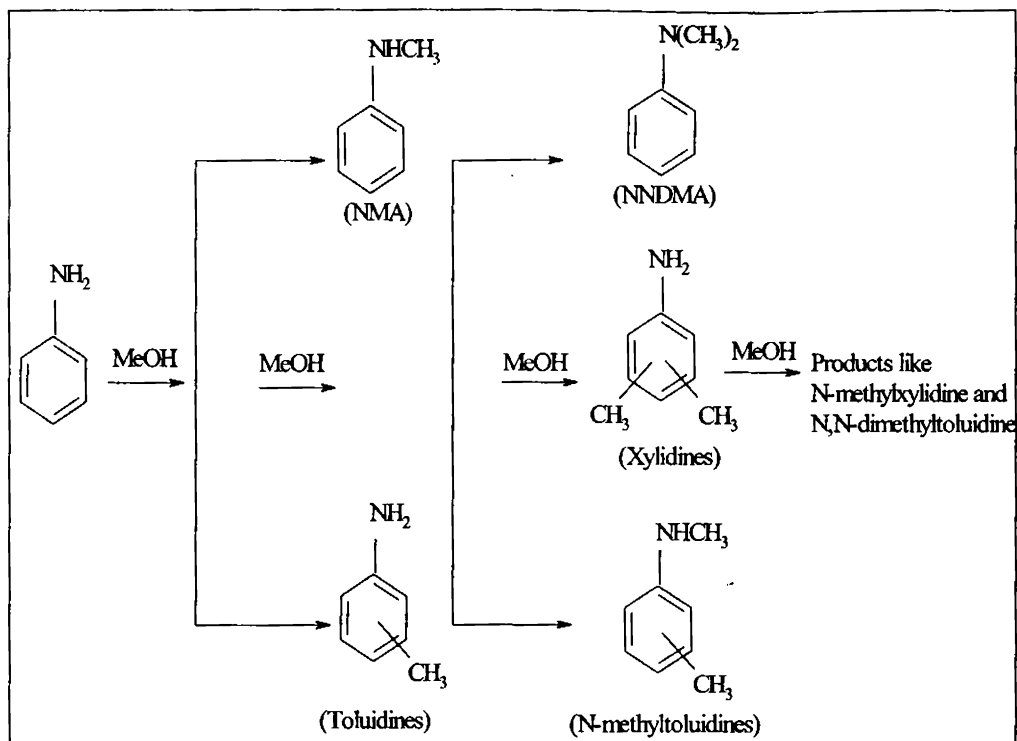
Figure 6.7

General scheme of aniline methylation

Sreekumar *et al* studied the kinetics of the N-monoalkylation of the aniline with methanol over $Zn_{1-x}Co_xFe_2O_4$ systems[39]. The low activation energy of the system can be probably due to the peculiar type of cation distribution in the spinel lattice, which provides active sites well suited for the adsorption and subsequent reactions of both aniline and methanol. Ferrospinel systems were found to be highly active and selective for the N-monomethylation of aniline using methanol as the alkylating agent[40-41]. High

yields of N- methyl aniline could be obtained even at sufficiently high methanol to aniline ratios.

Methylation of aniline with methanol was also carried out on a basic CsOH/Cs, Na-Y zeolite[42]. Here the detection of N-methyl aniline as an intermediate species can be accounted for by a mechanistic pathway, which includes dehydrogenation of methanol to formaldehyde, condensation of aniline with formaldehyde leading to N-methylene aniline and hydrogenation of N-methylene aniline to N-methyl aniline by hydrogen produced during the methanol dehydrogenation.

Ione and Kikhtyanin reported alkylation of aniline with methanol over ZSM-5 catalyst. N- and C- alkylation took place during the reaction between aniline and methanol[43]. It is reported that the product selectivity depends on reaction temperature; N-alkylated product decreases as temperature increases[44-45]. Chen *et al* found HZSM-5 zeolite modified by alkali metal species to boost the selectivity towards N,N-dimethyl aniline[46]. They suggested that N-alkylation could be promoted by the additional basicity introduced by metal oxide modifiers. Barthomeuf *et al* studying the reaction over zeolites concluded that it involves acidic (cations) and basic (oxygen) sites[47-48]. The more basic zeolites (X and Y exchanged with K, Rb or Cs) favour production of N-alkylates while zeolites with more acidic cations Li and Na lead to C-alkylation. Large pore zeolites favour both ring and side chain alkylation. Metal oxides show better selectivity for N-alkylation but majority of them favour both the mono and di-substitution on nitrogen. The acid base properties as well as the shape selectivity of zeolites plays a crucial role in determining the activity as well as the selectivity for aniline methylation.

The selective alkylation of aniline over several metallosilicates suggested the involvement of strong, medium and weak acid sites in the formation of C-alkylate and coke, NNMA and N-methyltoluidines and NMA respectively. Aramendia *et al* reported the activity and selectivity of various magnesium orthophosphates for the gas phase methylation of aniline[49-50]. No C-alkylates was detected, which is consistent with the weak acidity observed with magnesium orthophosphates. Elangovan *et al.* conducted methylation of aniline over AFI and AEL types of molecular sieves and obtained a direct relationship between conversion and total acidity[51]. The product distribution was influenced by reaction conditions like temperature, methanol to aniline molar ratio etc.

Dixon and Burgoyne reported the alkylation of substituted anilines with isobutene over zeolite catalysts[52]. N-alkylated and C-alkylated products were obtained. The selectivity is reduced for arylamine having ortho substituents such as chloro or methyl groups. With increase in temperature, N-alkylated, o-alkylated and p-alkylated anilines become the major products on alkylation of aniline with isobutene. Maurizio Seiva *et al* studied the selective mono-N-methylation of primary aromatic amines by dimethyl carbonate over faujasite X- and Y- type zeolites[53]. The reaction is an example of a synthesis with low environmental impact; it couples the use of a non-toxic methylating agent with ecofriendly zeolite catalysts in a waste free process.

6.7 Process Optimisation

Methylation of aniline can give N-alkylated products like N-methyl aniline (NMA) and N,N-dimethyl aniline(NNDMA) and also the C-alkylated

products such as toludines. The product distribution depends strongly on the nature of the catalyst and the reaction conditions employed. The catalytic activity studies were conducted in the vapour phase. Exactly 0.5g of the catalyst was used in the powder form for this reaction. A mixture of aniline and methanol was fed into a fixed bed, down flow reactor placed inside a double zone furnace, which was set at a particular temperature. The products and the unreacted reactants were fed condensed by a cold water circulating condenser and was analyzed by Gas Chromatography (Chemito GC 1000) using BP1 capillary column (12m×0.32m) with FID detector.

6.7.1 Effect of Reaction Temperature

Aniline methylation using methanol is carried out at five different reaction temperatures 250, 300, 350, 400 and 450°C using a mixture of methanol and aniline of molar ratio 7:1 over TiLa2 catalyst. The flow rate is maintained at 4ml/h. The dependence of temperature on the percentage conversion as well as the selectivity in aniline methylation is given in table 6.6. A drastic increase in the percentage aniline conversion from 40.0 to 75.4 is observed when the reaction temperature increases from 300 to 350°C. Further rise in temperature has an adverse effect in the percentage conversion. The variation in the product selectivity is more pronounced with the change in temperature. The percentage toludine selectivity increases with the increase in reaction temperature. The selectivity to NMA remains almost steady whatever be the temperature. These observations indicate that 350°C is the optimum reaction temperature for the reaction between aniline and methanol.

At higher temperature, aniline would probably undergo oxidation and also decompose, resulting in coke formation[54-55]. The possibility of certain side reactions of methanol forming polymeric aromatics or gaseous products or even coke could not be ignored. This may be the reason for the decrease in the catalytic activity at higher temperatures. Coke deposition is an important factor in deactivating the catalyst system. This can act as a catalytic poison and hence decreasing the number of available active sites in the reaction.

Table 6.6

Influence of reaction temperature on aniline methylation reaction

Temperature	Conversion	Selectivity (%)		
(°C)	(%)	NMA	NNDMA	Toludines
250	21.4	50.1	45.2	4.7
300	40.0	49.6	42.3	8.5
350	75.4	53.5	36.5	10.0
400	55.3	50.5	23.9	35.6
450	45.1	51.4	9. 9	38.7

Catalyst-0.5g TiLa2, Flow rate-4ml/h, Time on Stream-2h, Aniline : Methanol -1:7

6.7.2 Effect of Flow Rate

Each reaction requires an optimum contact time with which maximum conversion and desired product yield is achieved. The dependence of flow rate on aniline methylation over TiLa2 catalyst under otherwise identical conditions is given in table 6.7. A change in the flow rate from 3 to 4ml/h changes the percentage aniline conversion from 56.6 to 75.4. Thereafter the percentage conversion decreases with flow rate. So the optimum flow rate chosen for this

reaction is 4ml/h. The percentage NNDMA selectivity is high when the flow rate is only 3ml/h though the percentage aniline conversion is only 36.6. It is clear that very high contact time between the catalyst and the reactants is available when the flow rate is low, which results in the formation of N,N-disubstituted product of aniline. Aniline methylation is a sequential reaction and follows the order aniline → NMA → NNDMA.

Table 6.7

Influence of flow rate on aniline methylation reaction

Flow rate (ml/h)	Conversion (%)	Selectivity (%)		
		NMA	NNDMA	Toludines
3	36.6	30.5	49.5	19.7
4	75.4	53.5	36.5	10.0
5	46.3	49.2	23.8	26.5
6	35.3	46.7	23.4	29.9

Catalyst-0.5g TiLa2, Reaction temperature-350°C, Duration-2h, Aniline: Methanol-1:7

6.7.3 Effect of molar ratios of Aniline and Methanol

The optimum feed mix molar ratio is selected by carrying out the reactions by taking aniline-methanol premixed in various molar ratios at 350°C. The percentage aniline conversion together with its corresponding product distribution at different molar ratios of the reactants is given in table 6.8. With the increase in the amount of methanol, a gradual increase in the percentage conversion is noticed. After an optimum mole ratio, the percentage conversion dropped. The decrease in aniline conversion at high molar ratios may be attributed to the competitive adsorption of methanol. This invariably

hinders the adsorption of aniline, which ultimately results in a lowering of the aniline conversion. Also, in the presence of methanol as the alkylating agent, water is formed as one of the products. This may poison the active sites on the catalysts. The direct consequence of the increase in concentration of methanol in the feed mix is the enhanced percentage of NNDMA selectivity.

Table 6.8

Influence of molar ratios of Aniline and Methanol on aniline methylation reaction

Methanol/Aniline	Conversion (%)	Selectivity (%)		
		NMA	NNDMA	Toludines
3	20.1	37.6	36.0	26.1
5	36.9	38.9	31.6	29.5
7	75.4	53.5	36.5	10.0
9	51.0	27.1	57.0	16.0
11	32.9	12.3	62.3	25.4

Catalyst-0.5g TiLa2, Reaction temperature-350°C, Flow rate-4ml/h,

Duration-2h.

6.7.4 Effect of time on Stream

The time on stream studies were performed at 350°C with 0.5g of the catalyst at a feed rate of 4ml/h. The feed solution consisted of a 1:7 molar ratios of aniline and methanol. The product fractions were collected at 1h intervals and analyzed by GC. A plot of percentage conversion versus time gives an idea about the deactivation of the catalyst over the course of the

reaction. Retention of the catalytic activity and desired product selectivity is the most sought after property of a catalyst.
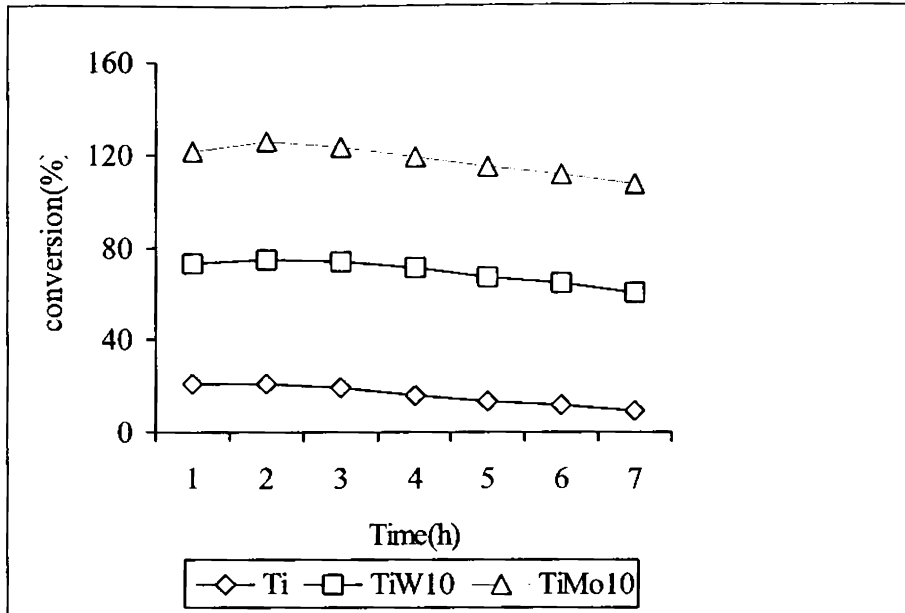
Figure 6.8

Deactivation studies on Ti, TiW10 and TiMo10

From the plots, it is evident that there is no appreciable change in the aniline conversion activity of the modified titania catalysts with time. In addition, the product selectivity also remained almost unchanged during 8h on stream. The modificaion of titania with both transition metals and rare earth metals improves the stability of the catalyst, thereby rendering a better catalytic performance. This indicates that there is no apparent deactivation of the catalysts at the selected reaction temperatures.
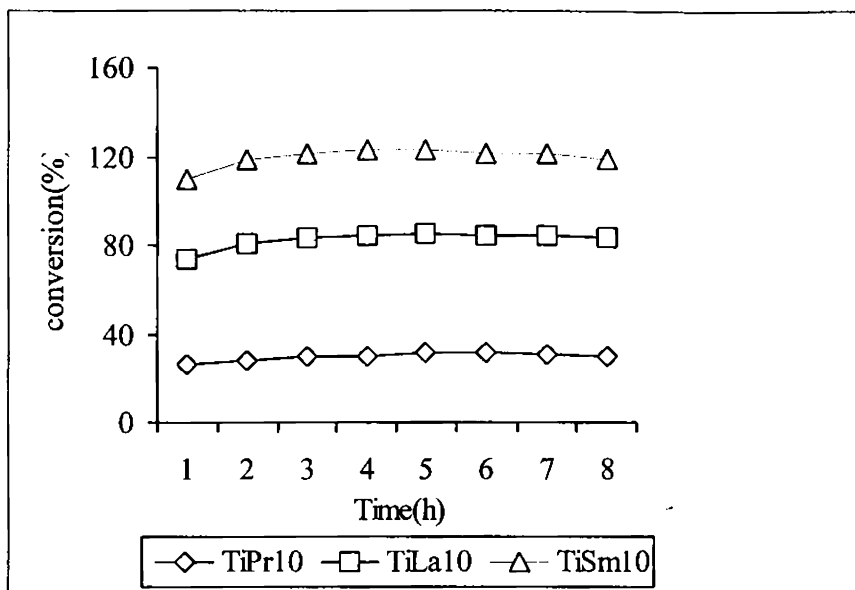
Figure 6.9

Deactivation studies on TiPr10, TiLa10 and TiSm10

6.8 Comparison of Catalyst systems

The methylation of aniline is carried out over the prepared systems under the optimized reaction conditions. A comparative evaluation of the catalytic activity of both transition metals and rare earth metals incorporated titania systems for the methylation of aniline is described in table 6.9 and 6.10 respectively. The catalyst systems predominantly give N-alkylated products like NMA and NNDMA in preference to the C-alkylated product like toludine. The percentage conversion varies from 21.1 in the case of pure titania to 75.4 in case of TiLa2. The metal incorporation has a profound influence in the percentage aniline conversion as well as product distribution.

Table 6.9

Influence of Transition Metals on Aniline Methylation

Systems	Conversion (%)	Selectivity (%)		
		NMA	NNDMA	Toludines
Ti	21.1	45.7	52.1	2.2
TiMo2	64.1	39.2	54.5	6.3
TiMo6	68.4	72.3	15.7	12.0
TiMo10	51.1	66.5	18.7	14.8
TiCr2	57.0	39.2	48.5	12.3
TiCr6	71.6	50.8	35.1	14.1
TiCr10	68.6	40.3	42.1	17.7
TiW2	30.2	44.0	42.6	13.4
TiW6	72.6	40.1	42.7	17.2
TiW10	53.8	61.4	26.1	12.5

Catalyst weight-0.5g, Reaction temperature-350°C, Flow Rate-4ml/h,

TimDuration-2h, Methanol:Aniline-7:1

In transition metal incorporated titania systems, maximum activity is shown by 6% metal incorporated systems, and thereafter the percentage conversion decreases. But in rare earth metal incorporated systems, the percentage conversion shows a regular decrease when the percentage of metal incorporation increases. Maximum catalytic activity is shown by 2% metal incorporated ones. An attempt was made to correlate the catalytic activity of the systems with their corresponding acidic properties. No apparent

dependence could be obtained between the catalytic activity and the relative amounts of strong, medium or weak acid sites.

Table 6.10

Influence of Rare Earth Metals on Aniline Methylation

Systems	Conversion (%)	Selectivity (%)		
		NMA	NNDMA	Toludines
Ti	21.1	45.7	52.1	2.2
TiLa2	75.4	53.5	36.5	10.0
TiLa6	62.6	63.1	27.1	9.8
TiLa10	52.6	62.3	16.2	7.7
TiPr2	58.9	44.5	40.4	15.1
TiPr6	32.4	54.1	23.5	22.4
TiPr10	28.1	64.3	8.2	29.3
TiSm2	52.1	41.3	32.9	25.8
TiSm6	48.5	41.8	36.6	21.6
TiSm10	38.1	40.6	39.7	19.8

Catalyst weight-0.5g, Reaction temperature-350°C, Flow Rate-4ml/h,

Duration-2h, Methanol:Aniline-:7:1

It was postulated that weak and moderate acid sites are sufficient for N-alkylation, whereas strong acid sites initiate C-alkylation[56-60]. A good correlation is obtained between the percentage selectivity of the products and the acidic properties of the system. The correlations between the %NMA selectivity and weak acidity is given in figures 6.10 to 6.11. Similarly a good correlation is obtained between the percentage toludine selectivity and strong acidity obtained from NH_3 TPD and it is represented in figures 6.12 and 6.13.
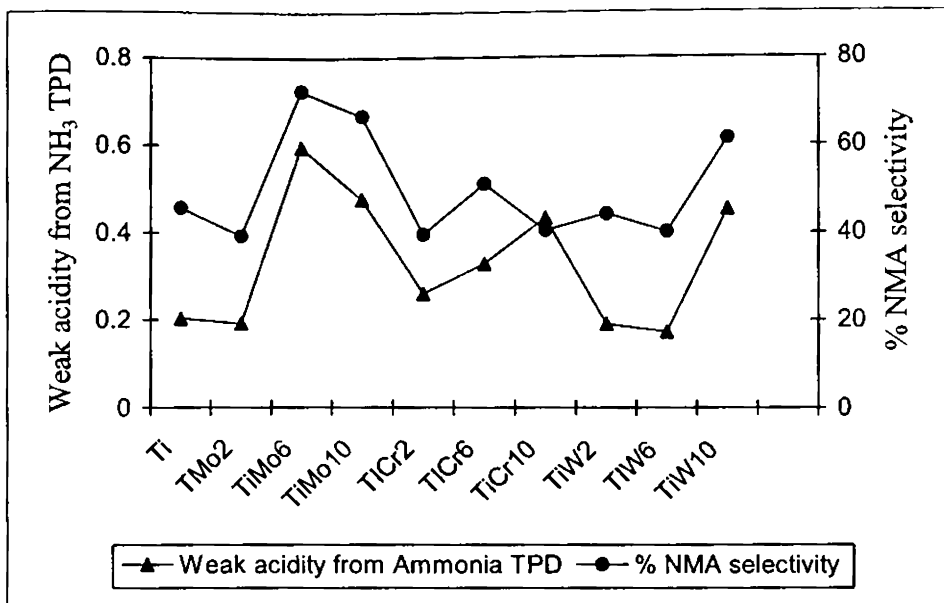
Figure 6.10

Correlation between weak acidity from NH$_3$ TPD and %NMA selectivity
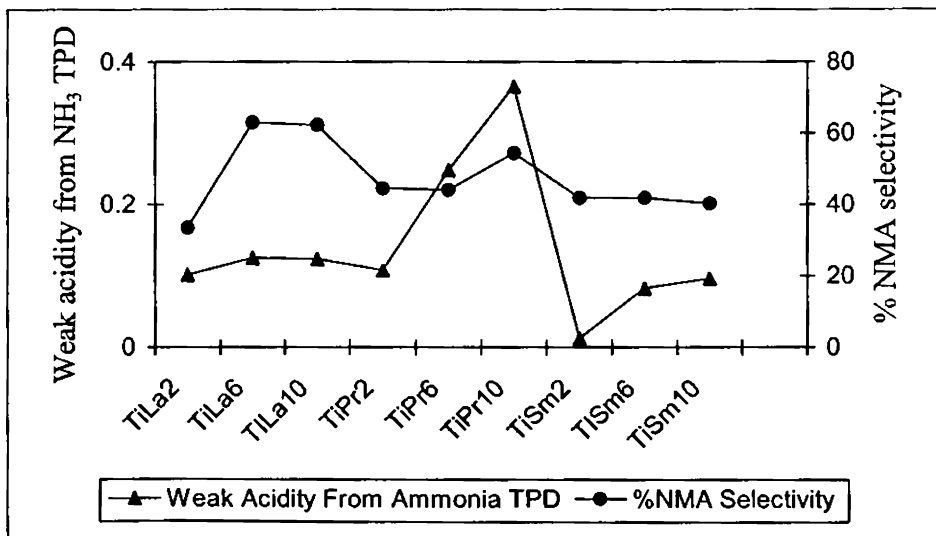
Figure 6.11

Correlation between weak acidity from NH$_3$ TPD and %NMA selectivity
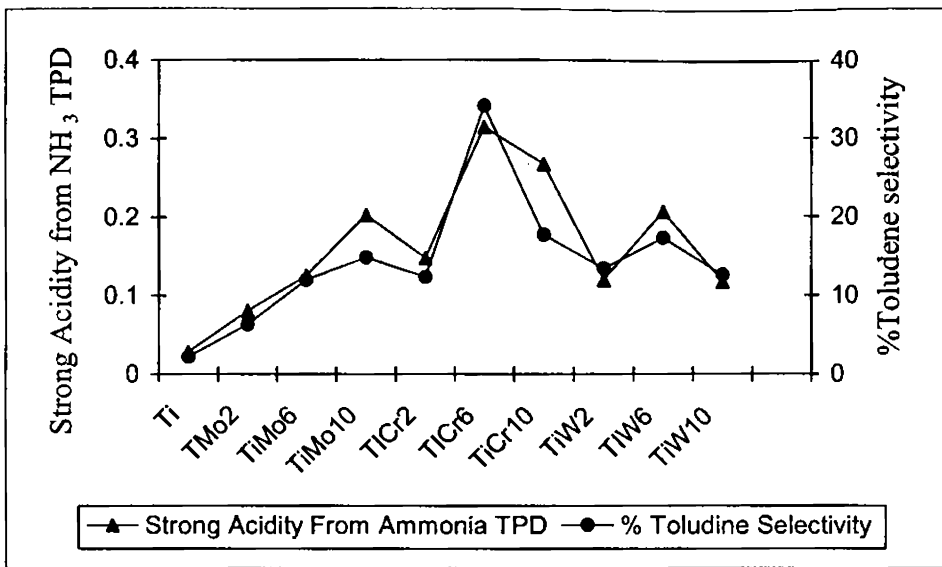
Figure 6.12

Correlation between strong acidity from NH_3 TPD and %Toludine selectivity
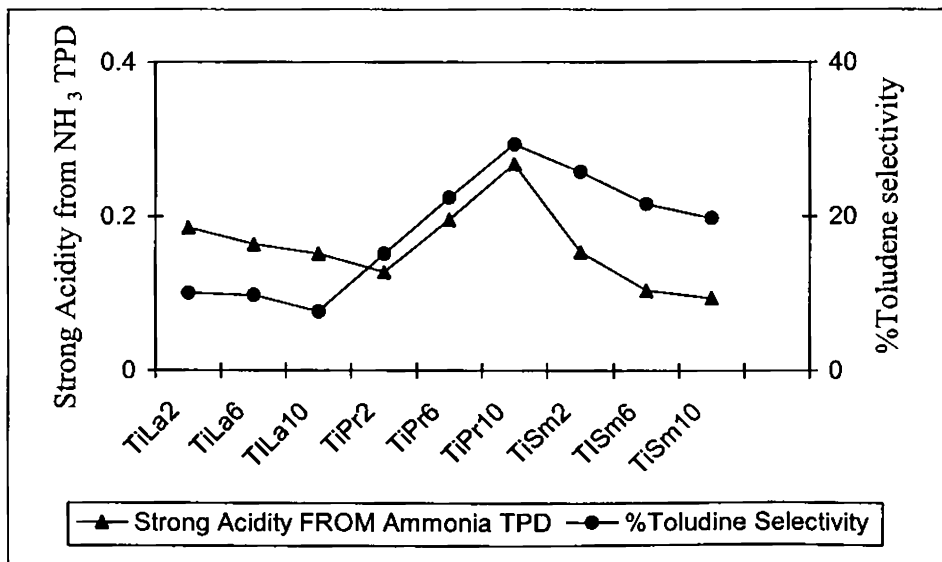
Figure 6.13

Correlation between strong acidity from NH_3 TPD and %Toludine selectivity

6.9 Mechanism of the Reaction

Aniline alkylation is a multistep acid catalyzed reaction and the amount and distribution of acidity influences the conversion of aniline and the product selectivity. In the present study, good correlations are obtained between the weak acidity and the %NMA selectivity and also the strong acidity and % toludine selectivity. From this, the role of weak acid sites in promoting N-alkylation and strong acid sites in promoting C-alkylation is clearly understood. Similarly no correlation could be observed between the Brönsted and Lewis acidity of the samples and the respective conversions and product selectivities. Thus, a combined effect of the different acidic sites along with the basic nature may be deciding the catalytic activity of the systems for methylation of aniline.

Due to the ortho / para orientation effect imparted by the delocalization influence of the unshared pair of electrons over the amino group into the benzene ring, the expected major products are ortho and/or para C-alkylated aniline[61]. But due to the adsorption of aniline over the surface, alkylation can give N-alkylated products. The catalyst also plays a major role in releasing the electrophile from the alkylating agent. Aniline being a stronger base than methanol, it gets adsorbed preferentially over the Lewis acidic sites[59-60]. A plausible mechanism involving both Bronsted and Lewis acidic sites are given in figure 6.14. The high electronegativity of the oxygen of methanol, leading to hydrogen bonding with hydroxyl protons of the Bronsted sites and thus methanol is adsorbed over the Bronsted sites. Protonation of alcohol, dehydration and subsequent formation of ether linkage of the released carbocation may follow.
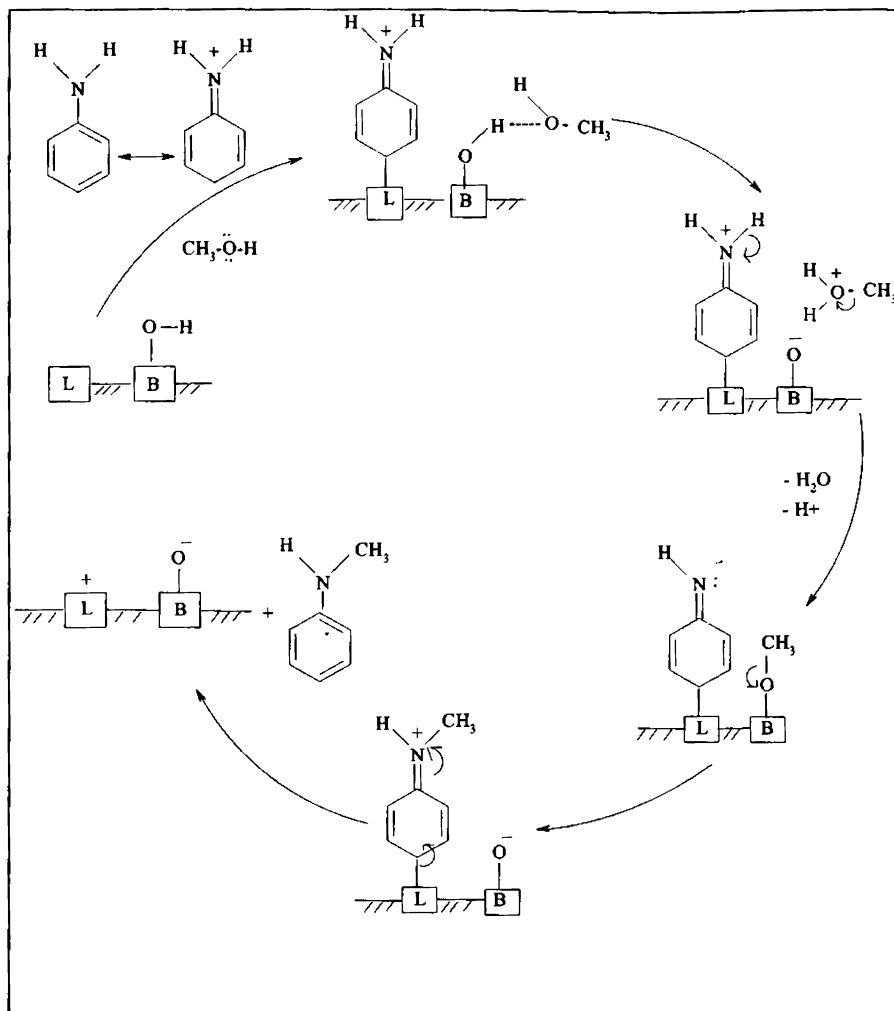
Figure 6.14

Mechanism of Aniline Methylation Reaction

On the Lewis sites, the adsorbrd aniline may lose a proton to balance the positive charge developed on the nitrogen. The high electronegativity of oxygen in the ether linkage results in the development of partial positive

charge on the alkyl side chain, initiating heterolytic cleavage of polar O-C bond and shift of alkyl carbocation to nitrogen. Thus the necessary condition for the reaction to take place in the desired direction is that aniline should adsorb on Lewis sites and methanol on Bronsted acid sites. In the present study, more than 70% selectivity of the N-alkylated product is obtained.

6.10 Conclusions

The methylation of aniline is carried out efficiently over the prepared catalytic systems. The percentage N-methyl selectivity is more than that of C-alkylated product selectivity in all the systems. The influence of various reaction parameters like reaction temperature, flow rate and aniline to methanol molar ratio were found to influence the catalytic activity and selectivity. An acceptable correlation is obtained between various types of acidity obtained from NH_3 TPD as well as percentage product selectivities. A reaction mechanism involving the combined action of Brönsted and Lewis acid sites has been proposed for the alkylation of aniline over titania and modified titania systems.

<div align="center">
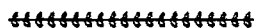
Section C

Methylation of Anisole

</div>

6.11 Introduction

There is currently a significant world wide interest in the use of solid acid and base catalysts to promote various organic reactions, of industrial importance, since such systems often give value added products with improved selectivity without creating major burdens to the environment. The selective synthesis of alkyl phenols especially o-cresol and 2,6-xylenol is receiving increasing interest in recent years because of their importance as intermediates for the synthesis of a variety of resins, herbicides, pesticides and other chemicals[62-64]. Xylenol or dimethylphenol is a benzene derivative with two methyl groups and a hydroxyl group. Six isomers exist for xylenol of which 2,6-xylenol with both methyl group in a ortho position with respect to the hydroxyl group is the most important. The name *xylenol* is a contraction of two similar compounds xylene and phenol. Together with cresols and cresylic acid, xylenols are an important class of phenolics with great industrial importance. Xylenols are used as pesticides and used in the manufacture of antioxidants. Xylenol orange is a redox indicator built on a xylenol skeleton. 2,6-xylenol is a monomer for Poly(p-phenylene oxide) engineering resins through carbon - oxygen oxidative coupling. In one study 2,6-xylenol is oxidized with iodosobenzene diacetate with a five fold excess of the phenol[65].

Alkylation of alkoxy benzenes thus becomes a very important reaction from the industrial point of view[66].The synthesis of 2,6-xylenol by the alkylation of phenol with methanol has been attempted over different metal oxide catalysts[67-71]. It is known that anisole can undergo intramolecular

rearrangement reaction to *o*-cresol or intermolecular rearrangement between two molecules to give methyl anisole and phenol. Also, dealkylation reactions can prevail depending upon the reaction conditions or acid–base properties of the catalyst. Apart from the acid–base properties of the catalysts, the product selectivity is often influenced by the operating conditions and the nature of alkylating agent. Bautista and co-workers found that dealkylation to phenol is predominant over $AlPO_4$–Al_2O_3 catalysts in the alkylation of anisole with methanol[72]. Jyothi *et al* reported the selective synthesis of 2,6-xylenol by the reaction of anisole and methanol over solid base catalysts comprising of tin oxide and rare earth elements like Lanthanum Cerium and Samarium as promoters[73]. It has also been reported that the incorporation of weak acid sites and comparatively stronger basic sites are responsible for the selective methylation of phenol to o-cresol and 2,6-xylenol[74-75].

6.12 Process Optimization

Methylation of anisole was carried out over a fixed bed down flow glass reactor under a constant flow of nitrogen. 0.5g of the powdered catalyst was loaded in the middle of the reactor and placed in a temperature controlled furnace with a thermocouple for measuring the reaction temperature. The feed, which contains a mixture of anisole and methanol, was passed using a syringe pump. The product was cooled in a water cooled condenser, collected in a receiver and analyzed using a Gas Chromatograph (Chemito GC 1000) using BP1 capillary column (12m×0.32m) with FID detector. The major product obtained in this reaction is 2,6-xylenol. Small amounts of phenol, o-cresol as well as methyl anisole are obtained during the course of the reaction. No peak

corresponding to the formation of trimethyl phenol is obtained from the GC results. The scheme of anisole methylation reaction is given in figure 6.15. The optimization of the reaction variables such as reaction temperature, flow rate and molar ratio of anisole and methanol is done to get maximum conversion as well as product selectivity.
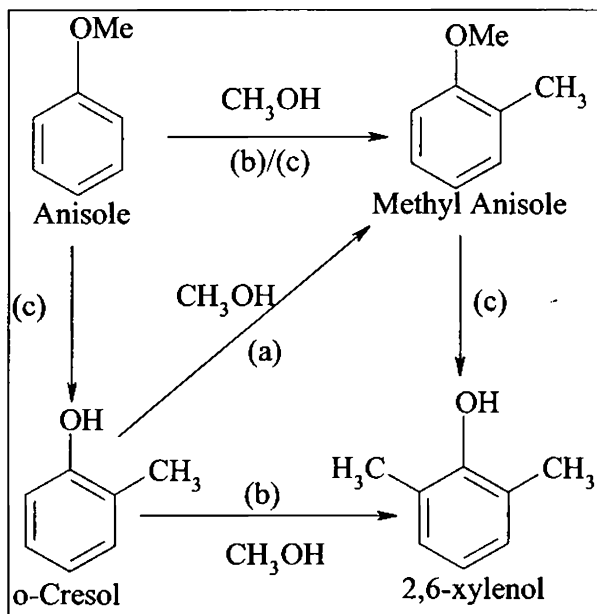
Figure 6.15

Pathways of Anisole Methylation

(a) Ortho Alkylation, (b) C-Alkylation, (c) Intermolecular Reaction

6.12.1 Influence of Reaction Temperature

The anisole conversion and product selectivity as a function of reaction temperature is shown in table 6.11. The anisole conversion increased with temperature and attained a maximum of 44.6% at 380°C. Thereafter the

percentage anisole conversion decreases considerably. This can be attributed to the decomposition of methanol at higher temperatures. Maximum 2,6-xylenol selectivity was attained at 380°C but at higher temperatures it decreases. The percentage selectivity of methyl anisole decreases appreciably as the temperature increases. Methyl anisole as soon as it is formed gets converted to other products. Another interesting observation is that the percentage phenol selectivity increases with the increase of reaction temperature. The possibility of forming the dealkylated product increases with temperature.

Table 6.11

Influence of Reaction Temperature on the Methylation of Anisole

Reaction	Percentage	Selectivity (%)			
Temperature°C	Conversion	2,6-xylenol	Phenol	Cresol	Methyl Anisole
340	19.5	43.6	3.1	22.8	30.6
360	22.9	39.9	6.2	26.2	27.7
380	44.6	65.5	7.3	12.6	14.6
400	22.9	50.9	18.7	45.6	4.8
420	18.8	47.5	41.3	30.2	1.0

Catalyst-0.5g TiLa10, Flow Rate-5ml/h, Anisole: Methanol-1:5

6.12.2 Influence of molar ratios of anisole and methanol

The effect of anisole to methanol molar ratio on the product selectivity was investigated at 380 °C taking several anisole to methanol molar ratios over TiLa10 catalyst to select an optimum feed mix. The major product formed was 2,6-xylenol along with small quantities of phenol, methyl anisole and cresol. The results are presented in table 6.12. The selectivity to methyl anisole

decreases with increase in the molar ratio of methanol and anisole. The percentage selectivity of the dealkylated product does not vary appreciably with the increase of methanol content. An optimum molar ratio of 1:7 (anisole:methanol) is chosen for the reaction as it gives good conversion and better selectivity.

Table 6.12

Influence of methanol/anisole molar ratio on the Methylation of Anisole

Methanol/ Anisole	Percentage Conversion	Selectivity (%)			
		2,6-xylenol	Phenol	Cresol	Methyl Anisole
3	25.4	54.2	6.5	10.5	28.8
5	44.6	65.5	7.3	12.6	14.6
7	32.1	46.7	6.3	30.9	16.1
9	19.6	45.2	7.1	34.5	13.3

Catalyst-0.5g TiLa10, Flow Rate-5ml/h, Reaction Temperature-380°C

6.12.3 Influence of Flow Rate

The effect of flow rate on anisole conversion as well as product selectivity is shown in table 6.13. The flow rate is varied from 3 to 7ml/h, keeping all other reaction parameters identical. When the flow rate increases from 3 to 5ml/h, a gradual increase of anisole conversion from 34.2 to 44.6 % is noticed. After that anisole conversion decreases with flow rate. It can be seen that the selectivity of methyl anisole increases with increase in flow rate with a concomitant decrease in the selectivity of 2,6-xylenol. This suggests that methyl anisole is the possible intermediate in the formation of 2,6-xylenol. The isomerisation of methyl anisole to 2,6-xylenol further supports this reaction

pathway. Hence, conversion of anisole to 2,6-xylenol in the presence of methanol must be taking place in two consecutive reactions (*a*) the formation of methyl anisole from anisole and (*b*) isomerisation of methyl anisole to 2,6-xylenol. When anisole alone was passed over the catalyst under similar conditions phenol and *o*-cresol were detected as major products but the conversion was low.

Table 6.13

Influence of flow rate on the Methylation of Anisole

Flow Rate ml/h	Percentage Conversion	Selectivity (%)			
		2,6-xylenol	Phenol	Cresol	Methyl Anisole
3	34.2	61.3	12.8	15.7	10.2
4	39.4	59.1	8.5	19.6	12.8
5	44.6	65.5	7.3	12.6	14.6
6	35.1	42.2	8.1	23.9	25.8
7	30.5	37.2	6.9	19.5	36.4

Catalyst-0.5g TiLa10, Anisole : Methanol-1:5, Reaction Temperature-380°C

6.12.4 Effect of Time on Stream

One of the major criteria required for a good catalyst is its stability over the course of the reaction. Retention of the catalytic activity and desired product selectivity is the most sought after property of a catalyst. Thus, a time on stream study becomes highly important in the field of catalysis. A time on stream study was performed with different systems under optimized reaction conditions (Catalyst-0.5g, Anisole: Methanol-1:5, Reaction Temperature-380°C, Flow rate-5ml/h). Figures 6.16 and 6.17 describe the effect of time on

stream on the conversion of anisole with methanol over various catalyst systems. The selectivity pattern is almost silimilar over the systems.
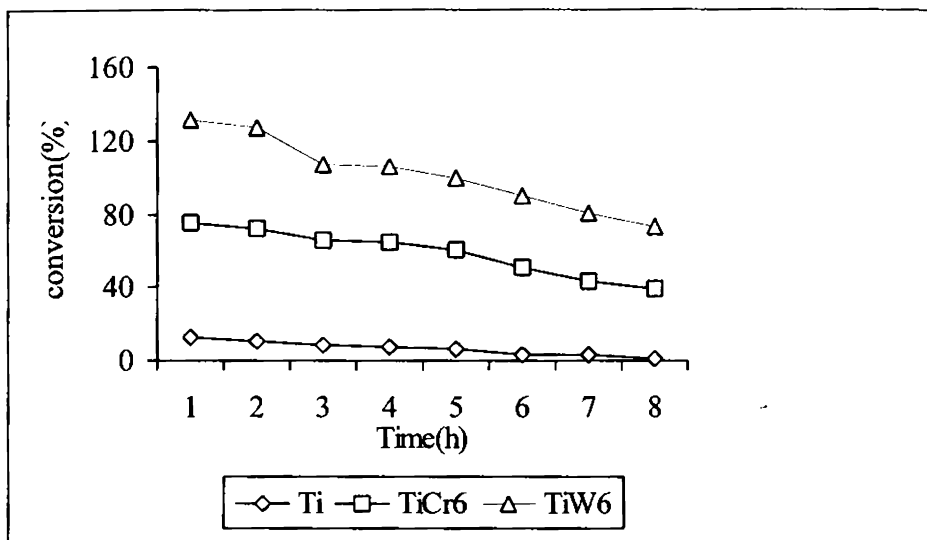
Figure 6.16

Effect of time on stream over Ti, TiCr6 and TiW6

The deactivation pattern of transition metals incorporated titania systems differs considerably from rare earth metals incorporated systems. In the earlier case, a continuous loss in the catalytic activity with time is observed. But in rare earth metal incorporated systems, an initial deactivation was observed over all the catalysts and thereafter attained a stable activity. The deactivation of pure titania is fast compared to their modified forms shows that modification with other metals improves the stability of titania, besides increasing their catalytic activity. The faster deactivation can be explained in terms of coke deposition.
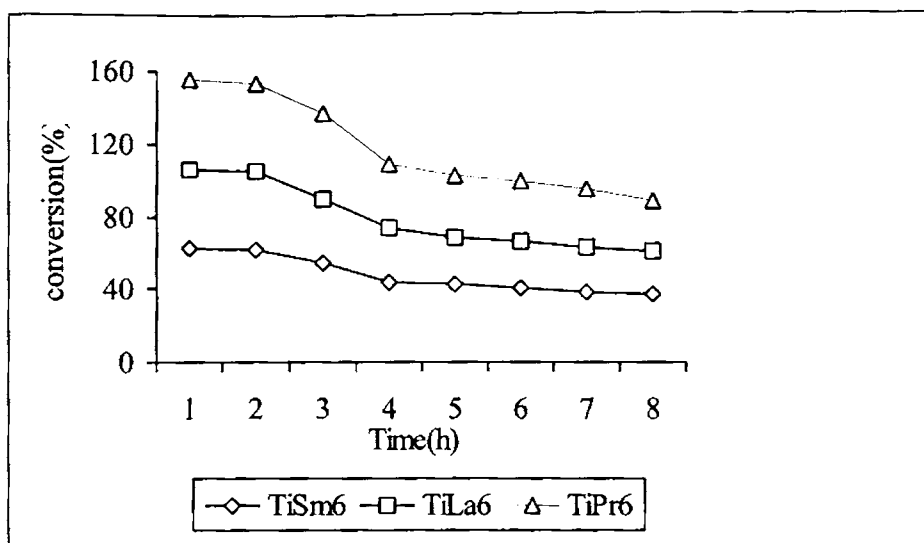
Figure 6.17

Effect of time on stream over TiLa6, TiSm6 and TiPr6

6.13 Comparison of Catalyst Systems

Anisole methylation is carried out under the optimized reaction conditions over the prepared catalyst systems. The effect of transition metals as well as the rare earth metals on the catalytic activity and selectivity of the systems is given in tables 6.14 and 6.15. Pure titania possess a catalytic activity of 10.5 in this reaction with a xylenol selectivity of 47.5%. The selectivity to methyl anisole is more in the case of pure titania than others. Both transition metals and rare earth metals enhance the catalytic activity of pure titania. In all the systems, the major product obtained is 2,6-xylenol. Among the various transition metals, chromium incorporated titania systems are found to be most active. These systems also show the highest xylenol selectivity.

Table 6.14

Effect of Transition Metals on Anisole Methylation

Systems	Conversion (%)	Selectivity			
		Phenol	Cresols	2,6-xylenol	Methyl Anisole
Ti	10.5	7.4	24.3	47.5	20.7
TiMo2	40.2	9.8	14.2	69.4	6.5
TiMo6	52.4	3.8	12.1	74.2	9.9
TiMo10	65.5	2.7	7.1	84.1	6.2
TiCr2	50.6	2.8	7.5	80.1	9.6
TiCr6	61.3	1.9	3.3	88.8	5.0
TiCr10	67.3	1.0	6.7	84.3	7.9
TiW2	48.6	5.9	19.9	63.3	11.0
TiW6	55.0	2.2	4.7	80.3	12.7
TiW10	56.0	1.0	18.5	72.5	8.0

Catalyst-0.5g TiLa10, Anisole : Methanol-1:5, Reaction Temperature-380°C, Flow Rate-5ml/h

Among the rare earth metals, praseodymium incorporated titania systems are showing maximum catalytic activity as well as xylenol selectivity in anisole methylation reaction. An attempt to investigate the influence of the metal loading on the catalytic activity is quite reasonable. As expected, the variation in metal loading had a significant impact on the catalytic activity as well as product selectivity. A common trend in the percentage anisole selectivity is observed among all the modified systems. As the percentage of metal incorporation increases, there is a reduction in the rate of dealkylation of

anisole to phenol. In all the metal incorporated systems, the percentage anisole conversion increases with the metal content.

Table 6.15

Effect of Rare Earth Metals on anisole methylation

Systems	Conversion	Selectivity			
	(%)	Phenol	Cresols	2,6-xylenol	Methyl Anisole
Ti	10.5	7.4	24.3	47.5	20.7
TiLa2	40.9	10.8	4.8	76.6	7.8
TiLa6	44.0	8.6	17.8	60.1	13.5
TiLa10	44.6	7.3	12.6	65.5	14.6
TiPr2	40.9	5.7	2.9	79.3	12.1
TiPr6	48.8	4.7	10.0	82.2	3.0
TiPr10	51.5	3.8	6.7	85.1	4.5
TiSm2	42.5	10.0	21.0	57.9	11.1
TiSm6	61.3	6.49	17.47	56.1	19.9
TiSm10	61.9	4.7	17.4	54.3	23.6

Catalyst-0.5g TiLa10, Anisole : Methanol-1:5, Reaction Temperature-380°C, Flow Rate-5ml/h

The acid base properties of the catalysts affect the final selectivity of heterogeneous catalysts[76]. Figures 6.18 and 6.19 gives the correlation between the percentage anisole conversion and the percentage cyclohexanol decomposition reaction. Similarly a good correlation is obtained between the 2,6-xylenol selectivity and strong acidity assessed by ammonia TPD and the results are compiled in figures 6.20 and 6.21.
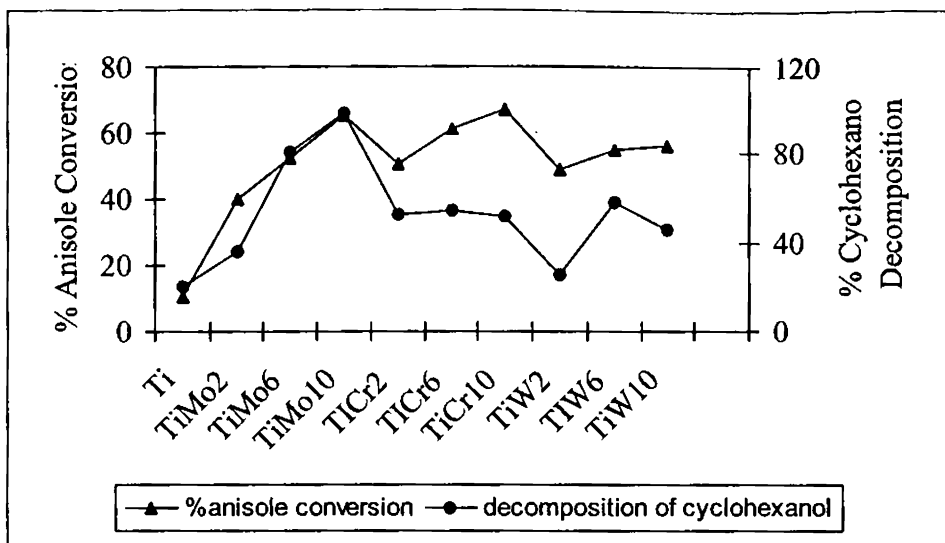
Figure 6.18

Correlation between % Anisole Conversion and % Cyclohexanol Conversion
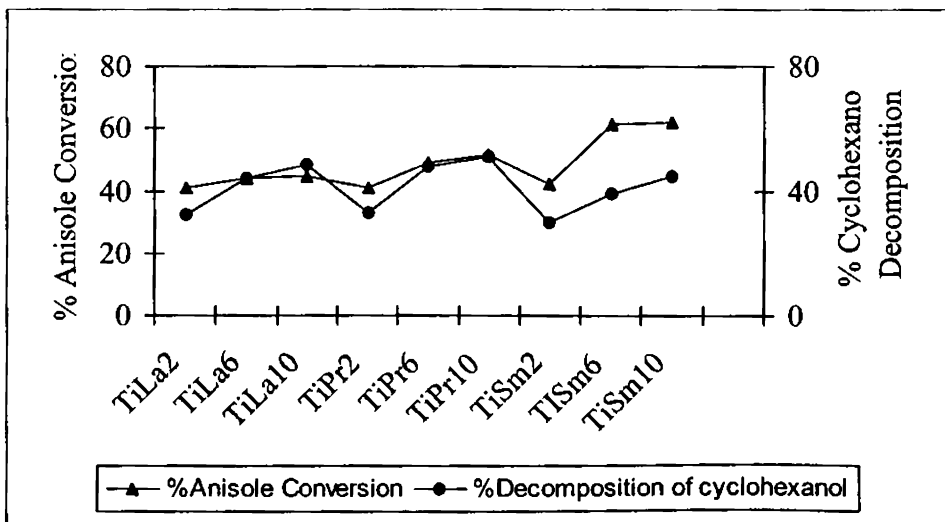
Figure 6.19

Correlation between % Anisole Conversion and % Cyclohexanol Conversion
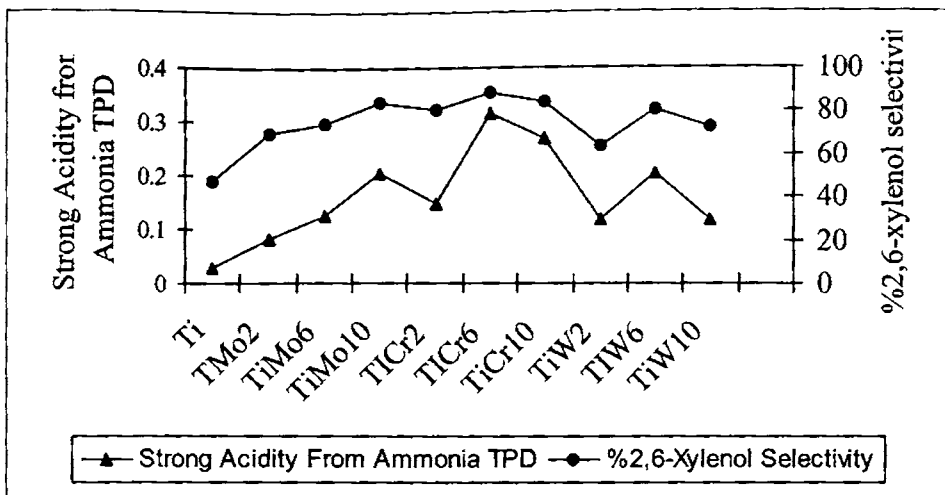
Figure 6.20

Correlation between strong acidity from NH_3 TPD and %2,6 Xylenol
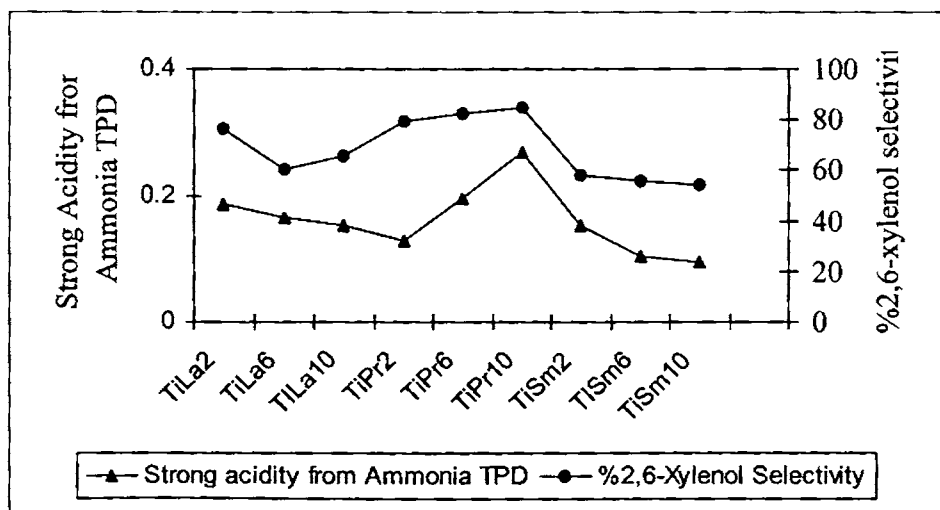
selectivity

Figure 6.21

Correlation between strong acidity from NH_3 TPD and %2,6-Xylenol

selectivity

Cyclohexanol decomposition reaction is a typical test reaction for investigating the acid-base properties of the catalytic sites on the metal oxides[77-79]. Studies utilizing different alcohols showed that acid sites on the catalyst cause dehydration of the alcohol molecule and the basic sites cause dehydrogenation[80]. So the percentage of cyclohexanol decomposition gives an idea about both the acidic and basic sites. In the present study, the percentage anisole conversion is well correlated with the percentage cyclohexanol decomposition reaction. So it can be concluded that the methylation of anisole occurs on the acidic as well as basic sites of the prepared catalysts. It is also clear that the strong acid sites present in the catalyst are responsible for the formation of 2,6-xylenol.

6.14 Conclusions

The formation of alkylated phenols is a major area of chemistry and clean processes are required. The conversion of anisole to 2,6-xylenol is an important target, and the prepared titania and modified titania catalyst systems may provide the answer. The acid-base properties of the prepared catalysts are responsible for the methylation of anisole. The high selectivity to 2,6-xylenol can be attributed to the presence of strong acidic sites present in the catalyst. The product selectivity is also influenced by reaction temperature, flow rate as well as the molar ratio of anisole and methanol.

References

1   S.H. Patinuin and B.S. Friedman, in; Alkylation of aromatics with Alkenes and alkanes in Friedel Crafts and related reactions, Vol.3, ed. G.A.Olah Interscience, New York, (1964) 75.

2   J.F. Lorenc, G. Lambeth and W. Scheffer, in; Kirk-Othmer Encyclopedia of Chemical Technology, Vol 2, eds. M.Howe-Grant and J.I.Kroschwitz Wiley, New York, (1992) 113.

3   D. Ganapati, Yadav, Nirav S. Doshi, Appl. Catal A; Gen, 236 (2002) 129.

4   BF.Cunill, J.Tejero, J.F.Izquierdo, Appl. Catal, 34 (1987) 341.

5   J.Tejero, BF.Cunill, S.Manazano, Appl. Catal, 38 (1988) 327.

6   G.D. Yadav, Bull. Catal. Soc India, 15 (1998) 21.

7   G.D. Yadav, N.Kirthivasan, in: J.P.Bitz, C.B. Little (Eds), Fundamentals and Applied Aspects of Chemically Modified Surfaces, Royal Society of Chemistry, UK (1999) 254.

8   G.D.Yadav, A.A.Pujari, A.V.Joshi, Green Chem, 1 (1999) 269.

9   O.N.Tsvetkov, K.D.Kovenev, Int. J. Chem. Eng, 6 (1966) 328.

10 U.S.4, 414, 233.

11 Ger. (East) DD 267,250

12 V.I. Korenskii, I.P. Kolenko, V.D. Skobeleva, Zh. Prikl, Khim, (Leningrad) 57 (1984) 2016

13 G. Sartori, F. Bigi, G. Casiraghi, G.casnati, L. Chiesi, A. Arduini, Chem. Ind, (London) 22 (1985) 762.

14 Japan 85 178, 836.

15 V.A. Koshchii, Y.B. Kozlikovskii, A.A. Matyusha, Zh.org.Khim, 24 (1988) 1508.

16   Japan 6100,036.

17   K.G. Chandra, M.M. Sharma, Catal.Lett, 19 (1993) 309.

18   Japan 5852,233.

19   R.A.Rajadhyaksha, D.D.Chaudhari, Ind.Eng.Chem.Res, 26 (1987) 1276.

20   Braz. Pedidv PIBR 8002,607.

21   Ger.often DE 3,443,736.

22   K.R.Sunajadevi and S.Sugunan, Catal.Lett, 99 (2005) 263.

23   A.Sakthivel, N.Saritha, and P.Selvam, Catal.Lett, 72 (2001) 225.

24   Yasuhiro Kamitori, Masaru Hojo, Ryoichi Masuda, Tatsuo Izumi and Shuichi Tsukamoto, J. Org. Chem, 49 (1984) 4161.

25   S. Subramanian, Anupam Mitra, C.V.V. Satyanarayana and D.K. Chakratarty, Appl. Catal A; General, 159 (1997) 229.

26   A. Sakthivel, S.K. Badamali, P. Selvam, Microporous and mesoporous materials, 39 (2000) 457.

27   A. Vinu, K. Usha Nandhini, V. Murugesan, Winfried Bohlmann, V. Umamaheswari, Andreas Poppl and Martin Hartmann, Appl. Catal A; General, 265 (2004) 1.

28   Kui Zhang, Changhua Huang, Huaibin Zhang, Shouhe Xiang, Shangyuan Liu, Dong Xu and Hexuan Li, Appl. Catal A; General, 166 (1998) 89.

29   Kui Zhang, Huaibin Zhang, Genhui Xu, Shouhe Xiang, Dong Xu, Shangyuan Liu and Hexuan Li, Appl. Catal A; General, 207 (2001) 183.

30   A.V.Krishnan, Keka Ojha and Narayan C. Pradhan, Organic Process Research & development, 6 (2002) 132.

31   Kui Zhang, Shouhe Xiang, Huaibin Zhang, Shangyuan Liu and Hexuan

Li, React. Kinet. Catal. Lett, 77 (1) (2002) 13.

32 Emil Dumitriu and Vasile Hulea, J. Catal, 218 (2003) 249.

33 A. Corma, H. Garcia, J. Primo, J. Chem. Res, (S) 1 (1988) 40.

34 R.F. Parton, J.M. Jacobs, H. Van Ootehem and P.A. Jacobs, Stud. Surf. Sci. Catal, 46 (1989) 211.

35 K. Tanabe, T. Nishizaki, in F.C Tompkins (Ed.) Proc. 6th Int. Congress on Catalysis, The Chemical Society, London (1977).

36 L.H. Klemm, C.F. Klopfenstein, J. Shabtai, J. Org. Chem, 35 (1970) 1069.

37 N. Nagaraju and George Kuriakose, New J. Chem, 27 (2003) 765.

38 Rahna Koyakutty Shamsudeen, Kanat Nisha and Sankaran Sugunan, React. Kinet. Catal. Lett, 81 (2) (2004) 341.

39 Kurungot Sreekumar, Thundimadathil Jyothi, Ramankutty. C. Govindankutty, Bollapragada S. Rao and Sankaran Sugunan, React. Kinet. Catal. Lett, 70 (1) (2000) 161.

40 K. Sreekumar, T. Raja, B.P. Kiran, S. Sugunan, B.S. Rao, Appl. Catal. A: Gen, 182 (1999) 327

41 K.Sreekumar, T.M.Jyothi, M.B.Talawar, B.P.Kiran, B.S.Rao, S.Sugunan, J. Mol. Catal. A: Chem, 152 (2000) 225.

42 Wei Wang, Michael Seiler, Irina I. Ivanova, Jens Weitkamp and Michael Hunger, Chem. Commun, (2001) 1362.

43 K.G. Ione and O.V. Kikhtyanin, Stud. Surf. Sci. Catal, 49 (1989) 1073.

44 R.B.C. Pillai, React. Kinet. Catal. Lett, 58 (1996) 145.

45 Nidhi Rammohan, V.G. Kumar Das and R.B.C. Pillai, Hungarian J. Industrial Chem, 27 (1999) 13.

46 P.Y.Chen, S.J.Chu, N.S.Chang, T.K.Chuang, Stud. Surf. Sci. Catal, 49 B

(1989) 1105.

47   B.L.Su, D.Barthomeuf, Appl. Catal. A: Gen, 124 (1995) 73.

48   B.L.Su, D.Barthomeuf, Appl. Catal. A: Gen, 124 (1995) 81.

49   M.A. Aramendia, V. Borau, C. Jimenez, J.M. Marinas, F.J. Romero, Appl. Catal. A: Gen, 183 (1999) 73.

50   M.A. Aramendia, V. Borau, C. Jimenez, J.M. Marinas, F.J. Romero, Colloids and Surfaces A: Physico-chemical and Engineering Aspects, 170 (2000) 51.

51   S.P. Elangovan, C. Kannan, B. Arabindoo, V. Murugesan, Appl. Catal. A: Gen, 174 (1998) 213.

52   D.D. Dixon and W.F. Burgoyne, Appl. Catal, 62 (1990) 161.

53   Maurizio Seiva, Andrea Bomben and Pietro Tundo, J. Chem. Soc, Perkin Trans, 1 (1997) 1041.

54   V.R. Choudhary, V.S. Nayak, Zeolites, 5 (1985) 328.

55   B. Gielen, M.G. Palekar, Zeolites, 9 (1989) 208.

56   F.M. Bautista, J.M. Campelo, A. Garcla, D. Luna, J.M. Marrinas, A.A. Romero, Appl. Catal. A: Gen, 166 (1998) 39.

57   S.I.Woo, J.K.Lee, S.B.Hong, Y.K.Park, Y.S.Uh, Stud. Surf. Sci. Catal, 49 (1989) 1905.

58   P.Y. Chen, M.C. Chen, H.Y. Chu, N.S. Chang, T.K. Chuang, Stud. Surf. Sci. Catal, 28 (1986) 739.

59   S. Narayanan, K. Deshpande, Appl. Catal. A. Gen, 193 (2000) 17.

60   S. Narayanan, K. Deshpande, Appl. Catal. A. Gen, 199 (2000) 1.

61   S. Prasad, B.S. Rao, J. Mol. Catal, 62 (17) 1990.

62   R. Dowbenko, in Encyclopedia of Chemical Technology, ed. J. I.

Kroschwitz and M. Houlgrant, Wiley, New York, 1992, p. 106.

63 H. Fiege, in B. Elvers, S. Hawkins and G. Schultz (Editors), Ullmann's Encylopedia of Industrial Chemistry, 5th ed., VCH Verlag, 1991, Vol. A19, p. 313.

64 S. Narayanan, Res. Ind, 34 (1989) 296.

65 Christophe Boldron, Guillem Aromí, Ger Challa, Patrick Gamez and Jan Reedijk Chem Commun, 46 (2005) 5808.

66 G.D. Yadav, P.K. Goel and A.V. Joshi, Green Chem, 3 (2001) 92.

67 M. C. Samolada, E. Grgoriadou, Z. Kiparissides and I. A. Vasalos, J. Catal, 52 (1995) 152.

68 S. Velu and C. S. Swamy, Appl. Catal, 211(1994) 119..

69 S. Sato, K. Koizumi and F. Nozaki, Appl. Catal, L7 (1995) 133.

70 S. Sato, K. Koizumi and F. Nozaki, J. Catal, 264 (1998) 178.

71 V. V. Rao, V. Durgakumari and S. Narayan, Appl. Catal, 161 (1984) 49.

72 F. M. Bautista, J. M. Campelo, A. Garcia, D. Luna, J. M. Marinas and A. A. Romero and M. R. Urbano, React. Kinet. Catal. Lett, 349 (1995) 56.

73 T.M. Jyothi, S. Sugunan and B.S. Rao, Green Chem, 2 (2000) 269.

74 T. M. Jyothi, B. S. Rao, S. Sugunan and K. Sreekumar, Indian J. Chem. Sect. A, 1253 (1999) 38.

75 Rajaram Bai and S. Sivasankar, Green Chem, 2 (2000) 106.

76 B. Coq, V. Gourves, F. Figueras, Appl. Catal. A, 100 (1993) 69.

77 M. Ai, Bull. Chem. Soc. Jpn, 50 (1977) 2579.

78 H. Nollery, G. Ritler, J. Chem. Soc. Faraday Trans, 80 (1984) 275.

79 C. Bezouhanava, M.A. al-Zihari, Catal. Lett, 11 (1991) 245.

80 A. Gervasini, A. Aurox, J. Catal, 131 (1991) 190.

Chapter 7

Catalytic Dehydrogenation

Abstract

The dehydrogenation of cyclic alkanes and alkenes to aromatic molecules is one of the key reactions during naphtha reforming. The hydrogenation of olefins is also an important reaction in the chemical technology. The area is rapidly developing due to a great deal of research effort. Developments in dehydrogenation should bring more selective and active catalysts and oxidative dehydrogenation to increase thermodynamically limited conversion. The vapour phase dehydrogenation of cyclohexane as well as cyclohexene is carried out over the prepared systems. The influence of reaction temperature and flow rate is investigated in detail. The percentage conversion as well as the selectivity to the dehydrogenated product has an intimate dependence with the reaction time. The surface acidity of the prepared systems can be correlated with the percentage cyclohexane conversion.

7.1 Introduction

Growing interest is observed towards the hydro-dehydrogenation catalysts due to the legal limits of aromatic emission in exhaust gases[1-2]. Hydrogenation and dehydrogenation of organic compounds is the oldest and most diverse catalytic process[3]. Six membered alicyclic rings can be aromatized in a number of ways. Aromatization can be easily accomplished if there are already one or two double bonds in the ring or if the ring is fused to an aromatic ring[4]. Direct non oxidative catalytic decomposition of hydrocarbons is an alternative one step process to produce hydrogen of the required purity. The dehydrogenation of cyclohexane as well as cyclohexene is carried out over different catalyst systems and benzene is reported to be the major product in both the cases[5-11].

Benzene cannot be considered to be a useful product because cyclohexane is mostly produced by hydrogenation of benzene itself[12]. However, cyclohexane is also available in large amounts in naphthas, so it can be recovered from them although with quite demanding procedures. In particular, a significant concentration of cyclohexane occurs in the side fraction of the so-called benzene heartcut tower, a refinery distillation tower, where a benzene-rich fraction (50% of benzene) is separated from a heavy gasoline bottom and a light gasoline head fraction, both fulfilling the 1% maximum limit for benzene in commercial gasoline[13]. This side fraction can be considered a relatively low-value by-product of the refinery and is used to provide benzene for petrochemical processes. Due to the important role of benzene as an intermediate in petrochemistry, processes for conversion of low-value hydrocarbons into benzene, such as aromatization of light alkanes[14], are

under development. In this context, the conversion of cyclohexane, either recovered from the benzene heartcut tower side fraction, or still in mixture with benzene, can be a way to enhance the production of benzene and to fulfill the need for benzene in some cases.

The dehydrogenation of cyclohexane to benzene on Pt catalysts as a prototypical hydrocarbon reforming reaction was first recognized by Zelinskii in 1911[15] and introduced commercially in 1949. The typical hydrocarbon reforming catalysts consists of 1 nm Pt particles supported on alumina. Cyclohexane dehydrogenation has been studied extensively on Pt single crystals using surface science techniques[16-32]. Grant *et al* studied *the* dehydrogenation of cyclohexane on Pt/ZnO (0001)-O model catalysts with temperature programmed desorption (TPD), low-energy ion scattering spectroscopy, and X-ray photoelectron spectroscopy[33].

Don A. Perry and John C. Hemminger described the effect of coadsorbed hydrogen on the initial step in the dehydrogenation of cyclohexane on Pt (111)[34]. The experiments show that the initial step in the dehydrogenation of cyclohexane is dramatically altered by the presence of saturation amounts of surface hydrogen or deuterium. The hydrocarbon-surface interaction is substantially weakened, yet the activation energy for initial dehydrogenation is lowered by approximately 20%. While other possible explanations may exist, their results are consistent with a σ-bond metathesis mechanism for the initial step in the dehydrogenation of cyclohexane on a hydrogenated Pt surface.

Tiscareno-Luchega *et al.* studied the dehydrogenation of cyclohexane to benzene in a porous alumina oxide reactor packed with platinum/ silica

oxide supported catalyst and potassium promoted iron oxide catalysts, respectively[35]. Terry *et al.* investigated in detail the catalytic dehydrogenation of cyclohexane using silica oxide coated ceramic membranes[36]. The effect on reaction yield, membrane permeability, and membrane selectivity of altering pore size by addition of successive thin film layers (silica oxide particles in an iron (III) supported solution) to the membrane surfaces was the primary focus of the study. The dehdrogenation of cyclohexane is also carried out over platinum-tin-alumina sol-gel catalysts. It is shown that the metal active exposed area, determined by the cyclohexane dehydrogenation rate is not a function of the platinum precursor used, but rather a function of the specific surface area of the support[37]. Pal Teenyi and Victor Galsan studied the correlation between cyclohexane and thiophene conversion on alumina supported Ni and NiMo catalysts. The electron transfer between Ni and Mo is significant in both the reactions[38,1].

The hydrogenation and dehydrogenation reactions of cyclohexene on Pt(111) crystal surfaces were investigated by surface vibrational spectroscopy via sum frequency generation (SFG) both under vacuum and high pressure conditions with 10 Torr cyclohexene and various hydrogen pressures[39]. Previous surface science studies of cyclohexene chemisorption on Pt(111) in vaccum found that the molecule dehydrogenates readily to benzene around 300K[40-49]. The dehydrogenation of cyclohexene over carbon deposited on alumina, C/Al$_2$O$_3$, which was prepared by contacting hydrocarbons such as cyclohexane, cyclohexene and cyclohexanone was investigated under non-oxidative conditions[50]. The selectivity to the dehydrogenated products such as benzene and 1,3-cyclohexadiene was maximized at specific carbon content.

7.2 Process Optimization

The vapour phase dehydrogenation of cyclohexane and cyclohexene were carried out in a fixed bed down flow glass reactor under the flow of nitrogen with 0.5 g of catalyst being placed. Prior to the reaction, the catalyst sample was activated at 500°C for 2h. Then it is placed in the middle part of the reactor, supported on either side with a thin layer of glass wool and ceramic beds. The reactor was placed in an electrical furnace, and the reaction temperature was monitored using a thermocouple located in the reactor center. The product stream at the reactor exit was collected in an ice cooled trap and then analyzed by Gas Chromatography (Chemito GC 1000) using BP1 capillary column (12m×0.32m) with FID detector. The catalytic performance was evaluated by the conversion and the selectivities obtained during the process time.

The reaction conditions like reaction temperature and flow rate is optimized to get good results for all the prepared catalyst systems. The influence of catalyst is very clear when a blank run is carried out. In the absence of the catalyst, the percentage conversion is less than one. In the catalytic dehydrogenation of cyclohexane, benzene and minor amounts of cyclohexene is obtained. A very small percentage of other products like methyl cyclopentenes are also formed besides the selective formation of benzene. In the present chapter, the optimization of reaction conditions are done for the dehydrogenation of cyclohexane only and under that optimized conditions, the dehydrogenation of cyclohexane as well as cyclohexene is carried out over the prepared catalyst systems.

7.2.1 Effect of Temperature

Preliminarily, the effect of reaction temperature on the catalytic conversion of cyclohexane as well as its selectivity was examined. The results are given in table 7.1. With the increase of reaction temperature, there is a gradual increase in the cyclohexane conversion from 6.0% to 35.3%. Benzene selectivity also increases with temperature. When the reaction temperature is 475°C, maximum benzene selectivity as well as least formation of other products like methyl cyclopentanes is observed. Further increase of temperature may change the structure of the catalyst and so a reaction temperature of 475°C was chosen for all the reactions. It was also assumed that the deactivating compound gets readily desorbed at elevated temperatures.

Table 7.1

Influence of Reaction Temperature on the dehydrogenation of cyclohexane

Reaction	Cyclohexane	Selectivity (%)		
Temperature (°C)	Conversion (%)	Benzene	Cyclohexene	Others
400	6.0	75.6	15.0	9.4
425	10.2	84.3	5.9	9.8
450	18.6	91.9	3.0	5.1
475	35.3	95.6	3.0	1.4

Catalyst chosen- 0.5g TiMo10, Duration-1h, Flow Rate-3ml/h

7.2.2 Effect of flow rate

Table 7.2 shows the influence of flow rate on the catalytic activity and product selectivity. The flow rate alters the contact time and at high flow rate, the encounter of the reactants and the products with the catalyst surface will be

less compared to that at lower feed rates. Progressive increase in the cyclohexane conversion is noticed with increase in flow rate upto 3ml/h and thereafter it decreases. As the flow rate increases, benzene selectivity increases initially, reaches a maximum and thereafter it decreases. The formation of other products is less at higher feed rates because the reactants are in contact for less time and hence side reaction is suppressed. An optimum flow rate of 3ml/h is chosen for all the reactions considering its highest percentage conversion as well as benzene selectivity.

Table 7.2

Influence of Flow rate on the dehydrogenation of cyclohexane

Flow Rate (ml/h)	Cyclohexane Conversion (%)	Selectivity (%)		
		Benzene	Cyclohexene	Others
1	12.1	75.9	8.6	15.6
2	25.3	89.2	4.9	5. 9
3	35.3	95.6	3.0	1.4
4	21.4	90.2	9.5	0.3
5	20.6	85.5	14.4	0.1

Catalyst chosen- 0.5g TiMo10, Duration-1h, Reaction Temperature-475°C

7.2.3 Effect of time on Stream

The lowering of activity with time on stream is a common problem associated with heterogeneous catalysts. To study this, the reaction was carried out continuously for 5h over the prepared catalysts under optimized reaction conditions and the product analysis was done at regular intervals of 30 minutes. The results obtained are shown in figures 7.1 and 7.2.
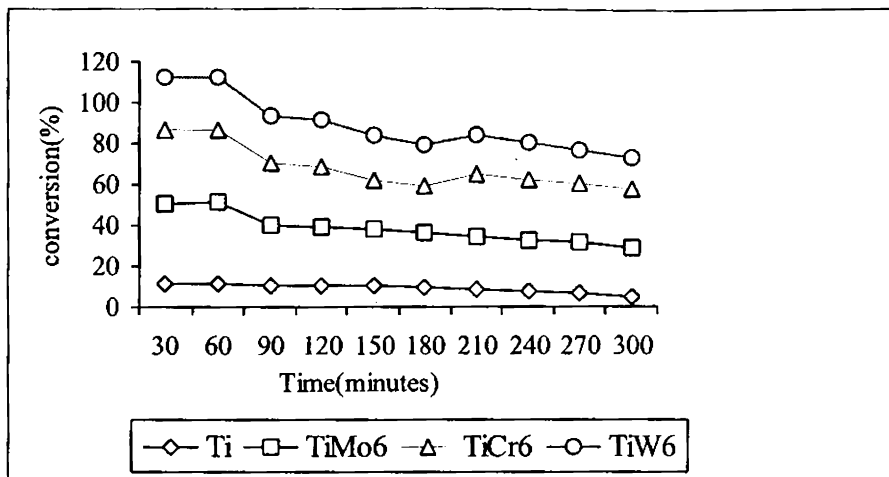
Figure 7.1

Deactivation studies of titania as well as transition metal incorporated titania in
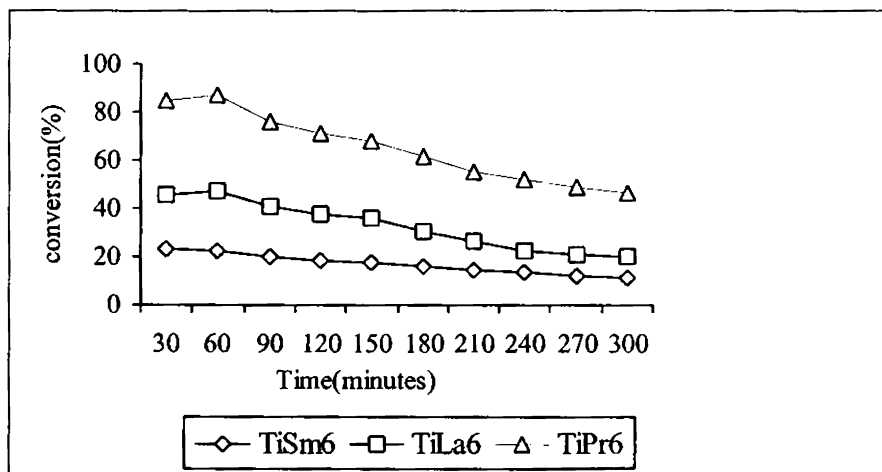the dehydrogenation of cyclohexane

Figure 7.2

Deactivation studies of rare earth metal incorporated titania in the
dehydrogenation of cyclohexane

The catalytic dehydrogenation of cyclohexene is also carried out effectively over the prepared systems. The deactivation studies of some of the systems were done under the optimized reaction conditions. The reaction mixture was collected at every 30 minutes and the results are depicted in figure 7.3.
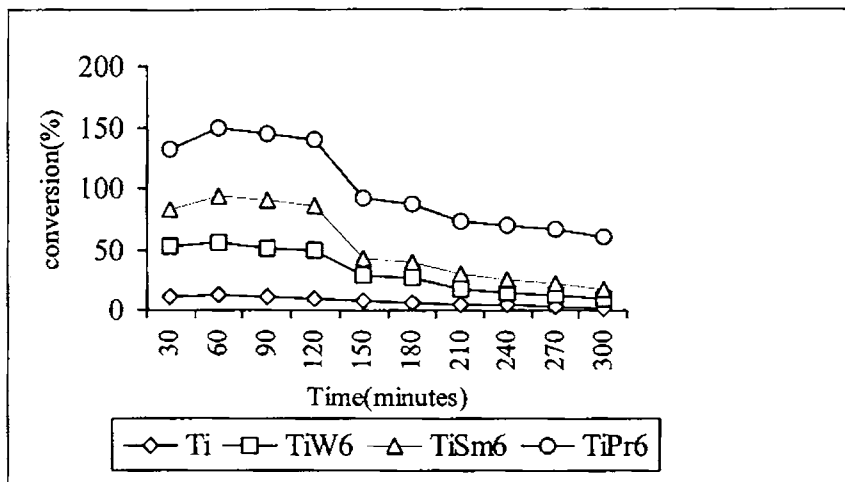
Figure 7.3

Deactivation studies of titania as well as metal incorporated titania in the dehydrogenation of cyclohexene.

The catalyst systems show small drops in the catalytic activity for 2h, but in the subsequent hour there is a sudden loss in catalytic activity. After that the deactivation rate is gradual in the dehydrogenation of cyclohexene. This indicates that when the reaction progresses, the number of active sites for dehydrogenation decreases upon coke deposition. Similar trends in benzene selectivity are also observed among the prepared catalytic systems. Similarly as the reaction time increases, there is chance for the formation of light hydrocarbons by decomposition.

7.3 Comparison of Catalyst Systems

After optimization studies, catalytic activity of all the prepared systems were evaluated using 0.5g of the catalyst and a reaction temperature of 475°C at a flow rate of 3 ml/h. The results for cyclohexane dehydrogenation over transition metal incorporated as well as rare earth metal incorporated systems are presented in tables 7.3 and 7.4 respectively.

Table 7.3

Influence of Transition metals on the dehydrogenation of cyclohexane

Systems	% Cyclohexane Conversion	Selectivity (%)		
		Benzene	Cyclohexene	Others
Ti	11.0	91.4	7.6	1.0
TiMo2	22.7	95.4	4.1	0.6
TiMo6	40.4	93.3	5.7	1.0
TiMo10	55.3	95.6	3.0	1.4
TiCr2	29.6	95.3	3.0	1.7
TiCr6	35.3	92.1	6.7	1.2
TiCr10	68.0	96.2	2.1	1.7
TiW2	22.2	80.5	18.4	1.1
TiW6	25.5	77.4	19.0	3.6
TiW10	30.3	71.0	25.6	3.4

Catalyst weight-0.5g, Duration-1h, Flow rate-3ml/h, Temperature-475°C

Pure titania gave only a very low conversion under the specified reaction conditions. An interesting observation is the enhanced benzene selectivity of the reaction. Titania alone is efficient enough to give a good selectivity of benzene during the reaction. Among the various metal

incorporated systems, a notable observation was the increase in percentage conversion with the increase in the metal content. Among the different transition metals, molybdenum incorporated systems are having highest catalytic activity in dehydrogenating cyclohexane with a better selectivity of benzene. This can be attributed to the enhanced amount of acidic sites present in the catalyst systems. Among the rare earth metals, praseodymia incorporated systems are having highest catalytic activity. The catalyst aids the transformation of cyclohexane to cyclohexene more easily and the formation of benzene from cyclohexene is a slow process in this case. But the selectivity to benzene is more in the case of lanthana modified systems.

Table 7.4

Influence of Rare Earth metals on the dehydrogenation of cyclohexane

Systems	% Cyclohexane Conversion	Selectivity (%)		
		Benzene	Cyclohexene	Others
Ti	11.0	91.4	7.6	1.0
TiLa2	17.3	88.5	10.4	1.1
TiLa6	24.8	90.1	7.5	2.5
TiLa10	26.5	93.1	4.9	2.0
TiPr2	30.8	78.2	17.9	3.8
TiPr6	40.6	75.3	22.8	2.0
TiPr10	46.0	73.9	24.1	2.0
TiSm2	19.0	82.8	14.1	3.1
TiSm6	22.1	75.3	18.8	5.9
TiSm10	24.6	72.3	23.5	4.1

Catalyst weight-0.5g, Duration-1h, Flow rate-3ml/h, Temperature-475°C

The dehydrogenation of cyclohexene is carried out over the prepared systems and the results are given in tables 7.5 and 7.6. The major product obtained in this reaction is benzene. The following three reactions are considered to be alternatives; release of hydrogen molecule, hydrogenation of cyclohexene to cyclohexane and formations of smaller hydrocarbons by hydrogenolysis of cyclohexene. When the second reaction is dominant, the overall reaction is described as disproportionation. In the present study, the dehydrogenation occurs predominantly over disproportionation. Comparatively lower temperature used in the present study leads to a very low formation of cracking products.

Table 7.5

Influence of Transition metals on the dehydrogenation of cyclohexene

Systems	Conversion (%)	Selectivity (%)		
		Benzene	Cyclohexane	Others
Ti	12.7	70.3	21.8	7.9
TiMo2	29.9	86.6	13.1	0.3
TiMo6	43.5	81.9	14.2	2.5
TiMo10	62.4	83.7	13.8	2.5
TiCr2	44.4	89.1	7.9	3.1
TiCr6	48.7	85.6	9.8	4.7
TiCr10	55.5	88.6	11.3	0.1
TiW2	38.8	75.6	19.9	5.6
TiW6	42.4	85.8	10.4	3.8
TiW10	43.9	80.7	18.1	1.1

Catalyst weight-0.5g, Duration-1h, Flow rate-3ml/h, Temperature-475°C

Pure titania is having a cyclohexene conversion of 12.73% with a benzene selectivity of 70.34%. Both transition metals and rare earth metals enhance the dehydrogenation of cyclohexene with good benzene selectivity.

Table 7.6

Influence of Rare Earth metals on the dehydrogenation of cyclohexene

Systems	Cyclohexene Conversion (%)	Selectivity (%)		
		Benzene	Cyclohexane	Others
Ti	12.7	70.3	21.8	7.9
TiLa2	34.0	81.6	9.4	9.1
TiLa6	38.6	80.7	15.8	3.5
TiLa10	37.6	79.8	10.3	9.9
TiPr2	48.7	78.1	13.7	8.2
TiPr6	55.2	82.5	14.6	3.0
TiPr10	60.3	81.0	9.9	9.2
TiSm2	40.6	78.6	11.8	9.6
TiSm6	39.2	81.2	10.5	8.3
TiSm10	40.5	83.6	12.4	4.1

Catalyst weight-0.5g, Duration-1h, Flow rate-3ml/h, Temperature-475°C

From the literature, there is evidence that surface acid sites play an important role in the dehydrogenation reaction. A good correlation is obtained between the total acidity obtained from ammonia TPD and the percentage cyclohexane as well as cyclohexene conversion among the various catalyst systems. Figures 7.4 to 7.7 illustrate that the total acidity plays a decisive role in the dehydrogenation of cyclohexane and cyclohexene.
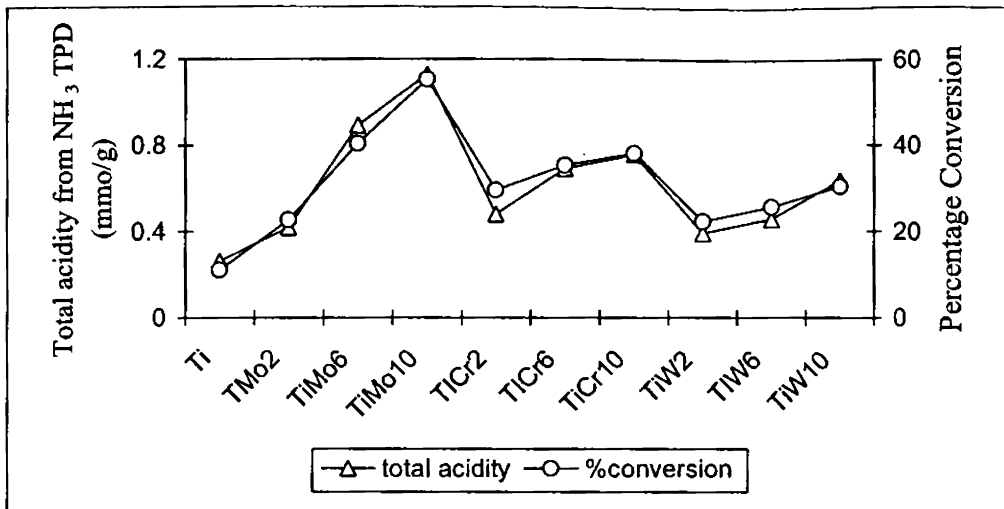
Figure 7.4

Correlation between the percentage cyclohexane conversion and total acidity

obtained from NH_3 TPD in transition metal modified TiO_2

Figure 7.5

Correlation between the percentage cyclohexane conversion and total acidity

obtained from NH_3 TPD in rare earth metal modified TiO_2

Figure 7.6

Correlation between the percentage cyclohexene conversion and total acidity obtained from NH_3 TPD in transition metal modified TiO_2
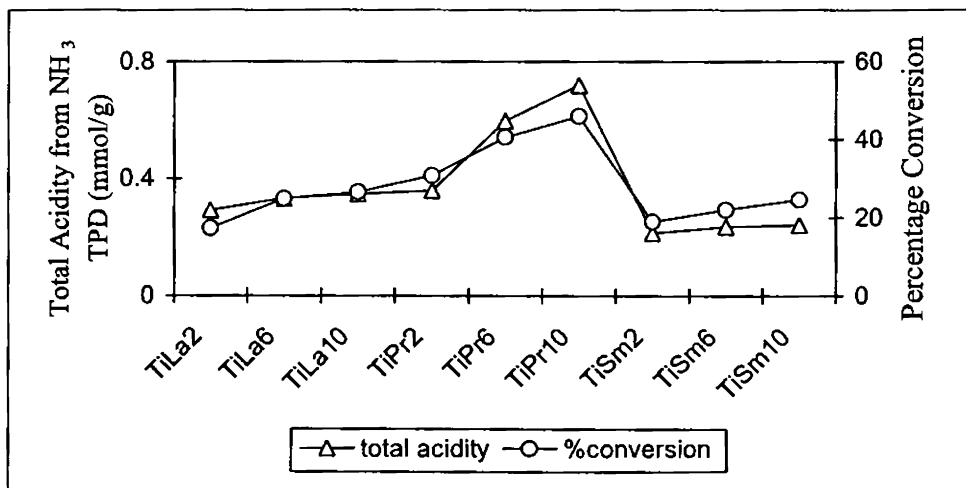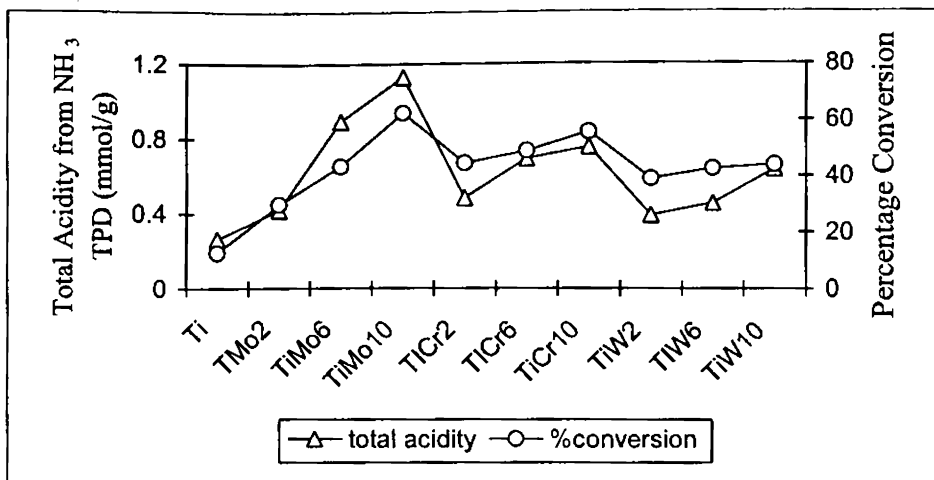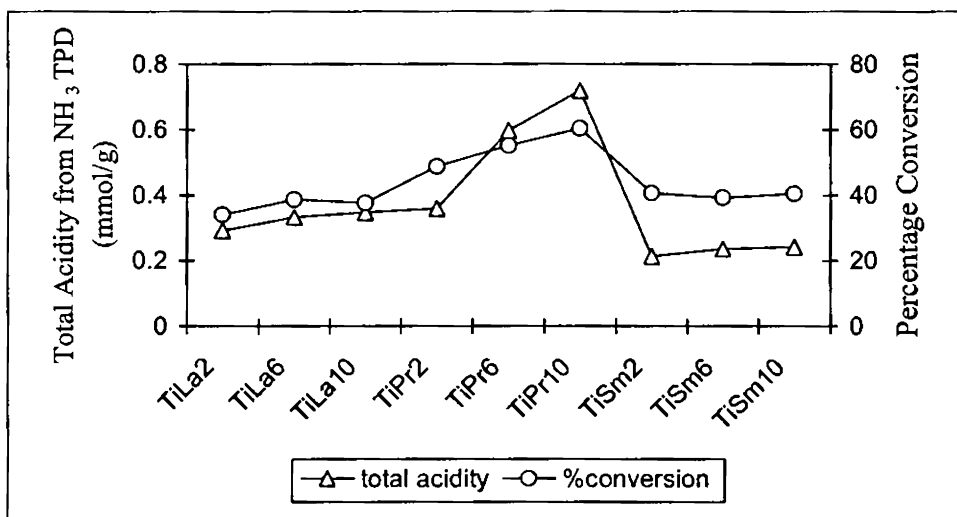

Figure 7.7

Correlation between the percentage cyclohexene conversion and total acidity obtained from NH_3 TPD in rare earth metal modified TiO_2

7.4 Conclusions

Modified titania catalysts are found to exhibit high activity and selectivity in the dehydrogenation of cyclohexane and cyclohexene. The reaction always yielded benzene as the predominat product. The catalytic activity is significantly affected by the reaction parameters like temperature of the reaction, flow rate and reaction time. The total surface acidity of the prepared catalyst systems plays an important role in determining the catalytic activity.

References

1   Pal Tetenyi ans Victor Galsan, React. Kinet. Catal. Lett, 74 (2) (2001) 251.

2   T. Kabe, W. Qian, Y. Hiazi, L. Li and A. Ishihara, J. Catal, 190 (2000) 191.

3   R. Farrauto and C.H. Bartholomew, React. Kinet. Catal. Lett, 70 (1) (2000) 195.

4   Jerry March, Advanced Organic Chemistry – Reactions, Mechanisms and Structure, Fourth Edition, Wiley Interscience Publication, New York.

5   F.C. Henn et al., J. Phys. Chem. 96 (1992) 5965

6   M.C. Tsai, C.M. Friend and E.L. Muetterties, J. Am. Chem. Soc, 104 (1982) 2539.

7   F. Patcas, A. Akbas, F.C. Buciuman and D. Honicke, Chem. Technik 52(5/6) (2001) 224.

8   F. Patcas, W. Krysmann, D. Honicke and F.C. Buciuman, Catal.Today, 69 (2001) 379.

9   E.C. Alyea and M.A. Keane, J. Catal, 164 (1996) 28.

10   M.C. Kung and H.H. Kung, J. Catal, 128 (1991) 287.

11   S. Hocine, C. Rabia, M.M. Bettahar and M. Fournier, Studies Surf. Sci. Catal, 130 (2000) 1895.

12   K. Weissermel and H.-J. Arpe, Industrial Organic Chemistry, 3rd Ed. p. 345.

13   J. Blomberg, P.J. Schoenmakers and U.A. Th. Brinkman, J. Chromatogr. A, 972 (2002) 137.

14   K. Nishi, S. Komai, K. Inagaki, A. Satsuma and T. Hattori, Appl. Catal.

A: Gen, 223 (2002) 187.

15   J.H. Sinfelt, J. Mol. Catal. A: Chem, 163 (2000) 123.

16   D.W. Blakely, G.A. Somorjai, J. Catal, 42 (1976) 181.

17   J.A. Rodriguez, C.T. Campbell, J. Phys. Chem, 93 (1989) 826.

18   M.E. Bussell, F.C. Henn, C.T. Campbell, J. Phys. Chem, 96 (1992) 5978.

19   C. T. Campbell, J. A. Rodriguez, F. C. Henn, J. M. Campbell, S. G. Seimanides, J. Chem. Phys, 88 (1988) 6585.

20   C. T. Campbell, Crit. ReV. Surf. Chem, 3 (1994) 49.

21   M.A. Newton, C.T. Campbell,J. Phys. Chem, 198 (1997)169.

22   C.L.A. Lamont, M. Borbach, W. Stenzel, H. Conrad, A.M. Bradshaw, Chem. Phys. Lett, 230 (1994) 265.

23   C.L.A. Lamont, M. Borbach, R. Martin, P. Gardner, T.S. Jones, H. Conrad, A.M. Bradshaw, Surf. Sci, 374 (1997) 215.

24   C.L.Pettiette-Hall, D.P. Land, R.T. McIver, J.C. Hemminger, J. Am. Chem. Soc, 113 (1991) 2755.

25   D.P. Land, C.L. Pettiettehall, R.T. McIver, J.C. Hemminger, J. Am. Chem. Soc, 111 (1989) 5970.

26   D.P. Land, W. Erley, H. Ibach, H. Surf. Sci, 289 (1993) 237.

27   R. Raval, M.A. Chesters, Surf. Sci, 219 (1989) L505.

28   C. Xu, Y.L. Tsai, B.E. Koel, J. Phys. Chem, 98 (1994) 585.

29   B.E. Koel, D.A. Blank, E.A. Carter,J. Mol. Catal. A: Chem, 131 (1998) 39.

30   L.Q. Jiang, B.E. Koel, J. Phys. Chem. Lett, 96 (1992) 8694.

31   D.H. Parker, C.L. Pettiettehall, Y.Z. Li, R.T. McIver, J.C. Hemminger, J. Phys. Chem, 96 (1992) 1888.

32 N. Sheppard, Annu. ReV. Phys. Chem, 39 (1988) 589.

33 Ann W. Grant, Lien T. Ngo, Karsten Stegelman, and Charles T. Campbell, J. Phys. Chem. B, 107 (2003) 1180.

34 Don A. Perry and John C. Hemminger, J. Am. Chem. Soc, 122 (2000) 8079.

35 F. Tiscareno-Lechuga, C.G. Hill, and M.A. Anderson, App. Catal, 96 (1993) 33.

36 P.A. Terry, M. Anderson and I. Tejedor, J. Porous Mater, 6 (1999) 267.

37 R. Gomez, T. Lopez, V. Bertin, R. Silva, P. Salas and L. Schifter, J. Sol-Gel Sci. Tech, 8 (1997) 847.

38 Pal Tetenyi ans Victor Galsan, React. Kinet. Catal. Lett, 70 (2) (2000) 265.

39 Xingcai Su, Jouko Lahtinen and Gabor A. Somorjai, Catal. Lett, 54 (1998) 9.

40 J.L. Gland, K. Baron and G.A. Somorjai, J. Catal, 36 (1975) 305.

41 L.E. Firment and G.A. Somorjai, J. Chem. Phys, 66 (1977) 2901.

42 D.W. Blakely and G.A. Somorjai, J. Catal, 42 (1976) 181.

43 C.E. Smith, J.P. Biberian and G.A. Somorjai, J. Catal, 57 (1979) 426.

44 J.A. Rodriguez and C.T. Campbell, J. Phys. Chem, 93 (1989) 826.

45 C.T. Campbell et al., J. Phys. Chem, 93 (1989) 806.

46 J.M. Campbell, S. Seimanides and C.T. Campbell, J. Phys. Chem, 93 (1989) 815.

47 J.W. Peck and B.E. Koel, J. Am. Chem. Soc, 118 (1996) 2708.

48 C.L. Petettiette-Hall et al., J. Am. Chem. Soc, 113 (1991) 2755.

49 J.E. Demuth, H. Ibach and S. Lehwald, Phys. Rev. Lett, 40 (1978) 1044.

50   Hidefumi Amano, Satoshi Sato, Ryoji Takahashi and Toshiaki Sodesawa, Phys. Chem. Chem. Phys, 3 (2001) 873.

Chapter 8

PHOTOCATALYSIS

Introduction and Literature Survey

Abstract

For the passed few years, research activities in the domain of photocatalysis have acquired a strong momentum. Today photocatalysis is regarded as a key technology, and consequently gives rise to research programmes and application developments in the world over. This established research methodology provides the framework for a broader outline of research into enhancement of indoor air quality via photocatalytic oxidation. As an "environmentally harmonious catalyst", titania photocatalysts have been some of the most actively investigated catalysts for applications in systems that can effectively address environmental pollution. The potential for the effective utilization and conversion of solar energy makes research into the modifications of the electronic properties of TiO_2 photo catalysts which are able to absorb and operate efficiently even under visible light irradiation. One of its main advantages is to make it possible to obtain complete mineralization of pollutants while not degrading the environment.

8.1 General Introduction

Heterogeneous photocatalysis has been intensively examined from both fundamental and practical perspectives especially in environmental remediation scenarios in recent years [1-3]. In 1972, Fujishima and Honda discovered the photocatalytic splitting of water on TiO_2 electrodes[4] and this event marked the beginning of a new era in heterogeneous photocatalysis. Since then, research efforts in understanding the photocatalytic efficiency of TiO_2 have come from extensive research performed by chemists, physicists, and chemical engineers. Such studies are often related to energy renewal and energy storage[5-9]. In recent years application to environmental clean up have been one of the most active areas in heterogeneous photocatalysis. This is inspired by the potential application of TiO_2 based photocatalysts for the destruction of organic compounds in polluted air and in wastewaters [10-11]. In addition, the discovery of Q-particles have turned the whole field in a new direction such that one can now think of reduction of CO_2 to various products like HCHO, HCOOH, CH_3COOH and CH_4.

Photocatalysis is a direct quantum conversion process and has been investigated for utilizing solar energy to produce value added chemicals[12]. Photochemical processes in heterogeneous systems have gained wide popularity in recent years because of their wide applications in xerography, photography, chemical synthesis, conversion and storage of solar light energy. Of particular interest are the photochemical processes on inorganic oxide surfaces. The surface as well as the intrinsic properties of the support material play an important role in influencing the course of a photochemical reaction[13]. The support materials, which can control the photochemical

behavour of an adsorbed substrate, can be broadly classified into two categories;

- ⋗ Nonreactive surfaces, such as silica or alumina which provide an ordered two dimensional environment for effecting and controlling the photochemical processes more efficiently than can be attained in homogeneous solutions.

- ⋗ Reactive surfaces, such as titania or metal chalcogenides, which directly participate in photochemical reactions by absorbing the incident photon and transferring the change to an adsorbed molecule or by quenching the excited state of the adsorbed molecule.

In a heterogeneous photocatalysis system, photoinduced molecular transformations or reactions take place at the surface of a catalyst[14]. Photocatalysis on a semiconductor powder is essentially a redox reaction. During a photocatalytic reaction, the irradiated surface of the semiconductor will act as a sink for the electrons (or holes) depending upon the direction of band bending. The other charge carrier will move under the influence of the electric field into the bulk of the semiconductor or to the surface that receives the lowest intensity of incident radiation. Thus, the separation of the charge carriers namely the electrons and the holes determines the efficiency of the photocatalytic reaction. Sometimes effective charge separation can be achieved by metallisation, doping or by coupling two semiconductors. The photoreactivity of the doped semiconductors appears to be a complex function of the dopant concentration, the energy level of the dopants, their oxidation states and the type of defects created in the host lattice.

A thorough and meticulous understanding of the photocatalytic processes will be necessary for the development and design of highly reactive photocatalysts, especially since such systems are to be applied to dilute concentrations of toxic reactants in the atmosphere and water on a huge global scale[15]. The preparation of well defined photocatalysts is necessary in order to identify and clarify the chemical features of the photo formed electrons and holes, to detect the reaction intermediate species and their dynamics, and to elucidate the reaction mechanisms at the molecular level, which in turn would necessitate a detailed and comprehensive investigation of the photogenerated active sites and the local structures[16-31]. Photocatalytic engineering is under development, now using deposited titania in a fixed bed. Some (solar) photocatalytic pilot reactors and prototypes are described. The use of solar energy as a source of activating UV irradiation is described as a sub discipline called "helio-photocatalysis"

8.2 Background on Photocatalysis

Photocatalysis and related phenomena are now well known and well recognized. Biogenic photocatalytic phenomena, such as those occurring in natural photosynthesis, have been known since prehistoric times and this without any knowledge of the intrinsic chemical mechanisms of plant growth. Abiogenic photocatalytic phenomena were recognized since the initial studies on photochemical phenomena. The term "photocatalysis" was introduced as early as the 1930s, if not sooner. Since then, this term has been used often in the scientific literature. The early workers saw no need to address the nomenclature until the field had matured enough. Nonetheless, the term was

taken to represent that field of chemistry that focused on catalytic reactions taking place under the action of light. Consequently, the totality of the phenomena related to both photochemistry and catalysis was considered to belong to the field of photocatalysis. Such phenomena seemed rather *exotic* and of interest only to a narrow group of specialists. Recent interest and studies in environmental photochemistry, in natural photosynthesis and in chemical methods for solar energy transformations has contributed greatly to our knowledge and understanding of the various phenomena related to both photochemistry and catalysis. Many of these phenomena differ qualitatively by their nature and, generally speaking, are often found in different fields of chemistry. For example, it is possible to distinguish such phenomena as catalyzed photochemical reactions, photoactivation of catalysts, and photoactivated catalytic processes, among several others.

Water splitting, photofixation of nitrogen, photoreduction of carbon dioxide and many other reactions do not occur on illumination with light alone. These reactions often require the use of Photocatalysts - a term that implies photon assisted generation of catalytically active species. The role of photons is to generate catalysts or electron-hole pairs in the case of semiconductor materials that yield fuels or chemicals in subsequent dark reactions.

Organic chemicals, which may be found as pollutants in wastewater effluents from industrial or domestic sources, must be removed or destroyed before discharge to the environment. Such pollutants may also be found in ground and surface waters, which also require treatment to achieve acceptable drinking water quality[31]. The increased public concern with these environmental pollutants has prompted the need to develop novel treatment

methods[32] with photocatalysis gaining a lot of attention in the field of pollutant degradation.

Much of the natural purification of aqueous system lagoons, ponds, streams, rivers and lakes is caused by sunlight initiating the break down of organic molecules into simpler molecules and ultimately to carbon dioxide and other mineral products. There are various natural sensitizers that accelerate the process. The utilization of colloidal semiconductors and the introduction of catalysis to promote specific redox processes on semiconductor surfaces were developed in 1976[33]. Since then, laboratory studies have confirmed that naturally occurring semiconductors could enhance this solar driven purification process[34].

The photocatalytic detoxification of wastewater is a process that combines heterogeneous catalysis with solar technologies. Semiconductor photocatalysis, with a primary focus on TiO_2 has been applied to a variety of problems of environmental interest in addition to water and air purification. The application of illuminated semiconductors for degrading undesirable organics dissolved in air or water is well documented and has been successful for a wide variety of compounds[35]. Organic compounds such as alcohols, carboxylic acids, amines, herbicides and aldehydes have been photocatalytically destroyed in laboratories and field studies. The photocatalytic process can mineralize the hazardous organic chemicals to carbon dioxide, water and simple mineral acids[36].

An important advantage of the photocatalytic process is that when compared to other advanced oxidation technologies, especially those using oxidants such as hydrogen peroxide and ozone, expensive oxidizing chemicals

are not required as ambient oxygen is the oxidant[36]. Photocatalysts are also self regenerated and can be reused or recycled. The solar photocatalytic process can be applied to destroy nuisance ordour compounds and naturally occurring organic matter, which contains the precursors to trihalo methanes formed during the chlorine disinfection step in drinking water treatment[37].

During the photocatalytic process, the illumination of a semiconductor photocatalyst with ultraviolet radiation activates the catalyst, establishing a redox environment in the aqueous solution[38]. Semiconductors act as sensitizers for light induced redox processes due to their electronic structure characterized by a filled valence band and an empty conduction band. The energy difference between the valence and conduction bands is called the band gap. The semiconductor photocatalyst absorbs impinging photons with energies equal to or higher than its band gap or threshold energy. Each photon of the required energy that hits an electron in the occupied valence band of the semiconductor atom can elevate that electron to the unoccupied conduction band leading to the excited state conduction band electron and positive valence band holes.

8.3 Definition of Photocatalysis

Some attempts were made in the past to determine the term "photocatalysis". Indeed, one of the IUPAC Commissions defined photocatalysis as "a catalytic reaction involving light absorption by a catalyst or a substrate"[39-40]. In a later revised glossary[40] a complementary definition of a photo-assisted catalysis was also proposed: "catalytic reaction involving production of a catalyst by absorption of light". Germane to the present discussion, an earlier Compendium of Chemical Terminology[41] described the

notion of catalysis and a catalyst as follows: "Catalysis is the action of a catalyst"; and a "Catalyst is a substance that increases the rate of reaction without modifying the overall standard Gibbs energy change in the reaction". Both of these descriptions are less than satisfactory as they lack some, if not many, of the details of the catalytic process. Addition of the extra reactant, namely light, inserts an extra dimension to an otherwise complex issue. An overview of some approaches in describing photocatalytic phenomena was given in a paper[42]. It is germane in this context to revisit this overview to attain a better appreciation and understanding of the complexity (ies) of photocatalysis, particularly heterogeneous photocatalysis.

Unlike the earlier terminology[41], it is relevant to recall that catalysis refers simply to a process in which a substance (the catalyst) accelerates, through intimate interaction(s) with the reactant(s) and concomitantly providing a lower energy pathway, an otherwise thermodynamically favored but kinetically slow reaction with the catalyst fully regenerated quantitatively at the conclusion of the catalytic cycle. When photons are also involved, the expression photocatalysis can be used to describe, without the implication of any specific mechanism, as the acceleration of a photoreaction by the presence of a catalyst. The catalyst may accelerate the photoreaction by interacting with the substrate(s) either in its ground state or in its excited state or with the primary product (of the catalyst), depending on the mechanism of the photoreaction [43]. The latter description is silent as to whether photons also interact with the catalyst. Such a description also embraces photosensitization[44] and yet such a process, defined officially[45] as a process whereby a photochemical change occurs in one molecular entity as a result of initial

photon absorption by another molecular species, known as the photosensitizer, is not necessarily catalytic without assessing a turnover quantity and/or the quantum yield. The issue rests entirely on the role of the photons. Chanon and Chanon[46] suggested that the non-descriptive term photocatalysis be taken simply as a general label to indicate that light and a substance (the catalyst or initiator) are necessary entities to influence a reaction[47]. Such a broad description indicates the required reagents without undue constraints as to the (often unknown) mechanistic details of the chemical process .
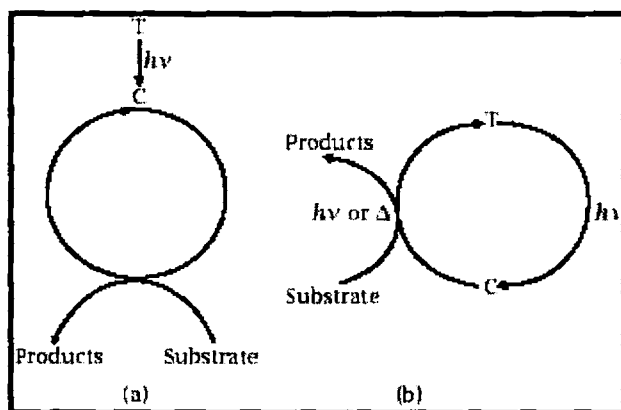
$$\text{Substrate} + \text{light} + \text{Catalyst} \rightarrow \text{Products} + \text{Catalyst}$$

Figure 8.1(a) Simple scheme of photogenerated catalysis

Figure 8.1(b) depicts an example of catalyzed photolysis.

In the early 1980s, Salomon[48] proposed that the broad description of photocatalysis be subdivided into two main classes: (i) photogenerated catalysis, which is catalytic in photons, and (ii) catalyzed photolysis, which is non-catalytic in photons .In photogenerated catalysis, ground states of the

catalyst and of the substrate are involved in the thermodynamically spontaneous (exoergic) catalytic step. By contrast, in catalyzed photolysis either the nominal catalyst T (Figure 8.1) or the substrate or both are in an excited state during the catalytic step.

8.4 Photocatalysis on Titania

Titanium dioxide, that stolid industrial mainstay has an alter ego. The continuing interest in such oxides originates from the fact that TiO_2 is an excellent catalyst for oxidizing a large variety of organic substances [49-50]. The capacity of titania to completely oxidize many toxic substances to form non-toxic compounds distinguishes it as being the most promising material for the photo detoxification of contaminated water. TiO_2, it appears has seemingly limitless potential under even indoor room light to break down organics in not only trivially annoying things like bad breath, but more dangerous contaminants, such as cigarette smoke.

In the eyes of chemical engineers, TiO_2 is an ideal substance for mass use. The semiconductive properties of titania are strongly dependent on its crystalline structure, non stoichiometry and doping procedure. Stoichiometric titania is a dielectric material; however it exhibits semiconductor properties when its stoichiometry is altered. Therefore large TiO_2 crystallites are not useful for photocatalysts [51].In spite of this vigorous activity and the search for the "ideal" photocatalyst for more than two decades, titania has remained as a benchmark against which any emerging material candidate will be measured. Attributes of an ideal photocatalyst[52] in a heterogeneous photocatalysis system for solar applications are.

♦ Stability and sustained photocatalytic activity.

♦ Good overlap of absorption cross-section with solar spectrum.

♦ High conversion efficiency and quantum yield.

♦ Compatibility with a variety of substrates and reaction environments.

♦ Low cost.

♦ Non-toxic.

A key characteristic of titanium dioxide is its high surface area, which allows the rate of reaction to increase, as the efficiency of a photocatalyst is proportional to its surface area. Despite the positive attributes of TiO_2 as an ideal photocatalyst, there are some drawbacks associated with its use; (i) charge carrier recombination occurs within nanoseconds, and (ii) the band edge absorption's threshold of TiO_2 is < 400nm[53]. To circumvent these two limitations, a number of strategies have been proposed to improve the light absorption features and lengthen the carrier lifetime characteristics of TiO_2. Titania's propensity for oxidation when exposed to light has been known for sometime. To show full catalytic potential, TiO_2 requires both oxygen and water, both of which are abundant in air. Photons impinging on titania dislodge electrons, creating holes and free electrons. The holes and free electrons oxidize water and oxygen respectively to form hydroxyl as superoxide radicals, both ruthless bond cleavers. Two different crystal structures of titania, rutile and anatase, are commonly used in photocatalysis with anatase showing a higher photocatalytic activity[54]. The structures of rutile and anatase can be described in terms of chains of TiO_6 octahedra. The two crystal structures differ by the distortion of each octahedron and by the assembly pattern of the octahedra chains. These differences in the lattice structures cause different

mass densities and electronic band structures between the two crystalline forms. Irradiation of TiO_2 using low energy UV radiation ($\lambda > 400nm$) promotes an electron from the valence band (VB) to the conduction band (CB), making it available for the transfer, while the positive equivalent, the hole (h^+) in the valence band is ready to accept an electron from the substrate (Figure 8.2) [55].
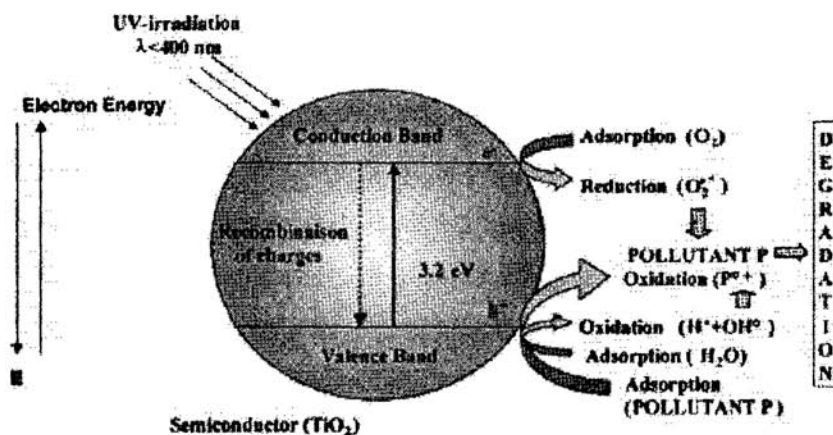

Figure 8.2 Energy band diagram of spherical titania particles.

A titania photocatalyst has outstanding hydrophilicity and durability, making it exceptionally well suited as a material for applying a hydrophilic treatment to outside mirrors. Irradiating titania with light having a wavelength of less than 380 nm produces photocatalytic reactions on the surface of titania, causing adsorbed organic matter to oxidize and decompose. The strong hydrophilicity shown by the titania film under irradiation by ultraviolet light is thought to stem from the exposure of a pristine surface following the decomposition of hydrophobic surface compounds.

8.5 Enhanancement of Photoactivity of titania

Metal modified titania systems have been extensively studied even in the early days of photoelectrochemistry/photocatalysis[56-57], although the reported results have been conflicting. Three main consequences of metal modification of TiO_2 can be distinguished; (a) induction of visible light photoresponse in the host material, (b) suppression (or in some cases enhancement) of carrier (electron-hole) recombination as a result of new states introduced in the band gap of TiO_2 by these dopants (c) generation of catalytic sites on the TiO_2 surface that serve to store electrons for subsequent transfer to acceptor species in the solution. Transition metal doping can expand the responsiveness of suspended metal oxide particles to the visible[58-66]. On such doped materials, enhanced photocatalytic activity for the reduction of CO_2 and N_2 [67-68] has been reported. Enhancement in the rate of photoreduction upon metal ion loading of the semiconductor can produce a photocatalyst with an improved trapping to recombination rate ratio. This effect seems to be sensitive to the dopant level. Therefore, significantly decreased activity has also been described as resulting from doping and the effects of transition metal ion dopants are understandably somewhat difficult to generalize for all systems. Some transition metal dopants[69-70], such as Fe^{3+} and V^{4+} inhibit e^-/h^+ pair recombination, while others such as Cr^{3+} are detrimental to the photocatalytic efficiency of the semiconductor.

A new outside mirror with enhanced rearward visibility on a rainy day has been developed using a TiO_2-SiO_2 coating on the glass base. Prepared by the sol-gel process, the coating spreads out rain droplets on the mirror surface into a thin film of water by a photocatalytic hydrophilic effect in the TiO_2-SiO_2.

This mirror maintains its good hydrophilicity for a long time, and when hydrophobic contaminations collect on the glass surface, the suns radiation induces a photocatalytic effect that serves to decompose the contaminations[71]. Furthermore, the new mirror has sufficiently high durability for use in the severe automotive environment.
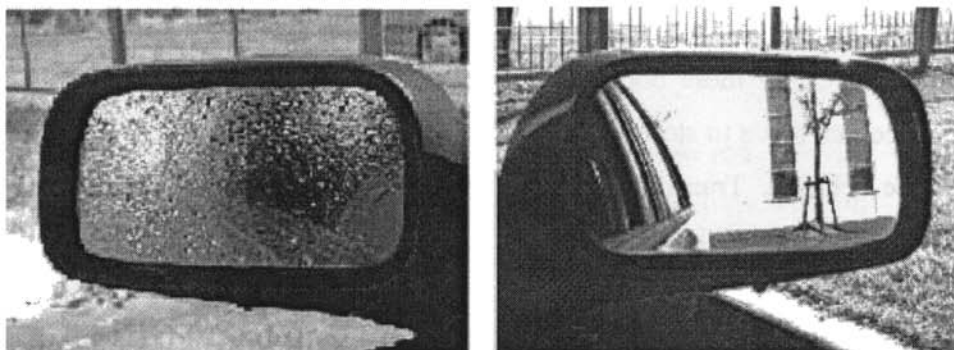

Figure 8.3 Hydrophilic outside mirror (right)

Photocatalytic enhancement can also be induced by derivatizing the TiO_2 surface with organic substances[72]. Photocatalytic reactions on semiconducting TiO_2 photocatalysts were shown to be remarkably enhanced by the addition of small amoints of noble metal such as Pt. Such an enhancement in the photocatalytic reactivity has been explained in terms of photoelectrochemical mechanism in which the electrons generated by the UV irradiation of the TiO_2 semiconductor quickly transfer to the Pt particles loaded on the TiO_2 surface. These Pt particles work to effectively enhance the charge separation of the electrons and holes, resulting in marked improvement in photocatalytic performance. Recent time resolved spectroscopic investigations clearly

indicate the important role of Pt particles in the dynamics of such photoformed charge carriers[73-76]. Ways of improving the photocatalytic activity of titania[77] is shown schematically in figure 4.
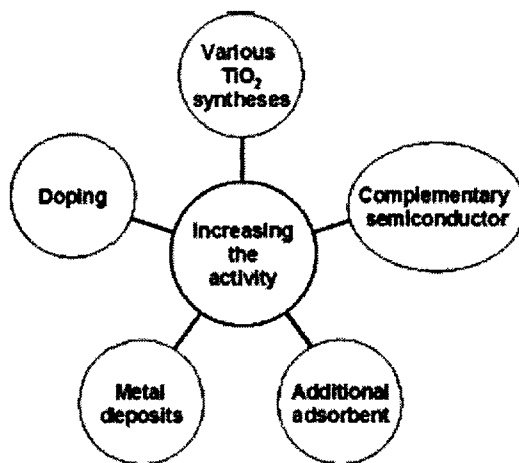
Figure 8.4

Ways of improving TiO_2 photocatalytic activity.

8.6 Quantum size effects

Semiconductor particles, which exhibit size dependent optical and electronic properties, are termed as quantized particles (Q particles) or semiconductor clusters[78]. Quantum size effects occur for such particles on the order of 10-100A° in size. The anomalies arise when the size of the semiconductor particles become comparable to the de Broglie wavelength of the charge carriers in the semiconductor[79-80]. The phenomenon of quantum size effect is due to electronic modification of the photocatalysts as well as the close existence of the photo formed electron and hole pairs and their efficient contribution to the reaction, resulting in a performance much enhanced over

that of semiconducting titania powders. The range of size for particles experiencing this effect is therefore dependent on the effective mass for the Q-particle semiconductor. These findings have provided us with new insights into photocatalysts such as highly dispersed titanium dioxide.

Kormann *et al* estimated the excitation radii for titania particles to be between 7.5 and 19 A°. The exciton radii were computed by using various literature values and calculated by the equation put forward by Brus[81]. Graztel[82] estimated an excitation radius of ~3A°. Quantization effect is also reported with 20-40A° titania particles. This effect is observed during the particle growth and at the final stage of synthesis of these transparent colloids. The electron and the hole produced in Q-partcles are confined in a potential well of small geometrical dimensions. The electron and the hole do not experience the electronic delocalization present in the bulk semiconductor possessing a conduction band and the valence band. Instead the confinement produces a quantization of discrete electronic states and increases the effective band gap of the semiconductor. Such effects can change the color of the material (due to the altered optical absorption maxima) and the photocatalytic properties. The increase in effective band gap and consequently the blue shift in the absorption threshold can become quite dramatic for bulk semiconductors with very small band gaps. While photocatalyst particles have not reached Q-particle sizes yet, it can be expected that this may happen in the future as new materials are produced.

When considering semiconductors other than titania, many reports have observed quantum size effects with many different particles. For example, CdS and PbS a few nanometers in size have been found to exhibit quantum

mechanical effects. Quantization effects have also been demonstrated with nanoclusters of hexagonal MoS_2 and several of its isomorphous Mo and W chalcogenides[83].

8.7 Literature Survey

	Systems	Reactions investigated	Remarks
1	TiO_2	Degradation of the herbicide cinosulfuron[84].	Degradation leads to the formation of CO_2, NO_3^- and SO_4^{2-} as final products and in addition cyanuric acid.
2	TiO_2	Oxidation of methyl orange aqueous solution[85]	Powdered TiO_2 showed higher photoactivity when irradiated under visible light.
3	TiO_2	Degradation of acid blue 9[86].	Dye decolourisation could be explained by the one dimensional diffusion model with a first order reaction.
4	TiO_2	Degradation of sulfonyl urea herbicide, prosulfuron[87].	Synthesis of titania by the molten salt method also is an effective photocatalyst.
5	TiO_2	Dichlorvos degradation to	A new approach to the

		dimethyl phosphate, which further reacted to form monomethyl phosphate, which was hydrolysed to phosphate. The reaction can be traced using ^{31}P NMR[88].	study of phosphorus containing products resulting from organophosphurus pesticide degradation.
6	TiO$_2$	Degradation of a textile dye, methylene blue in presence and absence of common inorganic salts[89].	The degradation follows the first order kinetics.
7	TiO$_2$	Destruction of 17 VOCs, which include alkanes, chlorinated alkanes, alkenes, ketones, alcohols, ethers, aromatic compounds, acetals and nitrogenated compounds[90].	The results strengthen the potential use of heterogeneous photocatalysis in the abatement of different classes of VOC's.
8	TiO$_2$	Degradation of methylene blue[91].	Degradation rate depends on both the specific surface area and the crystallinity of nanostructured titania film.
9	TiO$_2$	Oxygenation of naphthalene[92]	The reaction involves transfer of a hydroxy group to naphthalene and

			reduction of oxygen to super oxide followed by coupling of the two species.
10	TiO_2	Oxidation of naphthalene[93]	TiO_2 consisting of anatase and rutile crystalline phases efficiently catalyses the oxidation whereas pure anatase or rutile is ineffective.
11	TiO_2	Destruction of microcystins[94].	The pH dependence of microcystin destruction can be associated with changes to surface charge of the photocatalyst as well as altered hydrophobicity and net charge on the toxin.
12	TiO_2	Degradation of 3-nitro acetophenone[95].	The reaction follows a first order kinetics.
13	TiO_2	Degradation of anionic dyes like Alizarin S, azo methyl red, congo red, Orange G and cationic dyes like methylene blue[96].	The reaction occurs in the adsorbed phase at the surface of titania and not in the solution. The degradation rate is influenced by the chemical

			structure of different dyes as well as that of pH and of the presence of inorganic salts.
14	TiO_2	Oxidation of toluene at room temperature[97].	Temperature programmed hydrogenation was effective at hydrogenating the strongly bound intermediates formed during toluene oxidation.
15	TiO_2	Oxidation of toluene in the gas phase[98].	CO_2 is the main oxidation product and benzaldehyde is the stable intermediate in the photooxidation of toluene. FTIR spectra of the catalyst reveals the fact that benzaldehyde originates from toluene adsorbed on isolated hydroxyls.
16	TiO_2	Photocatalyzed epoxidation of 1-decene by H_2O_2 under visible light[99].	The selectivity of the production of 1,2-epoxydecane was higher under visible light than under uv light.

17	TiO$_2$	Oxidation of toluene[100].	Competetive adsorption of water and toluene on Titania samples confirm that titania has a highly elctrophilic surface.
18	TiO$_2$	Photosensitized oxidation of benzyl derivatives in aqueous media[101].	The single electron transfer process from the substrate to the photogenerated hole occurs.
19	TiO$_2$	Photocatalytic interconversion of nitrogen containing benzene derivatives[102].	The redox reactions at the nitrogen containing substituent have an important role than the hydroxylation of aromatic ring, which was the predominant degradation pathway for most of the other aromatic compounds.
20	TiO$_2$	Photodegradation of 1,4-dichloro benzene[103].	The volatile precursors result in the formation of titanium oxide samples, which exhibit a high photocatalytic activity.
21	TiO$_2$	Oxidation of Ethylene with O$_2$ to CO$_2$ and H$_2$O[104].	The large surface area of the photocatalysts is one of

			the most important factors in achieving a high efficiency of the reaction.
22	TiO_2	Photocatalytic decomposition of acetic acid[105]	Two parallel pathways leading to the formation of different products.
23	TiO_2	Photocatalytic degradability of substituted phenols[106]	Photoactivity affected by both electronic character and by the position of substituents in the aromatic ring. -
24	TiO_2 (Degussa P-25 and Millennium PC-500)	Oxidation in aqueous phase of imazapyr, a schematic herbicide characterized by its persistence and mobility in soils[107].	Higher photocatalytic efficiency of Millennium PC-500, together with its composition of anatse nanocrystallites was expected to overcome the adsorption and interfacial processes limitations with Degussa P-25.
25	Mesoporous TiO_2	Photodecomposition of cationic dye X-GL in aqueous solution[108].	High photocatalytic activity could be due to its larger BET surface area and mixed crystal containing 21.5% brookite

			and 78.5% anatase.
26	Nitrogen N_2 substituted TiO_2	Undergo hydrophilic conversion under visible light irradiation[109].	Hydrophilicity was enhanced by increasing the degree of nitrogen substitution at oxygen sites leading to an increase in the absorbed photon numbers.
27	N_2 doped TiO_2	Photocatalytic degradation of three azodyes (Acid orange 7, Procion red MX-5B and Reactive Black 5)[110]	High reactivity under visible light allowing more efficient usage of solar energy.
28	TiO_2/Hβ	Destruction of monochrotophos pesticide[111].	Higher activity is due to the capability of support to delocalise the conduction band electrons of excited titania.
29	Nd^{3+} modified TiO_2 hydrosol	Degradation of active brilliant red Dye X-3B[112].	Higher photocatalytic activity was ascribed due to the electron trapping effect of modified Nd^{3+} ion on TiO_2 sol particles.
30	Nd^{3+} doped titania	Effect of dopant on the anatase-rutile phase	Distortion along the c-axis of anatase titania is due to

		transition[113]	the combination of interstitial as well as substitutional accommodation of the dopant ions.
31	Ta on TiO_2	To study the influence of oxygen upon the electrical properties of titania films doped with Ta[114].	Electrical conductivity decreased significantly by introducing oxygen.
32	Ln_2O_3 doped TiO_2	Degradation of Salicylic acid and t-Cinnamic acid[115]	Complete mineralisation has been achieved in the case of lanthanide oxide doped TiO_2 in total contrast to the formation of intermediates in case of nonmodified TiO_2.
33	TiO_2-SiO_2	Decomposition of acetaldehyde in air[116]	The nanoscale combination of crystalline titania and mesoporous silica particles was successfully applied as a photocatalytic adsorbent for the rapid removal from air and complete decomposition of organic molecules.

34	TiO_2-SiO_2 aerogels	Removal of benzene in air[117].	The samples possess excellent benzene adsorption capacities and the adsorbate could be decomposed to CO_2 by photocatalytic degradation.
35	$TiO_2 - WO_3$	Study the energy storage of the composite photocatalysis system in gas phase[118].	Reductive energy generated at a TiO_2 photocatalyst under UV light can be stored in WO_3 by coupling them together, and the stored energy can be used after dark.
36	TiO_2/Cr_2O_3	Photoelectrolytic decomposition of water[119].	Promising candidate for photoanodes.
37	TiO_2, Pt/TiO_2, WO_3/TiO_2	Vapour phase degradation of butyl acetate[120].	Photocatalytic degradation is improved because of the prevention of initial deactivation and of photogenerated charge recombination.
38	TiO_2/$ZnFe_2O_4$ nanocomposite	Degradation of Phenol[121]	Inhibit anatase - rutile transformation. Also the nanocomposite is a promising solar energy

			material for applications in photocatalysis as well as in photoelectrochemical conversion.
39	SnO_2/ TiO_2 solar cell	Study of the photoelecrochemical behaviours of eosin Y-sensitized nanostructured coupled SnO_2/ TiO_2 solar cell[122].	The coupled film can be utilized to fabricate a low cost solar cell.
40	TiO_2 impregnated with functionalised Cu(II)-porphyrin or Cu(II)-pthalocyanin	Degradation of 4-Nitrophenol[123]	The presence of sensitizers is beneficial for the photoactivity and suggest an important role of Cu (II).
41	Fe^{III}-doped TiO_2	Photocatalyzed oxidation of methanol in aqueous solution[124].	The formation of formaldehyde is tentatively attributed to the conditions of particle growth more favourable in this novel preparation method.
42	Surfactant/	Photodegradation of a	The degradation proceeds

	TiO_2	cationic dye, malachite green[125].	at the semiconductor particle ssurface rather than in the bulk solution, ˙OH active species are generated and participates in the photodecomposition reaction.
43	TiO_2 modified with Ca, Sr or Ba ion additives.	Photocatalytic decomposition of oxalic acid[126]	The additives have a profound influence on the photocatalytic activity.
44	TiO_2 - PVP	Degradation of methylene red[127]	Higher efficiency in the transportation of photo induced electrons and holes in the photocatalyst and therefore a higher photoactivity.
45	TiO_2	Decomposition of 2,4-Dinitroaniline[128].	The photoactivity in the decomposition of 2,4-Dinitroaniline depends on the E_g and on the crystalline phases.
46	TiO_2	Destruction of Catechol[129].	Full catechol mineralisation is a multistep reaction with

47	CuO/TiO$_2$	Photocatalytic reduction of NO[130].	1,2,4-benzene triol and glycol as the intermediates. The increase of NO reaction rate increases with increasing CuO loading upto an optimum value and then decreases.

8.8 Photocatalysis; Views and Prospects

Many studies have been carried out with the aim of developing models of practical interest or attaining more refined understanding of the functioning of the photocatalyst. The development and application aspects of various semiconductor particulate models in heterogeneous photocatalysis constituted primarily the common aim of achieving efficient charge separation. The entry of nanosize semiconductor catalysts in heterogeneous photocatalysis has been addressed. The expanding area of the field of photocatalysis especially for applications in organic chemistry, light images, metallic patterns and pollution treatments, however makes us to believe the prospect of wide applicability of photocatalysis. The areas of applications of photocatalysis to water purification and treatment of water, area selective reactions polymer degradations and selective organic synthesis will probably gain priority as they appear to possess the potential to alter environmental and electronic scenarios.
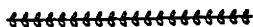
References

1   N. Serpone and E. Pelizzetti. Photocatalysis: Fundamentals and applications, Wiley Interscience, New York (1989).

2   M. Schiavello (Ed.). Heterogeneous photocatalysis, Wiley, Chichester (1997).

3   K. Rajeshwar and J.G. Ibanez. Environmental Electrochemistry, Academic, San Diego (1997).

4   A. Fujishima and K. Honda, Nature, 37 (1972) 238.

5   A.J. Bard, J. Phys. Chem., 86 (1982) 172; J. Photochem., 10 (1979) 59; Science, 207 (1980) 139.

6   M. Gratzel, Ed. Energy resources through Photochemistry and catalysis, Academic Press, New York (1983).

7   K.Kalyanasundaram, M.Gratzel, E.Pelizzetti, Coord.chem.Rev., 69 (1986) 57.

8   V.N. Parmon, K.I. Zamareav, In Photocatalysis-Fundamentals and Applications; N. Serpone, E. Pelizzetti, Eds, Wiley Interscience, New York (1989) 565.

9   E. Pelizzetti and M. Schiavello, Eds, Photochemical conversion and storage of solar energy; Kluwer Academic Publishers; Dordrecht (1991).

10   M. Schiavello, Ed., Photocatalysis and Environment. Kluwer Academic Publishers, dordrecht (1988).

11   D.F. Ollis, H. Al-Ekabi, Eds, Photocatalytic purification and treatment of water and air, Elseveir, Amsterdam (1993).

12   N. Nageswara Rao and P. Nagarajan, current science, 66(10) (1994)

13   Prashant V. Kamat, Chem.Rev, 93 (1993) 267.

14   Amy L. Linsebigler, Guangquan Lu and John. T. Yates, Chem. Rev, 95 (1995) 735.

15   Masakazu Anpo and Masato Takeuchi, J. Catal, 216 (2003) 505.

16   G. Calzaferri (Ed.), Solar Energy Materials and Solar Cells, in; Procceedings of the 10th International Conference on Photochemical Transfer and Storage of Solar Energy, Elsevier, Amsterdam (1995).

17   M. Anpo, Surface Phitochemistry, Wiley, Chichester, (1996).

18   Y. Kubokawa, K. Honda, Y. Saito, Hikarishokubai - Photocatalysis A Sakura-shoten, Tokyo, (1988).

19   M. Anpo, (Ed.), Photofunctional Zeolites, Nova (2000).

20   M. Anpo, S. Higashimoto, S. Tud, Surf. Sci. Catal, 135 (2001) 123.

21   A. Corma, Chem Rev, 97 (1997) 2373.

22   T. Maschmeyer, F. Rey, G. Sankar, J.M. Thomas, Nature, 378 (1995) 159.

23   K.I. Zamaraev, J.M. Thomas, Adv. Catal, 41 (1996) 335.

24   S. Bordiga, S, Coluccia, C. Lamberti, L. Marchese, F. Boscherini, F. Buffa, F. Genoni, G. Leofanti, G. Petrini, G. Vlaic, J. Phys, Chem, 98 (1994) 4125.

25   L. Marchese. T. Maschmeyer, E. Gianotti, S. Coluccia, J.M. Thomas, J. Phys. Chem. B, 101 (1997) 8836.

26   C.Lamberti, S.Bordiga, D.Arduino, A.Zecchina, F.Geobaldo, G.Span, F.Genoni, G.Petrini, A.Carati, F.Villain, G.Vlaic, J. Phys. Chem. B, 102 (1998) 6382.

27   M.S. Rigutto, H.Van Bekkum, Appl. Catal, 68 (1991) 297.

28 G. Centi, S. Perathoner, F. Trifiro, A. Aboukais, C.F. Aissi, M. Guelton, J. Phys. Chem, 96 (1992) 2617.

29 S. Dzwigaj, M. Atsuoka, R. Franck, M. Anpo, M. Che, J. Phys. Chem. B, 102 (1998) 6309.

30 S. Dzwigaj, M. Atsuoka, M. Anpo, M. Che, J. Phys. Chem. B, 104 (2000) 6012.

31 H. Yamashita, K.Yoshizawa, M. Ariyuki, S. Hijashimoto, M. Che, M. Anpo, J. Chem. Soc. Chem. Commun, (2000) 435.

32 Lindner M, D.Bahnemann, B.Hirthe and W. Griebler, Solar Engineering, 1 (1995) 399.

33 W.A. Zeltner and M.A. Anderson, Fine partcles science and Technology, Kluwer Academic Publishers. (1996) 643.

34 K. Kalyanasundaram, Energy resources through Photochemistry and Catalysis, Academic Press, (1983) 217.

35 R. Matthews, Photocatalytic purification and treatment of water and air, Elseveir Publishers, (1993) 121.

36 M.R. Hoffmann, S.T. Martin, W. Choi and D. Bahnemann, Chemical Reviews, 95 (1995) 69.

37 S. Ahmed, D.F. Ollis, Solar Energy, 32 (5) (1984) 597.

38 Y. Zhang, J.C. Crittenden, D.W. Hand, Chemistry and Industry, (1994) 714.

39 Y. Zhang, J.C. Crittenden, D.W. Hand, and D.L. Perram, Environmental Science and technology, 28 (1994) 435.

40 S. E. Braslavsky and K. N. Houk, Pure & Appl. Chem, 60 (1988) 1055.

41 J. W. Verhoeven, Pure & Appl. Chem, 68 (1996) 2223.

42   Compendium of Chemical Terminology, IUPAC Recommendations, A. D. McNaught and A. Wilkinson (eds.), London, Blackwell (1977).

43   N. Serpone and A. Salinaro, Pure & Appl. Chem, 71 (1999) 303.

44   H. Kisch, Photocatalysis - Fundamentals and Applications, N. Serpone and E. Pelizzetti (eds.), Wiley Interscience, New York (1989).

45   Glossary of Terms in Photochemistry, EPA Newsletter, 25 (1985) 13.

46   F. Chanon and M. Chanon, Photocatalysis – Fundamentals and Applications, N. Serpone and E. Pelizzetti (eds.), Wiley Interscience, New York (1989).

47   K. I. Zamaraev, Studies in Surface Science and Catalysis, J. W. Hightower, W. N. Delgass, E. Iglesia and A. T. Bell (eds.), Vol. 101, part A, Elsevier, Amsterdam (1996) p. 35.

48   R. G. Salomon, Tetrahedron, 39 (1983), 485.

49   A.Navio, G.Colon, M.Macias, C.Real and M.I.Litter, Appl.Catal.A, 177 (1999) 111.

50   G.Guzman, P.Babaux, J.Livage and J.Perriere, J.Sol-Gel Sci. Technol, 2 (1994) 619.

51   Eduardo Munoz, Jose L.Boldu, Eduardo Andrade, Octavio Novaro and Xi. Bokhimi, J.Am.Ceram.Soc, 84(2) (2001) 392

52   Krishnan Rajeshwar, C.R.Chenthamarakshan, Scott Goeringer and Miljana Djukic, Pure Appl.Chem, 73, 12, (2001) 1849.

53   B. Viswanathan, S. Sivasanker and A.V. Ramaswamy, Catalysis-Principles and applications, Narosa Publishing house, New Delhi.

54   Augustynski, J. Electrochim.Acta, 38 (1993) 43.

55   J.M. Herrmann, Topics in Catal, 34 (1–4) (2005) 49.

56   M.R. Hoffmamann, S.T. Martin, W. Choi, D.W. Bahnemann, Chem. Rev, 95 (1995) 69.

57   K. Rajeshwar, J. Appl. Electrochem, 25 (1995) 1067.

58   A.K. Ghosh, H.P. Maruska, J. Electrochem.Soc, 124 (1977) 1516.

59   H.P. Maruska, A.K. Ghosh, Sol. Energy Mater, 1 (1979) 237.

60   Y. Matsumoto, J. Kurimoto, Y. Amagasaki, E. Sato, J. Electrochem. Soc, 127 (1980) 2148.

61   Y. Matsumoto, J. Kurimoto, T. Shimizu, E. Sato, J. Electrochem. Soc, 128 (1981) 1040.

62   J.B. Goodenough, Adv. Chem. Ser, 186 (1980) 113.

63   P. Salvador, Sol. Energy Mater, 12 (1980) 413.

64   R.U.E. Lam, L.G.J. Dehaar, A.W. Wiersma, G. Blasse, A.H.A. Tinnemans, A. Mackor, Mater. Res. Bull, 16 (1981) 1593.

65   W.K. Wong, M.A. Malati, Sol. Energy, 36 (1986) 163.

66   T.R.N. Kutty, K. Avudaithai, Chem. Phys. Lett, 163 (1989) 93.

67   V. Augugliaro, F.D. Alba, L. Rizzuti, M. Schiavello, A. Sclafani, Int. J. Hydrogen Energy, 7 (1982) 851.

68   J.C. Conesa, J. Soria, V. Augugliaro, L. Palmisano, In structure and reactivity of surfaces; C. Morterra, A. Zecchina, G. Costa, Eds. Elsevier; Amsterdam (1989) 307.

69   J. Cunningham, S. Srijaranai, J. Photobiol. A.Chem, 43(1988) 329.

70   V.S. Escribano, G. Busca, V. Lorenzelli, J. Phys. Chem, 95 (1991) 5541.

71   Seiji Yamazaki and Hiroshi Honjo, Journal of Sol-Gel Science and Technology, 23 (2002) 267.

72   A. Maldotti, A. Molinari and R. Amadelli, Chem. Rev. 102 (2002) 3811.

73   A. Furube, T. Ashai, H. Masuhara, H. Yamashita, M. Anpo, J. Phys. Chem. B, 103 (1999) 3120.

74   A. Furube, T. Ashai, H. Masuhara, H. Yamashita, M. Anpo, Res. Chem. Intermed, 27 (2001) 177.

75   A. Furube, T. Ashai, H. Masuhara, H. Yamashita, M. Anpo, Chem. Phys. Lett, 336 (2001) 424.

76   A. Furube, T. Ashai, H. Masuhara, H. Yamashita, M. Anpo, Chem. Lett, (1997) 735.

77   Alexander G. Agrios and Pierre Pichat, J. Appl. Electrochemistry, 35 (2005) 655.

78   P.V. Kamat, Chemtech, (1995) 22.

79   A. Hagfeldt, M. Gratzel, Chem. Rev, 95 (1995) 49.

80   A. Henglein, Progress in Colloid Polymer Science, (1-4) (1987) 73.

81   C. Kormann, D.W. Bahnemann, M. Hoffmann, J. Phys. Chem, 92 (1988) 5196.

82   M. Gratzel, Heterogeneous Photochemical Electron Transfer, CRC Press, Boca Rato, FL, (1989).

83   D. Beydoun, R. Amal, G. Low and S. McEvoy, J. Nanoparticle Research, 1 (1999) 439.

84   E. Vulliet , C. Emmelin, J.M. Chovelon, C. Guillard, J.M. Herrmann, Environ Chem Lett 1 (2003) 62.

85   Lei E, Mingxia Xu, Lei Ge, Yuming Tian, Yan Li and Tiantian Xu, Key Engineering Materials, 280-283 (2005) 377.

86   Kazuhiro Doushita, Tetsuro Kawahara, Journal of Sol-Gel Science and Technology 22 (2001) 91.

87   T. Docters, J.M. Chovelon, J.M. Herrmann, J.P. Deloume, Applied Catalysis B: Environmental 50 (2004) 219.

88   F. Benoit-Marqui, C. de Montety, V. Gilard .R. Martino, M. T. Maurette, M. Malet-Martino, Environ Chem Lett,2 (2004) 93.

89   S. Senthilkumaar, K. Porkodi, R. Vidyalakshmi, Journal of Photochemistry and Photobiology A: Chemistry 170 (2005) 225.

90   Rosana. M. Alberici, Wilson. F. Jardim, Applied Catalysis B: Environmental, 14 (1997) 55.

91   Lili Zhao, Yun Yu, Lixin Song, Xingfang Hu, Andre Larbot, Applied Surface Science 239 (2005) 285.

92   Federica Soana, Michela Sturini, Laura Cermenati and Angelo Albini, J. Chem. Soc, Perkin Trans, 2 (2000) 699.

93   Teruhisa Ohno, Koji Sarukawa, Kojiro Tokieda and Michio Matsumura, J. Catal, 203 (2001) 82.

94   Linda A. Lawton, Peter. K. J. Robertson, Benjamin J. P. A. Cornish, Iain L. Marr and Marcel Jaspars, J. catal, 213 (2003) 109.

95   Didier Robert, Bini Dongui and Jean Victor weber, Journal of Photochemistry and Photobiology A: Chemistry, 156 (2003) 195.

96   Chantal Guillard, Hinda Lachheb, Ammar Houas, Mohamed Kisbi, Elimame Elaloui and Jean Marie Herrmann, Journal of Photochemistry and Photobiology A: Chemistry, 158 (2003) 27.

97   M. Catherine Blount and John. L. Falconer, J. Catal, 200 (2001) 21.

98   A.J. Maira, J.M. Coronado, V. Augugliaro, K.L. Yeung, J.C. Conesa

and J. Soria, J. Catal, 202 (2001) 413.

99   Teruhisa Ohno, Yuji Masaki, Seiko Hirayama and Michio Matsumura, J. Catal, 204 (2001) 163.

100   Lixin Cao, Zi Gao, Steven L. Suib, Timothy N. Obee, Steven O. Hay and James D. Freihaut, J. Catal, 196 (2000) 253.

101   Michele Ranchella, Cesare Rol and Glovanni V. Sebastiani, J. Chem. Soc, Perkin Trans, 2 (2000) 311.

102   Paola Piccinini, Claudio Minero, Marco Vincenti and Ezio Pelizzetti, J. Chem. Soc, Faraday Trans, 93 (10) (1997) 1993.

103   W. Lee, Y.M. Gao, K. Dwight and A. Woid, Mat. Res. Bull, 27 (1992) 685.

104   Dal Rung Park, Jinlong Zhang, Keita Lkeue, Hiromi Yamashita and Masakazu Anpo, J. Catal, 185 (1999) 114.

105   Darrin S. Muggli and John L. Falconer, J. Catal, 187 (1999) 230.

106   Mohamed Ksibi, Asma Zemezemi and Rachid Boukchina, Journal of Photochemistry and Photobiology A: Chemistry, 159 (2003) 61.

107   P. Pizarro, C. Guillard, N. Perol, and J. M. Herrmann, Catalysis Today 101 (2005).

108   Qiaorong Sheng, Shuai Yuan, Jinlong Zhang , Feng Chen, Microporous and Mesoporous Materials 87 (2005) 177.

109   Hiroshi Irie, Seitaro Washizuka, Norio Yoshino and Kazuhito Hashimoto, Chem. Commun, (2003) 1298.

110   Y. Liu, X. Chen, J. Li, C. Burda, Chemosphere 61 (2005) 11.

111   M.V. Shankar, K.K. Cheralathan, Banumathi Arabindoo, M. Palanichamy, V. Murugesan, Journal of Mole Catal A: Chemical 223

(2004) 195.

112 Yibing Xie, Chunwei Yuan, Xiangzhong Li, Colloids and Surfaces A: Physicochem. Eng. Aspects 252 (2005) 87.

113 Andrew Burns, G. Hayes, W. Lia, J. Hirvonen, J. Derek Demareed, S. Ismat Shah, Materials Science and Engineering B 111 (2004) 150.

114 Koichi Kajihara and Takeshi Yao, Phys. Chem. Chem. Phys, 1(1999) 1979.

115 K.T. Ranjit, I. Willner, S.H. Bossann and A.M. Braun, J. Catal, 204 (2001) 305.

116 Hiroaki Uchiyama, Keisei Suzuki, Yuya Oaki, Hiroaki Imai, Materials Science and Engineering B 123 (2005) 248.

117 Satoshi Yoda, Katsuto Ohtake, Yoshihiro Takebayashi, Tsutomu Sugeta, Takeshi Sako and Tsugio Sato, J. Mater. Chem, 10 (2000) 2151.

118 Tetsu Tatsuma, Shuichi Saitoh, Pailin Ngaotrakanwiwat, Yoshihisa Ohko and Akira Fujishima, Langmuir, 18 (2002) 7777.

119 M. Radecka, K. Zakrzewska, M. Wierzbicka, A. Gorzkowska and S. Komornicki, Solid state Ionics, 157 (2003) 379.

120 V. Keller, P. Bernhardt and F. Garin, J. Catal, 215 (2003) 129.

121 Zhi-hao Yuan and Li-de Zhang, J. mater. Chem, 11 (2001) 1265.

122 Weon Pil Tai and Kozo Inoue, Mat. Lett, 57 (2003) 1508.

123 Giuseppe Mele, Roberta Del Sole, Giuseppe Vasapollo, Elisa Garcia Lopez, Leonardo Palmisano and Mario Sciavello, J. Catal, 217(2003) 334.

124 Chuan -Yi Wang, Detlef W. Bahnemann and Jurgeon K. Dohrmann,

Chem. Commun, (2000) 1539.

125 Jincai Zhao, Kaiqun Wu, Taixing Wu, Hisao Hidaka and Nick Serpone, J. Chem. Soc, Faraday Trans, 94 (5) (1998) 673.

126 Najeh I. Al-Salim, Stephen A. Bagshaw, Antoine Bittar, Tim Kemmitt, A. James McQuillan, Ann M. Mills and Martin J. Ryan, J. Mater. Chem, 10 (2000) 2358.

127 Wenjie Wang, Mingyuan Gu and Yanping Jin, Materials Lett, 57 (2003) 3276.

128 Tessy Lopez, R. Gomez, E. Sanchez, F. Tzompantzi and L. Vera, J. Sol-Gel Sci and Tech, 22 (2001) 99.

129 Andrzej Sobezynski and Lakasz Duczmal, React. Kinet. Catal. Lett, 82 (2) (2004) 213.

130 Tak-Hyoung Lim, Sang-Mun Jeong, Sang-Done Kim and Janos Gyenis, React. Kinet. Catal. Lett, 71 (2) (2000) 223.

Chapter 9

Photooxidation of Benzhydrol

Abstract

Photocatalysts are likely to provide a versatile means of producing several organic compounds. The present chapter provides a detailed study on the oxidation of benzhydrol, a secondary alcohol on irradiated surfaces of titania. The titanium dioxide photocatalyzed oxidation of benzhydrol in oxygen purged acetonitrile gives benzophenone as the sole product. The influence of various reaction parameters like irradiation time, amount of catalyst, concentration of the reactant and the nature of the solvent has been investigated. The proposed mechanism envisages the oxidation of benzhydrol by a hole to give the radical cation of benzhydrol and its subsequent reaction with a superoxide radical anion produced by the transfer of a conduction band electron to oxygen. The nature of the incorporated metal as well as its amount upon the rate of photocatalytic oxidatioin of benzhydrol is also discussed.

9.1 Introduction

Heterogeneously dispersed semiconductor surfaces provide both a fixed environment to influence the chemical reactivity of a wide range of adsorbates and a means to initiate light induced redox reactivity in these weakly associated molecules. Semiconductor photocatalysis, particularly with TiO_2 as the catalyst has been employed in photoelectrochemical cells/ photoelectrochemical production of hydrogen, photocatalytic degradation of pollutants and organic functional group transformations[1-11]. Upon photo excitation of several semiconductors nonhomogeneously suspended in either aqueous or non aqueous solutions or in gaseous mixtures, simultaneous oxidation and reduction reactions occur. This conversion often accomplishes either a specific, selective oxidation or a complete oxidative degradation of an organic substrate present. Molecular oxygen is often assumed to serve as the oxidizing agent although details about the mode of its environment have not been unambiguously demonstrated in a few gas/solid reactions[12].

Photooxidation is, by far, the most numerous classes of the known photocatalytic reactions of organic substrates. It is typical that high (in some cases nearly quantitative) chemical yields of oxidation products are formed, although sometimes with quantum yields of only a few percent or less[13]. Irradiation in the presence of a semiconductor powder, most commonly of the inexpensive titanium dioxide is an appealing method for the oxidation of organic molecules[14-19]. Such heterogeneous photocatalysis has been carried out both in organic solvents[20-24] and in aqueous solution[14-17]. In the former case, the reaction is initiated by electron transfer at the interface leading to the radical cation of the substrate and the superoxide anion, while in the latter one,

the actual species are assumed to be hydroxy radicals formed by the oxidation of the solvent[25-26]. The charge recombination in the semiconductor is extremely fast[27], and thus electron transfer from the solute is thought not to compete in aqueous solution. Of appreciable interest would be a means for selecting one oxidation pathway over another through heterogeneous photocatalysis, a goal that demands considerable mechanistic insight.

Although there are several photocatalytic studies with TiO_2 directed mainly towards the mineralisation of pollutants, there are only a few photocatalytic studies on organic transformations. Virtually, every functional group bearing either a nonbonded lone pair of any π conjugation can be activated toward TiO_2 photocatalyzed oxidative reactivity, either by dehydrogenation, oxygenation or oxidative cleavage. The gaseous dehydrogenation of ethanol to acetaldehyde occurs effectively over irradiated titania powder[28].

$$CH_3CH_2OH \xrightarrow[O_2]{TiO_2^{\bullet}} CH_3CHO$$
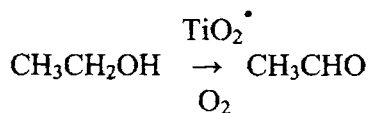
$TiO_2^{\bullet}$ indicates the excited state formed by band gap excitation of the suspended photocatalysts.

Irradiation of β-chlorodiethyl sulfide suspended in aerated aqueous, non aqueous or mixed solvents in the presence of suspended TiO_2 leads to the formation of the corresponding sulphoxide in high yield and subsequently the sulphone[29].

$$ClCH_2CH_2SCH_2CH_3 \xrightarrow[\substack{O_2 \\ CH_3CN}]{TiO_2^{\bullet}} ClCH_2CH_2SOCH_2CH_3$$
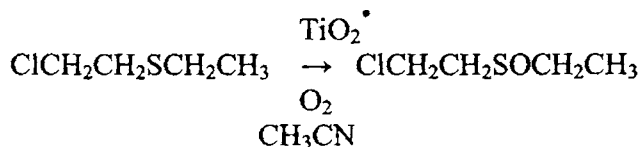
Nearly quantitative conversion of the C=C double bond of 1,1-diphenyl ethylene to benzophenone and formaldehyde in the irradiation of TiO_2 suspended in oxygenated acetonitrile[30].

$$C_6H_5CH_2C_6H_5 \xrightarrow[\substack{O_2 \\ CH_3CN}]{TiO_2{}^\bullet} C_6H_5COC_6H_5$$
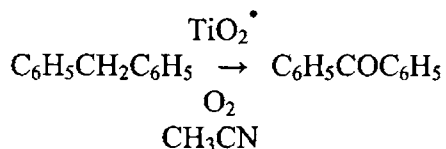
Even with the organic compounds with the simplest functionality (the alkanes) oxidation products often result when a gaseous stream of substrate passes over an irradiated solid semiconductor film. Federica Soana *et al* studied the photocatalyzed oxygenation of naphthalene in water[31]. They obtained (E, Z)-2-formylcinnamaldehydes and 1,4-naphthoquinones besides traces of naphthols. It is now well established that the photocatalytic oxidation of several organic molecules by optically excited semiconductor oxides is thermodynamically allowed in the presence of oxygen at room temperature. The oxidation of secondary alcohols on irradiated TiO_2 in general yields the corresponding ketones.

Metal oxides can sometimes also act as high temperature thermal oxidation catalysts, but better oxidative selectivity is often observed in the room temperature photocatalytic oxidations[33]. For example, although the oxidation of cyclohexane by oxygen over native or chemically modified titania is thermodynamically permissible, its rate at room temperature is impossibly slow without photoassistance, and at higher temperatures little oxidative selectivity is observed. In contrast, TiO_2 photocatalysis produces 83% cyclohexanone, 5% cyclohexanol and 12% CO_2[32].

Vijaikumar *et al* reported the oxidation of benzhydrol under solar radiation[33]. Though titania is a cheap material, for its effective use, it is economically desirable to get good results with solar radiation as the source of light. The weak UV light available in the solar radiation is used in organic redox reactions in the presence of photocatalysts. Therefore, an oxygen purged solution of benzhydrol in the presence of suspended TiO_2 was exposed to direct solar radiation on a sunny day. Benzophenone was formed on exposure to sunlight and the amount increased with exposure time. Fujishima[2] *et al* have succeeded in developing transparent titania coatings on various substrates such as glass and ceramic tiles. These coatings could photodegrade in the presence of solar radiation various noxious, malodorous chemicals, smoke residues and cooking oil residues.

9.2 Process Optimization

The photooxidation of benzhydrol was carried out in a Heber photoreactor (Multilamp type, model HML-MP88) containing concentrically arranged eight numbers of 8W mercury lamps of 365nm wavelength. The only product obtained in this reaction is benzophenone. In a typical experiment, benzhydrol (10ml of 1mM) in acetonitrile was taken in a 20ml glass tube and 0.01g of TiO_2 was added to it. The reaction mixture was stirred vigorously to get a uniform suspension of the catalyst. After being purged with oxygen for 15 min, it was irradiated in an annular photoreactor. The reaction mixture was centrifuged to remove TiO_2 and analyzed by using a gas chromatograph using BP-1 capillary column (12m X 0.32mm). Products were confirmed by comparison with authentic samples. The results of an extensive study of the

photocatalytic oxidation of benzhydrol in acetonitrile by TiO_2 in the presence of oxygen are discussed below.

9.2.1 Influence Of Catalyst Weight

The photocatalytic activity strongly depends on the amount of the catalyst. To study this influence, the weight of the catalyst is varied from 0.0025 to 0.0125g using Ti catalyst for the same volume of a fixed concentration of the solution and irradiating for 80 minutes. . The variation in the product distribution with the amount of titania is plotted in figure 9.1.
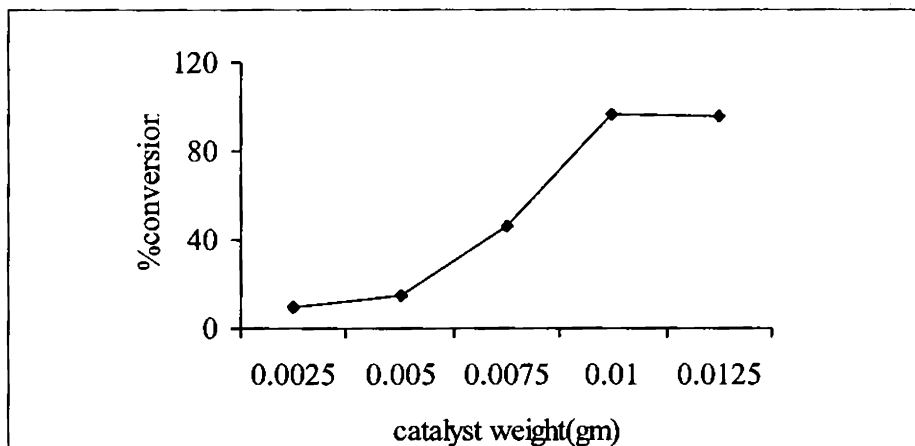

Figure 9.1

Dependence of product formation on the amount of TiO_2

1 mmol benzhydrol, Time of study – 80minutes, Lamp Intensity-48W

All other parameters were kept similar. There is a drastic rise in the percentage conversion as the catalyst weight is increased. A saturation point is

obtained when the weight of the titania catalyst is 0.01g, above which further rise in catalyst weight doesn't have a significant influence on the activity. Therefore, in all the studies, the optimum concentration of TiO_2 for the photocatalytic oxidation has been fixed as 0.01g. Whatever be the amount of the catalyst, benzophenone is obtained as the sole product.

9.2.2 Influence Of Light Intensity

The light intensity plays a significant role in any photocatalytic reaction. With an increase in light intensity, the number of photons striking the semiconductor per unit area of the TiO_2 catalyst powder increases. This has resulted in an increased amount of the product when the intensity of the lamps increases from 16W to 48W for the irradiation of 1mmol benzhydrol in acetonitrile. The percentage conversion remains more or less similar when the light intensity is varied from 48W to 64W. The results are given in table 9.1.

Table 9.1

Influence Of Light Intensity on the Photooxidation of Benzhydrol

Light Intensity (W)	% Conversion
16	21.6
32	57.1
48	96.5
64	96.9

TiO2 catalyst-0.01g, 1 mmol benzhydrol, Time of study – 80minutes

9.2.3 Influence of Concentration of Benzhydrol

The effects of concentration of benzhydrol on the photocatalytic oxidation was studied be taking solutions of different initial concentrations of benzhydrol, and keeping all other factors identical. The amounts of benzophenone formed at different concentrations of the substrate are given in table 9.2. The amount of benzophenone varies linearly with the initial concentration of benzhydrol.

Table 9.2

Influence Of Concentration of Benzhydrol on the Photooxidation

Concentration of Benzhydrol	0.4	0.6	0.8	1.0	1.2	1.4
Percentage Conversion	47.2	57.1	79.9	96.5	98.3	98.5

TiO2 catalyst-0.01g, Lamp Intensity-48W, Time of study – 80minutes

9.2.4 Influence of Solvent

The photocatalytic reaction is also solvent dependant just like any catalyzed reaction. The mechanism and hence the product distribution varies with the nature of the solvent. Under different conditions in the TiO_2 photo assisted oxidation of benzhydrol dissolved in acetonitrile, benzophenone was found to be the sole product. When the photooxidation of benzhydrol was investigated in methanol and ethanol, benzophenone was not formed and the solvents have been oxidized. Acetonitrile is used as a solvent in all cases, considering the fact that acetonitrile is stable under photocatalytic conditions.

9.2.5 Influence of Irradiation time

When an oxygen-purged solution of benzhydrol in acetonitrile was irradiated with light for several minutes in the absence of the photocatalyst, benzophenone was not formed. In another set of experiments, a solution of benzhydrol was saturated with oxygen and mixed with TiO_2. This solution was kept in the dark; product analysis at various time intervals indicated the absence of formation of benzophenone. However, when an oxygenated solution of benzhydrol in the presence of semiconductor photocatalyst, TiO_2, was irradiated with light, oxidation of the reactant resulted in the formation of benzophenone. The amount of benzophenone increased with increase in time of irradiation, which is illustrated in Fig. 9.2. We have also observed that, when the photocatalytic oxidation of benzhydrol was conducted in the presence of purged nitrogen (i.e. in the absence of oxygen), the substrate was not oxidized.

This observation, along with the results shown in Fig. 9.2, clearly reveal that TiO_2, oxygen and light are essential for the sustained photocatalytic oxidation of benzhydrol to benzophenone. The presence of oxygen is also beneficial, as it prevents carrier recombination by trapping the photogenerated electrons and forming a superoxide anion radical. Irradiation carried out for more than 100 min has not improved the yield of benzophenone and almost a saturation level is reached. The reaction is carried out in the presence of solar radiation on a sunny day. The GC results show the presence of the one and only product, benzophenone, but the percentage conversion didn't increase beyond 19.5% even after 4h.
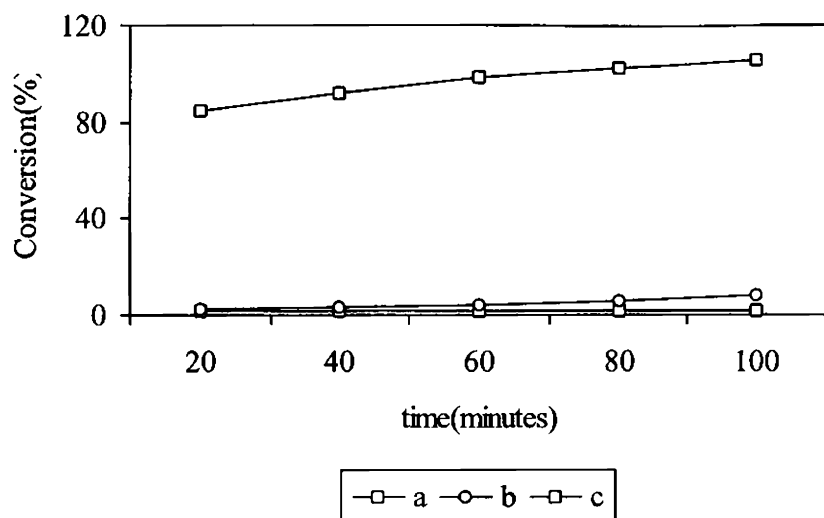
Figure 9.2

Dependence of Product formation on irradiation time

TiO2 catalyst-0.01g, Lamp Intensity-48W, 1 mmol benzhydrol

(a) Benzhydrol in acetonitrile (1mM) solution with titania in the absence of light

(b) Photolysis of benzhydrol in acetonitrile (1mM) with light in the absence of titania catalyst

(c) Irradiation of a solution of benzhydrol in acetonitrile (1mM) with titania catalyst and oxygen

The photooxidation reaction is carried out over TiLa6, TiCr6 and TiPr6 systems and their product distribution with time is given in figure 9.3. All the systems are found to be stable with a good percentage conversion and

selectivity over the course of the reaction. The photostability of rare earth metal incorporated titania systems are more than that of transition metal incorporated systems.
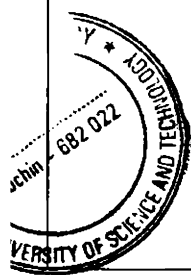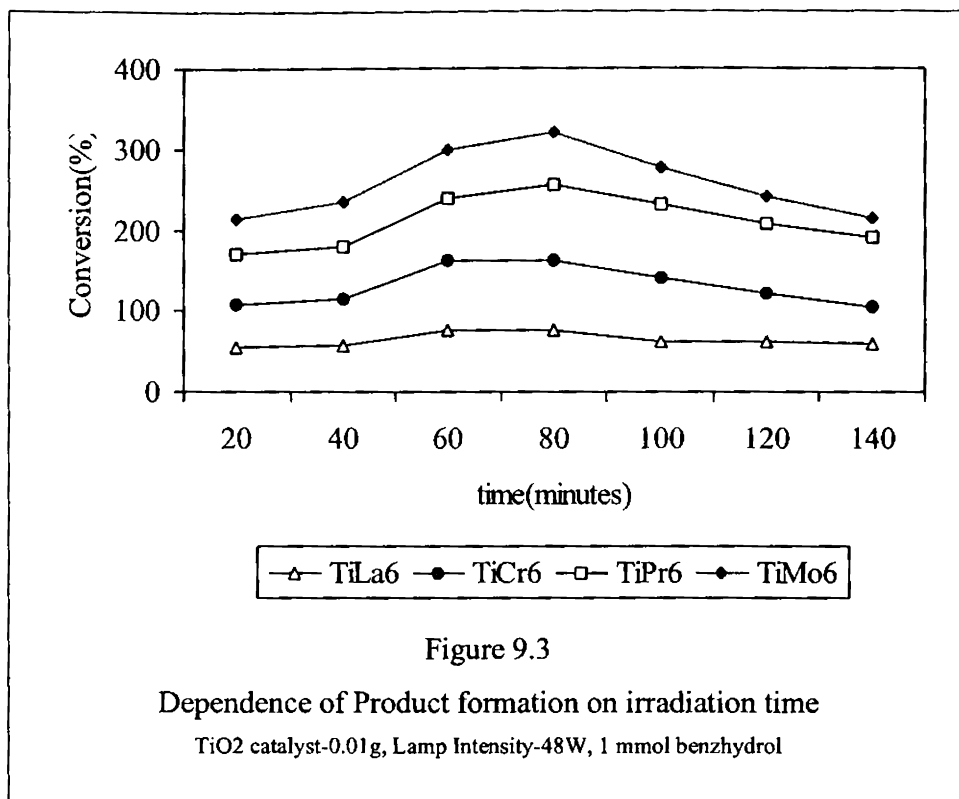

Figure 9.3

Dependence of Product formation on irradiation time

TiO2 catalyst-0.01g, Lamp Intensity-48W, 1 mmol benzhydrol

9.3 Comparison of Catalyst Systems

The results obtained for the photooxidation of benzhydrol over the prepared catalytic systems under the optimized reaction conditions is given in in table 9.3. Pure titania shows comparatively higher catalytic activity in the

photooxidation reaction. All the transition metals are having a deteriorating influence on the photocatalytic activity of titania.

Table 9.3

Comparison of Catalyst Systems

Catalyst	% Conversion	Catalyst	%Conversion
Ti	96.5	TiLa2	65.6
TiMo2	77.2	TiLa6	77.0
TiMo6	66.5	TiLa10	93.6
TiMo10	57.3	TiPr2	90.2
TiCr2	90.3	TiPr6	92.6
TiCr6	86.6	TiPr10	94.6
TiCr10	76.7	TiSm2	68.3
TiW2	52.3	TiSm6	75.6
TiW6	49.8	TiSm10	89.3
TiW10	46.1		

Catalyst-0.01g, Lamp Intensity-48W, 1 mmol benzhydrol,

Solvent- Acetonitrile

Another interesting observation is that as the percentage of the incorporated transition metals increases, the photocatalytic activity decreases. 2% transition metal loaded systems exhibiting highest conversion while 10% loaded systems exhibiting least conversion. But the trend is reverse in the case of rare earth metal incorporated systems. Here 10% rare earth metal incorporated titania systems are having highest activity. Except in the case of praseodymia incorporated titania systems, all the other systems are having comparatively lower capacity of oxidizing benzhydrol under identical reaction

conditions. Zhang *et al* reported that improved crystallinity has a beneficial effect on the increase of photocatalytic degradation of phenol by titania powders[34]. They also reported that the mixtures of anatase and rutile are found to be more active than anatase crystallites or rutile crystallites at the same calcinations temperatures. The same explanation can be highlighted in the case of praseodymia incorporated systems. The XRD spectra of these systems are an indicative of its reduced crystallinity. Also a small amount of the rutile phase is present along with the anatase phase.

9.4 Mechanism of the Reaction

It is recognized that the heterogeneous photooxidation of organic compounds sensitized by TiO$_2$ powder in acetonitrile, an inert solvent under oxidative conditions, involves a single electron transfer from the adsorbed substrate to the photogenerated hole in the valence band (VB), while the electron in the conduction band (CB) is captured by a suitable acceptor. In all cases the intermediate cations are responsible for the primary oxidation products[35]. In the proposed mechanism, the oxidation of benzhydrol by the hole to give the corresponding radical cation and the subsequent oxidation of this radical by superoxide anion radical are suggested. The formation of radical cation and superoxide anion radical on irradiated TiO$_2$ is depicted in Fig. 9.4.

The occurrence of this reaction only in the presence of a solvent like acetonitrile in presence of purged oxygen, supports the proposed mechanism shown in scheme1. It has also been reported the result of photooxidation of benzhydrol carried out in the presence of a sensitizer 9,10-dicyanoanthracene (DCA) in acetonitrile[33]. This supports the oxidation of a radical cation of
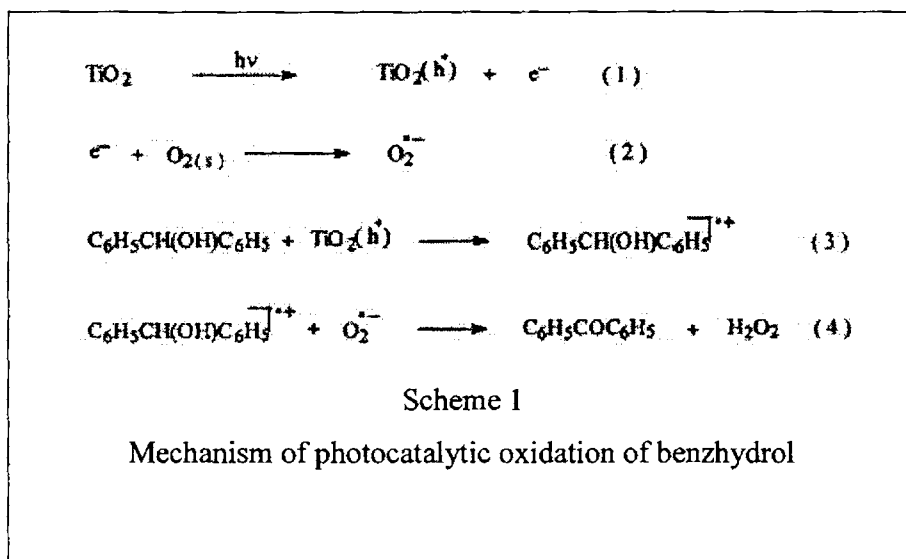
benzhydrol by a superoxide radical anion. An oxygen purged solution of benzhydrol and DCA in acetonitrile yielded benzophenone. It is well known that, on excitation of DCA, the resulting singlet DCA accepts an electron from the electron donor to give the radical anion of DCA and the radical cation of the donor. The DCA radical anion can transfer an electron to oxygen to give the superoxide anion. The superoxide can oxidize the cation radical[36]. In this case, the cation radical of benzhydrol would have been formed in the DCA sensitized reaction and that would have been oxidized to the ketone by the superoxide anion radical.

Figure 9.4

Schematic diagram for the formation of radical cation and superoxide anion
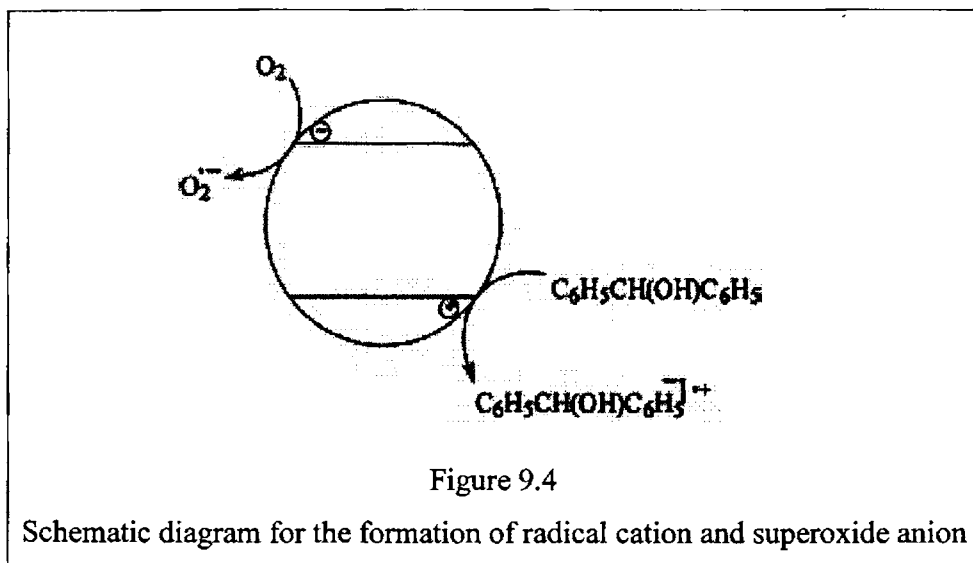
In an independent experiment, irradiation of a mixture of 1mM benzhydrol and 0.2mM benzophenone in acetonitrile in the presence of 0.1% TiO_2 has yielded the same amount of the oxidized product as in the absence of added benzophenone. This result indicates that, though benzophenone is a

sensitizer for generation of singlet oxygen, our experimental results above indicate that singlet oxygen, if generated, at all has not played any role.

$$TiO_2 \xrightarrow{\;h\nu\;} TiO_2(\overset{\bullet}{h}) + e^- \quad (1)$$

$$e^- + O_{2(s)} \longrightarrow O_2^{\bullet -} \quad (2)$$

$$C_6H_5CH(OH)C_6H_5 + TiO_2(\overset{\bullet}{h}) \longrightarrow \left[C_6H_5CH(OH)C_6H_5\right]^{\bullet +} \quad (3)$$

$$\left[C_6H_5CH(OH)C_6H_5\right]^{\bullet +} + O_2^{\bullet -} \longrightarrow C_6H_5COC_6H_5 + H_2O_2 \quad (4)$$

Scheme 1

Mechanism of photocatalytic oxidation of benzhydrol

The formation of H_2O_2 in several TiO_2 photocatalyzed reactions has been proposed. It is noted that in the light-activated TiO_2 oxidation of 2-propanol in aqueous solution or in pure liquid, the mechanism may involve the oxidation of surface hydroxyl groups, which participate in the photocatalytic oxidation process[34-35]. The oxidation of benzhydrol with 0.2mM H_2O_2 (the maximum amount that would have formed in our reaction) has not oxidized benzhydrol under the present experimental conditions. Therefore, it is concluded that the hole and superoxide radical anion are mainly responsible for the oxidation.

9.3 Conclusions

Photocatalyzed oxidation of benzhydrol occurs effectively in acetonitrile in the presence of oxygen to give benzophenone. The proposed mechanism involves the reaction between a cation radical of benzhydrol formed by the oxidation of the alcohol by a hole and a superoxide radical anion produced by the transfer of a conduction band electron to oxygen. Pure titania prepared in the particulate sol-gel route is regarded as a very effective photocatalyst in this context. The transition metals are having a negative influence in photooxidising benzhydrol. Among the rare earth metals, praseodymia incorporated titania systems are having comparable activity with that of pure titania. The photocatalytic oxidation of benzhydrol to benzophenone opens a very effective path for the selective formation of benzophenone.

References

1 A. Fujishima, K. Honda, Nature, 238 (1972) 37.

2 A. Fujishima, T.N. Rao, D.A. Tryk, J. Photochem. Photobiol. Chem, Photochem. Rev, 1 (2000) 1

3 M.R. Hoffmann, S.T. Martin, W. Choi, D.W. Bahnemann, Chem. Rev, 95 (1995) 69.

4 J. Peral, X. Domenech, D.F. Ollis, J. Chem. Tech. Biotech, 70 (1997) 117.

5] M.A. Fox, M.T. Dulay, Chem. Rev, 93 (1993) 341.

6 M.A. Fox, in: N. Serpone, E. Pelizzetti (Eds.), Photocatalysis-Fundamentals and Applications, Wiley, New York, 1989,p. 420.

7 M.A. Fox, Top. Curr. Chem, 142 (1991) 71

8 H. Al-Ekabi, in: V. Ramamurthy (Ed.), Photochemistry in Organized and Constrained Media, VCH Publishers, New York, 1991, p. 495.

9 M.A. Fox, ACS Symposium Series 278, American Chemical Society, Washington, DC, 1985, p. 43.

10 Y. Li, in: V. Ramamurthy, K.S. Schanze (Eds.), Organic Photochemistry, Marcel Dekker, New York, 1987, p. 295

11 C. Srinivasan, Curr. Sci. 76 (1999) 535.

12 Marye Anne Fox and Maria T. Dulay, Chem. Rev, 93 (1993) 341.

13 F. sabin, T. Turk, A. Vogler, J. Photochem. Photobiol. A; Chem, 63 (1992) 99.

14 A. Mills and S. Le Hunte, J. Photochem. Photobiol. A; Chem, 108 (1997) 1.

15 P. Pichat, Handbook of Heterogeneous Photocatalysis, eds, G. Ertl, H. Knoezinger and J. Wietkamp, Wiley, New York (1997) p. 2111.

16   M. R. Hoffnannn, S.T. Martin, W. Choi and D.W. Bahnemann, Chem. Rev, 93 (1993) 671.

17   P. Pichat, Catal. Today, 19 (1994) 313.

18   P.V. Kamal, Chem. Rev, 93 (1993) 267.

19   N.N. Rao and P. Natarajan, Curr. Sci, 66 (1994) 742.

20   M.A. Fox, Top. Curr. Chem, 142 (1987) 71.

21   H. Kisch, J. Prakt. Chem, 336 (1994) 635.

22   E. Baciocchi, C. Rol, G.V. Sebastiani and L. Taglieri, J. Org. Chem, 59 (1994) 5272.

23   R. Kuenneth, C. Feldmer, F. Knoch and H. Kisch, Chem. Eur. J, 1 (1995) 441.

24   L. Cermenati, M. Mella and A. Albini, Tetrahedron, 54 (1998) 2575.

25   J. Schwitzgebel, J.G. Ekerdt, H. Gerisher and A. Heller, J. Phys. Chem, 99 (1995) 5633.

26   Y. Sun and J. Pignatello, J. Environ. Sci. Technol, 29 (1995) 2065.

27   N. Serpone, D. Lawless, R. Khairutdinov and E. Pelizzetti, J. Phys. Chem, 90 (1993) 16655.

28   P. Pichat, M.N. Mossanega, H. Courbon, J. Chem. Soc, Faraday Trans, 83 (1987) 697.

29   M.A. Fox, A.A. Abdel Wahab, Y.S. Kim, M.J. Dulay, J. Catal, 126 (1990) 693.

30   M.A. Fox, C.C. Chen, J. Am. Chem. Soc, 103 (1981) 6757.

31   Federica Soana, Michela Sturini, Laura Cermenati and Angelo Albini, J. Chem. Soc, Perkin Trans, 2 (2000) 699.

32   W. Mu, J.M. Herrmann, P. Pichat, Catal. Lett, 3 (1989) 79.

33   S. Vijaikumar, N. Somasundaram, C. Srinivasan, App. Catal A: Gen, 223 (2002) 129.

34   Q. Zhang, L. Gao, J. Guo, Appl. Catal. B, Environ, 26 (2000) 207.

35   M. Ranchella, C. Roi, G.V. Sebastiani, J. Chem. Soc, Perkin Trans, 2 (2000) 311.

36   N. Soffiu, H. Cardy, J.L. Habib Jiwan, I. Leray, J.Ph. Soumillion, S. Lacombe, J. Photochem. Photobiol. A: Chem,124 (1999) 1.

37   .R. Harvey, R. Rudham, S. Ward, J. Chem. Soc., Faraday Trans. 79 (1983) 1381.

38   Y. Ohko, K. Hashimoto, A. Fujishima, J. Phys. Chem. A,101 (1997) 8057.

Chapter *10*

Photodegradation of Methyl Orange

Abstract

Over the past decade, there has been growing interest in photocatalytic oxidation as a means of pollution destruction. The efficient photocatalytic degradation of hazardous wastes is one of the most desirable and challenging goals in the research of the development of environmentally friendly catalysts. The present chapter focuses on the photocatalytic activity of titania as well as its modified forms towards the degradation of methyl orange. The dependence of photodegradation of the dye on various parameters such as dye concentration, photocatalyst concentration, irradiation time and intensity of radiation were also investigated in detail. The percentage degradation of various systems for this reaction is correlated with the band gap energy of the prepared systems.

10.1 Introduction

Dyestuffs are important class of synthetic organic pigments, which represent an increasing environmental problem. The wastewater containing these organic dyes is highly coloured, and the dyes are not easily removed in biological wastewater treatment plants because most dyes are resistant to biodegradation. Azo compounds are an important class of synthetic dyes commonly used as coloring agents in the textile, paint, ink, plastics and cosmetics industries. They are characterized by the presence of one or more azo group bound to aromatic rings. Azo dye, comprising various synthetic dyestuffs, even can be potentially reduced into carcinogenic aniline[1]. With in the overall category of azo dye stuffs, methyl orange is one of the most important dye, used in different applications such as dyeing and printing industries. The structure of methyl orange aqueous solution in alkaline solution is given in figure 10.1. The release of azo dyes into the environment is of great concern due to the coloration of natural waters, the toxicity, the mutagenicity, and carcinogenicity[2-5]. The consequence of this release in the eco-system is a dramatic source of aesthetic pollution, eutrophication and perturbation in aquatic systems[6]. The available physical, chemical and biological methods are available for the treatment of textile wastewater is cost effective. However, it has been reported that most of the dyes are adsorbed on the adsorbent and are not degraded. Hence, physical, chemical and biological methods are not cost effective to Indian context[7]. This leads to search for highly effective method to degrade the dyes into environmentally compatible products. It has been revealed from the literature that photocatalysis can be used to destroy the dyes using semiconductor catalyst under light irradiation[8-11].

TiO$_2$ based nanoparticles are materials that recently demonstrated enhanced photocatalytic efficiency. The application of these materials for relevant industrial dyes is an important step in order to establish semiconductor based photocatalysis for environmental use. TiO$_2$ photocatalysis has become increasingly important in recent years for environmental improvement such as the photodegradation and complete mineralization of organic pollutants [12-20]. TiO$_2$ nanoparticles have large specific surface areas and high catalytic performance in which reactions take place on the TiO$_2$ surface[21].
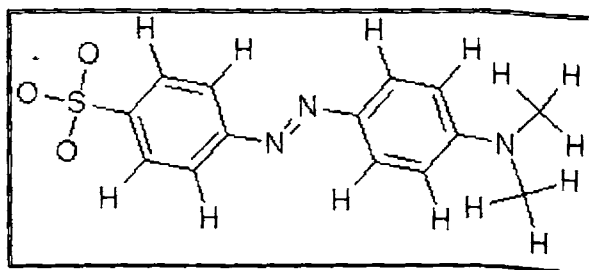

Figure 10.1, Structure of methyl orange in basic form

Most of the photocatalytic investigations have focused on TiO$_2$, for which a high reactivity and a good chemical stability under ultraviolet light have been obtained[22]. Among the semiconductors used, TiO$_2$ is considered particularly efficient owing to the formation of electron-hole pair under illumination with near UV light. Nevertheless, the recombination of electron-hole inhibits the photocatalytic reaction process[23]. TiO$_2$ semiconductor has high bandgap (3.2 eV), which limits its wide application in visible light range of solar spectrum. So, it only absorbs in the ultraviolet range, and efficient collection of the solar spectrum requires sensitization by a modification molecule absorbing in the visible range. Therefore, in order to realize the solar

decontamination process, many efforts are contributed to develop the second-generation photocatalysts that can drive the photodegradation reaction under visible light[24].

Photocatalytic destruction of different classes of organic dyes using highly concentrated solar light and TiO_2 suspension have been reported[25] where hetero atoms such as S and N in the dye molecules transform into SO_4^{2-} and NO_3^-. Mineralisation is reported to vary between 80 and 100% in <30min irradiation. This work suggests that high potential for the use of highly concentrated solar light in the destruction of textile dyes and biological stains from waste waters[26]. The photocatalytic activity of titania towards the degradation of various anionic dyes such as Alizarin S, Azo methyl red, Congo red, Orange G and cationic dyes like methylene blue and malachite green was reported in literature[27-30]. Nitrogen doped TiO_2 is very effective towards the photocatalytic degradation of three azodyes like Acid orange 7, Procion red MX-5B and Reactive Black. Illuminated titania is also capable of degrading dyes like Acid blue 9, X-GL, active Brilliant red Dye X-3B[31-33].

Photocatalytic experiments were conducted using the silica coated titania nanoparticles with tunable coatings to photocatalytically degrade methyl orange in water solutions[34]. The change of effective titania surface area available for methyl orange caused by silica coatings and the dispersion stability were used to explain the difference in photocatalytic activity. Ping Cheng *et al* studied the enhancement in photocatalytic activity of silica-titania binary oxides by comparing their efficiency towards photocatalytic degradation of methyl orange[35]. The photocatalytic properties of titania silica mixed oxide mesoporous materials was also tested by the degradation of

methyl orange[36]. E. Lei *et al* investigated the photocatalytic activity of titania by studying their rate of photocatalytic degradation in UV light as well as visible light. The results showed that the absorption intensity in visible-light was dependent on the concentration of the materials, pH value and heat-treatment temperature[37].

10.2 Process Optimization

The photoactivity of the prepared systems was investigated in the oxidation of methyl orange aqueous solution. The reaction was carried out in a Heber photoreactor (Multilamp type, model HML-MP88) containing concentrically arranged eight numbers of 8W mercury lamps of 365nm wavelength. The distilled water solution of methyl orange with a concentration of 25 mg/l was chosen for photodegradation. 0.1g catalyst powder was uniformly dispersed into 20ml of the above solution with vigorous agitation under the mercury light. After photooxidation, the suspended catalyst powder was separated from methyl orange aqueous solution. The concentration of methyl orange was measured using Shimadzu UV-Vis spectrophotometer (UV-160A). All the photocatalytic experiments were carried out at room temperature.

10.2.1 Effect of Time

The degradation of methyl orange is conducted over titania photocatalyst. The measurement of absorbance is done at regular time intervals and calculated the corresponding percentage degradation. Figure 10.2 illustrates the influence of time on the degradation rate of methyl orange at two

different initial concentrations of 25mg/l and 35mg/l. In both the cases, the percentage conversion first increases upto an irradiation time of 80 minutes and then it starts decreasing. The increased amount of radiation is the dominating factor that facilitates the degradation upto a time of 80 minutes. Obviously, the rate of degradation depends on the initial concentrations of methyl orange. It is seen that the decrease in the rate of degradation of a methyl orange solution after an irradiation time of 80 minutes having a concentration of 25mg/l is more than that containing 35mg/l of methyl orange.
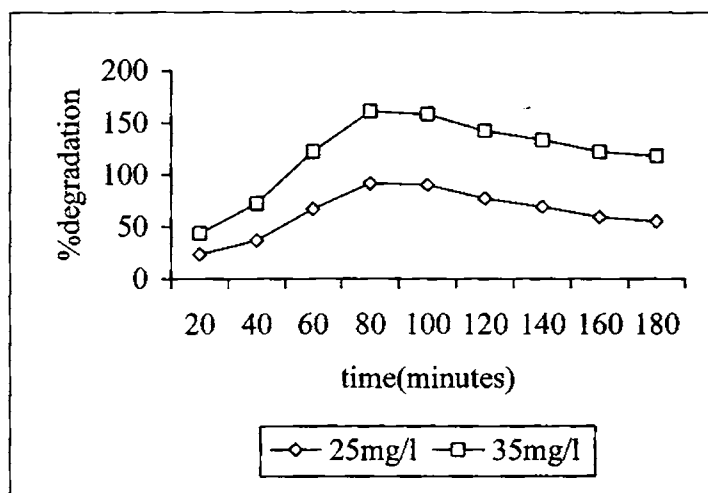

Figure 10.2

Influence of time on degradation of methyl orange

0.1g pure titania, 20ml methyl orange, Intensity-48 Watts

Further, Davis *et al* and Mathew[38-39] explained this behavior that the path length of the photons entering the solution decreases and in low concentration the reverse effect has observed, there by increasing the number

of photon absorption by the catalyst in low concentration. Mengyue *et al*[40]. suggests that as the initial concentration of the dye increases, the amount of catalyst required for the degradation also increases. Since irradiation time and the amount of catalyst are constant, the OH. (primary oxidant) formed at the surface of the catalyst is also constant. So the relative number of free radicals attacking the dye molecule increases with the amount of catalyst[41]. Hence, at higher concentration the degradation decreases with increase in the concentration of dye.

10.2.2 Effect of catalyst concentration

The mass of catalyst used in the photoreactor has to be properly selected since it plays an important role on the global efficiency of the reaction. Experiments were carried out with different concentrations of catalyst (0.025–0.150 g) at fixed methyl orange concentration (25 mg/l). It has been observed that the initial rate increases with an increase in the amount of catalyst and that it remains almost constant above a certain level and is presented in figure 10.3. As the concentration of the catalyst is increased, the number of photons absorbed and the number of dye molecules adsorbed are increased with respect to an increase in the number of catalyst molecules. The density of the molecule in the area of illumination also increases and thus the rate gets enhanced. After a certain level, the dye molecules available are not sufficient for adsorption by the increased number of catalyst molecule. Hence, the additional catalyst powder is not involved in the photocatalytic activity and the rate does not increase with increase in the amount of catalyst beyond certain limit. It is also expected that the aggregation of the catalyst molecules

at high concentration must also be considered, which causes the decrease in the number of active surface sites. The experimental data are found in good agreement with those reported by Sauer *et al.* for the degradation of Safira dye using Degussa P-25[42]. Neppolian *et al*[43] also reported the decreased percent degradation of reactive dyes at higher catalyst concentration. Further, it is explained that the deactivation of activated molecule by collision with the ground state molecule with the shielding of TiO_2 may also take place.
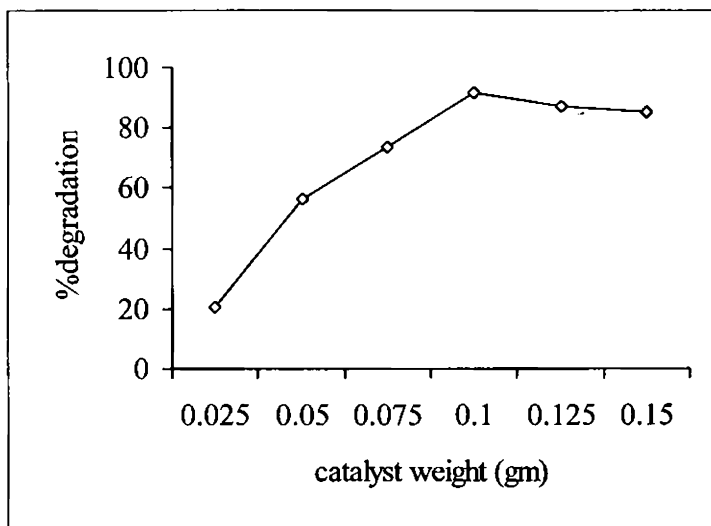

Figure 10.3

Influence of catalyst concentration in the degradation of methyl orange

20ml methyl orange (25mgl-1), Intensity-48 Watts, Irradiation time-80 min

10.2.3 Effect of methyl orange concentration

Various initial concentrations of methyl orange from 15mg/l to 40mg/l were used to evaluate the influence of the amount of the dye on the efficiency

of the reaction with otherwise identical reaction conditions. It can be seen from figure 10.4 that the concentration has a significant effect on the degradation rates. As the concentration of methyl orange increases, there is an increase in percentage degradation upto a concentration of 25mg/l, and thereafter it starts decreasing. This behaviour is expected since the ratio of methyl orange molecules/active sites of TiO_2 is lower leading to a faster overall disappearance of the compound.
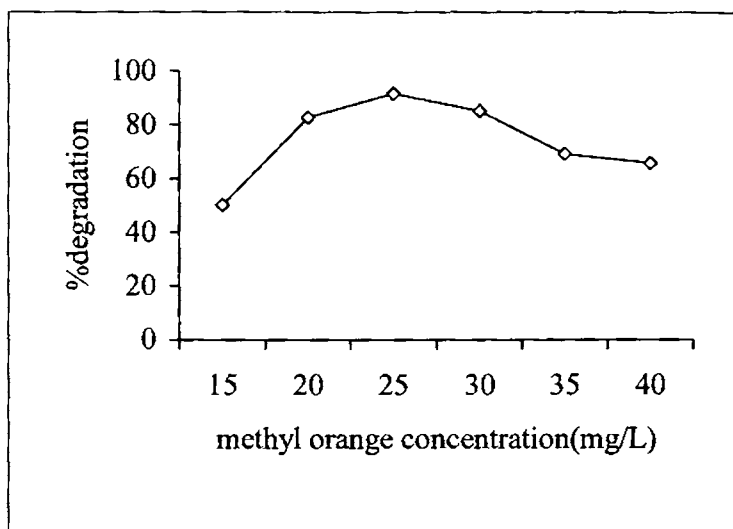

Figure 10.4

Influence of dye concentration on the degradation rate of methyl orange

0.1g pure titania, 80 minutes reaction time, Intensity-48 Watts

10.2.4 Effect of lamp intensity

The intensity of radiation falling on the catalyst surface plays an important role in any photocatalytic process. Here, the degradation of methyl orange,

having a concentration of 25mg/l is monitored using 0.1g of titania for 80 minutes with varying intensities of radiation. Figure 10.5 clearly illustrates the dependence of light intensity in the percentage degradation of methyl orange. The reaction doesn't occur actually in the dark, indicating the efficiency of the photocatalyst in the degradation of methyl orange. The percentage degradation of methyl orange rises steeply with intensity upto 48 Watts and thereafter it remains almost steady. So an optimum of 48W is chosen for the comparison of all the catalyst systems.
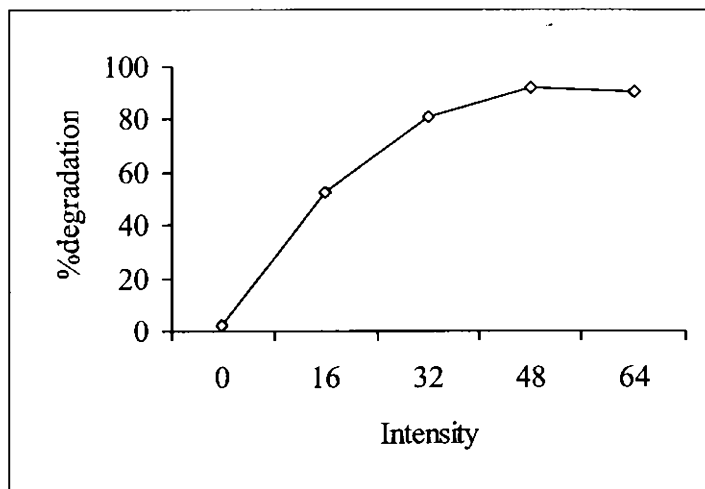

Figure 10.5

Influence of Lamp intensity on degradation of methyl orange

20ml methyl orange (25mgL-1), 0.1gm TiO2 catalyst, reaction time-80min

10.3 Comparison of Catalyst Systems

The results obtained for the photocatalytic degradation of methyl orange over the prepared systems are given in the tables 10.1 and 10.2. Pure

titania is a good photocatalyst in the degradation of methyl orange. Rare earth incorporated titania systems are having more photocatalytic activity than that of transition metal loaded systems in this reaction. 2% molybdenum, tungsten as well as chromium incorporated systems are having almost the same percentage conversion. 10% chromium incorporated titania systems are having exceptionally high percentage degradation which is very clear from the band gap energy calculated from UV-Vis DRS spectra.

Table 10.1

Influence of the nature of the incorporated of metal ion in the photodegradation of methyl orange

Catalyst	Percentage degradation Of methyl orange	Catalyst	Percentage degradation Of methyl orange
Ti	91.6	TiLa2	92.7
TiCr2	69.7	TiPr2	69.8
TiMo2	65.4	TiSm2	89.2
TiW2	66.7		

20ml methyl orange (25mgl-1), 0.1g TiO2 catalyst, reaction time-80min, Intensity-48W.

Among the rare earth metals, praseodymium doped metals are photocatalytically least active than lanthanum and samarium doped ones. The heterogeneous photocatalysis was mainly occurred in interfacial layers. So, the affinity and adsorption properties between reactants and photocatalyst surface play an important role on determining overall reaction rate[44,45]. Regarding the strong adsorption capability of methyl orange on the surface of the systems, the key factor was ascribed to the positive charge characteristic of the incorporated metal ion on the TiO_2 nanoparticle surface.

Table 10.2

Influence of the amount of the incorporated of metal ion in the
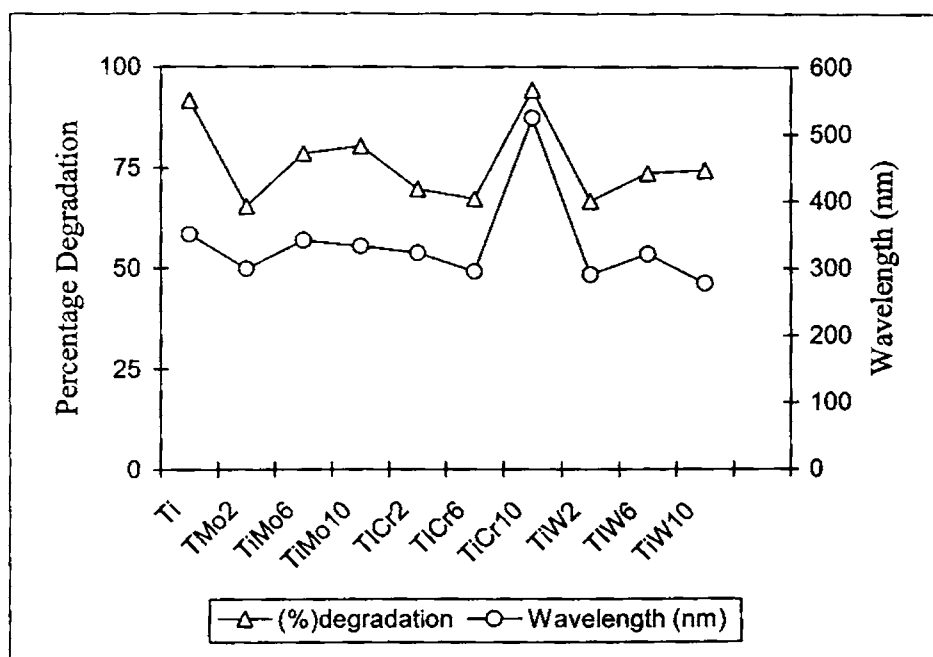
photodegradation of methyl orange

Catalyst	Percentage degradation Of methyl orange	Catalyst	Percentage degradation Of methyl orange
TiMo6	78.5	TiLa6	89.3
TiMo10	80.3	TiLa10	93.6
TiCr6	67.3	TiPr6	68.5
TiCr10	94.3	TiPr10	69.2
TiW6	73.7	TiSm6	91.2
TiW10	74.3	TiSm10	93.1

20ml methyl orange (25mgl-1), 0.1g TiO2 catalyst, reaction time-80min, Intensity-48W.

The amount of the metal incorporated also has a significant impact on the photocatalytic activity. In all the cases, a regular increase in the percentage degradation is noticed as the percentage of the incorporated metal increases, eventhough the increase is to a lesser extend. Lanthanum as well as Samarium incorporated systems are having slightly higher photocatalytic activity than other systems. The lesser activity of praseodymium incorporated systems can be explained from the respective XRD results. The presence of lower percentage of rutile in the system can decrease the photocatalytic activity in this reaction. It has been reported that the rutile phase of titanium dioxide has a lesser photocatalytic activity than the anatase phase since the rutile phase possesses a slightly lower degree of surface hydroxylation[46].

The values of the band gap are of great importance since they are indicative of the energy necessary to initiate the photocatalytic process[47]. For the

photodegradation of methyl orange, these values must be taken into account. The increase in band gap energy, evident from UV-vis DRS studies due to a red shift in the λ_{max} values can be well correlated with the percentage degradation of methyl orange. Figures 10.6 and 10.7 gives the relationship between these two variables in case of transition metal as well as rare earth metal loaded systems.
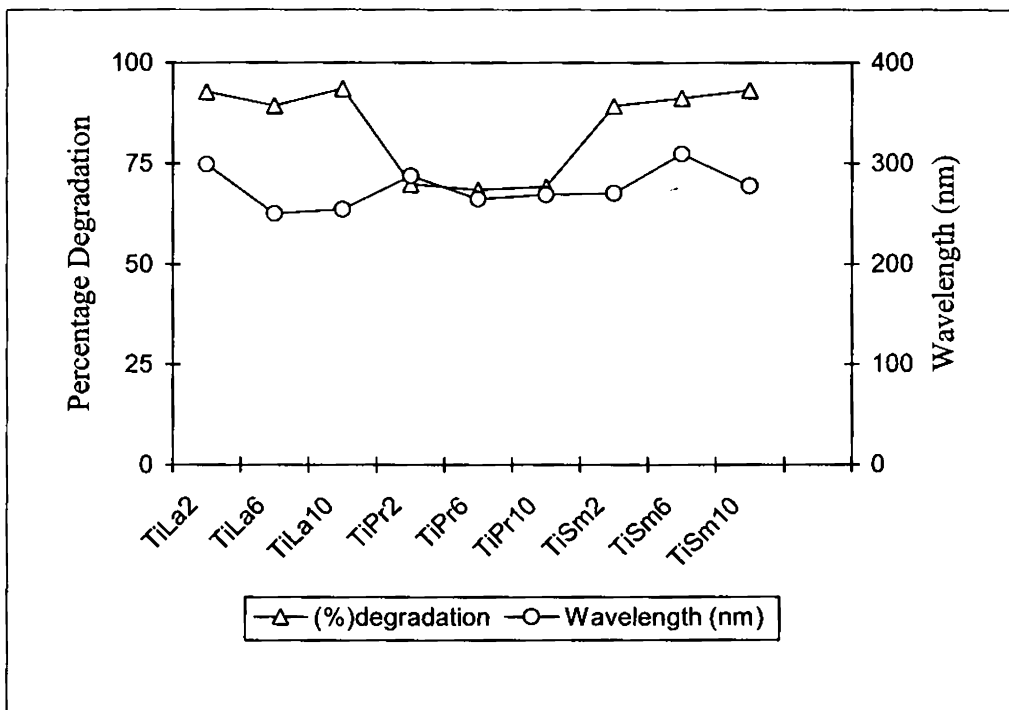

Figures 10.6

Correlation between λ_{max} and % degradation of methyl orange

It was reported that the pore structure, pore size, particle size and activation temperature of titania can affect the photocatalytic activity of organic pollutants in wastewater[48,49]. There were two competing factors to influence

the photocatalytic activity of the modified titania systems. The effective titania surface area available for methyl orange would decrease due to incorporation of the metals, which induced the decrease of photocatalytic activity. On the other hand, the dispersion stability, improved by incorporation of metals would expose more titania surface to methyl orange.

Figures 10.7

Correlation between λ_{max} and % degradation of methyl orange

The enhancement of photoactivity for lanthanide ion doped titania systems can be attributed to the concentrated organic materials at the semiconductor surface by the formation of a complex between the doped lanthanide ions and

the substrates. However our results reveal slight enhancement in the photoactivity and that too is not proportional to the concentration of the lanthanide ion. Theoretically, a greater amount of the incorporated metal should be favorable for more complex formation, and thus enhanced catalytic activity should be observed with higher lanthanide concentration[50]. Therefore, the concentration of the substrate is not the only factor that influences the activity. The manner in existence of Ln^{3+} may also play an important role in the activity of lanthanide doped titania. Usually Ln^{3+} is smaller than Ti^{4+}, and because of this mismatch of their ionic sizes, the possibility of their migration to the interstitial positions cannot be ruled out.

The photocatalytic activity should have some implications for the specific synthesis method followed. In addition, the increase of better surface acidity and larger surface area in rare earth mortal doped titania should be important factors that induce the improvement of the activity as well[51]. The well-dispersed titania nanoparticles with high surface area allow high access of the reactants to the TiO_2 surface in aqueous medium. In the photocatalysis system, the dye molecule was excited by absorption of a suitable visible light photon. The electrons of excited dye molecule can inject into conduction band (CB) of TiO_2. Then these electrons could be trapped by electron scavengers (usually oxygen molecule). But it was also extremely susceptible for the cation radicals and the electrons to recombine if the injected electrons accumulated in the CB of TiO_2. So, electrons trapping and electrons transfer would be two key steps to inhibit electron–cation radical recombination. The cation radical (dye^+) produced by electron injection was less stable than the ground state of the compound (dye). As a result, unstable cation radical dye may directly be

degraded to products or reacted with superoxide radial anion (O_2^-) to produce degradation products.

According to the principles of semiconductor TiO_2 photocatalysis, the photoactivity is mainly dependent on three factors: (a) electron–hole generation capacity; (b) electron transfer route and efficiency; (c) separation efficiency of photogenerated charge pairs. The sensitized photocatalysis mechanism is very different from UV light induced photocatalysis mechanism. The dye sensitization process involves the excitation of the dye molecule with visible light and subsequent electron injection or electron transfer from excited state dye molecule to conduction band of semiconductor TiO_2. The electron generation capacity mainly depends upon the intensity of incident photons with matchable energy and absorption amount of dye molecule on photocatalysts surface. The separation of electron–cation radical and electron transfer efficiency depend on the electron acceptor (usually TiO_2 conduction band, triplet ground state O_2 or other scavengers) and transferring route. Indeed, it could even be agreed that a tendency to strongly adsorb a given substrate may be deleterious to the photocatalytic efficiency.

10.4 Conclusions

The photocatalytic degradation of methyl orange can take place effectively over the prepared systems. The crystal structure as well as the effective surface area plays a significant role in the photocatalytic efficiency. Among the different systems, pure titania as well as their lanthanum and samarium modified analogues are found to be good photocatalysts. A good correlation between the band gap energy and percentage degradation of methyl

orange is obtained among the various systems studied. In a sense, the effective photodegradation of methyl orange by TiO_2 is a very exciting respect in photocatalytic area.

❦❦❦❦❦❦❦❦❦❦❦❦❦❦❦❦❦❦❦❦

References

1   Yibing Xie, Chunwei Yuan, Xiangzhong Li, Colloids and Surfaces A: Physicochem. Eng. Aspects, 252 (2005) 87.

2   J. Li, P.L. Bishop, Wat. Sci. Technol, 46 (1–2) (2002) 207.

3   J. Li, P.L. Bishop, Wat. Sci. Technol, 49 (11–12) (2004) 237.

4   Y. Liu, X. Che, J. Li, C. Burda, Chemosphere, 61 (2005) 11.

5   C. Burda, Y. Lou, X. Chen, A.C.S. Samia, J. Stout, J.L. Gole, NanoLetters, 3 (2003) 1049.

6   F. Nerud, P. Baldrian, J. Gabriel, D. Ogbeifun, Chemosphere, 44 (2001) 957.

7   S. Senthilkumaar, K. Porkodi, R. Vidyalakshmi, Journal of Photochem. Photobiol. A: Chem, 170 (2005) 225.

8   M.R. Hoffmann, S.T. Martin, W. Choi, D.W. Bahnemann, Chem. Rev, 95 (1995) 69.

9   B. Neppolian, S. Sakthivel, M. Palanichamy, B. Arabindoo, V. Murugasen, Stud. Surf. Sci. Catal, 113 (1998) 329.

10 B. Neppolian, S. Sakthivel, M. Palanichamy, B. Arabindoo, V. Murugasen, J. Environ. Sci. Health A, 43 (1999) 1829.

11 B. Neppolian, S. Sakthivel, M. Palanichamy, B. Arabindoo, V. Murugasen, Bull. Cat. Soc. India, 81 (1999) 164.

12 A. Linsebigler, G. Lu, J.T. Yates, Chem. Rev, 95 (1995) 735.

13 A. Fujishima, N.T. Rao, D.A. Rryk, J. Photochem. Photobiol. C, 1 (2000) 1.

14 D.F. Ollis, E. Pellizzetti, N. Serpone, Environ. Sci. Technol, 25 (1991) 1522.

15   M.A. Fox, M. Dulay, Chem. Rev, 93 (1993) 341.

16   O. Legrini, E. Oliveros, A.M. Braun, Chem. Rev, 93 (1993) 671.

17   D.F. Ollis, H. Al-Ekabi (Eds.), Photocatalytic Purification and Treatment of Water and Air, Elsevier, Amsterdam, 1993.

18   M.R. Hoffmann, S.T. Martin, W. Choi, D.W. Bahnemann, Chem. Rev, 95 (1995) 69.

19   J.M. Herrmann, Catal. Today, 53 (1999) 115.

20   Maria-Jose, Lopez-Munoz, Rafael van Grieken, Jose, Aguado, Javier Marugan, Catalysis Today 101 (2005) 307.

21   Xin Zhang, Feng Zhang, Kwong Yu Chan, Appl. Catal A: Gen, 284 (2005) 193.

22   T. Docters, J.M. Chovelon, J.M. Herrmann, J.P. Deloume, Appl. Catal B: Environmental, 50 (2004) 219.

23   I.K. Konstantinou, T.A. Albanis, Appl. Catal. B, 42 (2003) 319.

24   R. Asahi, T. Morikawa, T. Ohwaki, K. Aoki, Y. Taga, Science, 293 (2001) 269.

25   P. Reeves, R. Ohlhausen, D. Sloan, K. Pamplin, T. Scoggins, C. Clark, B. Hutchinson and D. Green, Solar Energy, 48 (1992) 413.

26   N. Nageswara Rao and P. Natarajan, Current Science, 66 (10) (1994) 742.

27   Chantal Guillard, Hinda Lachheb, Ammar Houas, Mohamed Kisbi, Elimame Elaloui and Jean Marie Herrmann, Journal of Photochemistry and Photobiology A: Chemistry, 158 (2003) 27.

28   Jincai Zhao, Kaiqun Wu, Taixing Wu, Hisao Hidaka and Nick Serpone, J. Chem. Soc, Faraday Trans, 94 (5) (1998) 673.

29   Wenjie Wang, Mingyuan Gu and Yanping Jin, Mat. Lett, 57 (2003) 3276.

30   Lili Zhao, Yun Yu, Lixin Song, Xingfang Hu, Andre Larbot, Applied Surface Science, 239 (2005) 285.

31   Kazuhiro Doushita, Tetsuro Kawahara, Journal of Sol-Gel Science and Technology, 22 (2001) 91.

32   Qiaorong Sheng, Shuai Yuan, Jinlong Zhang , Feng Chen, Microporous and Mesoporous Materials, 87 (2005) 177.

33   Yibing Xie, Chunwei Yuan, Xiangzhong Li, Colloids and Surfaces A: Physicochem. Eng. Aspects, 252 (2005) 87.

34   Q.Y. Li, Y.F. Chen, D.D. Zeng, W.M. Gao and Z.J. Wu, J. Nanoparticle Research, 7 (2005) 295.

35   Ping Cheng, Mao Ping Zheng, Qiang Huang, Yan Ping Jin and Ming Yuan Gu, J. Mat. Sci. Lett, 22 (2003) 1165.

36   Xin Zhang, Feng Zhang, Kwong Yu Chan, Appl Catal A: Gen, 284 (2005) 193.

37   Lei E, Mingxia Xu, Lei Ge, Yuming Tian, Yan Li and Tiantian Xu, Key Eng. Mat, (280-283) (2005) 377.

38   R.J. Davis, J.L. Gainer, G.O. Neal, I. Wenwu, Water Environ. Res, 66 (1994) 50

39   R.W. Matthews, J. Chem. Soc., Faraday Trans, 85 (1989) 1291.

40   Z. Mengyue, C. Shifu, T. Yaown, J. Chem. Tech. Biotechno 1 64 (1995) 339.

41   L. Zang, C.Y. Liu, X.M. Ren, J. Photochem. Photobiol. A, 85 (1995) 239.

42   T. Sauer, G. Cesconeto Neto, H.J. Jose, R.F.P.M. Moreira, J. Photochem. Photobiol. A, 149 (2002) 147.

43   B. Neppolian, S. Sakthivel, M. Palanichamy, B. Arabindoo, V.

Murugasen, J. Hazard. Mater B, 89 (2002) 303.

44 C. Hu, Y.Z. Wang, H.X. Tang, Appl. Catal. B, 35 (2001) 95.

45 M.S. Chiou, H.Y. Li, Chemosphere, 50 (2003) 1095.

46 Wenjie Wang, Mingyuan Gu, Yanping Jin, Mat. Lett, 57 (2003) 3276.

47 Tessy Lopez and R. Gomez, E. Sanchez, F. Tzompantzi and L. Vera, J. Sol-Gel Sci. Tech, 22 (2001) 99.

48 N. Xu, Z. Shi, Y. Fan, J. Dang, J. Shi, M.Z.C. Hu, Eng. Chem. Res, 33 (2) (1999) 373.

49 A. Soni, R. Amcta, B. Sharma, S.C. Amcta, J. Ind. Pollut. Control, 15 (1) (1999) 117.

50 K.T. Ranjit, I. Willner, S.H. Bossmann and A.M. Braun, Environ. Sci. Technol, 35 (2001) 1544.

51 C.P. Sibu, S. Rajeshkumar, P. Mukundan and K.G.K. Warrier, Chem. Mater, 14 (2002) 2876.

Chapter *11*

Summary and Conclusions

Abstract

   Nowadays the chemical industries are facing challenges to reduce the use of environmentally hazardous chemicals. Central to this problem, the search for a better methodology for chemical industries has been of great interest to scientists throughout the world. Catalysis is a fascinating field of science because it deals with processes, which may provide solutions for many of the key problems we face. The fundamental aspects giving prime importance to the preparation of titania and their modified analogues by particulate sol-gel route and its physico-chemical characterization are briefly reviewed in this thesis. The great versatility of the prepared catalysts for carrying out some industrially important organic reactions is also included in the thesis. This chapter deals with the summary and the conclusions of the results described in the preceding chapters of the thesis.

11.1 Summary

The present work concentrates on the preparation of the catalyst starting from a comparatively cheaper inorganic precursor like metatitanic acid through sol-gel route. The incorporation of transition metals like chromium, molybdenum and tungsten as well as rare earth metals like lanthanum, praseodymium and samarium is done in small amounts to titania, thus improving the surface characteristics, thermal stability and surface acidity of the composite catalysts and consequently their catalytic performance. It is well known that supported oxides of transition metals and rare earth metals are widely used as catalysts for various reactions. A systematic investigation of the physico-chemical characterization of the prepared catalysts is necessary considering their industrial relevance. The catalytic and photocatalytic properties of titania systems are systematically studied in this work. Thus the thesis gives emphasis to various aspects like catalyst preparation, characterization and their versatile applications in carrying out some industrially important organic transformations. The chapter wise organization of the thesis is as follows.

Chapter 1 gives an overview about solid acid catalysis carried out by titania. The importance of titania based catalysts in current environmental aspects is discussed in detail. The present chapter gives major stress to the various structural aspects of titania as well as different methods for its preparation. A brief literature survey is also included in this chapter.

Chapter 2 is devoted to a complete description of the materials used in the present work and the experimental techniques employed for the catalyst characterization. The flow chart describing the mode of preparation of the catalyst systems are also included in this chapter. The experimental details for the evaluation of catalytic activity are also incorporated in this chapter. The surface acidity determination by different techniques including the test reactions like cumene cracking and cyclohexanol decomposition is the additional features of this chapter.

Chapter 3 focuses on the physico-chemical characterization of the prepared catalytic systems. The catalyst systems were characterized by BET surface area and pore volume measurements, XRD analysis, TG/DTG studies, UV-Vis DRS and FTIR spectroscopy. The elemental composition of the systems were revealed by EDX analysis and the Scanning Electron Micrograms of the representative systems gives an insight into their surface morphology. The results obtained from ammonia TPD and thermodesorption studies using 2,6-dimethyl pyridine as probe molecule is also described in detail. Cumene conversion discriminates the Bronsted as well as Lewis acidity of the prepared systems. Cyclohexanol decomposition reaction is carried out to know the acid base properties of the catalysts prepared.

Chapter 4 discusses the applicability of titania and their modified analogues towards the epoxidation of cyclohexene. The influence of various reaction parameters like reaction temperature, flow rate, nature and amount of the solvent as well as the oxidant is investigated in detail in this section.

Chapter 5 illuminates the application of titania and their modified analogues in the hydroxylation of phenol. Here also, the variation in the catalytic activity and product selectivity with experimental parameters has been taken care of. A possible mechanism has been suggested after a critical analysis of the catalytic performance.

Chapter 6 deals with the catalytic activity of the prepared systems towards the alkylation of aromatics. Tert-butylation of phenol as well as the methylation of anline and anisole is carried out efficiently in a vapour phase reactor. Various factors, which influence the percentage conversion as well as the product selectivity, are also considered in detail. Attempt has been made to correlate the catalytic activity with the surface acidic properties of the catalyst systems.

Chapter 7 presents the dehydrogenation of cyclohexane and cyclohexene. The influence of reaction temperature and flow rate is investigated in detail. The dependence of surface acidity of the prepared systems on the percentage conversion is also investigated in detail.

Chapter 8 lays the foundation of photocatalysis. A brief literature review on titania as well as their modified systems are tabulated in this section showing their applications in the vast field of photocatalysis. The applications of titania based systems in today's world of growing environmental concern are also dealt in this chapter.

Chapter 9 describes the photooxidation of benzhydrol over titania and their modified systems. The influence of various reaction parameters like irradiation time, amount of catalyst, concentration of the reactant and the nature of the solvent has been investigated. The chapter also discusses the mechanistic aspects of this reaction.

Chapter 10 narrates the photodegradation of methyl orange. The dependence of photodegradation of the dye rates on various parameters such as dye concentration, photocatalyst concentration, irradiation time and intensity of radiation were also studied in detail. The percentage degradation of various systems for this reaction is correlated with the band gap energy of the prepared systems.

Chapter 11 presents the summary and important general conclusions of the work done.

11.2 Conclusions

The following conclusions that can be drawn from the present research work are the following.

&ex Particulate sol-gel method is found to be an efficient method for the preparation of high surface area titania systems together with their transition metal and rare rare earth metal analogues. The high cost of alkoxide precursor widely used in the sol-gel synthesis is avoided in the present preparation route, which adds to its economical importance.

❧ The enhanced anatase phase stability of the modified systems is an important consequence of metal incorporation. The high dispersion of the incorporated metals on the surface of the titania support is evident from the XRD patterns.

❧ Modified titania systems are capable of improving the physico chemical characteristics and the surface properties of pure titania. The XRD and SEM analysis emphasizes the agreement between the increase in surface area and decrease in the crystallite size.

❧ The high thermal stability of the prepared systems can be understood from the TG-DTG curves. The characteristic peak of pure titania is obtained from the FTIR analysis. UV-Vis DRS helped in the identification of tetrahedrally coordinated titanium ions and calculation of the band gap energy of the prepared systems.

❧ The surface acidic properties of titania supports improve considerably upon incorporation of transition metal as well as rare earth metals. There is a good correlation between the surface acidity measured by ammonia TPD, thermodesorption of 2,6-dimethyl pyridine adsorbed samples and catalytic test reactions such as cumene cracking and cyclohexanol decomposition reaction.

❧ The epoxidation of cyclohexene is carried out efficiently over the prepared systems with the selective formation of cyclohexene epoxide. The excellent activity and selectivity in the epoxidation of cyclohexene is due to highly dispersed Lewis acidic titanium sites. The activity of the prepared catalysts and their stability with time in the epoxidation of

cyclohexene by tert-butyl hydroperoxide hints that it might be possible to create cleaner nylon chemistry.

❧ The prepared systems are highly active in the hydroxylation of phenol. Selection of an optimum reaction time also demands prime importance in order to achieve maximum activity and selectivity of the products. The performance of the catalytic systems points to its potential in the degradation of phenolic wastes.

❧ Friedel Crafts alkylation of arenes is successfully carried out over the prepared systems and thus introducing green and clean processes replacing the conventional hazardous acid catalysts. Tert-butylation of phenol gives 4-tertiary butyl phenol as the major product, which is catalyzed by medium acid sites. In the methylataion of aniline, the percentage N-methyl selectivity is more than that of C-alkylated product selectivity in all the systems. Good correlation exists between various types of acidity obtained from NH₃ TPD as well as percentage product selectivities, which give clear-cut evidence about the reaction mechanism. The vapour phase methylation of anisole over the prepared catalyst systems results in the selective formation of 2,6-xylenol. The acid-base properties of catalysts are responsible for the methylation of anisole.

❧ In the catalytic dehydrogenation of cyclohexane and cyclohexene carried out over the prepared systems, benzene is obtained as the major product. The total surface acidity of the systems plays an important role in determining the catalytic activity.

❧ The photooxidation of benzhydrol is efficiently carried out over the prepared systems resulting in the formation of benzophenone as the sole

product. The proposed mechanism involves the reaction between a cation radical of benzhydrol formed by the oxidation of the alcohol by a hole and a superoxide radical anion produced by the transfer of a conduction band electron to oxygen.

* The photochemical degradation of methyl orange occurs effectively over the prepared catalysts. The large surface area of the photocatalyst is one of the most dominating factors in achieving a high efficiency in the reaction. The percentage degradation of various systems for this reaction is correlated with the band gap energy of the prepared systems.

Future Outlook

Catalysis is a fascinating, interdisciplinary and future oriented area. Indeed the chemistry of catalysis is as varied as chemistry itself. With its versatility and excellent control over products characteristics, sol-gel processing has played an important role in catalyst preparation and no doubt will continue to do so. The use of metatitanic acid as the precursor in the preparation of high surface area titania catalysts receives special attention. From the viewpoint of green chemistry, the use of heterogeneous catalysts like modified titania is desirable. The present investigation on the catalytic activity of modified titania catalysts reveal their high efficiency for various types of reaction like epoxidation of cyclohexene as well as hydroxylation of phenol. The work can be extended in the epoxidation of other cycloolefins and the products of which are of independent significance and/or are valuable chemicals for synthesis of biologically active species. The application of the prepared catalysts makes the wet air oxidation process more attractive by

achieving high conversion at considerably lower temperature and pressure. The higher activity and selectivity in the alkylation of aromatics carried out over the prepared systems is another important observation we got. Since the prepared catalysts are highly acidic, studies can be extended for various industrially important acid catalyzed alkylation and rearrangements of other aromatic molecules.

Good photocatalytic activity is shown by titania systems towards the photo degradation of methyl orange and photooxidation of benzhydrol. Being a photocatalyst, the work can be extended in this vast ever growing field too. The photocatalytic activity of the prepared systems can be utilized to establish an effective method for the remediation of volatile organic compounds from indoor air, which poses a significant health risk. Titania based catalysts can also be applied in the degradation of various types of dye stuffs which represent an increasing environmental problem. Their effective removal is a challenging task as environmental laws and regulations are becoming more and more stringent. The areas of application of photocatalysis to water purification and treatment of water, area selective reactions, polymer degradation and selective organic synthesis will probably gain priority as they appear to possess the potential to alter environmental and electronic scenarios.